ALEJANDRA RODRÍGUEZ MARTÍNEZ

Expression Profiling of Novel Iron-Related Genes in Mouse Models of Iron Overload

■

ACADEMIC DISSERTATION
To be presented, with the permission of
the Faculty of Medicine of the University of Tampere,
for public discussion in the Small Auditorium of Building B,
Medical School of the University of Tampere,
Medisiinarinkatu 3, Tampere, on October 30th, 2009, at 12 o'clock.

UNIVERSITY OF TAMPERE

ACADEMIC DISSERTATION
University of Tampere, Institute of Medical Technology
Tampere Graduate School in Biomedicine and Biotechnology (TGSBB)
Finland

Supervised by
Professor Seppo Parkkila
University of Tampere
Finland

Reviewed by
Professor Markku Heikinheimo
University of Helsinki
Finland
Professor Debbie Trinder
University of Western Australia
Australia

Distribution
Bookshop TAJU
P.O. Box 617
33014 University of Tampere
Finland

Tel. +358 3 3551 6055
Fax +358 3 3551 7685
taju@uta.fi
www.uta.fi/taju
http://granum.uta.fi

Cover design by
Juha Siro

Acta Universitatis Tamperensis 1460
ISBN 978-951-44-7862-8 (print)
ISSN-L 1455-1616
ISSN 1455-1616

Acta Electronica Universitatis Tamperensis 894
ISBN 978-951-44-7863-5 (pdf)
ISSN 1456-954X
http://acta.uta.fi

Tampereen Yliopistopaino Oy – Juvenes Print
Tampere 2009

CONTENTS

TIIVISTELMÄ

Raudalla on hyvin keskeinen tehtävä elimistössä. Vaikka se on terveydelle välttämätön alkuaine, liian suuri määrä rautaa on elimistölle haitallista. Ylimääräinen rauta edistää vapaiden radikaalien muodostumista aiheuttaen soluissa ns. oksidatiivista stressiä. Elimistössä ei ole säädeltyä raudan poistomekanismia. Sen takia raudan imeytymistä pohjukaissuolessa on säädeltävä tarkasti rautatasapainon säilyttämiseksi.

Perinnöllinen hemokromatoosi on geneettisesti heterogeeninen sairaus, jossa elimistöön kertyy liikaa rautaa. Sen yleisin geneettinen syy on mutaatiot *HFE*-geenissä. Perinnöllistä hemokromatoosia sairastavilla potilailla hepsidiini-hormonin ilmentyminen on poikkeavan matala, minkä seurauksena raudan imeytyminen lisääntyy ohutsuolessa. Ylimääräinen rauta kertyy kudoksiin, pääasiallisesti maksaan, sydämeen ja haimaan. Yleisimpiä kliinisiä komplikaatioita hoitamattomilla potilailla ovat maksafibroosi, maksakirroosi, maksasyöpä, diabetes, kardiomyopatia, seksuaalitoimintoihin liittyvät ongelmat ja niveltulehdus.

Tällä tutkimuksella oli kolme päätavoitetta. Ensimmäisessä osassa tavoitteena oli selvittää hemojuveliini- ja neogeniini-proteiinien ilmentymistä eri kudoksissa. Sekä hemojuveliini että neogeniini ovat vastikään löydettyjä proteiineja, jotka osallistuvat raudan säätelyn signalointiin. Hemojuveliinin ja neogeniinin ilmentymistä tutkittiin lähetti-RNA- ja proteiinitasoilla. Tutkimusmenetelminä käytettiin käänteiskopioijaentsyymiin perustuvaa RT-PCR-menetelmää, kvantitatiivista RT-PCR-menetelmää, western blottausta sekä immunohistokemiallista värjäystä. Geenien ilmentymistä genominlaajuisesti tutkittiin cDNA-mikrosirutekniikalla.

Toinen päätavoite oli karakterisoida raudan ylikuormituksen seurauksena tapahtuvia geenien ilmentymisen muutoksia hiiren sydämessä ja luurankolihaksessa. Kolmantena tavoitteena oli tutkia ja verrata koko genomin laajuisesti geenien transkriptiossa tapahtuvia muutoksia, joita rautakuormitus aiheuttaa maksassa ja pohjukaissuolessa. Sekundaarinen raudan ylikuormitus saatiin aikaan ruokkimalla

hiiriä rautarikkaalla dieetillä. *Hfe*-poistogeenisiä hiiriä käytettiin primaarisen eli geneettisen hemokromatoosin mallina.

Ensimmäiseen tavoitteeseen liittyvät tutkimukset osoittivat, että hemojuveliinin ilmentyminen on neogeniiniin verrattuna rajoittuneempaa. Sekä hemojuveliinin että neogeniinin lähetti-RNA:ta ja proteiinia ilmentyi sydämessä, luurankolihaksessa ja maksassa. Neogeniinin ilmentyminen oli voimakkainta sukuelimissä ja aivoissa.

Tutkimuksen toisessa osassa rautarikas dieetti vaikutti hiirellä merkittävästi 75 geenin ilmentymiseen sydämessä ja 54 geeniin luurankolihaksessa. Monet näistä geeneistä osallistuvat hiilihydraattien ja rasvojen aineenvaihduntaan, solun stressivasteeseen ja geenien transkriptioon. Jotkut löydetyistä geeneistä voivat liittyä myös perinnöllisen hemokromatoosin vakavien komplikaatioiden, kuten kardiomyopatian ja diabeteksen, kehittymiseen.

Tutkimuksen kolmannen osan merkittävin tulos $Hfe^{-/-}$-hiirten osalta oli maksassa akuutin vaiheen proteiineja ja pohjukaissuolessa monia ruoansulatusentsyymejä koodaavien geenien yli-ilmentyminen. Rautadieetti aiheutti voimakkaimmat muutokset oksidatiiviseen stressiin liittyvien geenien ilmentymisessä. Maksassa rautadieetti aiheutti sellaisia muutoksia geenien ilmentymisessä, jotka voivat liittyä maksasolujen hyperplasiaan ja maksasyövän kehittymiseen.

Geenien ilmentymistutkimusten perusteella raudan ylimäärä elimistössä muuttaa useiden, potentiaalisesti kiinnostavien kohdegeenien ilmentymistä, joista osa on huonosti tunnettuja tai toiminnaltaan kokonaan tuntemattomia. Jatkotutkimuksissa on mielenkiintoista selvittää niiden yhteyttä raudan aineenvaihduntaan ja raudan ylikuormituksen patofysiologiaan.

ABSTRACT

Iron is crucial to the survival of organisms and plays a critical role in the catalysis of many important enzymatic reactions. Despite its essential properties, iron can also cause damaging at the cellular level if present in excess and may promote the formation of free radicals resulting in oxidative stress. Importantly, there is no controlled mechanism for excretion of iron from the body. Thus, iron absorption in the duodenum must be tightly regulated to maintain iron homeostasis.

Hereditary hemochromatosis (HH) is a genetically heterogeneous disorder characterized by iron overload. Mutations of the *HFE* gene are the most common cause of HH in which abnormally low expression of the iron hormone hepcidin results in increased iron absorption. Iron is accumulated in various tissues, mainly in the liver, heart and pancreas. Common clinical complications in the absence of treatment include hepatic fibrosis, cirrhosis, hepatocellular carcinoma, diabetes, cardiomyopathy, hypogonadism, and arthritis.

The aims of the present study can be divided into three sections. In the first section, the aim was to elucidate the expression profiles of hemojuvelin and neogenin, two recently discovered proteins involved in iron-regulatory signaling pathways. In the second section, the goal was to characterize gene expression changes in response to dietary iron overload in the murine heart and skeletal muscle. The third aim was to explore and compare the genome-wide transcriptome response to *Hfe* deficiency and dietary iron overload in the murine liver and duodenum.

The expression profiles of hemojuvelin and neogenin were studied at the mRNA and protein levels by means of reverse transcription-PCR (RT-PCR), quantitative RT-PCR (Q-RT-PCR), western blotting and immunohistochemistry. Regulation of global gene transcription was explored using a cDNA microarray technique.

Secondary iron overload was induced by feeding mice with an iron-supplemented diet, while *Hfe*$^{-/-}$ mice, a mouse model of HH, were used as a model for genetic iron overload syndrome.

The first studies revealed that hemojuvelin is expressed in a more limited set of tissues than neogenin. Transcripts and proteins of both hemojuvelin and neogenin are present in the heart, skeletal muscle and liver. Neogenin protein shows an interesting profile with the highest expression in reproductive organs and the brain.

In the second part of the study, we found that dietary iron overload affected the expression of 75 genes in the heart and 54 genes in the skeletal muscle. Among the regulated genes, many are involved in the regulation of glucose and lipid metabolism, cellular stress responses and regulation of transcription. Some genes could be involved in the development of cardiomyopathy and diabetes, two pathologies common in HH patients.

In the third section, the most striking results in *Hfe*$^{-/-}$ mice were the overexpression of genes for acute phase reactants in the liver and the strong induction of digestive enzyme genes in the duodenum. In contrast, the iron-rich diet caused a more pronounced change of gene expression responsive to oxidative stress in both tissues. In the liver, dietary iron overload affected gene expression that may be implicated in liver hyperplasia and development of hepatocellular carcinoma.

The expression studies in the second and third sections revealed many genes of potential interest, most of which are poorly characterized and some previously unknown. The role of these genes in iron metabolism and the pathology of iron overload should be further explored.

LIST OF ORIGINAL COMMUNICATIONS

The thesis is based on the following original publications, referred to in the text by their Roman numerals (I-IV):

I **Rodriguez Martinez A**, Niemelä O and Parkkila S (2004): Hepatic and extrahepatic expression of the new iron regulatory protein hemojuvelin. Haematologica 89:1441-1445.

II **Rodriguez A**, Pan P and Parkkila S (2007): Expression studies of neogenin and its ligand hemojuvelin in mouse tissues. J Histochem Cytochem 55:85-96.

III **Rodriguez A**, Hilvo M, Kytömäki L, Fleming RE, Britton RS, Bacon BR and Parkkila S (2007): Effects of iron loading on muscle: genome-wide mRNA expression profiling in the mouse. BMC Genomics 8:379.

IV **Rodriguez A**, Luukkaala T, Fleming RE, Britton RS, Bacon BR and Parkkila S (2009): Global transcriptional response to *Hfe* deficiency and dietary iron overload in the mouse liver and duodenum. PLoS ONE 4: e7212. doi:10.1371/journal.pone.0007212.

ABBREVIATIONS

8-OHdG	8-hydroxy-2'-deoxyguanosine
ACTB	β-actin
ANGPTL4	Angiopoietin-like 4
B2M	β-2-microglobulin
BMP	Bone morphogenetic protein
BMPR	Bone morphogenetic protein receptor
Cp	Crossing point
CYBRD1	Duodenal cytochrome b
DAB	3,3'-diaminobenzidine tetrahydrochloride
DCYTB	Duodenal cytochrome b
DMT1	Divalent metal transporter 1
EGR	Early growth response
ERK	Extracellular signal-regulated kinase
Fe^{2+}	Ferrous iron
Fe^{3+}	Ferric iron
Fe-Tf	Iron-loaded transferrin
FLVCR	Feline leukemia virus subgroup C receptor
GAPDH	Glyceraldehyde-3-phosphate dehydrogenase
GDF15	Growth differentiation factor-15
GPI	Glycosylphosphatidylinositol
GPX	Glutathione peroxidase
HAMP	Hepcidin
HCP1	Heme carrier protein 1
HDL	High density lipoprotein
HFE2	Hemojuvelin
HH	Hereditary hemochromatosis
HIF	Hypoxia-inducible transcription factor
HJV	Hemojuvelin

HMOX	Heme oxygenase
HPRT1	Hypoxanthine phosphoribosyl-transferase I
HRP	Horseradish peroxidase
IL	Interleukin
IMP	Integrin-mobilferrin pathway
IRE	Iron responsive (or regulatory) element
IRP	Iron regulatory protein
JH	Juvenile hemochromatosis
LPL	Lipoprotein lipase
MAP	Mitogen-activated protein
MHC	Major histocompatibility complex
NEO1	Neogenin
NTBI	Non-transferrin-bound iron
PAGE	Polyacrylamide gel electrophoresis
PBS	Phosphate buffered saline
PCNA	proliferating cell nuclear antigen
PCR	Polymerase chain reaction
PDK4	Pyruvate dehydrogenase kinase 4
PVDF	Polyvinylidene fluoride
Q-RT-PCR	Quantitative reverse transcription-polymerase chain reaction
RGM	Repulsive guidance molecule
rSMAD	receptor-activated SMAD
RT-PCR	Reverse transcription-polymerase chain reaction
SD	Standard deviation
SDHA	Succinate dehydrogenase complex subunit A
SDS	Sodium dodecyl sulphate
sHJV	Soluble hemojuvelin
SLC40A1	Ferroportin gene
SMAD	Son of mother against decapentaplegic
STAT	Signal transducer and activator of transcription
STEAP	Six transmembrane epithelial antigen of the prostate
TF	Transferrin
TFR	Transferrin receptor

TFRC	Transferrin receptor 1
TGF-β	Transforming growth factor β
TMPRSS6	Membrane bound serine protease matriptase-2
TRPC6	Transient receptor potential cation channel 6
TXNIP	Thioredoxin interacting protein
USF2	Upstream stimulatory factor 2
UTR	Untranslated region

1. INTRODUCTION

Iron has critical functions in the organism as a component in proteins with roles ranging from oxygen transport and energy production to the replication, transcription and reparation of DNA. However, excessive iron may promote the formation of free radicals causing oxidative stress and damage to cell components (Britton 1996). Since there is no regulated pathway for body iron excretion, precise control of iron absorption in the duodenum is essential for the maintenance of iron homeostasis.

Hereditary hemochromatosis (HH) is a disorder of iron overload in which inappropriately high absorption of dietary iron leads to iron accumulation in a variety of tissues, primarily in the liver, heart and pancreas (Fleming et al. 2005). HH can be attributed to various genetic defects, and *HFE* mutations are the most common cause (Feder et al. 1996).

Hepcidin (HAMP) is a peptide hormone crucial in the regulation of iron homeostasis, and its expression is inappropriately low in HH. Hemojuvelin (HJV or HFE2) and neogenin (NEO1) are involved in iron-regulatory signaling pathways (Lin et al. 2005, Zhang et al. 2007). The present study elucidated the tissues in which the *HJV* and *NEO1* genes are expressed as well as the cellular localization of their protein products.

Cardiomyopathy is a common clinical complication in HH patients (Fleming et al. 2005). This study includes the first genome-wide analysis of transcriptional changes induced by iron overload in the murine heart and skeletal muscle. It reveals genes that may represent links between iron overload and the development of cardiomyopathy and diabetes.

The liver has a crucial role in the maintenance of iron homeostasis, as it is the main site of hepcidin production (Krause et al. 2000, Park et al. 2001, Pigeon et al. 2001). The role of the duodenum in iron metabolism is obvious since it is the site of iron absorption. The present study reveals that a lack of Hfe protein in mice induces expression of genes for acute phase reactants in the liver and genes for digestive

enzymes in the duodenum. In the liver, dietary iron overload affects transcription of genes that may be implicated in liver hyperplasia and the development of hepatocellular carcinoma.

2. REVIEW OF THE LITERATURE

2.1 Body iron homeostasis

Iron has the ability to alter its oxidation state and redox potential according to the ligand environment. At pH 7.4 and physiologic oxygen tension, free iron in the ferrous form (Fe^{2+}) is readily oxidized to ferric iron (Fe^{3+}). Iron is an extremely useful biological catalyst due to the efficiency of both Fe^{2+} as an electron donor and of Fe^{3+} as an electron acceptor. Iron is a component in both heme and non-heme proteins that play vital roles in a range of cellular functions, including oxygen transport, electron transfer and DNA synthesis (Aisen et al. 2001). Paradoxically, however, these same properties of iron can potentially become hazardous. The spontaneous oxidation of iron mentioned previously is easily coupled with reduction of other molecules leading to the formation of free radicals. These are very reactive species that may cause oxidative damage to cellular lipids, enzymes and even DNA. Moreover, Fe^{3+} is virtually insoluble at physiological pH. Therefore, binding of iron to specialized proteins prevents iron toxicity and maintains the metal in a bioavailable form.

Organisms have evolved mechanisms to maintain iron homeostasis, consisting of the coordinated regulation of iron absorption, iron recycling and mobilization of stored iron. However, despite these mechanisms, organisms have a limited capability to excrete excess iron, probably due to lack of evolutionary forces towards this ability.

2.1.1 Iron distribution in humans

The average adult woman and man contain 45 and 55 mg of iron per kilogram of body weight, respectively (equivalent to a total iron content of around 3 and 5 g, respectively), distributed as represented in Figure 1. This amount is maintained

throughout the adult life because of a tight balance between absorption and loss of iron in the body. Adults absorb around 1-2 mg of dietary iron every day and approximately the same amount is lost through passive means such as cell desquamation and blood losses. Because there is no controllable mechanism of iron purge from the body, balance can be achieved only by tightly regulating the absorption of dietary iron in the small intestine. Normally, about 60-70% of total body iron is contained in circulating erythrocytes as part of hemoglobin (Andrews 1999, Ponka 1997). A further 10% is present in myoglobin, cytochromes and other iron-containing enzymes. The remaining 20-30% is stored mainly in the liver as ferritin, which can be readily mobilized when needed, and as hemosiderin representing a less mobile iron pool.

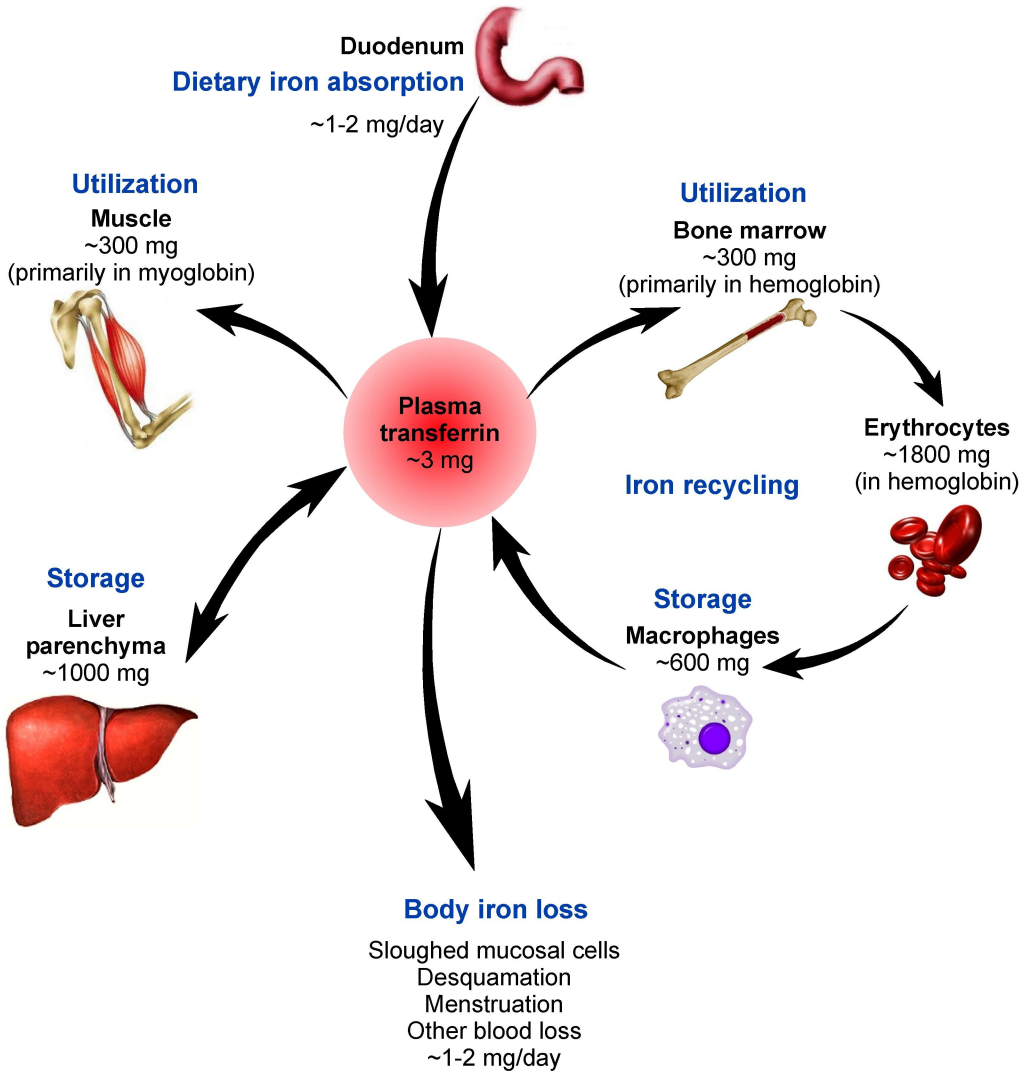

Figure 1. *Iron distribution in the adult human body. Adapted from (Andrews 1999).*

2.1.2 Intestinal iron absorption

2.1.2.1 Iron transport across the apical mucosal surface

Iron is absorbed from the diet in the duodenum and upper jejunum (Conrad and Umbreit 2002). Most diets contain two primary forms of iron: non-heme ferric iron from vegetables and grains and heme iron (ferrous iron protoporphyrin IX) from red meat. These forms are absorbed in a non-competitive manner. To reach the blood stream, iron must traverse both the apical and basolateral membranes of the absorptive enterocytes.

Non-heme iron is present in the chyme mainly in the ferric state, which precipitates at a pH greater than 3, becoming insoluble. This iron must be solubilized and chelated in the stomach to keep it in solution and available for absorption in the duodenum, where the pH is less acidic. This is achieved by dietary components (such as certain amino acids, sugars, amines and amides) and by intestinal mucines (Conrad et al. 1991). Contrastingly, other dietary constituents, such as phytates, carbonates, phosphates, oxalates, and tanates cause ferric iron to precipitate and form macromolecular complexes, rendering this iron unavailable for absorption. Reduction of ferric iron to the ferrous form makes it soluble at neutral pH and thus bioavailable. Numerous dietary components are capable of reducing iron, including ascorbic acid (Han et al. 1995) and amino acids such as cysteine (Glahn and Van Campen 1997) and histidine (Swain et al. 2002). However, ferrous iron is not a stable form in the presence of oxygen and it must be continuously reduced or chelated to protect it from oxidation. The duodenal cytochrome b (DCYTB, also known as CYBRD1) is a reductase located in the apical membrane of duodenal absorptive enterocytes and is the major reductase that facilitates the absorption of iron (McKie et al. 2001) (Figure 2). Other candidates for brush border reductases include members of the six transmembrane epithelial antigen of the prostate (STEAP) protein family (Ohgami et al. 2006). Once it has been reduced, ferrous iron is transported inside the cell by divalent metal transporter 1 (DMT1 or SLC11A2, formerly called NRAMP2, DCT1) (Canonne-Hergaux et al. 2001, Fleming et al. 1998, Fleming et al. 1997) (Figure 2). Intestinal DMT1 localizes primarily to the apical membrane of the enterocytes and subapical endosomes (Canonne-Hergaux et al. 1999). The transport of iron by DMT1 is coupled to proton

transport and the protons needed are derived from the gastric acid that flows from the stomach into the first portion of the duodenum (Gunshin et al. 1997, Sacher et al. 2001).

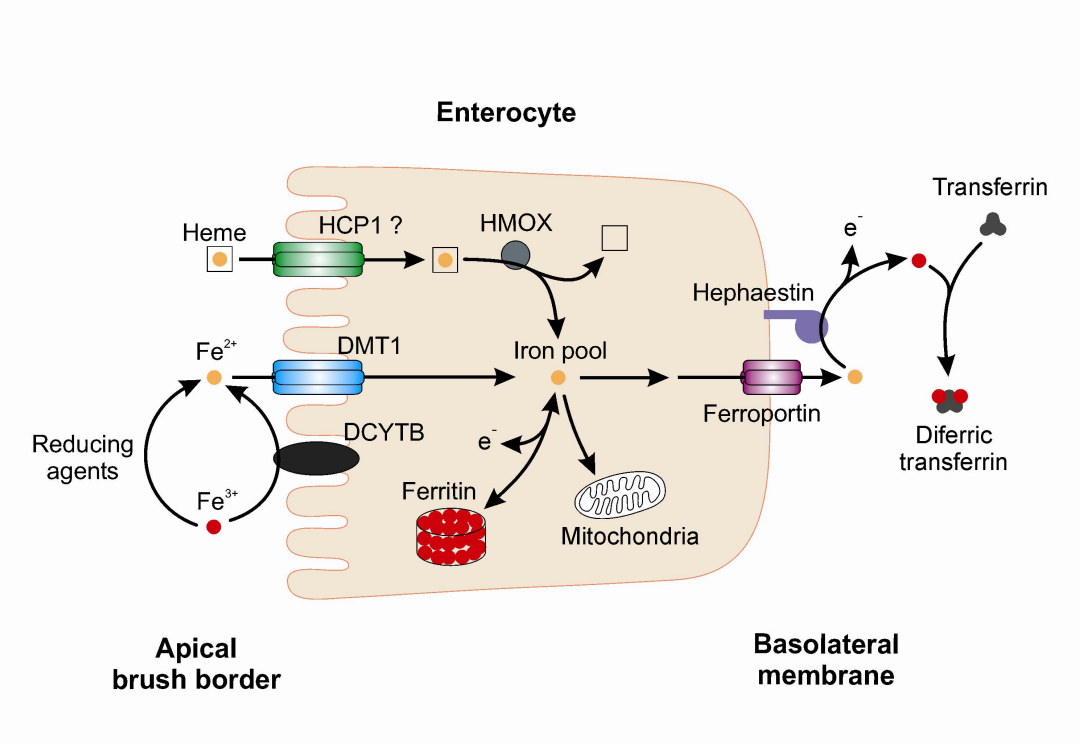

Figure 2. *The cellular mechanisms involved in iron absorption. Adapted from (Sharp and Srai 2007).*

There is also a proposed pathway for the absorption of ferric iron, called the integrin-mobilferrin pathway (IMP) (Conrad et al. 2000). The proteins involved in this pathway are mobilferrin and a β3-integrin, which associate with each other and bind ferric iron that can then enter the cell. Once in the cytosol, this protein-iron complex combines with flavin monooxygenase and β2-microglobulin. The resulting macromolecular complex is called paraferritin and has ferrireductase activity (Umbreit et al. 1996). It has been observed that DMT1 is also a component of this complex (Umbreit et al. 2002). Paraferritin may reduce the ferric iron and transport it into intracellular organelles, such as mitochondria, for the synthesis of iron-containing proteins (Conrad and Umbreit 2002).

Ferritin (section 2.2.2) is present in the diet in low concentrations, and is derived from animal and vegetal sources. Evidence indicates that ferritin-bound iron is well absorbed by intestinal enterocytes via what seems to be a mechanism unlike that of non-heme iron (Davila-Hicks et al. 2004). The kinetics of ferritin binding to human

colonic adenocarcinoma Caco-2 cells are characteristic of a receptor-mediated process (Lonnerdal 2007). However, the receptor has not been identified yet.

Lactoferrin is an iron-binding protein that is extremely abundant in human milk. It is believed to be the principal source of iron in infants and may also be an important source in adult females (Lonnerdal and Bryant 2006). Accordingly, fetal enterocytes express a receptor for lactoferrin (Kawakami and Lonnerdal 1991).

Heme iron is more efficiently absorbed than inorganic iron because it is soluble at the pH of the duodenal lumen and its absorption is not influenced by dietary components (Conrad et al. 1967). Prior to absorption, the heme in hemoglobin is released from the globin protein by proteolytic activity in the gastric and intestinal lumen. Heme iron is transported inside the enterocytes mediated by a specific heme transporter. Heme carrier protein 1 (HCP1), a protein that seems to also act as a folate transporter, is possibly this long sought after molecule, although this issue is still controversial (Laftah et al. 2008, Latunde-Dada et al. 2006, Qiu et al. 2006, Shayeghi et al. 2005) (Figure 2). Following absorption, iron is excised from the protoporphyrin ring by the action of heme oxygenases. Two isoforms of this enzyme, heme oxygenase 1 and 2 (HMOX1 and HMOX2), are present in the enterocyte and the specific isoform involved in the catabolism of dietary heme has not been established with certitude yet (West and Oates 2008). The released ferrous iron enters a common intracellular pool along with the iron absorbed via the non-heme iron pathways (Figure 2).

2.1.2.2 Iron export to plasma

The cytosolic iron in intestinal enterocytes has at least two possible fates. Part of it will stay inside the cell to be used or stored. This iron will be lost with the enterocyte when it senesces and is sloughed into the gut lumen. The other iron pool will be exported through the basolateral membrane of the enterocyte and only this iron is considered truly absorbed. The mechanism by which iron is translocated from the apical pole of enterocytes to the basolateral membrane is poorly understood. In this regard, several studies suggest that the process is mediated by transcytosis, with a crucial role of apotransferrin (apo-TF, the iron-free form of

transferrin) and involvement of DMT1 (Alvarez-Hernandez et al. 1998, Ma et al. 2002, Nunez and Tapia 1999).

Export of iron from enterocytes is mediated by ferroportin (also known as IREG1, MTP1, SLC39A1 and now SLC40A1) (Figure 2), the only known iron exporter molecule (Abboud and Haile 2000, Donovan et al. 2000, McKie et al. 2000). Ferroportin has a predicted mass of 67 kDa, contains 12 putative transmembrane domains (Liu et al. 2005) and seems to function as a dimer (De Domenico et al. 2007c). The species of iron transported by ferroportin is thought to be Fe^{2+}, whereas transferrin (TF) binds only Fe^{3+}. Therefore, iron oxidation is required for iron export, and in the intestine it is catalyzed by a membrane-bound multicopper ferroxidase, hephaestin, a basolateral membrane protein that is highly expressed in enterocytes (Figure 2) (Kuo et al. 2004, Vulpe et al. 1999). Ceruloplasmin, a serum protein homologous to hephaestin, also seems to participate in the export of iron from enterocytes under stress conditions (Cherukuri et al. 2005). It was long thought that the only functional meaning of iron oxidation upon export was to allow its uptake by serum TF. Instead, recent data shows that ferroxidase activity is necessary to maintain the cell surface localization of ferroportin (De Domenico et al. 2007a).

2.1.3 The transferrin iron pool

Transferrin transports iron in the blood stream between sites of absorption, storage and utilization (Hentze et al. 2004). Normally, the majority of the non-heme iron in circulation is bound to TF and non-transferrin bound iron (NTBI) is very scarce. In spite of this fact, only about 30% of the iron-binding sites in TF are occupied, meaning that most of the protein is free of iron. The high iron-binding affinity of TF and the presence of a high concentration of apo-TF ensure that when iron enters plasma it is rapidly chelated by apo-TF, preventing iron toxicity. Iron bound to TF is less than 0.1% (~3 mg) of total body iron (Figure 1). However, it represents the most dynamic iron pool in the body, with the highest rate of turnover, and it is the major iron source for most cell types, with the exception of macrophages and absorptive enterocytes. The turnover of TF iron is approximately 30 mg/d and about 80% of this iron (around 25 mg/day in humans) is transported to the bone marrow in

humans and also to the spleen in rodents for hemoglobin synthesis in developing erythroid cells. Reticulocytes are released from these sites into the circulation, where they develop into mature erythrocytes in about 24 h and subsequently circulate in the blood stream for approximately 120 days (in humans).

Transferrin is a ~80 kDa plasma glycoprotein expressed in the liver, retina, testis and brain. In the liver, it is synthesized predominantly by hepatocytes (Beutler et al. 2000). Cell types expressing TF include testicular Sertoli cells, ependymal cells, and oligodendroglial cells (Gomme et al. 2005). It contains two specific high-affinity binding sites ($K_d = 10^{-23}$ M) for Fe^{3+} (Surgenor et al. 1949). The affinity of TF for iron is extremely high at the physiological blood pH (7.4), but it decreases progressively with lower pH. This pH-dependence of iron binding has important physiological implications, such as in the trasferrin cycle (section 2.2.1.1).

2.1.4 Iron recycling

Senescent erythrocytes are phagocytosed by macrophages of the reticuloendothelial system in the liver and spleen (Figure 1) (Brittenham 1994). Inside the macrophages, erythrocytes are degraded in lysosomes and the heme moiety is split from hemoglobin and catabolized by the enzyme HMOX1 (Poss and Tonegawa 1997). The iron released is translocated to the macrophage cytosol, where it can be stored in ferritin or exported by ferroportin. The ferroxidase activity of ceruloplasmin facilitates the movement of iron across the cellular membranes of macrophages (Sarkar et al. 2003) and allows its incorporation back to plasma TF. The heme can also be exported directly into the circulation via the heme exporter feline leukemia virus subgroup C receptor (FLVCR) on macrophage plasma membranes (Keel et al. 2008) (The mechanisms of iron export from other cell types are described in section 2.2.3). Through the hemoglobin-haptoglobin receptor CD163, macrophages take up extracellular hemoglobin as well, which is essential to prevent oxidative toxicity (Kristiansen et al. 2001, Schaer et al. 2007). Recycling of iron from senescent erythrocytes in macrophages constitutes the major iron supply for hemoglobin synthesis. Furthermore, it occurs at a rate that normally matches the needs of iron transport for erythropoiesis.

2.2 Cellular iron metabolism

2.2.1 Cellular acquisition of iron

Cells need iron for many important metabolic functions and they have evolved mechanisms to obtain it from plasma. Under normal conditions, the vast majority of iron in serum is bound to TF and NTBI is very scarce. Thus, cellular acquisition of iron is normally mediated by TF. The main process by which the uptake of TF-bound iron from plasma to cells is mediated is the transferrin-transferrin receptor 1 (TF-TFR1) complex in the so-called transferrin cycle.

2.2.1.1 The transferrin cycle

The TF-Fe^{3+} complex in plasma is transported into cells through receptor-mediated endocytosis by TFR1 (Figure 3) (Ponka and Lok 1999). At the cell surface pH (7.4), TFR1 binds iron-bearing TF, either monoferric or diferric, with higher affinity than apo-TF. This prevents competition of iron-free TF, which is the predominant form in plasma under normal conditions. TF-receptor complexes cluster into clathrin-coated pits. Subsequently, the pit matures and internalizes into an endocytic vesicle, an endosome, aided by an adaptor protein complex called AP-2 (Conner and Schmid 2003). The proton pumps present in the endosomal membrane transport H^+ ions inside the endosome through a temperature- and energy-dependent process. The result is acidification of the endosome, which facilitates the release of iron from TF (Morgan 1981, van Renswoude et al. 1982). Endosomal Fe^{3+} is then reduced by the ferrireductase STEAP3 (Ohgami et al. 2005, Ohgami et al. 2006). After that, Fe^{2+} is transported through the endosomal membrane by DMT1 (Fleming et al. 1998). The protons needed for iron cotransport by DMT1 are provided by the acidic pH inside the endosome. This also keeps apo-TF and TFR bound to each other until the complex returns by exocytosis to the cell surface. In the more neutral pH of the cell surface iron-free TF is released from the receptor and is then ready to bind iron and initiate a new round of the transferrin cycle (Figure 3).

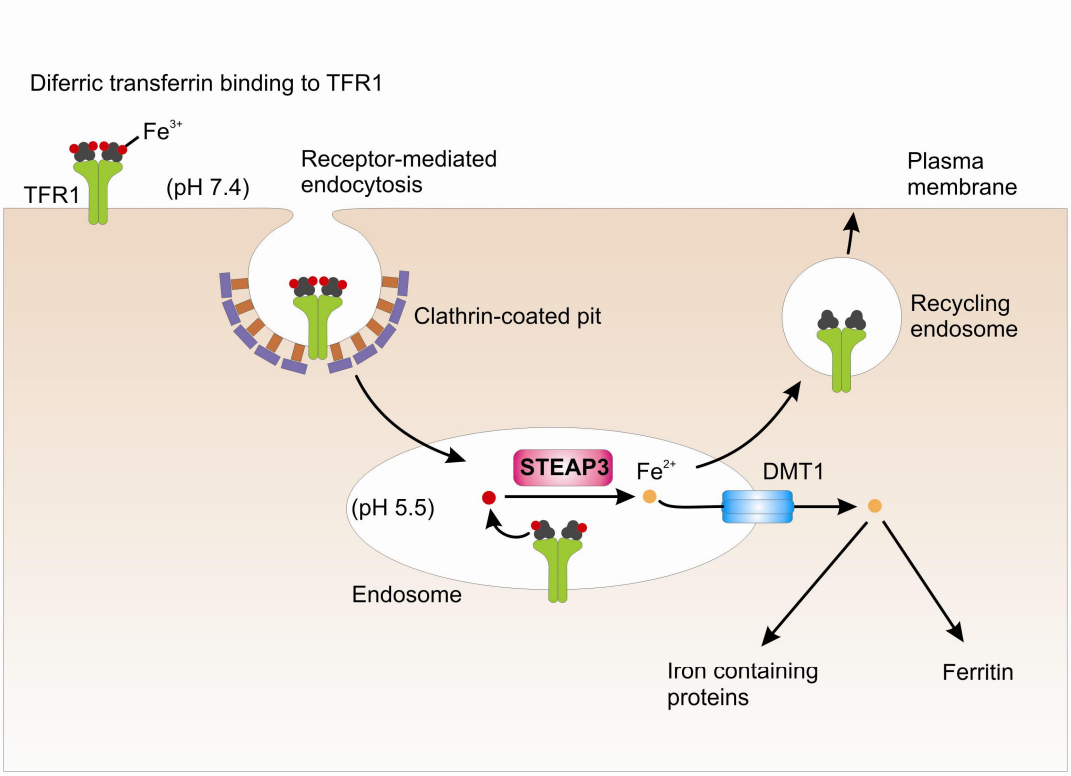

Figure 3. *The transferrin cycle. Endocytosis of the complex of iron, TF and TFR1 through a clathrin-coated pit and exocytosis of the TF-TFR1 complex by a recycling endosome. The export of iron from the endosome and the fates of iron once in the cytoplasm are also depicted. Adapted from (De Domenico et al. 2008).*

2.2.1.2 Other means of transferrin-iron uptake

A second transferrin receptor, TFR2, is also capable of mediating the internalization and recycling of transferrin and the delivery of iron to cells by a mechanism similar to that described for TFR1 (Graham et al. 2008, Kawabata et al. 1999). However, in comparison with TFR1, TFR2 seems to play a minor role in mediating cellular iron uptake. Specifically, data indicate that *in vivo* TFR2 accounts for only about 20% of total TF-bound iron uptake by the liver (Drake et al. 2007).

Studies performed by disruption of genes in specific cell types have shown that TFR1 is required for differentiation only in erythroid precursors, early lymphoid cells and neuroepithelial cells (Levy et al. 1999a). Similarly, DMT1 is the principal means of plasma iron supply only for erythroid precursors, while most other cell types do not seem to require DMT1 for iron uptake (Gunshin et al. 2005). These data suggest that the TF cycle is not an indispensable pathway for iron acquisition in every cell type and hints at the existence of other transmembrane iron importers.

Candidate additional mechanisms for TF-iron uptake have been discovered. Polarized epithelial cells of the kidney uptake TF-bound iron through megalin-dependent, cubilin-mediated endocytosis (Kozyraki et al. 2001). This may provide the major iron supply for renal proximal tubules. An additional recently discovered candidate is glyceraldehyde-3-phosphate dehydrogenase (GAPDH). According to recent data, GAPDH acts as a receptor for TF in macrophages and mediates iron uptake by these cells in a process that involves endosomal internalization of the GAPDH-TF complex (Raje et al. 2007).

2.2.1.3 Uptake of non-transferrin-bound iron

When serum iron levels exceed the binding capacity of TF, such as in iron overload, NTBI levels in the serum increase. NTBI consists of iron bound with low affinity to molecules other than TF, with the major component identified as ferric citrate (Grootveld et al. 1989). It is believed that under iron overload conditions, cellular mechanisms of NTBI uptake become particularly important, accounting for the continued uptake of iron, particularly by hepatocytes, as reviewed by Breuer and colleagues (Breuer et al. 2000). Cellular uptake of NTBI has also been demonstrated in cultured human and rat hepatocytes, K562 (human erythromyeloblastoid leukemia) cells and HeLa (human cervical adenocarcinoma) cells (Barisani et al. 1995, Inman et al. 1994, Parkes et al. 1995, Sturrock et al. 1990).

Several molecules have been proposed as mediators of NTBI uptake, including L-type calcium channels in cardiac cells (Oudit et al. 2003, Oudit et al. 2006), ZIP14 (SLC39A14) in hepatocytes (Liuzzi et al. 2006) and the transient receptor potential cation channel 6 (TRPC6) in neuronal cells (Mwanjewe and Grover 2004). Hepatocytes are also capable of taking up heme iron via the heme-hemopexin receptor, CD91 (Hvidberg et al. 2005). Hemopexin was thought to be recycled back to the circulation, like transferrin (Smith and Hunt 1990, Smith and Morgan 1978, Smith and Morgan 1979). However, this has been questioned by recent evidence showing that hemopexin is degraded in lysosomes (Hvidberg et al. 2005).

2.2.2 Cellular iron storage

The primary site for iron storage in the organism is the liver. Hepatocytes are capable of storing large quantities of iron in ferritin, a heteropolymer of 24 subunits of H- (heavy or heart) and L- (light or liver) types, which can hold up to 4500 iron atoms (Harrison et al. 1967). Ferritin is an exceptional enzyme in that it stores its substrate after acting upon it (Munro 1986). Expression of ferroportin induces mobilization of ferritin iron and results in ferritin degradation by the proteasome (De Domenico et al. 2006b). Therefore, iron storage in ferritin is an alternative pathway that takes place only in the absence of cellular iron export. The majority of ferritin is stored within cells and only a small proportion is glycosylated and released into serum. The biological role of serum ferritin is not known. Although there is a receptor for ferritin in B cells, as well as liver and kidney tissue, its physiologic function has not been well defined (Chen et al. 2005). In addition to ferritin, hepatocytes can also store iron as hemosiderin, a heterogeneous aggregate composed of products of ferritin breakdown and intracellular digestion (Wixom et al. 1980).

2.2.3 Cellular iron export

Iron is exported from cells by ferroportin, located in the cellular membranes of cells capable of regulated iron export, such as enterocytes (Figure 2), reticuloendothelial macrophages, hepatocytes and placental cells (Abboud and Haile 2000). A study in which the murine ferroportin gene, *Slc40a1*, was inactivated globally and selectively showed that ferroportin is essential for iron export in enterocytes as well as in macrophages and hepatocytes (Donovan et al. 2005). Ceruloplasmin, the secreted homolog of hephaestin, is a ferroxidase expressed in hepatocytes and macrophages and aids iron export mainly from these cell types (Harris et al. 1995, Roeser et al. 1970, Sarkar et al. 2003). It has been shown that there is also a glycosylphosphatidylinositol (GPI)-linked form of ceruloplasmin in brain cells and in macrophages (De Domenico et al. 2007a, Jeong and David 2003).

Cells such as immature erythrocytes, macrophages and hepatocytes are capable of exporting not only iron ions, but also excess heme. FLVCR is a critical player in this process (Keel et al. 2008).

2.3 Regulation of iron homeostasis

Every cell in the organism must control its gains, losses and storage of iron to prevent the generation of free iron and its toxic consequences. Cellular iron homeostasis seems to be principally determined by the intracellular concentration of iron. At a systemic level, iron homeostasis is achieved and maintained through an adequate rate of absorption and an appropriate distribution of iron in various body compartments. Iron efflux from duodenal enterocytes, hepatocytes and macrophages seems to be the key control point for systemic iron homeostasis and it is modulated according to a number of systemic signals. These two levels of iron homeostasis are discussed in the present section.

2.3.1 Regulation of cellular iron homeostasis

Cellular iron homeostasis is maintained by appropriate expression of proteins involved in iron uptake, storage, utilization and export. Regulation of the expression of these proteins may be exerted on transcription, mRNA stability, translation or posttranslationally. The posttranscriptional regulation of gene expression mediated by the iron-responsive element/iron regulatory protein (IRE/IRP) system, is the best characterized and appears to be crucial for iron homeostasis (Hentze et al. 2004, Muckenthaler et al. 2008). The *trans*-acting iron regulatory proteins 1 and 2 (IRP1 and IRP2) recognize the *cis*-regulatory iron-responsive elements (IREs), stem-loop structures that are found in the untranslated regions (UTRs) of mRNAs encoding iron-related proteins. There are single IREs in the 5' UTRs of mRNAs encoding ferritin H and L chains, erythroid 5-aminolevulinic acid synthase (the first enzyme in the process of heme synthesis), mitochondrial aconitase (an enzyme of the citrate cycle), and ferroportin. The 3' UTR of TFR1 mRNA presents multiple IREs and a single IRE is found in the 3' UTR of a DMT1 isoform.

Binding of IRPs to IREs located in the 5′-UTRs of mRNAs, inhibits translation (Muckenthaler et al. 1998), whereas binding in the 3′-UTRs of TFR1 stabilizes the mRNA and prevents its degradation (Hentze and Kuhn 1996). In the case of DMT1 transcripts, however, the precise molecular mechanisms of regulation by IRPs remain to be determined, although there is evidence suggesting that it is a positive form of regulation (Galy et al. 2008).

The IRE-binding activity of IRPs is modulated in response to the intracellular labile iron pool (Hentze and Kuhn 1996). Under iron-replete conditions, IRP1 incorporates an iron-sulfur cluster and is converted into a cytoplasmic aconitase, losing its IRE-binding ability. Conversely, when iron levels are low, IRP1 binds to target IREs. The functional significance of the aconitase activity in IRP1 is not known. The IRE-binding activity of IRP2 is regulated by a different mechanism than IRP1. IRP2 accumulates in iron-deficient cells, whereas high cellular iron stores induce IRP2 ubiquitination and proteasomal degradation. Other effectors regulating the IRE-binding activity of IRPs are reactive oxygen species, nitric oxide and hypoxia (Hentze et al. 2004).

The importance of IRPs *in vivo* has been demonstrated in mice, where the double knockout of *Irp1* and *Irp2* is embryonic lethal (Smith et al. 2006). Additionally, the double knockout of these genes in the intestine results in the death of intestinal epithelial cells, presumably by iron depletion (Galy et al. 2008). One example of the functionality of the IRP-IRE system is the "mucosal block", a phenomenon by which, shortly after exposure to a large dose of iron, enterocytes become refractory to absorbing more iron (Crosby 1966). Interestingly, in rat enterocytes, the ingestion of high iron-containing food causes increased cellular iron content and reduced mRNA levels of Dmt1 and Dcytb (Frazer et al. 2003).

2.3.2 Regulation of systemic iron homeostasis

At a systemic level, iron transfers are regulated according to various physiological stimuli. When iron stores are high, iron transport into plasma is decreased. The same response follows inflammation. Increased erythropoiesis and hypoxia elicit an increase in iron absorption. The iron hormone hepcidin seems to be a pivotal mediator behind these homeostatic mechanisms.

2.3.2.1 Hepcidin, a negative regulator of iron transport

Hepcidin was first identified as an antimicrobial peptide in human blood ultrafiltrate (Krause et al. 2000) and urine (Park et al. 2001). The mature form is a 25-amino acid long peptide, which results from the processing of an 84-amino acid

long prepropeptide (Park et al. 2001, Pigeon et al. 2001). Hepcidin contains eight cysteine residues forming four intrachain disulfide bonds (Nicolas et al. 2001, Park et al. 2001, Pigeon et al. 2001). The hepcidin gene (*HAMP*) is strongly expressed in the liver and to a much lesser extent in the heart and brain (Park et al. 2001, Pigeon et al. 2001). Humans have one hepcidin gene (*HAMP*), while mice possess two (*Hamp1* and *Hamp2*) (Nicolas et al. 2001, Pigeon et al. 2001). The two mouse hepcidin genes have similar genomic organization and the expression of both is induced by enteral and parenteral iron overload in mice (Ilyin et al. 2003). However, it seems that only hepcidin1, but not hepcidin2, has a key role in the regulation of body iron levels (Lou et al. 2004).

The link between hepcidin and iron metabolism was established early after its discovery, when hepcidin was found to be upregulated in the liver of iron overloaded mice (Pigeon et al. 2001). Furthermore, a contemporary study using upstream stimulatory factor 2 (*Usf2*) knockout mice showed that lack of hepcidin causes hepatic iron overload and iron depletion in the reticuloendothelial system (Nicolas et al. 2001). Thereafter, the relationship between hepcidin and iron pathophysiology has been explored through a number of experiments and clinical observations. Hepcidin-deficient mice develop severe iron overload (Lesbordes-Brion et al. 2006), while mice overexpressing hepcidin present with serious iron refractory anemia (Nicolas et al. 2002a, Roy et al. 2007). Moreover, mutations in the *HAMP* gene were identified in families with grave juvenile hemochromatosis (Roetto et al. 2003) while hepatic adenomas overexpressing hepcidin were described in patients with severe iron refractory anemia. Most interestingly, the anemia was resolved upon removal of the tumor (Weinstein et al. 2002).

Hepcidin binds cell-surface ferroportin, triggering its tyrosine phosphorylation, internalization and ubiquitin-mediated degradation in lysosomes (De Domenico et al. 2007b, Nemeth et al. 2004b). This explains how hepcidin regulates iron metabolism at the systemic level. By removing ferroportin from the plasma membrane, hepcidin blocks iron absorption from the intestine, iron recycling from macrophages and mobilization of stored iron from hepatocytes. The outcome is decreased levels of serum iron.

2.3.2.2 *Regulation of hepcidin expression*

The expression of hepcidin is regulated by the same physiological factors that modulate iron homeostasis. In addition to the previously mentioned induction by iron overload, an iron deficient diet causes decreased hepcidin expression in the liver of rats (Frazer et al. 2002) and mice (Nicolas et al. 2002b). Transcription of hepcidin in hepatocytes is repressed in response to hypoxia and ineffective erythropoiesis (Adamsky et al. 2004, Nicolas et al. 2002b) but is induced in response to treatment with lipopolysaccharide and inflammation of other etiologies (Nicolas et al. 2002b, Pigeon et al. 2001).

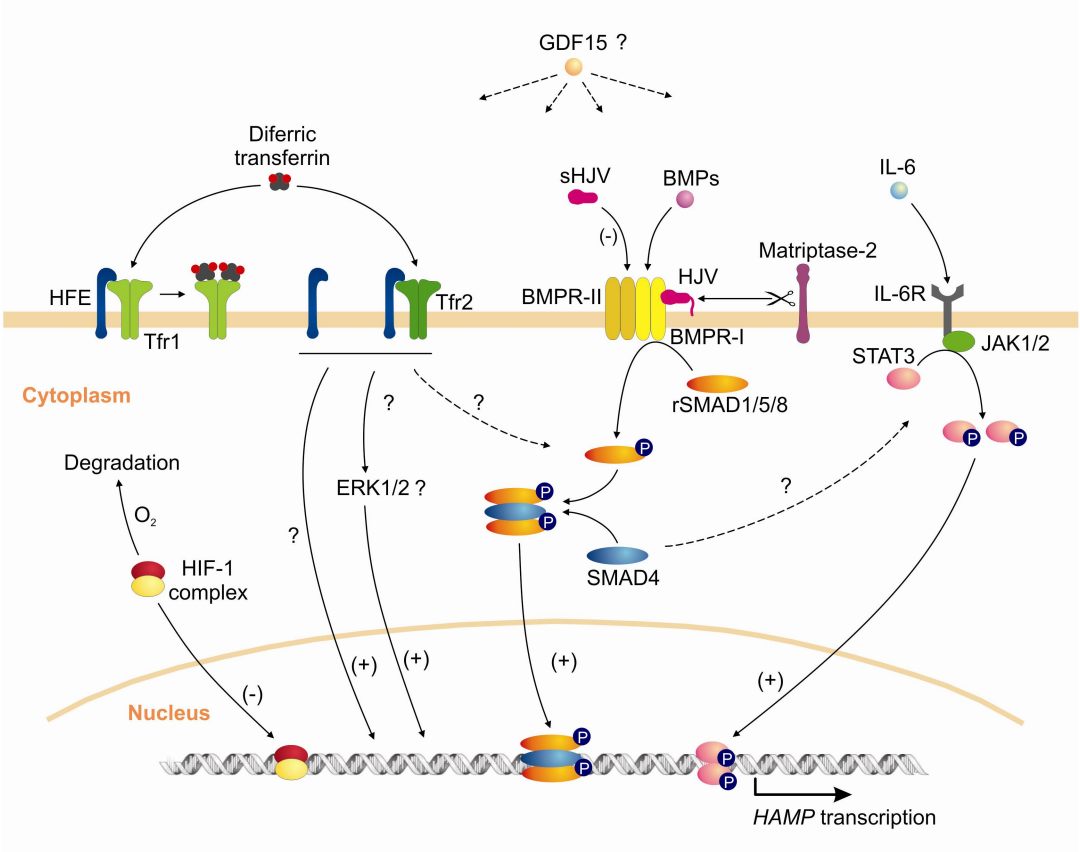

Figure 4. *Regulation of hepatic hepcidin expression. The solid lines indicate known pathways, whereas broken lines and interrogation marks indicate pathways where the links have yet to be proven or where information is incomplete. Adapted from (Darshan and Anderson 2009).*

The modulation of hepatic expression of hepcidin is pivotal in the regulation of systemic iron metabolism. At the molecular level, several pathways are known that regulate hepcidin transcription (Figure 4). The involvement of HFE, HJV and TFR2 in hepcidin regulation was elucidated through the study of the hereditary disorder of

iron overload hemochromatosis, and it is discussed in sections 2.4.2.1-3. It has been well documented that bone morphogenetic protein (BMP) treatment is a strong stimulus of hepcidin expression in both cell culture (Babitt et al. 2006, Babitt et al. 2007, Truksa et al. 2006, Wang et al. 2005) and animal models (Babitt et al. 2007). Indeed, the BMP/SMAD (son of mother against decapentaplegic) signaling pathway has a chief role in hepcidin regulation (Figure 4). BMPs are a subfamily of cytokines that belong to the transforming growth factor-β (TGF-β) superfamily. The interaction of specific BMPs with BMP receptors (BMPR-I and BMPR-II) in the cell membrane of hepatocytes triggers phosphorylation of receptor-activated SMADs (rSMADs) (SMAD1, SMAD5 and SMAD8) in the cytosol. Once phosphorylated, rSMADs form heterodimeric complexes with SMAD4, the central mediator of TGF-β/SMAD signaling. The resulting complex translocates into the nucleus where it activates *HAMP* transcription. The fact that liver-specific disruption of *Smad4* in mice results in reduced transcription of *hamp* and severe iron accumulation in the liver and other organs (Wang et al. 2005) offers support for the role of the BMP/SMAD pathway in the regulation of hepcidin expression. The consensus sites for SMAD binding are very variable and thus difficult to find in the promoters of genes by sequence analysis alone. Although it is likely that activated SMADs bind directly to the hepcidin promoter, a binding site has not been localized yet. In contrast, putative BMP-responsive elements have been identified in the promoter of *hamp* (Truksa et al. 2006).

A second pathway for transcriptional regulation of hepcidin is activated during inflammatory conditions by interleukin-6 (IL-6) (Nemeth et al. 2004a). Binding of signal transducer and activator of transcription-3 (STAT3) to a consensus STAT3 binding site in the *HAMP* gene promoter activates its transcription (Figure 2) (Verga Falzacappa et al. 2007, Wrighting and Andrews 2006). Growing evidence shows that the BMP/SMAD pathway and the JAK/STAT pathway converge at some point and that a fully functional BMP/SMAD pathway is required for the hepcidin response to inflammation through the JAK/STAT pathway (Wang et al. 2005, Verga Falzacappa et al. 2008, Yu et al. 2008). It is believed that the purpose of activating hepcidin synthesis in response to inflammation is to reduce iron availability in plasma, since it is an essential nutrient for pathogens.

Regulation of *HAMP* transcription by hypoxia is mediated by hypoxia-inducible transcription factors (HIFs) (Peyssonnaux et al. 2007). The promoter of the *HAMP*

gene contains a HIF-binding site, allowing HIF1α to bind to the promoter and repress *HAMP* transcription. In the absence of oxygen, HIF1α is stabilized and hepcidin expression is maintained in a repressed state (Figure 4). The same scenario occurs in the absence of iron, supposedly because low iron results in limited red blood cell production, which in turn leads to increased hypoxia.

A cytokine member of the TGF-β superfamily, the growth differentiation factor-15 (GDF15), might be the long sought after erythroid regulator of iron acquisition. GDF15 negatively regulates hepcidin expression *in vitro* and its transcription is increased in erythroblasts during maturation (Tanno et al. 2007). Hence, in the event of stimulation of erythropoiesis, the expansion of the erythroid compartment would lead to enhanced expression of GDF15 and decreased hepcidin levels.

The most recent addition to the puzzle of hepcidin regulation is the membrane-bound serine protease matriptase-2 (TMPRSS6). Negative regulation of hepcidin expression by matriptase-2 has been evidenced (Du et al. 2008, Folgueras et al. 2008). Moreover, Silvestri and co-workers have shown that this negative regulation is mediated by proteolysis of membrane bound hemojuvelin (Figure 4) (Silvestri et al. 2008b).

There are potential binding sites for other widely expressed transcription factors in the *HAMP* promoter, such as C/EBPα, USF2, HNF4α and p53, but their functionality *in vivo* is unknown (Bayele et al. 2006, Courselaud et al. 2002, Weizer-Stern et al. 2007).

2.4 Iron overload

2.4.1 General

The inability to adequately repress iron absorption in response to increased iron stores results in a situation in which the amount of iron in the plasma exceeds the binding capacity of transferrin. This state is known as iron overload. Its original cause can be excessive iron intake, a genetic defect or repeated blood transfusions. In any case, NTBI appears and is taken by cells through transferrin-independent processes. Consequently, iron accumulates in parenchymal tissues and leads to

tissue damage and fibrosis. Iron-overload diseases owing to genetic defects are referred to as primary iron-overload disease or HH.

2.4.2 Hereditary hemochromatosis

HH is a disorder of iron overload in which increased intestinal absorption of iron results in deposition of the metal, primarily in the liver, heart and pancreas and leads to cell injury and organ failure (Fleming and Sly 2002). The most common consequences of iron accumulation are hepatic fibrosis, cirrhosis, hepatocellular carcinoma, diabetes, cardiomyopathy, hypogonadism, and arthritis (Parkkila et al. 2001). Phlebotomy is an inexpensive and safe treatment for iron overload. If initiated at an early stage, this treatment is effective for preventing the symptoms of HH and providing a normal life expectancy to the patient. If left untreated, however, HH can be lethal (Adams et al. 2000).

Table 1. *Genetic defects in Hereditary Hemochromatosis.*

HH type	Protein (Gene)	Inheritance	Protein function	References
HH type **I**	HFE (*HFE*)	Autosomal recessive	Regulates hepcidin expression, mechanism uncertain; interacts with TFR1 and TFR2; may participate in a signaling complex with TFR2	Feder *et al*. 1996
HH type **II**/ Juvenile H	Hepcidin (*HAMP*)	Autosomal recessive	Iron regulatory hormone, binds ferroportin to cause its inactivation and degradation	Roetto *et al*. 2003 Lee *et al*. 2004
HH type **II**/ Juvenile H	Hemojuvelin (*HJV*)	Autosomal recessive	Bone morphogenetic protein coreceptor	Papanikolaou *et al*. 2004
HH type **III**	Transferrin receptor-2 (*TFR2*)	Autosomal recessive	Sensor for diferric transferrin; regulates hepcidin expression; may participate in a signaling complex with HFE	Camaschella *et al*. 2000
HH type **IV**/ Ferroportin disease	Ferroportin (*SLC40A1*)	Autosomal dominant	Transmembrane iron transporter (exporter)	Montosi *et al*. 2001 Njajou *et al*. 2001

HH is classified into 4 different types according to the genetic background and the severity of the symptoms (Table 1). So far, mutations in 5 genes have been identified in HH patients. Defects in *HFE*, *HAMP*, *HJV* and *TFR2* are recessive and are all characterized by inadequate production of hepcidin relative to body iron stores (Bridle et al. 2003, Nemeth et al. 2005, Papanikolaou et al. 2004, Roetto et al. 2003). Mutations in a fifth gene, *SLC40A1*, cause a dominant trait and do not affect

hepcidin expression, but rather cause hemochromatosis by rendering ferroportin insensitive to hepcidin regulation (De Domenico et al. 2006a).

2.4.2.1 HH type 1: mutated HFE

The gene mutated in the majority of cases of HH is the human hemochromatosis gene, *HFE*. The mutation most frequently found converts cysteine to tyrosine in location 282 of the HFE protein (C282Y mutation) (Feder et al. 1996). In the United States, the carrier frequency of this mutation is approximately 1 in 9 for Northern European descendants. In Northern Europeans, frequency of homozygosity has been estimated to be about 1:200 (Adams et al. 2005, Olynyk et al. 1999). There seems to be a considerable individual variation among the homozygous patients in the age of onset, the severity of clinical features, the pace of iron accumulation in the liver, and the response to phlebotomy. Hence, no consensus has been reached about the penetrance of this mutation and estimates range from 1:400 to 1:10,000 individuals developing the disease (Allen et al. 2008). According to a population-based study conducted in Busselton, Australia, the penetrance is 50% (Olynyk et al. 1999). A similar study in the United States reported increased total body iron in over 50% of homozygous individuals, but clinical penetrance of about 1% (Beutler et al. 2002). However, it is clear that penetrance is much higher in men than it is in women (Allen et al. 2008). In mice, on the contrary, the disease-associated mutations in *Hfe* do always cause the iron overload phenotype of HH (Andrews 2000). There are two major physiological characteristics of HH: Patients have an increased rate of mucosal iron transfer into plasma (McLaren et al. 1991) and their macrophages show an enhanced capacity to purge themselves of iron (Fillet et al. 1989, McLaren et al. 1991).

HFE (originally *HLA-H*) encodes an atypical major histocompatibility complex (MHC) class I protein. The HFE protein is present in the small and large intestine, stomach, esophagus, biliary tract, and liver (Parkkila et al. 2001). There is controversy about the expression of HFE in the liver. Some results show expression in Kupffer cells and endothelial cells (Bastin et al. 1998), whereas others evidence HFE mainly in the hepatocytes (Zhang et al. 2004). In the duodenum, HFE is found predominantly in the cryptal enterocytes (Parkkila et al. 1997b). HFE binds β2-

microglobulin (B2M) and this association is essential for membrane targeting of HFE (Feder et al. 1997, Waheed et al. 1997). HFE binds also TFR1 (Parkkila et al. 1997a, Waheed et al. 1999) and TFR2 (Goswami and Andrews 2006). There is an overlap between the binding sites of HFE and TF to TFR1 and the two molecules compete for TFR1 binding (Bennett et al. 2000, Lebron et al. 1998, Lebron et al. 1999). The binding of HFE to soluble TFR1 decreases its affinity for iron-loaded TF (Fe-TF) (Feder et al. 1998, Lebron et al. 1999). However, it has been shown that HFE binds to TFR1 with lower affinity than does Fe-TF (Giannetti and Bjorkman 2004), thus Fe-TF can displace HFE from TFR1.

The C282Y mutation in the HFE protein eliminates its ability to bind B2M and prevents the cell surface expression of HFE (Feder et al. 1997, Waheed et al. 1997). *B2m* knockout mice develop similar iron overload than *Hfe* knockout mice do (de Sousa et al. 1994, Santos et al. 1996), evidencing the importance of the association between Hfe and B2m for normal iron homeostasis. Likewise, the capability of HFE to associate with TFR1 is considerably reduced in these mutant HFE proteins, thus allowing high affinity binding of TF to the uncomplexed TFR1 (Feder et al. 1998). In addition, a second missense mutation, histidine 63 to aspartate (H63D), is enriched among C282Y heterozygotes (Beutler et al. 1996, Feder et al. 1996). However, the H63D mutation does not alter either the interaction with B2M or the surface expression of the protein in COS-7 cells (Waheed et al. 1997). Although H63D mutant HFE binds normally to TFR1, this association does not affect the affinity of the interaction of trasferrin and its receptor TFR1 (Feder et al. 1998).

It is obvious that HFE plays an important role in monitoring the status of iron in the body. However, there is still controversy about the how and where. Two main hypotheses are considered in this regard. The “crypt program” hypothesis (Waheed et al. 1999) suggests that iron absorption by mature intestinal absorptive enterocytes is regulated by programming of the immature enterocytes located in the crypts of Lieberkuhn. Programming would involve interaction of HFE and TFR1 and body iron sensing by TFR1-mediated Fe-TF uptake in the crypt enterocytes. Expression of iron transporters in the absorptive enterocytes would be determined by the amount of Fe-TF taken up by the cell before it reached the crypt-villus junction. There are controversial data on whether HFE has a role of physiological importance in iron homeostasis in the duodenum or not (Oates 2007). The disruption of *Hfe* leads to a reduction in the Fe-Tf uptake in the duodenum that is independent of

plasma iron levels (Trinder et al. 2002). By contrast, the specific deletion of *Hfe* in enterocytes has no effect on iron homeostasis (Vujic Spasic et al. 2007). On the other hand, the specific overexpression of *Hfe* in enterocytes has been shown to induce body iron overload (Fergelot et al. 2002). Certainly, additional experiments are needed to clarify this issue.

Given that hepcidin has inappropriately low expression in the liver of patients with *HFE* mutations and that, in *Hfe* knockout mice, the overexpression of hepcidin prevents hepatic iron overload (Nicolas et al. 2003), it seems clear that dysregulation of hepcidin expression is a key event underlying the development of iron overload in HH patients. Based on this information, the question that naturally follows is how HFE regulates hepcidin expression in the liver. A recent hypothesis maintains that, under conditions of low iron-Tf levels, HFE in the hepatocyte membrane is bound to TFR1. When iron-TF levels increase, this complex binds to the TFR1 binding site and displaces HFE (Figure 4). In turn, HFE somehow exerts a positive effect on hepcidin expression (Schmidt et al. 2008).

2.4.2.2 HH type II or juvenile hemochromatosis: mutated hepcidin and hemojuvelin

Causes of HH that result from mutations in *HJV* and *HAMP* genes are usually called juvenile hemochromatosis (JH) because of the early onset of the disease (Papanikolaou et al. 2004, Roetto et al. 2003). It can cause death even before the age of 30 and seems to affect men and women equally (Camaschella et al. 2002). In contrast to HH, JH patients often present severe cardiac and endocrine complications, rather than hepatic disease (Camaschella 1998).

Hemojuvelin is the protein product of the gene *HJV* (also named *HFE2*), which is strongly expressed mainly in skeletal muscle, the heart and, at lower levels, in the liver (Papanikolaou et al. 2004). HJV is a GPI-bound protein. Homozygous or compound heterozygous mutations in the *HJV* gene result in JH (Papanikolaou et al. 2004). In mice, the disruption of both *Hjv* alleles ($Hjv^{-/-}$) results in a significant increase in the iron content of the liver, pancreas and heart (Huang et al. 2005, Niederkofler et al. 2005). JH patients with mutated *HJV* as well as mice with disruptions of this gene present severely decreased expression of hepcidin,

indicating that HJV plays a crucial role in the regulation of hepatic hepcidin expression.

Given the pivotal role of hepcidin in regulation of iron homeostasis, it is easy to understand the connection between mutated hepcidin and the development of JH. In the case of mutations in HJV, the mechanism is not so straightforward. HJV is a member of the repulsive guidance molecule (RGM) family of proteins that function as BMP co-receptors. HJV increases hepatic hepcidin expression via enhancing the BMP signaling pathway (see section 2.3.2.2 and Figure 4) (Babitt et al. 2006, Babitt et al. 2007). HJV mutants associated with juvenile hemochromatosis are unable to signal through BMP (Babitt et al. 2006).

The HJV protein is synthesized in two forms: a membrane bound heterodimer that results from autocatalytic cleavage and a soluble (sHJV) full-length protein that is processed by the protease furin (Kuninger et al. 2006, Lin et al. 2008, Silvestri et al. 2008a). sHJV also binds to BMP and acts as a competitive antagonist of the hepatocyte membrane-bound HJV, resulting in decreased hepcidin expression (Lin et al. 2005). The shedding of HJV from the cell membrane is a regulated process and it depends on its interaction with neogenin, but seems to be independent of BMP signaling (Zhang et al. 2007) and it is repressed by holo-TF (Zhang et al. 2007). Based on these results, it seems that the generation of soluble HJV might be a link between transferrin saturation and iron acquisition: high levels of holo-TF, by preventing cleavage of HJV, lead to increased hepcidin production, which leads to decreased ferroportin-mediated iron transport.

HJV also binds to neogenin (NEO1) (Zhang et al. 2005), a type I transmembrane receptor that belongs to the N-CAM family of cell adhesion molecules. Diverse functions of NEO1 through interaction with different ligands have been reported, such as the repulsive guidance of retinal axons, the regulation of neuronal survival and a role in myotube formation (Kang et al. 2004, Matsunaga et al. 2004, Monnier et al. 2002). According to some data, the interaction between HJV and NEO1 has implications for intracellular iron homeostasis in cultured HEK293 (human embryonic kidney) cells (Yang et al. 2008, Zhang et al. 2005). Other experiments suggest that NEO1 mediates the shedding of membrane HJV (Zhang et al. 2007). However, a report by Xia and colleagues showed no effect of *NEO1* knockdown or overexpression on HJV-mediated BMP signaling nor on hepcidin expression (Xia et al. 2008). Thus, the role of NEO1 in relation to HJV needs to be explored further.

2.4.2.3 HH type III: mutated TFR2

Mutations in the *TFR2* gene are associated with a rare form of HH, called HH type III (Camaschella et al. 2000, Roetto et al. 2002). The phenotype of these HH patients is indistinguishable from that of those with HFE-related hemochromatosis (Camaschella 2005). The disruption of *Tfr2* in mice (*Tfr2*$^{-/-}$) causes similar iron overload as that seen in the HH patients (Wallace et al. 2007). Patients of HH with mutated *TFR2* and *Tfr2*$^{-/-}$ mice exhibit reduced hepcidin levels (Kawabata et al. 2005, Nemeth et al. 2005).

TFR2 is a homolog of TFR1 that was discovered in 1999 (Kawabata et al. 1999). Like TFR1, TFR2 is a type II membrane glycoprotein with a large C-terminal extracellular domain and a small N-terminal cytoplasmic domain. The binding site for TF is located on the extracellular domain, where TFR1 and TFR2 share 45% amino acid identity. However, there are important differences between these two genes. *TFR1* is expressed in many tissues but very faintly in the liver. In contrast, *TFR2* is abundantly expressed only in the liver, with very weak expression in a few other tissues and is absent in the placenta (Fleming et al. 2000, Kawabata et al. 1999). Additionally, the *TFR2* transcript lacks the IREs found in the 3' UTR of *TFR1*, thus it is not regulated by cellular iron status (Fleming et al. 2000). Furthermore, there are no sequence similarities in their cytoplasmic domains. TFR2 is much less stable than TFR1, which allows much faster changes in the levels of TFR2 (Johnson and Enns 2004, Robb and Wessling-Resnick 2004). The affinity of TFR2 for diferric TF is about 30-fold lower than that of TFR1 (West et al. 2000). Like TFR1, TFR2 forms complexes with HFE (Goswami and Andrews 2006) although the binding site for HFE in the two receptors is not homologous (Chen et al. 2007).

The function of TFR2 in iron metabolism is not clear. However, some observations support a role in controlling the levels of body iron by sensing changes in the plasma concentration of iron-bound TF. Diferric TF stabilizes TFR2 protein by increasing its half-life *in vitro* and *in vivo*, a novel mechanism of regulation at the level of protein degradation (Johnson and Enns 2004, Robb and Wessling-Resnick 2004). This response of TFR2 to diferric TF seems to be exclusive to hepatocytes. Interestingly, a mutant form of TFR2 that does not detectably bind diferric TF does not show the response observed in wild-type TFR2 (Johnson et al. 2007). In the

light of these data, it is tempting to suggest that TFR2 acts as a sensor of body iron that regulates the rate of hepcidin synthesis. High iron conditions would involve higher TFR2 levels in the cell membrane of the hepatocyte and induction of hepcidin expression would be then consistent. The mechanism of the signal transduction involved is unknown, but since ERK1/ERK2 and P38 MAP kinase pathways are activated when Fe-TF binds TFR2 they are possible candidates (Figure 4) (Calzolari et al. 2006).

2.4.2.4 HH type IV: mutated ferroportin

HH due to mutations in the ferroportin gene (*SLC40A1*) is also called ferroportin disease and it presents dominant inheritance (Montosi et al. 2001). Two types of ferroportin mutations with different functional consequences result in different phenotypes (Liu et al. 2005). Mutations that hinder ferroportin targeting to the cell surface or make it unable to transport iron cause iron accumulation in macrophages, low transferrin saturation (normally ranging from 20-30%) and iron-limited erythropoiesis (McGregor et al. 2005). Other ferroportin mutations may cause "resistance" to hepcidin action, leading to constitutive iron export (Drakesmith et al. 2005). These mutations include two types, those that prevent binding to hepcidin and those that impede the internalization of ferroportin after hepcidin binding (De Domenico et al. 2007b). In these cases, patients present a typical HH phenotype. There is a lack of consensus when it comes to explaining the dominant inheritance of ferroportin disease. Some studies propose a dominant-negative effect of the mutant protein on the ferroportin homo-multimer (De Domenico et al. 2007c, De Domenico et al. 2005). In support of this theory, mice heterozygous for a deletion of *Slc40a1* do not exhibit ferroportin disease (Donovan et al. 2005). Contrastingly, other reports indicate that ferroportin is a monomer and the dominant transmission of the disease is due to haploinsufficiency (Goncalves et al. 2006).

2.4.3 Animal models of iron overload

There is a large variety of animal models for the investigation of iron overload. These can be divided into two main groups: those induced genetically and those

generated by delivering exogenous iron. According to the route of iron administration, two main groups may be distinguished from animal models obtained through exogenous iron (Ramm 2000). Enteral or dietary iron overload is achieved by administering carbonyl iron, ferrocene, and ferric ammonium citrate to experimental animals. Parenteral iron overload models involve delivering iron chelates such as iron-dextran, iron-sorbitol, or ferric nitrilotriacetate.

Dietary supplementation with carbonyl iron reproduces the HH pattern of hepatic iron loading, with iron deposition predominantly in parenchyma (Ramm 2000) and that is strongest in the periportal zone (Park et al. 1987). This model has been extensively used, especially in rats, to study the effects of iron loading on many aspects of metabolism. Some studies have shown liver fibrosis in rats exposed to the carbonyl iron diet for long periods (Park et al. 1987, Roberts et al. 1993), whereas others have failed to see this (Asare et al. 2006). There is abundant evidence of lipid peroxidation, specifically microsomal lipid peroxidation, in the liver of these rats (Bacon et al. 1986, Brunet et al. 1999, Houglum et al. 1990, Khan et al. 2002, Masini et al. 1989, Wu et al. 1990). The levels of plasma lipids such as triglycerides, free cholesterol, cholesteryl ester and HDL-cholesterol are increased in this model as well (Brunet et al. 1999). DNA oxidation has been proven by measuring 8-hydroxy-2'-deoxyguanosine (8-OHdG) (Kang et al. 1998). Signs of oxidative stress and protein peroxidation are observed in rats after 6-8 weeks of 3% carbonyl iron diet and, interestingly, these signs decrease by 8-12 weeks (Cornejo et al. 2005).

Mice homozygous for a null allele of *Hfe* (*Hfe*$^{-/-}$) provide a genetic animal model of HH, showing elevated transferrin saturation and liver iron content with a periportal to pericentral gradient (Zhou et al. 1998). However, in contrast to the human disease, these mice do not develop liver fibrosis or cirrhosis. This may be due to the fact that humans are among the few mammals that cannot synthesize ascorbic acid (Chatterjee et al. 1975). The antioxidant activity of ascorbic acid may provide some protection against oxidative damage resulting from iron overload.

Hfe$^{-/-}$ mice and carbonyl iron-fed mice both develop iron overload. In spite of this, a key difference between the two models is that *Hfe*$^{-/-}$ mice lack Hfe protein and therefore have decreased expression of hepcidin (Ahmad et al. 2002, Bridle et al. 2003), whereas mice with dietary iron overload express functional Hfe protein and their hepcidin expression is induced (Pigeon et al. 2001).

3. AIMS OF THE STUDY

The present work was aimed to characterize gene expression changes in response to iron overload in tissues with functional relevance in iron metabolism and in the pathogenesis of iron overload. The underlying hypothesis was that iron overload would significantly alter gene expression in these tissues.

The specific aims of this study were to:

1) Elucidate the expression profiles of hemojuvelin and neogenin, two recently discovered proteins involved in the regulation of hepcidin expression.
2) Characterize gene expression changes in response to dietary iron overload in the murine heart and skeletal muscle.
3) Explore and compare the genome-wide transcriptome response to Hfe protein deficiency and dietary iron overload in murine liver and duodenum.

4. MATERIALS AND METHODS

4.1 Protein expression analyses

4.1.1 Antibody production (**I**)

The rabbit anti-human/mouse hemojuvelin serum was raised by Innovagen AB (Lund, Sweden) against the synthetic peptide (NH2-)SRSERNRRGAITIDTARRLC(-COOH), which was designed based on the predicted amino acid sequences of human and mouse hemojuvelin (amino acids 328-347 and 321-340 from human and murine hemojuvelin molecules, respectively). Thus, anti-hemojuvelin recognizes the protein from both species. The amino acid sequences of human and murine hemojuvelin are available in SwissProt (accession numbers Q6ZVN8 and Q7TQ32, respectively).

4.1.2 Western blotting (**I**)

Western blot analysis was performed to study the expression of hemojuvelin protein in the mouse. Samples of the heart, lung, stomach, duodenum, jejunum, liver, ileum, colon, spleen, kidney, muscle, testis and brain were obtained from adult BALB/c mice. The tissue samples were homogenized in phosphate-buffered saline (PBS) in the presence of protease inhibitors, and approximately 1 mg of protein from each sample was analyzed by sodium dodecyl sulphate-polyacrylamide gel electrophoresis (SDS-PAGE) (NuPAGE 10% Bis-Tris, Invitrogen) under reducing conditions. The separated proteins were transferred electrophoretically from the gel to a polyvinylidine fluoride (PVDF) membrane (Macherey-Nagel, Düren, Germany) in a Novex XCell II blot module (Invitrogen). The membranes were blocked with cow colostral whey (Biotop Oy, Oulu, Finland) diluted 1:10 in TBST buffer (20 mM Tris, 500 mM NaCl, 0.3% Tween-20, pH 7.5) for 25 min. The membranes were then incubated with primary antibody diluted 1:2000 in TBST buffer for 1 h and washed

in TBST buffer five times for five min. Preimmune rabbit serum (1:1000) was used as a negative control. The secondary antibody was horseradish peroxidase (HRP)-labeled donkey anti-rabbit IgG, and the rest of the procedure was performed according to the instructions of the manufacturer of the ECL electrochemiluminescence detection system (Amersham Biosciences).

4.1.3 Immunohistochemistry (**II**)

Tissue specimens were obtained from eight adult mice, including four NMRI (two male and two female), two BALB/c (male and female), and two C57BL/6 (male and female) mice. All the available samples were used for neogenin studies while hemojuvelin staining was performed on samples from female C57BL/6 mice. After extraction, the samples were fixed in 4% neutral-buffered formaldehyde at 4°C for 24 hours and then dehydrated in an alcohol series, treated with xylene and embedded in paraffin wax. Sections (4 μm) were cut and placed on Superfrost PlusTM microscope slides.

After deparaffinization, immunostaining was performed by the biotin-streptavidin-peroxidase complex method. Briefly, antigen retrieval was performed in an autoclave at 95°C. The parameters for neogenin were 30 min in 10 mmol/L citrate buffer, pH 6.0. For hemojuvelin experiments, the slides were treated for 25 min in 10 mmol/L citrate buffer, pH 9. After the endogenous peroxidase activity was quenched and non-specific binding was blocked, the slides were incubated overnight at 4°C with the rabbit anti-neogenin polyclonal antibody (sc-15337, Santa Cruz Biotechnology, Santa Cruz, CA, 1:50 dilution), previously characterized (Lee et al. 2005), or alternatively with the rabbit anti-hemojuvelin polyclonal antibody (see section 4.1.1) diluted 1:250. The slides were then washed three times with phosphate-buffered saline (PBS) for 10 min. The biotinylated goat anti-rabbit secondary antibody (Zymed Laboratories Inc., South San Francisco, CA) was used at a dilution of 1:500 in a 60-min incubation step at room temperature. After washing, the sections were incubated with Streptavidin-HRP Conjugate (Zymed Laboratories Inc; diluted 1:750) for 30 min at room temperature. The slides were then washed again four times for 5 min in PBS and the staining reaction was carried out using 3,3'-diaminobenzidine tetrahydrochloride (DAB) as a chromogen. Finally,

a 4-min incubation in hematoxylin was performed to stain the nuclei of the cells and facilitating the interpretation of the results. Neogenin experiments were accompanied with negative and positive control stainings to detect possible nonspecific signals. Negative controls were processed by replacing the primary antibody with diluent. As a positive control parallel tissue sections were immunostained using a polyclonal rabbit anti-mouse proliferating cell nuclear antigen (PCNA) antibody (Santa Cruz Biotechnology). Two kinds of negative control were used to detect possible non-specific signals in the hemojuvelin staining. The preimmune serum controls consisted of replacing the primary antibody with normal preimmune rabbit serum. The diluent controls were performed as described above.

4.2 mRNA expression analyses

4.2.1 Conventional reverse transcription PCR (I)

The reverse transcription polymerase chain reaction (RT-PCR) method was used to test the expression of *HJV* mRNA in human and mouse tissues. For this purpose, we used cDNA kits purchased from BD Biosciences (Palo Alto, CA, USA), as well as cDNA samples produced in our laboratory from 5 adult male BALB/c mice. The human MTC^{TM} digestive panel, panel I and panel II and mouse MTC^{TM} panel I (BD Biosciences) contained first-strand cDNA preparations produced from total poly(A) RNA isolated from a number of different tissues. All human cDNA were derived from adult tissues. The tissues represented in the cDNA samples of our own production included blood, heart, lung, stomach, duodenum, jejunum, liver, ileum, colon, spleen, kidney, muscle, testis and brain.

Two primers for amplifying human HJV cDNA were chosen based on the human mRNA sequence (GenBank database accession NM_213653), which is the translated portion of the gene's longest transcript; forward 5´-TCACTTTCACACATGCCG-3' (nucleotides 540-557 in exon 3) and reverse 5'-GATCGAGAGAGTCGCTGAC-3' (nucleotides 971-989 in exon 4), which generated a 450-bp product corresponding to amino acids 180-330 of the protein sequence. The primers were produced by Sigma Genosys (Cambridgeshire, UK).

Primers for B2M were used to monitor the quantity of mRNA in the study samples; forward 5'-TATCCAGCGTACTCCAAAGATTCA -3' and reverse 5'-GAAAGACAAGTCTGAATGCTCCAC -3', which amplify a 169 bp product.

To amplify mouse Hjv cDNA, two primers (Sigma Genosys) were chosen based on the mouse Hjv mRNA sequence published in GenBank (NM_027126); forward 5'-AGGCTGAGGTGGACAATC-3' (nucleotides 945-962) and reverse 5'-CAAGAAGACTCGGGCATC-3' (nucleotides 1382-1399), which generated a 455-bp product corresponding to amino acids 230-381 of the murine Hjv protein sequence. Primers for beta-actin (Actb) were used to assess the quantity of mRNA; forward 5'-GCCGCATCCTCTTCCTCCCT-3' and reverse 5'-GTTGGCATAGAGGTCTTTACG-3', which amplify a sequence 205 bp long.

Amplification was performed using 2-3 ng of total cDNA as a template. The PCR reactions were amplified in a thermal cycler (Biometra, Göttingen, Germany). After initial denaturation at 94°C for 1 min, amplification was performed for 30-31 cycles of denaturation at 94°C for 30 s, annealing at 55-56°C for 30 s and extension at 72°C for 1 min 30 s, followed by a final extension at 72°C for 3 min. The PCR products were analyzed by electrophoresis on 1.5% agarose gel containing 0.1 mg/mL ethidium bromide with DNA standard (100 bp DNA Ladder, New England Biolabs, Beverly, MA, USA). Primers for glyceraldehyde 3-phosphate dehydrogenase (GAPDH, BD Biosciences) were used in all the performed experiments to monitor the amplification reaction.

4.2.1.1 Sequencing of PCR products

Some of the results from the PCR analysis were validated by sequencing the DNA from the gel band of interest. The amplification products obtained from the human liver and muscle as well as from mouse blood and 17-day-old embryos were purified from the agarose gel using a GFX™ PCR DNA and Gel Band Purification kit (Amersham Biosciences, Buckinghamshire, UK). DNA sequencing reactions were performed using an ABI PRISM™ Big Dye Terminator Cycle Sequencing Ready Reaction Kit, version 3.1 (Applied Biosystems, Foster City, CA, USA) according to the manufacturer's protocol. The sequencing was performed on the ABI PRISM™ 3100 Genetic Analyzer (Applied Biosystems).

4.2.2 Quantitative reverse transcription PCR (**II-IV**)

4.2.2.1 Murine tissue samples

To study Neo1 and Hjv mRNA expression in mouse tissues (**II**), 10-week-old NMRI mice (4 male and 4 female) were used. The tissues used in these analyses were the lung, brain, muscle, heart, spleen, thymus, pancreas, liver, esophagus, stomach, duodenum, jejunum, ileum, colon, kidney, testis, ovary, and uterus.

For the analysis of Neo1, Hjv, Hamp1 and Hamp2 expression in the heart, skeletal muscle and liver, samples of these tissues were collected from 3 strains of mice with or without enterally induced iron overload (see section 4.3.1) (**III**). Heart and skeletal muscle samples from male C57BL/6 mice were used to validate the microarray results (**III**).

Q-RT-PCR confirmation of the microarray results in article **IV** was performed on liver and duodenum samples from C57BL/6 mice of 2 experimental models: *Hfe*$^{-/-}$ and dietary iron overload.

4.2.2.2 RNA extraction and cDNA synthesis

Tissue specimens were snap frozen (**II**) or immersed in RNAlater (Ambion, Huntingdon, UK) (**III-IV**) immediately upon extraction and stored at -80°C until use. Total RNA was isolated using TRIZOL® reagent (Invitrogen, Carlsbad, CA) (**II**) or RNeasy RNA isolation kit (Qiagen, Valencia, CA) (**III-IV**) according to the manufacturers' instructions. In all the purifications, a digestion step with RNase-free DNase I (Novagen, Madison, USA in **II** and Qiagen in **III-IV**) was included to remove any residual DNA. The concentration and purity of the RNA was determined by optical density measurements at 260 and 280 nm. In articles **II** and **III**, the RNA extracts from males and females were separately pooled. In article **IV** RNA samples from different individuals were processed separately. A total of 3 µg of each total RNA isolate (5 µg in **IV**) was converted into first strand cDNA with a First Strand cDNA Synthesis kit (Fermentas, Burlington, Canada) and random hexamer primers, according to the protocol recommended by the manufacturer.

4.2.2.3 Quantitative reverse transcription PCR

The quantitative RT-PCR method was used to assess the relative mRNA expression levels of mouse Neo1 and Hjv in different tissues (**II**), that of Neo1, Hjv, Hamp1 and Hamp2 in the heart, skeletal muscle and liver of 3 mouse strains (**III**), and to validate the microarray results (**III, IV**). The reactions were run in the Roche LightCycler detection system (Roche, Rotkreuz, Switzerland). The majority of the primer sets used in these analyses (Table 2) was designed using Primer3 (http://primer3.sourceforge.net/). The specificity of the primers was verified using NCBI Blast (http://blast.ncbi.nlm.nih.gov/Blast.cgi). Whenever possible, both primers from each set were specific to different exons to avoid amplification of contaminating genomic DNA. Hjv primers amplify the mouse Hjv transcripts 1 and 3. The primers for Car4 have been described elsewhere (Pan et al. 2007).

The *Actb*, *Gapdh*, *Hprt1*, and *Sdha* genes were used as internal controls to normalize for potential quality and quantity differences between samples. Every PCR reaction was performed in a total volume of 20 µl containing 1 µl (**II**) or 0.5 µl (**III** and **IV**) of the first strand cDNA, 1x concentrated QuantiTect SYBR Green PCR Master Mix (Qiagen, Hilden, Germany), and 0.5 µmol/L of each primer. Amplifications and subsequent detection were carried out as follows: after an initial activation step of 15 min at 95°C, amplification was performed in a three step cycling procedure: denaturation at 95°C, 15 s, ramp rate 20°C/s; annealing according to the melting temperature of the primers, 20 s, ramp rate 20°C/s; and elongation at 72°C, 20 s, ramp rate 20°C/s for 45 cycles, and a final cooling step. A melting curve analysis was always performed for each PCR amplicon to verify specific amplification.

Table 2. *Primer sequences used in Q-RT-PCR analyses in original papers **II-IV**.*

Name	Direc-tion	Sequence (5'-3')	Size (bp)	Ann. temp. (°C)	GenBank number	Primer source	Original paper
Actb	F	AGAGGGAAATCGTGCGTGAC	138	57	NM_007393	QPPD ID:664	II, III, IV
Actb	R	CAATAGTGATGACCTGGCCGT					
Gapdh	F	ATGGTGAAGGTCGGTGTG	186	57	NM_008084	Primer3	II, III, IV
Gapdh	R	CATTCTCGGCCTTGACTG					
Hprt1	F	AGCTACTGTAATGATCAGTCAACG	180	55	NM_013556	QPPD ID:10050	II, III, IV
Hprt1	R	AGAGGTCCTTTTCACCAGCA					
Sdha	F	GCTTGCGAGCTGCATTTGG	145	53	NM_023281	PrimerBank ID:15030102a2	II, III, IV
Sdha	R	CATCTCCAGTTGTCCTCTTCCA					
Hamp1,2	F	CCTATCTCCATCAACAGATG	171	53	NM_032541	Ilyin et al.[a]	III
Hamp1	R	AACAGATACCACACTGGGAA					
Hamp1,2	F	CCTATCTCCATCAACAGATG	171	50	NM_183257	Ilyin et al.[a]	III
Hamp2	R	AACAGATACCACAGGAGGGT					
Pdk4	F	GATTGACATCCTGCCTGACC	119	55	NM_013743	Primer3	III
Pdk4	R	TCTGGTCTTCTGGGCTCTTC					
S100a8	F	GGAAATCACCATGCCCTCTAC	173	56	NM_013650	Primer3	III
S100a8	R	GCCACACCCACTTTTATCACC					
S100a9	F	CGACACCTTCCATCAATACTC	127	55	NM_009114	Primer3	III
S100a9	R	GAGGGCTTCATTTCTCTTCTC					
Fos	F	CGGGTTTCAACGCCGACTA	166	56	NM_010234	RTprimerDB, ID:3328	III
Fos	R	TTGGCACTAGAGACGGACAGA					
Myl4	F	GGGTAAAGCACGTTTCTCCA	119	55	NM_010858	Primer3	III
Myl4	R	AGGGAAGGTTGTGGGTCAG					
Myl7	F	TCACCGTCTTCCTCACACTC	129	55	NM_022879	Primer3	III
Myl7	R	GCTGCTTGAACTCTTCCTTG					
Cxcl7	F	GCCCACTTCATAACCTCCA	208	52	NM_023785	Primer3	III
Cxcl7	R	ATCACTTCCACATCAGCACA					
Tfrc	F	TCATGAGGGAAATCAATGATCGTA	101	56	NM_011638	QPPD ID:1607	III, IV
Tfrc	R	GCCCCAGAAGATATGTCGGAA					
Scd1	F	TGGGTTGGCTGCTTGTG	150	52	NM_009127	QPPD ID:1847	III
Scd1	R	GCGTGGGCAGGATGAAG					
Mup1	F	CTCTATGGCCGAGAACCAGA	115	55	NM_031188	Primer3	III
Mup1	R	AGCGATTGGCATTGGATAGG					
Dnajb1	F	CGACCGCTATGGAGAGGAA	133	55	NM_018808	Primer3	III, IV
Dnajb1	R	GCCACCGAAGAACTCAGCA					
Hspa1b	F	GAGGAGTTCAAGAGGAAGCA	169	54	NM_010478	Primer3	III
Hspa1b	R	GCGTGATGGATGTGTAGAAG					
Acaa1b	F	TGTCCCAGAGAGGGAACCA	135	55	NM_146230	Primer3	IV
Acaa1b	R	CCTGCTTCTGCCGTGAAAC					
Acot3	F	ACTTTGAGGAAGCTGTGACC	168	55	NM_134246	Primer3	IV
Acot3	R	CGCCGATGTTGGATATAGAG					
Acta1	F	CCAAAGCTAACCGGGAGAA	135	52	NM_009606	Primer3	III
Acta1	R	CCCCAGAATCCAACACGA					
Adn	F	AACCGGACAACCTGCAATC	151	55	NM_013459	Primer3	III
Adn	R	CCCACGTAACCACACCTTC					
Angptl4	F	CACGCACCTAGACAATGGA	174	52	NM_020581	Primer3	III, IV
Angptl4	R	AGAGGCTGGATCTGGAAA					
Cp	F	CAGCCGTAGAGGTGGAATG	153	53	NM_001042611	Primer3	IV
Cp	R	TAAACTGGCGATACACAACC					
Cpb1	F	GGTTTCCACGCAAGAGAG	138	52	NM_029706	Primer3	IV
Cpb1	R	GTTGACCACAGGCAGAACA					
Creld2	F	GAACGAGACCCACAGCATC	128	55	NM_029720	Primer3	IV
Creld2	R	CCACATCCACACAGGCATC					
Ctse	F	CACACCCAGTATTCCATCCA	137	56	NM_007799	Primer3	IV
Ctse	R	ATCCACAGTCAACCCTTCCA					

Cyp26b1	F	CAAGCTCGGCAGATCCTTCA	166	57	NM_175475	Primer3	IV
Cyp26b1	R	ACTCCAGGGTTCCATCCTTC					
Cyp2c54	F	TATTGGTGGGACAGAGTCAA	164	53	NM_206537	Primer3	IV
Cyp2c54	R	CATTTGTATAGGGCATGTGG					
Cyp4a14	F	CAAGACCCTCCAGCATTTCC	186	58	NM_007822	Primer3	IV
Cyp4a14	R	CCCAGAACCACCTTCACATAG					
Dbp	F	TGAGGAACAGAAGGATGAGAAG	192	59	NM_016974	Primer3	IV
Dbp	R	ACAGCACGGTAGTGGGACAG					
Ddb1	F	GAACCGACTCAATAAGGTCA	200	53	NM_015735	Primer3	IV
Ddb1	R	GCTTCATACCACTGCCATC					
Dmt1	F	ACTTGGGTTGGCAGTGTTTG	149	55	NM_008732	Primer3	IV
Dmt1	R	CTGGGCTGTTAGTCATCTGG					
Egr1	F	AGCGGCGGTAATAGCAGCA	186	56	NM_007913	Primer3	IV
Egr1	R	GGGATAACTCGTCTCCACCA					
Ela3	F	TGCCTGTGGTGGACTATGAA	193	55	NM_026419	Primer3	IV
Ela3	R	CAGCCCAAGGAGGACACAA					
Erdr1	F	TTTCTCTGTGGGCGTGAATG	192	54	NM_133362	Primer3	IV
Erdr1	R	GCAGGCTTCCTACCTTGTG					
Foxq1	F	ACTCCTACATCGCTCTCATC	178	55	NM_008239	Primer3	IV
Foxq1	R	AGCACCTTGACGAAACAGTC					
Gprc5a	F	AGAGCTATGGTGTGGAGAA	101	51	NM_181444	Primer3	IV
Gprc5a	R	CTGAAAATGGGTGGAATAAG					
Gstm1	F	ACGCCTTCCCAAACCTGA	135	52	NM_010358	Primer3	IV
Gstm1	R	GGGCCTACTTGTTACTCCA					
Hfe2	F	TCTGACCTGAGTGAGACTGC	187	56	NM_027126	Primer3	II, III
Hfe2	R	GATGATGAGCCTCCTACCTA					
Hmox1	F	CAGAGGAACACAAAGACCAGA	174	57	NM_010442	Primer3	IV
Hmox1	R	CCAACAGGAAGCTGAGAGTG					
Hsd3b5	F	GTGAGCTGTACCTGCCTTCA	171	56	NM_008295	Primer3	IV
Hsd3b5	R	GCACCAACATTCGGACAATC					
Hsph1	F	TCACCATCTCCACGGCTTC	148	55	NM_013559	Primer3	IV
Hsph1	R	GCTTCACTGTTGTCTTGCTG					
Id2	F	ACCACCCTGAACACGGACA	209	55	NM_010496	Primer3	IV
Id2	R	CTCCTGGTGAAATGGCTGA					
Id3	F	ATCTCCAAGGACAAGAGGAG	188	55	NM_008321	Primer3	IV
Id3	R	AGGCGTTGAGTTCAGGGTAA					
Lcn2	F	CAATGTCACCTCCATCCTG	166	53	NM_008491	Primer3	IV
Lcn2	R	CTGGTTGTAGTCCGTGGTG					
Ltf	F	CGGAGAAGTATCTGGGAAAG	198	54	NM_008522	Primer3	IV
Ltf	R	ACAGCAGGGAGTGAGGAGA					
Mt1	F	CCTCACTTACTCCGTAGCTC	118	55	NM_013602	Primer3	IV
Mt1	R	GCACTTGCAGTTCTTGCAG					
Neo1	F	CCCTGGTCTCTACTCGCTTC	139	59	NM_008684	Primer3	II, III
Neo1	R	CCTGGCTGGCTGGTATTCTC					
Rsad2	F	TGGTGCCTGAATCTAACC	128	49	NM_021384	Primer3	IV
Rsad2	R	TTCTTCCACGCCAACATC					
Saa1	F	CATTTGTTCACGAGGCTTTC	103	51	NM_009117	Primer3	IV
Saa1	R	CGAGCATGGAAGTATTTGTC					
Saa2	F	TGGTCTTCTGCTCCCTGCTC	140	58	NM_011314	Primer3	IV
Saa2	R	GTATTTGTCTCCATCTTTCCAG					
Slc46a3	F	GTGTGACCAAAACAAAAGCAG	192	55	NM_027872	Primer3	IV
Slc46a3	R	CCCAGAGAGCCAAGAGATG					

QPPD is the Quantitative PCR Primer Database (http://web.ncifcrf.gov/rtp/gel/primerdb/).
PrimerBank (http://pga.mgh.harvard.edu/primerbank/).
Primer3 (http://primer3.sourceforge.net/).
[a] (Ilyin et al. 2003)

To quantify the concentration of each transcript in the evaluated samples, a standard curve for each gene was established using 5-fold serial dilutions of known concentrations of purified PCR products generated from the same primer sets. Every cDNA sample was tested in duplicate (**II**) or in triplicate (**III, IV**). The mean and standard deviation (SD) of the 3 crossing point (Cp) values were calculated for each sample and, in article **IV**, a SD cutoff level of 0.2 was set. Accordingly, when the SD of the triplicates of a sample was greater than 0.2, the most outlying replicate was excluded and the analysis was continued with the two remaining replicates. Using the standard curve method, the Cp values were then transformed by the Lightcycler software into copy numbers. The expression value for each sample was the mean copy number of the sample replicates. This value was normalized by dividing it by the geometric mean of the four internal control genes, which is an accurate normalization method (Vandesompele et al. 2002). The normalization factor was always considered as a value of 100 and the final result was expressed as the relative mRNA expression level.

*4.2.2.4 Statistical analyses (**III, IV**)*

In article **III**, the mean and SD values were calculated from technical triplicates and the Student's *t*-test (unpaired, 2-tailed) was used to statistically analyze the differences in gene expression between the control and iron-loaded mice. In article **IV**, the distributions of *Hfe*$^{-/-}$ mice vs. wild-type mice and mice with dietary iron overload vs. untreated mice were shown by means with SDs and, due to the small sample size, tested by a Mann-Whitney test. Also due to the small sample size within each group, the statistical significance was considered only as orientative. Theoretically, the Q-RT-PCR technology used herein can detect a minimum of 100 copies of starting material. To avoid inaccurate use of the statistical methods, these were not applied to data with raw values below 300 copies. Values are expressed as the mean ± SD.

4.2.3 cDNA Microarray (**III, IV**)

4.2.3.1 Experimental procedure

Microarray studies were performed in the Finnish DNA Microarray Centre at Turku Centre for Biotechnology. In article **III**, total RNA was extracted from heart and skeletal muscle specimens derived from 3 male C57BL/6 mice of each group (iron diet and control diet). In article **IV**, liver and duodenal samples from 3 *Hfe*$^{-/-}$ mice and 3 mice with dietary iron overload and, as controls, samples from the liver and duodenum of 4 wild-type mice (2 controls of the *Hfe*$^{-/-}$ mice and 2 controls of the mice with dietary iron overload), were subjected to total RNA extraction.

The resulting samples were analyzed individually. A total of 200 ng in **III** and 300 ng in **IV**, of total RNA from each sample were amplified using the Illumina™ RNA TotalPrep Amplification kit (Ambion) following the manufacturer's instructions. The in vitro transcription reaction, which was conducted for 14 h, included labeling of the cRNA by biotinylation.

Labeled and amplified material (1.5 μg/array) was hybridized to Illumina's Sentrix Mouse-6 Expression BeadChips™ (Illumina, Inc., San Diego, CA) (12 samples, 2 chips) at 55°C for 18 h according to Illumina BeadStation 500X™ protocol. Arrays were washed and then stained with 1 μg/ml cyanine3-streptavidin (Amersham Biosciences, Buckinghamshire, UK). The Illumina BeadArray ™ reader was used to scan the arrays according to the manufacturer's instructions. In article **III**, samples were analyzed using the BeadStudio™ software from Illumina. The hybridization control report showed problems in two of the arrays, corresponding to two heart samples, one from a control mouse and the other from an iron-loaded mouse. In both cases, 228 probes failed to hybridize, and therefore, these probes were excluded from the analyses of these two samples.

4.2.3.2 Data analysis

Array data were normalized with Inforsense KDE version 2.0.4 (Inforsense, London, UK) (**III**) or with Chipster (v1.1.1) (**IV**) using a quantile normalization method. Quality control of the data in Chipster included non-metric multidimensional scaling, dendrograms, hierarchical clustering, and 2-way

clustering (heatmaps). These analyses showed that data from one of the three duodenal samples from *Hfe*$^{-/-}$ mice were highly divergent from the other two (**IV**). Thus, this sample was excluded from further analyses.

The fold-change values were calculated for each gene using the same software (**III, IV**). In **IV**, the data were then filtered according to the SD of the probes. The percentage of the data that was filtered out was adjusted to 99.4%, implicating a SD value of almost 3. At this point, statistical analysis was performed using the empirical Bayes t-test for the comparison of 2 groups (**IV**). Due to the small number of samples, the statistical results were considered as orientative and thus no filtering was applied to the data according to p-values. The resulting data (**III, IV**) were filtered according to a fold-change of 1.4 and -1.4 for up and downregulated expression, respectively. This value has been proposed as an adequate compromise above which there is a high correlation between microarray and quantitative PCR data, regardless of other factors such as spot intensity and cycle threshold (Morey et al. 2006).

Finally, the functional annotation tool DAVID (Database for Annotation, Visualization and Integrated Discovery, http://david.abcc.ncifcrf.gov) (Dennis et al. 2003) was used to identify enriched biological categories among the regulated genes compared to all the genes present in Illumina's Sentrix Mouse-6 Expression Beadchip. The annotation groupings analyzed were: Gene Ontology biological process and molecular functions, SwissProt Protein Information Resources keywords, SwissProt comments, Kyoto Encyclopedia of Genes and Genomes and Biocarta pathways. Redundant categories with the same gene members were removed to yield a single representative category.

4.3 Mouse models of iron overload

4.3.1 Dietary iron overload (**III, IV**)

The experiments with mice were performed in the laboratory animal center of the University of Oulu, where mice were kept under specific pathogen-free conditions. Five male and five female mice from each of three strains (BALB/c, C57BL/6, and DBA/2) were placed on a diet (Lactamin, Stockholm, Sweden) supplemented with

2% carbonyl iron (Sigma-Aldrich Sweden AB, Stockholm, Sweden, #C3518) at the age of 10-12 weeks. Equivalent groups of littermates were fed control chow diet without iron supplementation (0.02% iron). After 6 weeks of treatment, blood was collected from the mice under anesthesia. Animals were then sacrificed and liver, duodenum, skeletal muscle (extensor digitorum longus, EDL) and heart samples were immediately collected and immersed in RNAlater (Ambion, Huntingdon, UK). Liver samples were also collected and stored frozen before measurement of iron content.

*4.3.1.1 Determination of tissue iron content and statistical analysis (**III**)*

Liver and heart tissue samples were analyzed for nonheme iron content using the bathophenanthroline method as described by Torrance and Bothwell (Torrance and Bothwell 1968). The values are expressed as micrograms of iron per gram of dry weight. The mean and SD values were calculated from the individuals in each group. The Student's *t*-test (unpaired, 2-tailed) was used to statistically analyze the differences in iron content between control and iron-loaded mice.

4.3.2 *Hfe*$^{-/-}$ mice (**IV**)

A total of 5 mice homozygous for a disruption of the *Hfe* gene and 5 wild-type control mice were used in this study. All 10 mice were male C57BL/6 and approximately 10 weeks old. Tissue specimens were immersed in RNAlater (Ambion) immediately upon extraction. The knockout mouse model for *Hfe* used in this work has been developed and characterized elsewhere (Ahmad et al. 2002, Fleming et al. 1999, Zhou et al. 1998). At the age of 10 weeks, these mice present significantly elevated transferrin saturation (77% vs. 96%) and liver iron content (2071 vs. 255µg/g) compared with normal littermates. Iron is deposited in the liver of these mice following a periportal to pericentral gradient. In the small intestine, iron is deposited in epithelial cells of the villi and absent in cryptal enterocytes (Zhou et al. 1998). Duodenal upregulation of IRE-containing Dmt1 has been demonstrated in this mouse model (Fleming et al. 1999). Additionally,

downregulation of hepatic hepcidin expression has also been proven (Ahmad et al. 2002).

4.4 Ethical approval (**II-IV**)

The experimental induction of dietary iron overload in mice was approved by the Animal Care and Use Committee of the University of Oulu (permission No 102/05) (**III, IV**). The use of *Hfe*$^{-/-}$ mice for experimentation was approved by the Institutional Animal Care and Use Committee at Saint Louis University.

5. RESULTS

5.1 Iron content in the liver and heart of iron-fed mice (**III**, **IV**)

The mice were fed either standard (0.02 % carbonyl iron) or high-iron (2 % carbonyl iron) diet during 6 weeks. Iron concentrations in liver and heart specimens were determined to confirm the validity of the animal model (Figure 1 in **III**). Basal iron levels were higher in the liver than in the heart. C57BL/6 mice fed a standard chow had lower hepatic iron than BALB/c and DBA/2 mice kept on the same diet (158 vs. 287 and 389µg/g). The livers of mice of all three strains (BALB/c, C57BL/6 and DBA/2) were highly iron-loaded as a result of the extra iron ingestion. In C57BL/6 male mice in particular, hepatic iron content increased from 158 to 4429µg/g. A much smaller increment was observed in cardiac iron content after a high-iron diet in all three strains and in both genders, although statistical significance was not reached in all the cases (132 to 152µg/g in C57BL/6 male mice). In general, hepatic and cardiac iron levels were slightly higher in females than in males.

5.2 Expression of Hemojuvelin

5.2.1 Hemojuvelin mRNA in human and mouse tissues (**I, II**)

First of all we determined the tissues in which the human and mouse *Hjv* gene, coding for hemojuvelin, is transcribed (**I**). In humans, a strong signal was seen in the liver, esophagus, heart and muscle while weaker reactions where evident in the descending colon and pancreas. A faint signal was also observed in the ileocecum. The rectum, cecum, stomach, ascending colon, transverse colon, duodenum, ileum, jejunum, brain, lung, placenta, kidney, ovary, colon and leukocytes were negative. In mice, the Hjv transcript was detected in the blood, heart, lung, stomach,

duodenum, jejunum, liver, ileum, colon, kidney, muscle and testis (Table 3, second column). A strong positive signal was amplified from the brain and spleen cDNA prepared in our laboratory while no expression was detected in the commercial cDNA samples of these tissues. There was no signal in the 7-days-old embryo, but the three oldest embryos showed positive bands. Even though the PCR method was not quantitative, the signal became stronger with increasing age of the embryo, which could indicate a developmental regulation.

Later, we quantified the levels of Hjv transcripts in tissues of male and female mice by Q-RT-PCR (**II**) (Table 3, third column). Positive tissues included the skeletal muscle, heart, esophagus, and liver in which the signal intensities were approximately at the same levels in both males and females. Very weak signals were also evident in the lung, thymus and stomach of male mice.

5.2.2 Hemojuvelin protein in mouse tissues (**I, II**)

Compared with the transcript, the hemojuvelin protein showed a more limited pattern of distribution, as analyzed by western blotting (**I**) (Table 3, fourth column). A 26 kDa positive band was observed in the liver, heart, kidney, brain, and muscle. A 30 kDa band was also observed in the jejunum, liver, kidney, and testis. These two bands most likely correspond to different hemojuvelin isoforms. The lung, stomach, duodenum, ileum, colon, and spleen were negative for hemojuvelin protein.

Hemojuvelin protein expression and localization was further examined by immunohistochemical analyses (**II**) (Table 3, fifth column). There was a faint intracellular reaction in the skeletal muscle, while the expression of hemojuvelin was negligible in the heart and liver.

Table 3. *Expression profile of hemojuvelin in mouse and human.*

Tissue	h RT-PCR	m RT-PCR	m Q-RT-PCR	m Western blotting	m IHC
Skeletal muscle	+	+	+	+	+
Heart	+	+	+	+	negligible
Esophagus	+	NT	+	NT	NT
Liver	+	+	+	+	negligible
Lung	-	+	+	-	NT
Stomach	-	+	+ ♂	-	NT
Thymus	NT	NT	+ ♂	NT	NT
Blood	NT	+	NT	NT	NT
Duodenum	-	+	-	-	NT
Jejunum	-	+	-	+	NT
Ileum	-	+	-	-	NT
Colon	+	+	-	-	NT
Pancreas	+	NT	-	NT	NT
Kidney	-	+	-	+	NT
Testis	NT	+	-	+	NT
Ovary	-	NT	-	NT	NT
Uterus	NT	NT	-	NT	NT
Brain	-	?	-	+	NT
Spleen	NT	?	-	-	NT
Embryo 7d	NT	-	NT	NT	NT
Embryo 11d	NT	+	NT	NT	NT
Embryo 15d	NT	+	NT	NT	NT
Embryo 17d	NT	+	NT	NT	NT

The tissues are arranged according to the mRNA expression by Q-RT-PCR (third column), in descending order. h, human; m, mouse; ?, results were different in commercial cDNA samples and those obtained in our laboratory from 5 BALB/c mice; ♂, hemojuvelin was detected only in male mice; NT, not tested; IHC, immunohistochemistry.

5.2.3 Hemojuvelin transcript in the heart, skeletal muscle and liver of mice with dietary iron overload (**III**)

The results for hemojuvelin expression did not indicate any clear regulation by iron overload, strain or gender in the murine heart, skeletal muscle or liver (Figure 7 in **III**). This is in agreement with previous studies of hepatic expression (Bondi et al. 2005, Krijt et al. 2004). Hjv expression only showed a minor trend downwards in the skeletal muscle and heart of mice fed with a high-iron diet.

5.3 Expression of Neogenin

5.3.1 Neogenin transcript in mouse tissues (**II**)

The expression levels of Neo1 mRNA were examined in a broad range of mouse tissues by Q-RT-PCR. Neo1 transcripts were detectable in each of the tissues tested for both genders with the highest expression observed in the testis, ovary, and uterus (Figure 1 in **II**). A relatively high signal was also observed in the brain, followed by lung, skeletal muscle, and heart. In the digestive system, the highest expression for Neo1 was found in distal parts of the intestine (the ileum and colon). However, moderate signal levels were also observed in the esophagus, stomach, duodenum, and jejunum, with a similar intensity as in the kidney, outside of the digestive system. The lowest Neo1 transcript levels were observed in the liver, thymus, spleen, and pancreas. There were no marked differences in the levels of expression observed in males vs. females.

5.3.2 Neogenin protein in mouse tissues (**II**)

Table 4. *Expression profile of neogenin in mouse.*

Q-RT-PCR	Immunohistochemistry
Testis	Cytoplasm of sperm cells in different developmental stages
Uterus	Cytoplasm of epithelial cells of endometrium (also in epithelial cells of oviduct)
Ovary	Cytoplasm of follicular cells. Follicles mainly negative
Brain	Neuronal bodies and weaker in nervous fibers, nuclei negative. Basolateral membrane of choroid epithelial cells.
Heart	Sarcolemma and weaker in sarcoplasm, nuclei negative
Ileum	Cytoplasm of enterocytes, homogeneous intensity throughout the crypt
Lung	Mainly round cells in alveolar walls (probably type II pneumocytes)
Skeletal muscle	Sarcolemma and weaker in sarcoplasm, nuclei negative
Colon	Cytoplasm of epithelial cells
Stomach	Mucus secreting cells and chief cells. Mainly absent in parietal cells
Kidney	Glomeruli and some renal proximal and distal tubules. Negative in renal medulla
Esophagus	Not tested
Jejunum	Cytoplasm of enterocytes, stronger in crypts and weakens towards villi tips
Duodenum	Strong in Brunner gland cells, weaker in enterocytes
Liver	Weak in cytoplasm of hepatocytes. Stronger in sinusoid lining cells
Thymus	Not tested
Spleen	Not tested
Pancreas	Negative

The tissues are arranged according to the expression level in Q-RT-PCR results, in a descending scale.

The localization of neogenin protein in mouse tissues was examined by immunohistochemistry, which revealed no marked differences in the staining patterns between different strains or genders (data not shown). Examples of neogenin localization in the testis and liver are shown in Figure 5 and a summary of the results is presented in Table 4.

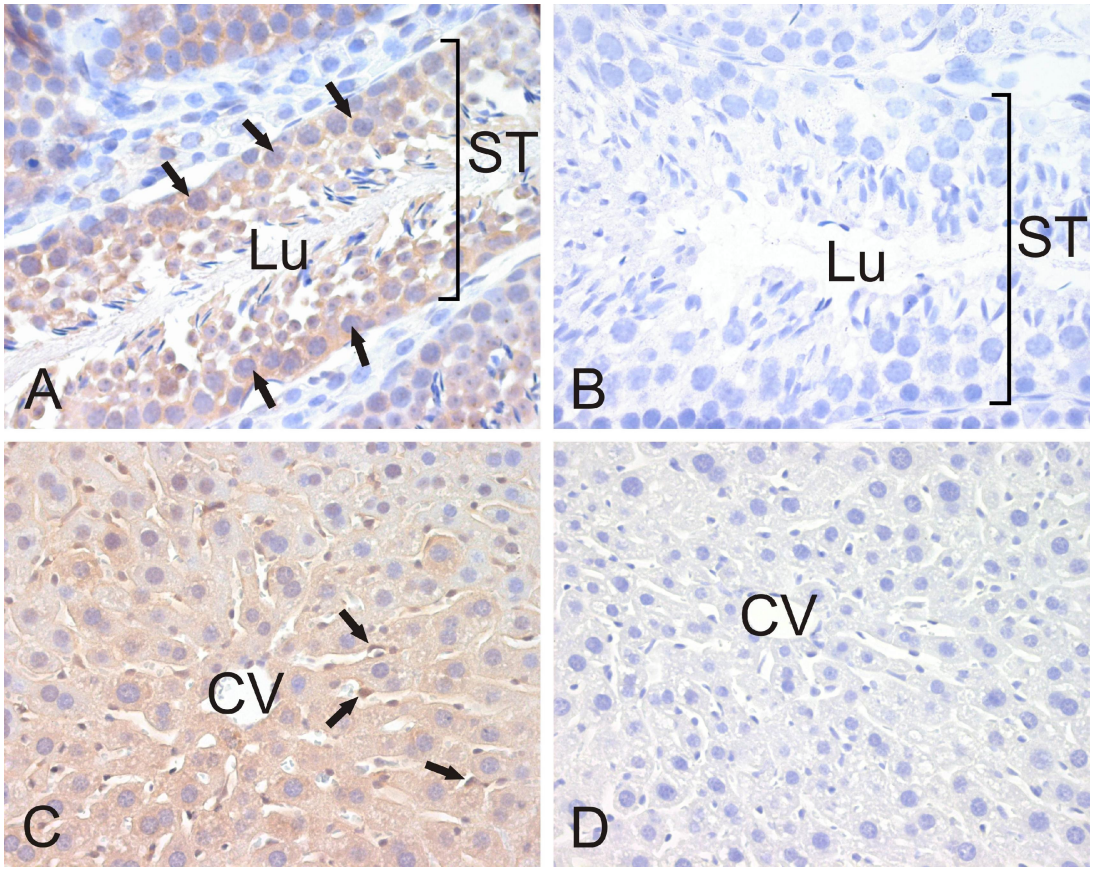

Figure 5. *Immunolocalization of neogenin in mouse seminiferous tubules of the testis (A) and liver(C). In testis, a positive cytoplasmic signal is observed in the developing sperm cells (arrows). The liver shows positive neogenin staining in the sinusoid lining cells (arrows in C), which are most probably Kupffer cells. There is also a faint signal in the hepatic parenchyma. No signal is present in the negative controls (B and D).*

5.3.3 Neogenin mRNA in heart, skeletal muscle and liver of mice with dietary iron overload (**III**)

The results show that neogenin transcription is not regulated by dietary iron overload as studied in heart, skeletal muscle, and liver (Figure 8 in **III**). Strain and gender neither affected neogenin expression in any of the three tissues.

5.4 Expression of iron-related genes in the heart, skeletal muscle, liver and duodenum of iron-loaded mice (**III, IV**)

5.4.1 Hepcidin

The expression of the hepcidin genes, *hamp1* and *hamp2,* was studied in the heart, skeletal muscle and liver of 3 strains of carbonyl iron overloaded mice using Q-RT-PCR (**III**). *Hamp1* expression in the heart showed a tendency downwards in the iron-fed mice, except for the BALB/c females. Even though the baseline signal in control mice was rather low, it was above the lower sensitivity limit of the method. The fold-changes were -8.25 for BALB/c males, -2.5 and -1.4 for C57BL/6 and -7.18 and -3.8 for DBA/2 males and females, respectively (Figure 5B in **III**). In the skeletal muscle, *hamp* expression was negligible (Figure 5A in **III**). Expression of *hamp2* in the skeletal muscle and heart was only observed in DBA2 mice and it did not show any clear tendency toward regulation by iron overload (Figure 6 in **III**). The expression of *hamp1* and *hamp2* was greatly upregulated in the liver of carbonyl iron-loaded mice, in concordance with published results (Figure 5C in **III** and Figure 2 in **IV**) (Krijt et al. 2004, Pigeon et al. 2001). Hepatic transcript levels of both genes varied according to mouse strain and gender, similar to previous observations (Courselaud et al. 2004, Krijt et al. 2004). In BALB/c and C57BL/6 mice, *hamp1* was the predominant gene expressed in the liver, while in DBA2 mice, the hepatic expression of *hamp2* was dominant (Figure 6C in **III**).

The mRNA levels of the murine *hamp* genes were also examined in the duodenum of C57BL/6 mice with dietary iron overload (**IV**) and the transcription levels were negligible (data not shown).

5.4.2 Other iron-related genes

Genome-wide profiling of the skeletal muscle of carbonyl iron-loaded mice showed no regulation of the expression of any gene known to be involved in iron metabolism. In the heart tissue of these mice, on the other hand, *Tfr1* was downregulated (Figure 3B in **III**). Dietary iron overload changed the expression of three iron-related genes in the liver. *Lcn2* and *Cp* were upregulated using both

microarray analysis and Q-RT-PCR, while *Tfr1* expression was downregulated by 1.74-fold in microarray (Table 3 in **IV**) and by 1.93-fold by Q-RT-PCR (Figure 4E in **III**). The mice fed the iron-supplemented diet displayed downregulated duodenal expression of *Tfr1* and upregulated *Hmox1*: both of these results were validated by Q-RT-PCR (Figure 3 in **IV**).

5.5 Expression of iron-related genes in the liver and duodenum of *Hfe*$^{-/-}$ mice (**IV**)

5.5.1 Hepcidin

The expression of the murine *hamp* genes was examined in the liver of C57BL/6 *Hfe*$^{-/-}$ mice (Figure 1 in **IV**). mRNA levels of hamp1 and hamp2 were reduced by 3.24- and 1.32-fold, respectively. The expression of both genes was also analyzed in the duodenum of the same mice and the transcription levels were negligible (data not shown).

5.5.2 Other iron related genes

The expression of *Tfr1* was decreased and that of *Lcn2* was induced in the liver of *Hfe*$^{-/-}$ mice as studied by microarray and these results were confirmed using Q-RT-PCR (Figure 1 in **IV**). In contrast, no iron-related gene was regulated in the duodenum of *Hfe*$^{-/-}$ mice.

5.6 Global transcriptional response to dietary iron overload in murine heart and skeletal muscle (**III**)

We studied the changes in gene expression caused by dietary iron overload in the heart and skeletal muscle of C57BL/6 male mice by DNA microarray. In the heart, iron loading resulted in increased expression of 35 genes (Table 3 in **III**), while 40 genes had decreased expression after iron overload (Table 4 in **III**). A total of 14 genes had induced expression as a result of dietary iron overload in skeletal muscle

(Table 1 in **III**) and 40 genes showed repressed expression (Table 2 in **III**). Functional annotation of the gene lists was performed to identify the biological processes that may be modified by iron overload in murine heart (Appendix 1) and skeletal muscle (Appendix 2). The most enriched functional categories were highly coincident for the two tissues, including response to stress, protein folding, carbohydrate metabolism, regulation of angiogenesis, calcium ion binding, negative regulation of apoptosis and transcriptional regulation. The expression results from the heart and skeletal muscle were compared at the gene level (Table 5). There were seven genes that were upregulated in both tissues, with functions related to carbohydrate and lipid metabolism, inflammation and response to stress, among others. Nine genes were downregulated in both tissues, with roles connected with protein folding and response to stress, regulation of cell cycle and apoptosis.

Table 5.*Genes whose expression was altered in heart and skeletal muscle by dietary iron overload.*

Function	Gene Symbol	Gene name	GenBank Number	FC H	FC SM
Regulation of glucose and fatty acid metabolism	*Angptl4*	angiopoietin-like 4	NM_020581	2.79	1.45
Regulation of glucose metabolism	*Pdk4*	pyruvate dehydrogenase kinase, isoenzyme 4	NM_013743	2.06	1.40
Inflammation	*S100a8*	Calgranulin A, S100 calcium binding protein A8	NM_013650	1.96	2.80
Inflammation	*S100a9*	Calgranulin B, S100 calcium binding protein A9	NM_009114	1.95	2.26
Inactivation of all-trans-retinoic acid	*Cyp26b1*	cytochrome P450, family 26, subfamily b, polypeptide 1	NM_175475	1.62	1.49
Response to stress	*Cirbp*	cold inducible RNA binding protein	NM_007705	1.49	1.48
Transcriptional coregulator	*Cited2*	Cbp/p300-interacting transactivator, with Glu/Asp-rich carboxy-terminal domain, 2	NM_010828	1.41	1.46
Transcription factor, proto-oncogene	*Fos*	FBJ osteosarcoma oncogene	NM_010234	1.49	-2.10
Synthesis of fatty acids	*Scd1*	Stearoyl-Coenzyme A desaturase 1	NM_009127	-2.40	1.75
Innate immunity	*Adn*	Adipsin, complement factor D	NM_013459	-1.92	1.62
Inhibitor of transcription	*Idb1*	inhibitor of DNA binding 1	NM_010495	-1.40	-1.66
Protein folding and response to stress	*Hspb1*	heat shock protein 1	NM_013560	-1.48	-1.48
Negative regulation of mTOR signaling pathway, apoptosis	*Ddit4*	DNA-damage-inducible transcript 4	NM_029083	-1.49	-1.54
Response to stress, regulation of cell cycle progression	*Cdkn1a*	cyclin-dependent kinase inhibitor 1A	NM_007669	-1.49	-1.62
Protein folding and response to stress	*Hspca*	heat shock protein 1, alpha	NM_010480	-1.53	-1.91
Inhibition of protein kinase signaling pathway	*Errfi1*	ERBB receptor feedback inhibitor 1	NM_133753	-1.81	-1.69
Protein folding and response to stress	*Dnajb1*	DnaJ (Hsp40) homolog, subfamily B, member 1	NM_018808	-1.90	-2.52
Protein folding and response to stress	*Hsp105*	heat shock protein 105	NM_013559	-2.25	-1.72
Protein folding and response to stress	*Hspa1b*	heat shock protein 1B	NM_010478	-2.25	-2.40

pink = upregulated in both tissues; green = downregulated in both tissues; white = oppositely regulated in the two tissues; FC, fold-change (obtained by DNA microarray method); H, heart; SM, skeletal muscle.

From the lists of microarray results, we selected 15 genes that presented the highest fold-change values. The expression levels of these genes were then analyzed by Q-RT-PCR in samples from the same strain of mice used in the microarray experiments (C57BL/6). Certainly, the results from these analyses showed an excellent correlation between the two methods; the expression of all the genes proved to be regulated and displayed the same direction of change (Figures 2 and 3 in **III**). All of the fold-change values obtained from Q-RT-PCR experiments exceeded 1.4 except for the Tfr1 gene whose downregulation in the skeletal muscle reached the value of -1.36 in the iron-fed mice compared to the controls.

The hepatic mRNA levels of these 15 genes were also analyzed by Q-RT-PCR. The expression of 4 of the 15 genes (*Myl4, Myl7, Acta1 and Adn*) was considered negligible in the liver because of very low signal intensity. Among the 11 remaining genes *S100a8*, *S100a9*, *Scd1* and *Fos* were upregulated; *Mup1*, *Hspa1b*, *Dnajb1*, Tfr1 and *Angptl4* were downregulated, and *Pdk4* and *Cxcl7* were not significantly regulated by dietary iron. Few of these results are presented in the Figure 4 of original publication **III**.

5.7 Global transcriptional response to *Hfe*$^{-/-}$ and dietary iron overload in liver and duodenum of mice (**IV**)

A genome-wide microarray analysis was used to study gene expression in the liver and duodenum of *Hfe*$^{-/-}$ mice and carbonyl iron-loaded mice, and was compared with that of wild-type mice fed a standard diet. This approach allowed the identification of genes that are differentially expressed during iron overload and those influenced by the lack of Hfe protein. All the mice used for this purpose were C57BL/6 males.

5.7.1 Hepatic transcriptional response to *Hfe* deficiency and dietary iron overload

Hepatic RNA from 3 *Hfe*$^{-/-}$ mice and 2 wild-type mice was subjected to microarray analysis. The results revealed 86 induced genes and 65 repressed genes (Appendix 3). The fold-changes ranged from 9.83 to -3.47. Functional annotation of

the gene lists highlighted the biological processes that may be modified by Hfe deficiency. This analysis revealed enrichment of heat shock proteins and proteins related to inflammatory responses or antigen processing and presentation, among others (Table 2 in **IV**).

In the liver of mice with dietary iron overload, the expression of 123 genes was upregulated and that of 95 genes was downregulated (Appendix 4). The fold-changes ranged between 13.58 and -7.46. The list of regulated genes was functionally annotated, showing enrichment of cytochrome P450 proteins as well as others involved in glutathione metabolism, the acute-phase response, organic acid biosynthesis and cellular iron homeostasis, in addition to other processes (Table 3 in **IV**).

The genes upregulated in the livers of mice from both models comprised a proposed iron transporter (*Lcn2*), genes involved in transport and metabolism of carbohydrates and lipids, and genes involved in protection against oxidative stress (Table 6). Downregulated genes, by contrast, included *Tfr1* and two heat shock proteins. Even more interestingly, the gene regulation showing opposite direction in the two models is likely affected by the presence or absence of Hfe (Table 6). Among the genes regulated in the opposite direction in the liver of the two mouse models, those upregulated in the *Hfe*$^{-/-}$ mice were associated with the acute phase response, lipid transport and regulation of carbohydrate and lipid metabolism. The genes repressed in the *Hfe*$^{-/-}$ mice and induced in the iron-fed mice included *hamp1* and genes involved in antigen processing and presentation and regulation of cytokine signaling, among others.

Table 6. *Comparison of hepatic gene expression regulation by Hfe deficiency and dietary iron overload.*

Function	Gene Symbol	Gene name	GenBank Number	FC $Hfe^{-/-}$	FC diet
Transporter (of iron?); Acute phase response	*Lcn2*	lipocalin 2	NM_008491	9.54	2.10
Signal transduction inhibitor	*Rgs16*	regulator of G-protein signaling 16	NM_011267	4.61	5.06
Protection against oxidative stress	*Mt1*	metallothionein 1	NM_013602	4.17	3.95
Lipid transport; Activation of LPL	*Apoa4*	apolipoprotein A-IV	NM_007468	2.36	6.56
Glucose transporter	*Slc2a2*	solute carrier family 2 (facilitated glucose transporter), member 2	NM_031197	1.92	2.17
Carbohydrate transport and metabolism	*Mfsd2*	major facilitator superfamily domain containing 2	NM_029662	1.68	3.59
Hormone metabolism, heme binding	*Cyp2a5*	cytochrome P450, family 2, subfamily a, polypeptide 5	NM_007812	1.67	1.65
Protection against oxidative stress	*Gstt2*	glutathione S-transferase, theta 2	NM_010361	1.58	1.86
Stimulation of glycogen synthesis	*Ppp1r3c*	protein phosphatase 1, regulatory (inhibitor) subunit 3C	NM_016854	1.57	1.53
Transcription factor	*Bhlhb2*	basic helix-loop-helix domain containing, class B2	NM_011498	1.52	2.35
Regulation of MAP Kinase pathways	*Dusp1*	dual specificity phosphatase 1	NM_013642	1.50	2.15
Acute phase response; Lipid transport	*Saa2*	serum amyloid A 2	NM_011314	9.83	-2.79
Acute phase response; Lipid transport	*Saa1*	serum amyloid A 1	NM_009117	6.30	-3.96
Acute phase response; Lipid transport	*Saa3*	serum amyloid A 3	NM_011315	2.89	-1.82
Regulation of glucose and fatty acid metabolism	*Angptl4*	angiopoietin-like 4	NM_020581	2.30	-2.03
Hemoglobin binding	*Hp*	haptoglobin	NM_017370	2.23	-1.69
Peptidase inhibitor	*Serpina12*	serine (or cysteine) peptidase inhibitor, clade A, member 12	NM_026535	2.01	-2.19
Adipocyte development and triglyceride metabolism	*Lpin1*	lipin 1	NM_015763	1.92	-1.59
Cytokine receptor	*Il6ra*	interleukin 6 receptor, alpha	AK020663	1.70	-2.08
Thyroid hormone metabolism	*Dio1*	deiodinase, iodothyronine, type I	NM_007860	1.57	-1.87
Stimulation of glycogen synthesis	*Ppp1r3b*	protein phosphatase 1, regulatory (inhibitor) subunit 3B	NM_177741	1.55	-1.95
Melanin synthesis	*Dct*	dopachrome tautomerase	NM_010024	1.50	-2.72
Binding pheromones	*Mup4*	major urinary protein 4	NM_008648	1.44	-4.28
Inactivation of all-trans-retinoic acid	*Cyp26b1*	cytochrome P450, family 26, subfamily b, polypeptide 1	NM_175475	-2.39	2.24
Regulation of apoptosis	*Phlda1*	pleckstrin homology-like domain, family A, member 1	NM_009344	-2.20	1.51
Response to stress; Activates MAPKKK cascade	*Gadd45g*	growth arrest and DNA-damage-inducible 45 gamma	NM_011817	-1.97	1.66
Inhibitor of cytokine signaling	*Socs3*	suppressor of cytokine signaling 3	NM_007707	-1.96	1.89
Inhibitor of cytokine signaling	*Cish*	cytokine inducible SH2-containing protein	NM_009895	-1.93	2.37
Antigen processing and presentation	*H2-Aa*	histocompatibility 2, class II antigen A, alpha	NM_010378	-1.81	1.81
Transcription factor	*Egr1*	early growth response 1	NM_007913	-1.77	2.55
Antigen processing and presentation	*H2-Ab1*	histocompatibility 2, class II antigen A, beta 1	NM_207105	-1.77	1.68
Protection against oxidative stress	*Gsta2*	glutathione S-transferase, alpha 2 (Yc2)	NM_008182	-1.71	1.83
Antigen processing and presentation	*H2-Eb1*	histocompatibility 2, class II antigen E beta	NM_010382	-1.63	1.43
Regulation of antigen presentation	*Cd74*	CD74 antigen (invariant polypeptide of major histocompatibility complex, class II antigen-associated)	NM_010545	-1.59	1.65
Oxidation of fatty acids, steroids and xenobiotics	*Cyp4a14*	cytochrome P450, family 4, subfamily a, polypeptide 14	NM_007822	-1.44	6.97
Oxygen transport	*Hbb-b1*	hemoglobin, beta adult major chain	AK010993	-1.42	1.45
Zinc ion binding	*Rnf186*	ring finger protein 186	NM_025786	-1.41	1.81
Maintenance of iron homeostasis	*Hamp1*	hepcidin antimicrobial peptide 1	NM_032541	-1.41	1.73
Unknown	*Creld2*	cysteine-rich with EGF-like domains 2	NM_029720	-3.47	-1.64
Protein folding and response to stress	*Hsph1*	heat shock 105kDa/110kDa protein 1	NM_013559	-2.16	-2.13
Cellular uptake of iron	*Tfr1*	transferrin receptor	NM_011638	-1.92	-1.74
Protein folding and response to stress	*Hspb1*	heat shock protein 1	NM_013560	-1.66	-1.81
Transcription factor	*Hhex*	hematopoietically expressed homeobox	NM_008245	-1.55	-2.05
Initiation of genome replication	*Mcm10*	minichromosome maintenance deficient 10	NM_027290	-1.55	-1.55
Biosynthesis of catecholamine	*Ddc*	dopa decarboxylase	NM_016672	-1.48	-1.97

pink = induced in both models; green = repressed in both models; white = oppositely regulated in both models; FC, fold-change obtained by DNA microarray.

5.7.1.1 Confirmation of hepatic microarray results by Q-RT-PCR

Microarray results for the expression of several genes were confirmed by performing Q-RT-PCR on hepatic samples from 5 *Hfe*$^{-/-}$ mice, 4 wild-type control mice, 5 iron-fed mice and 4 mice fed a standard diet. For this purpose, we selected those genes that are related to iron metabolism and others whose expression was considerably altered in the experimental groups. A total of 29 results from the hepatic microarray data, corresponding to 24 different genes, were tested by Q-RT-PCR, and 27 (93.1%) of them showed concordant results by these two methods (Figures 1 and 2 in **IV**). Changes in *Foxq1* and *Dmt1* expression were false positives in the microarray analysis for *Hfe*$^{-/-}$ and dietary iron overload mice, respectively. The upregulation of *Ltf* expression in the liver of mice with dietary iron overload was confirmed but the expression levels in samples from all but one of the treated mice and all controls were below the detection threshold of the PCR method.

5.7.2 Duodenal gene expression response to *Hfe* deficiency and dietary iron supplementation

Microarray analysis of duodenal RNA from 2 *Hfe*$^{-/-}$ mice and 2 wild-type mice revealed that the expression of 143 genes was upregulated while the expression of 30 genes was downregulated (Appendix 5). Fold-changes range from 15.67 to -3.14. Functional categories overrepresented among the genes regulated by *Hfe* deficiency included proteins with endopeptidase activity, and others involved in lipid catabolism and antimicrobial activity (Table 5 in **IV**).

Global transcriptional regulation was also studied in the duodenum of mice fed an iron-supplemented diet, using 3 treated mice and 2 controls. The expression of 49 genes was induced and 59 genes were repressed (Appendix 6). Fold-changes ranged between 6.07 and -5.64. Functional annotation of the gene list evidenced enrichment of genes involved in glutathione metabolism, antigen processing and presentation as well as the inflammatory response, in addition to other processes (Table 6 in **IV**).

Comparison of the microarray results in the duodenum of *Hfe*$^{-/-}$ versus iron-fed mice revealed limited similarities (Table 7). Genes upregulated in both mouse models were involved in inhibition of apoptosis, detoxification of oxidative stress intermediates, maintenance of the gut barrier and biosynthesis of the cell membrane.

Downregulated genes, conversely, had roles in antimicrobial defense, protein folding and response to stress. Three genes were upregulated in *Hfe*$^{-/-}$ mice and downregulated in the iron-fed mice, coding for proteins involved in the stress response to bacterial colonization, chymotrypsin activity and amino acid transport. The expression of one gene (*Defcr20*), with antimicrobial defense function, was induced by dietary iron supplementation and repressed by Hfe deficiency.

Table 7. *Comparison of genes regulated in the duodenum of mice by Hfe deficiency and dietary iron overload.*

Function	Gene Symbol	Gene name	GenBank Number	FC Hfe$^{-/-}$	FC diet
Lectin; Growth factor; Antiapoptotic	*Reg2*	regenerating islet-derived 2	NM_009043	10.34	2.14
Maintenace of gut barrier	*Alpi*	alkaline phosphatase, intestinal	NM_001081082	2.09	1.71
Detoxification of oxidative stress intermediates	*Akr1b8*	aldo-keto reductase family 1, member B8	NM_008012	1.60	4.17
Membrane phospholipid biosynthesis	*Mboat1*	membrane bound O-acyltransferase domain containing 1	NM_153546	1.46	1.81
Lectin; Stress response to bacterial colonization	*Reg3b*	regenerating islet-derived 3 beta	NM_011036	6.87	-2.13
Chymotripsin activity	*Klk1b27*	kallikrein 1-related peptidase b27	NM_020268	2.22	-1.87
Transport of amino acids	*Slc38a5*	solute carrier family 38, member 5	NM_172479	2.14	-2.31
Antimicrobial defense	*Defcr20*	defensin related cryptdin 20	NM_183268	-2.69	1.72
Protein folding and response to stress	*Hspb1*	heat shock protein 1	NM_013560	-2.07	-2.17
Antimicrobial defense	*Defcr-rs1*	defensin related sequence cryptdin peptide (Paneth cells)	NM_007844	-1.60	-3.23
Unknown	*LOC620017*	PREDICTED: similar to Ig kappa chain V-V region L7 precursor	XM_357633	-1.44	-2.31

pink = induced in both models; green = repressed in both models; white = oppositely regulated in both models; FC, fold-change obtained by DNA microarray.

5.7.2.1 Confirmation of microarray results by Q-RT-PCR

Q-RT-PCR analyses were carried out on duodenal RNA samples from 5 *Hfe*$^{-/-}$ mice, 4 wild-type control mice, 5 iron-fed mice and 4 mice fed a standard diet to verify the microarray results. The mRNA expression of a total of 18 different genes was tested and 17 (94.4%) showed concordant results between microarray analysis and Q-RT-PCR (Figures 3 and 4 in **IV**). The sole discrepant result concerned the expression of *Ddb1* that was downregulated according to the microarray data, while Q-RT-PCR revealed a slight expression induction (1.25-fold).

6. DISCUSSION

6.1 Expression profiles of hemojuvelin and neogenin

The expression of human HJV mRNA had been previously studied by northern blot analysis (Papanikolaou et al. 2004). Our results agreed with the previous data except for the colon, which we found to be positive. We tested some tissues for the first time (the esophagus, stomach, pancreas and ovary) and observed expression of *HJV* in the esophagus and pancreas, while the stomach and ovary were negative. Mouse Hjv mRNA expression had also been analyzed previously by northern blot (Niederkofler et al. 2004). We observed a similar profile except for few tissues, such as the lung, kidney and intestine, where we saw a positive signal. This is probably the result of the higher sensitivity of RT-PCR, compared to northern blot. The expression of Hjv mRNA had not been tested before in the esophagus, stomach, thymus, blood, colon, pancreas, testis, ovary or uterus. We observed the transcript in all of these tissues except for the pancreas, ovary and uterus. A strong positive signal was amplified from the brain and spleen cDNA prepared in our laboratory while no expression was detected in the commercial cDNA samples of these tissues. Our cDNA samples were obtained from 5 BALB/c adult mice and the commercial samples from 200 male/female BALB/c mice 8-12 weeks of age. Thus, the differences in expression between the two types of samples cannot be due to strain differences. It is possible that some age differences exist between the groups, as well as variability between mice of the same strain but from different colonies (see section 6.6). The expression profiles of human and murine hemojuvelin were coincident in several tissues. Hemojuvelin mRNA was detected in the skeletal muscle, heart, esophagus, liver and colon and it was absent in the ovary and brain in both species. The protein expression profile for mouse hemojuvelin proved to be more limited than the manifestation of the transcript. This is probably due to a higher sensitivity of the PCR amplification method as compared to immunodetection methods which depend on the specificity of an antibody.

The results of our western blot analyses of Hjv protein expression showed the existence of two bands of approximately 26 and 30 kDa. Since the publication of our data, several groups have characterized the processing of HJV and tried to offer an explanation for the band sizes observed (Kuninger et al. 2006, Kuninger et al. 2008, Lin et al. 2005, Silvestri et al. 2007, Zhang et al. 2005). According to these experiments, treatment of HJV in reducing conditions causes breakage of its disulfide bonds leading to a smaller N-terminal form of about 14-16 kDa and a longer C-terminal form of 30-35 kDa. The sequence recognized by our antibody is located in the C-terminal part of HJV. Hemojuvelin contains three consensus sequences for N-linked glycosylation, two of them in the C-terminal part of the protein. Furthermore, the level of glycosylation strongly influences the migration distance of the proteins in the SDS-PAGE (Kuninger et al. 2006). Thus, the sizes we observed likely represent different levels of glycosylation of the C-terminal form of hemojuvelin.

Neogenin is mainly known for its role in the regulation of developmental processes, such as neural tube and mammary gland formation, myogenesis and angiogenesis (Cole et al. 2007). Many studies are focused on its role in the development of the central nervous system (De Vries and Cooper 2008). The expression profile of human and mouse NEO1 mRNA has been studied by northern blot (Keeling et al. 1997, Meyerhardt et al. 1997, Vielmetter et al. 1997). The expression profile we observed for mouse Neo1 mRNA by Q-RT-PCR was concordant with that previously shown (Keeling et al. 1997). We extended the existing profile by testing the expression in the testis, colon, esophagus, uterus and pancreas. All these tissues were positive, with very low levels in the pancreas and very high levels in the testis and uterus. Currently, the function of neogenin in reproductive tissues is a completely unexplored subject. We performed the first analysis of mouse neogenin protein expression by immunohistochemistry. The results revealed the localization of neogenin in many tissues, showing interesting cell type specificity in many of them (Figure 5 and Table 4).

6.2 The RNA microarray technique

In this study, we used current RNA microarray technology, a powerful technique that allows expression profiling of the whole transcriptome simultaneously. Validation by Q-RT-PCR revealed that the microarray data was highly reliable (93.5% in the liver and duodenum, 100% in the heart and skeletal muscle). In most cases, the fold-change values obtained by microarray analysis were smaller than those determined by Q-RT-PCR. This phenomenon has been described previously and is probably due to the fact that array analyses are less quantitative than Q-RT-PCR (DeNardo et al. 2005).

6.3 Transcriptional changes in the heart and skeletal muscle of iron-loaded mice

Cardiomyopathy is a common complication in HH patients (Niederau et al. 1996). It is logical to reason that oxidative stress induced by excessive iron in the heart muscle mediates the development of cardiac pathologies in these patients. However, the underlying mechanism at the gene level is unknown. With this study, which is the first work to analyze genome-wide transcriptional regulation induced by iron overload in heart and skeletal muscle, we wanted to shed some light on this question. Particularly, we observed changes in expression of genes involved in cellular stress responses, the regulation of carbohydrate and lipid metabolism and transcription. Most interestingly, some of the genes whose expression was affected by dietary iron overload in the heart and muscle could be involved in the development of cardiomyopathy and diabetes, two pathologies common in HH patients.

The functional categories most overrepresented among the genes regulated in the heart and skeletal muscle were highly coincident. Nevertheless, the degree of agreement when comparing the genes contained in each category, was variable. The expression of several heat-shock proteins was reduced in both tissues as a result of iron overload, a phenomenon that is discussed later. Curiously, iron excess affected the expression of genes encoding myosin and actin proteins, well known for their pivotal function in muscular physiology. Among the enzymes involved in cellular

antioxidant protection, only glutathione peroxidase (Gpx3) had weakly altered transcription (fold-change of 1.35, data not shown) in the iron-loaded heart, probably representing a mechanism of cellular defense against iron-induced oxidative stress. Iron overload affected expression of several transcriptional regulators in the heart and skeletal muscle, although the majority of these genes were different in the two tissues. Interestingly, the transcription factors thioredoxin interacting protein (Txnip) and early growth response 1 (Egr1), both upregulated in the heart tissue of iron-fed mice, are believed to have key regulatory roles in cardiovascular pathological processes (Khachigian 2006, World et al. 2006).

Iron overload in the heart and skeletal muscle did not affect the transcription of many classical iron regulatory genes, such as *Dcytb*, *Dmt1*, *Slc40a1*, *Ferritin*, *Hfe*, *Hjv* or *Tfr2*. In contrast, the mRNA levels of *Tfr1* were reduced by iron overload in both tissues, which is in agreement with the post-transcriptional regulation mediated by the IRP/IRE system. Cellular iron loading reduces IRE-binding activity of IRPs, which renders *Tfr1* mRNA susceptible to degradation.

The presence of hepcidin mRNA in the human heart has been known since the identification of the gene (Krause et al. 2000, Park et al. 2001). Interestingly, in contrast to the liver, in which dietary iron overload results in greatly increased hepcidin expression, we found that cardiac hepcidin mRNA levels are decreased in response to dietary iron overload in the three mouse strains tested, with the exception of the BALB/c females. Moreover, in rats, the effect of hypoxia on hepcidin expression in the liver and the heart is also opposite. This result led others to suggest that cardiac hepcidin expression may have a predominantly local effect in the heart (Merle et al. 2007). According to this hypothesis, and in the context of dietary iron overload, decreased hepcidin expression in the heart may locally help reduce cellular iron burden, although it was insufficient to prevent iron overload in the heart of these mice. However, since the basal expression of hepcidin in the heart is rather low and the regulation is not seen in all the mice, its biological meaning is doubtful and these results should be interpreted with caution.

Angiopoietin-like 4 (Angptl4) mRNA levels were increased in the heart and skeletal muscle of iron-fed mice. Angptl4 is directly involved in regulating glucose homeostasis, lipid metabolism, and insulin sensitivity. Angptl4 inhibits the activity of lipoprotein lipase (LPL), thus inhibiting lipoprotein metabolism and increasing plasma triglyceride levels. Most importantly, transgenic mice with Angptl4

overexpression directed to heart muscle (lipoprotein-derived fatty acids are the major energy source in this tissue) show reduced cardiac LPL activity, decreased triglyceride utilization and impaired cardiac function resulting in cardiomyopathy (Yu et al. 2005). There is a hypothesis about how Angptl4 acts, and it proposes that Angptl4 has LPL-dependent actions (Li 2006). According to this hypothesis, in LPL-expressing tissues (muscle, heart and adipose tissue) Angptl4 acts as an autocrine/paracrine factor, binding directly to LPL and inactivating it locally, thus decreasing the acquisition of free fatty acids to these sites. Conversely, in the liver, which has low LPL expression, Angptl4 is shed to plasma and acts as an endocrine factor, inducing a general reduction of triglyceride utilization. In fact, dietary iron overload leads to increased plasma triglycerides in rats (Brunet et al. 1999). Interestingly, we showed a 5- and 2.26-fold increase in the expression of Angptl4 transcripts in the heart and skeletal muscle of iron-loaded mice, respectively. In contrast, liver expression of Angptl4 was weekly repressed (-1.48). These results raise the possibility that early induction of Angptl4 expression could contribute to the pathogenesis of cardiomyopathy in HH.

Pyruvate dehydrogenase kinase 4 (Pdk4) was also upregulated in both tissues of mice fed an iron-supplemented diet. Pdk4 has hyperglycemic effects. Increased Pdk4 expression and activity has been observed in both skeletal muscle (Feldhoff et al. 1993, Fuller and Randle 1984) and heart (Wu et al. 1998) of insulin-resistant mouse models. However, it is not clear whether Pdk4 overexpression causes insulin resistance or vice versa, but it seems likely that a vicious cycle may exist between these two phenomena.

6.4 Transcriptional changes in the liver of mice with iron overload

The molecular mechanisms of the pathology of iron overload remain obscure. It is not clear how excess iron is related to the clinical features observed in HH patients. The current believe is that iron-generated reactive oxygen species cause lipid peroxidation in the membranes of organelles such as mitochondria (Bacon et al. 1985) and lysosomes (Myers et al. 1991). Additionally, peroxidation of lipids, proteins and DNA is believed to contribute to hepatocyte apoptosis, which will lead

ultimately to fibrosis, cirrhosis and hepatocellular carcinoma (Ramm and Ruddell 2005). The development of hepatocellular carcinoma is commonly associated with HH, affecting approximately 30% of patients with pathological iron deposition in parenchymal tissue (Deugnier and Turlin 2001). It appears that C282Y homozygosity but not heterozygosity increases the risk of developing hepatocellular carcinoma (Cauza et al. 2003). In rats, the effect of iron overload on the development of hepatocellular carcinoma has been studied on several occasions using the carbonyl iron overload model, with controversial results (Asare et al. 2006, Stal et al. 1995, Stal et al. 1999).

According to our results, dietary iron overload in the liver caused transcriptional regulation most robustly in response to oxidative stress and related to acute-phase response, organic acid biosynthesis and cellular iron homeostasis, as well as other processes. Interestingly, the changes observed in the expression of some genes may be implicated in liver hyperplasia, such as the induction of cyclin D1 expression (Brown et al. 2006) and the development of hepatocellular carcinoma, such as the genes encoding inhibitors of DNA binding (Damdinsuren et al. 2005).

The most striking changes in the liver of *Hfe*$^{-/-}$ mice were the downregulation of heat shock proteins and proteins involved in antigen processing and presentation, the overexpression of genes involved in inflammatory responses such as serum amyloids and orosomucoids and the regulation of genes of the cytochrome P450 family.

In these studies we used a mouse model of primary iron overload, induced by *Hfe* disruption, and one model of secondary iron overload, induced enterally. Even though there were some differences in the age of the mice and in the hepatic iron levels between the two models, a comparative analysis of the gene expression response between them may reveal interesting information. Coincident results likely represent gene regulation due to iron overload that is independent of *Hfe*. Opposite results, on the other hand, are probably affected by the presence or absence of Hfe protein, regardless of the iron status. In the first category, there was upregulation of genes that provide protection against oxidative stress (*Mt1* and *Gstt2*), genes involved in transport and metabolism of carbohydrates and lipids (*Apoa4*, *Slc2a2*, *Mfsd2* and *Ppp1r3c*) and Lipocalin2, an APP with antimicrobial properties (Goetz et al. 2002), putative iron transporter (Devireddy et al. 2005) and adipokine with potential importance in insulin resistance associated with obesity (Yan et al. 2007).

Genes with decreased expression in both models included heat shock proteins, Tfr1 and other poorly known genes such as *Creld2*. The functions of genes induced by Hfe deficiency regardless of iron status included acute phase response (*Saa1*, *Saa2* and *Saa3*) and regulation of carbohydrate and lipid metabolism (*Angptl4*, *Lpin1* and *Ppp1r3b*). Genes whose expression was repressed as a result of *Hfe* disruption and independently of iron levels included genes involved in antigen processing and presentation as well as those that regulate cytokine signaling. Hamp1 also presented this pattern of regulation, which had been observed previously by others (Ahmad et al. 2002).

Gene expression profiling had been performed previously in the liver of iron-loaded mice (Table 8). There is one study on genome-wide expression in carbonyl iron-loaded mice (Kautz et al. 2008) in which the authors focused on a few genes whose expression was regulated in the same fashion as that of hepcidin. In comparison with our data, the upregulation of *Id1* was a coincident result.

Table 8. *Comparison of expression studies in the liver of mice with iron overload.*

	Method	**Mouse model**	**Mouse strain and gender**	**Mice age (weeks)**	**Reference**
Iron-loaded mice	Illumina **whole genome** array	2% **carbonyl iron** during 6 weeks	C57BL/6 ♂	16-18	**IV**
	Agilent **whole genome** array	8,3g/Kg **carbonyl iron** during 3 wk	C57BL/6 and DBA/2 ♂	7	(Kautz et al. 2008)
	Dedicated iron array	Iron dextran	129/SvEvTac ♀	8	(Muckenthaler et al. 2003)
	2D-PAGE + MALDI-MS	2% **carbonyl iron** during 8 days	C57BL/6 ♂	5	(Petrak et al. 2007b)
Hfe$^{-/-}$ mice	Illumina **whole genome** array	(Zhou et al. 1998)	C57BL/6 ♂	10	**IV**
	Affimetrix **whole genome** array	(Bahram et al. 1999)	C57BL/6 and DBA/2 ♂	7	(Coppin et al. 2007)
	Dedicated iron array	(Levy et al. 1999b)	C57BL/6 x 129/SvEvTac ♀	8	(Muckenthaler et al. 2003)
	2D-PAGE + MALDI-MS	(Zhou et al. 1998)	C57BL/6 ♂	5	(Petrak et al. 2007a)

The transcriptional response to Hfe deficiency in the liver of mice has also been explored previously (Table 8), and there is one report of a genome-wide analysis (Coppin et al. 2007). Comparing those earlier data with ours, only a few analogous changes in gene expression are found, even for mice of the same genetic

background. In a study using an array of iron-related genes (Muckenthaler et al. 2003) there were several similarities with our data, such as in the upregulation of *Mt1* and *Mt2* and downregulation of *Hamp1*, *Tfr1* and *Hspa5*. Interestingly, metallothioneins (Mt1 and Mt2) have been shown to scavenge harmful oxidant radicals, such as superoxide and hydroxyl radicals (Kumari et al. 1998), thus having a role in protection against oxidative stress.

Our experiments were set to analyze transcriptional changes. It is indeed of great interest to also know the response to iron overload in the liver at the protein level. This has been investigated in recent studies using carbonyl iron-loaded mice (Petrak et al. 2007b) and the same model of *Hfe*$^{-/-}$ mice that was used in this study (Petrak et al. 2007a) (Table 8). There are no similarities in the gene expression profile between these proteomics studies and our data. It should be noted that laboratory mice reach sexual maturity around 8 weeks, and are commonly considered adult by approximately 10-12 weeks (Hedrich 2004). Hence, there is an important age difference between the mice in our experiments and those used in the proteomics studies. Furthermore, the conventional 2D electrophoresis used in the mentioned protein studies has a significant drawback: it identifies soluble, relatively hydrophilic proteins, but not highly hydrophobic membrane proteins (Santoni et al. 2000).

6.5 Transcriptional changes in the duodenum of mice with iron overload

In the duodenum of *Hfe*$^{-/-}$ mice, we observed a strong induction of digestive enzyme genes, including elastases, carboxypeptidases, trypsins, chymotrypsins, amylases, and lipases. This response is not induced by dietary iron overload which, by contrast, caused upregulation of numerous genes encoding antioxidant enzymes of glutathione metabolism. It is known that the enterocytes of *Hfe*$^{-/-}$ mice are iron depleted, whereas in mice fed an iron-supplemented diet the enterocytes are iron-loaded. This fact or the lack of Hfe protein may explain these discrepancies in gene regulation between mice from the two models.

On the other hand, there were also similarities in the duodenal transcriptional response between the two models. These were activation of genes involved in solute

fluxes across epithelia and endothelia (claudins), epithelial repair or protection against intestinal inflammation (*Reg2*) and regulation of the homeostasis with commensal flora (*Alpi*). Likewise, we observed in both models repression of the regulators of the inflammatory response cryptdins.

The global transcriptional response to Hfe deficiency in the duodenum of mice has been explored previously (Table 9) (Coppin et al. 2007). It is notable that only a few analogous changes in gene expression are found when comparing our data with those of the previous study, even for mice of the same genetic background. Two other studies have explored expression of selected genes in the duodenum by using dedicated arrays in *Hfe*$^{-/-}$ mice and in mice with secondary iron overload produced by intraperitoneal injection of iron-dextran (Abgueguen et al. 2006, Muckenthaler et al. 2003). In one report, duodenum samples were analyzed using an array of iron-related genes (Muckenthaler et al. 2003). The results for duodenal gene expression in *Hfe*$^{-/-}$ mice have no concordance with ours. The second study focused on gene expression in the duodenum (Abgueguen et al. 2006), and again, there is little agreement between their observations and ours. The lack of accordance between these studies is probably due to differences in the animal models, age of the mice and in the microarray methodology.

Table 9. *Comparison of expression studies in the duodenum of mice with iron overload.*

	Method	**Mouse model**	**Mouse strain and gender**	**Mice age (weeks)**	**Reference**
Iron-loaded mice	Illumina **whole genome** array	2% **carbonyl iron** during 6 weeks	C57BL/6 ♂	16-18	**IV**
	Dedicated duodenum array	Iron dextran	129/Ola x C57BL/6 x DBA/2	12	(Abgueguen et al. 2006)
	Dedicated iron array	Iron dextran	C57BL/6 x 129/SvEvTac♀	8	(Muckenthaler et al. 2003)
Hfe$^{-/-}$ mice	Illumina **whole genome** array	(Zhou et al. 1998)	C57BL/6 ♂	10	**IV**
	Affimetrix **whole genome** array	(Bahram et al. 1999)	C57BL/6 and DBA/2 ♂	7	(Coppin et al. 2007)
	Dedicated duodenum array	(Bahram et al. 1999)	129/Ola x C57BL/6 x DBA/2	12	(Abgueguen et al. 2006)
	Dedicated iron array	(Levy et al. 1999b)	C57BL/6 x 129/SvEvTac ♀	8	(Muckenthaler et al. 2003)

6.6 General observations

We found repressed expression of many heat shock proteins in the heart, skeletal muscle and liver of mice fed an iron-supplemented diet, as well as in the liver of *Hfe*$^{-/-}$ mice. These genes are known to be induced under certain stress conditions, such as heat and ischemia-reperfusion, their expression can be decreased by iron overload (Brown et al. 2007, Muckenthaler et al. 2003). Currently, the physiological implications of this downregulation are unknown.

According to previous studies, the expression of *Dmt1* is induced in the duodenum of HH patients (Zoller et al. 1999) as well as in *Hfe*$^{-/-}$ mice (Fleming et al. 1999) and in carbonyl iron overloaded mice (Ludwiczek et al. 2004). However, we did not find a significant change in the expression of *Dmt1* in the *Hfe*$^{-/-}$ duodenum. The reason behind this apparent disagreement is that our microarray probes and PCR primers recognize a Dmt1 transcript that does not contain the IRE.

The effect of dietary iron overload on gene expression (represented by the number of genes whose expression is changed) was more pronounced in the liver than in the duodenum, heart or skeletal muscle. This is probably due to the fact that the liver, but not the other tissues, is the primary target of iron loading and that iron accumulation in this tissue is faster and greater.

In our experimental setup we had two mouse models and their corresponding controls. The *Hfe*$^{-/-}$ mice and their wild type littermates were bred in a different place than the mice fed a carbonyl iron-supplemented diet and their controls, fed a standard diet. Taking into account that all the mice belonged to the C57BL/6 strain, we assumed that control mice could be used as a single group for comparisons with either model. Strikingly, the microarray data showed that the samples from control mice from different laboratories diverged highly, while those from the same laboratory clearly grouped together. One reason for such a phenomenon may be the difference in age. The control mice for carbonyl iron loading were 6-8 weeks older than those for *Hfe*$^{-/-}$. Furthermore, it may be that such variability among different colonies of the same strain exists in spite of the same genetic background, due to epigenetic and environmental factors.

6.7 Conclusions

The iron regulatory protein hemojuvelin is expressed in a more limited set of tissues than neogenin. The transcript and protein of both hemojuvelin and neogenin are present in the heart, skeletal muscle and liver. Neogenin protein shows an interesting profile with the highest expression in reproductive organs and the brain.

Dietary iron overload in the heart and skeletal muscle affects the expression of genes that are involved in the regulation of glucose and lipid metabolism, cellular stress responses and regulation of transcription. Some genes may be involved in the development of cardiomyopathy and diabetes, two pathologies common in HH patients.

In the liver of mice with iron overload, regardless of the underlying cause, there is induction of genes involved in transport and metabolism of carbohydrates and lipids and genes encoding antioxidant enzymes. The disruption of *Hfe* induces expression of acute phase reactant genes and represses that of genes involved in antigen processing and presentation. Interestingly, dietary iron overload affected the expression of antioxidant genes and also gene expression that may be implicated in liver hyperplasia and development of hepatocellular carcinoma.

Both models of iron overload, genetic and dietary, show duodenal induction of genes involved in detoxification of oxidative stress intermediates, maintenance of the gut barrier, inhibition of apoptosis and cell membrane biosynthesis. The lack of Hfe protein results in a strong induction of digestive enzyme genes in the duodenum, while the iron-supplemented diet induces many antioxidant enzymes of glutathione metabolism.

The expression studies presented herein reveal many genes of potential interest, most of which are poorly characterized or previously unknown. Their relation with iron metabolism and the pathology of iron overload should be further explored.

ACKNOWLEDGEMENTS

This work was conducted in the Institute of Medical Technology, University of Tampere, during the years 2004-2009.

Firstly, I want to express my deepest gratitude to my supervisor Professor Seppo Parkkila, for granting me the opportunity to work in his laboratory under his guidance. I wish to thank him for his expertise and advice, his support and patience and his never-ending optimism, which have made possible the completion of this study.

I also wish to thank my thesis committee members Professor Terho Lehtimäki and Professor Onni Niemelä for their guidance during my thesis project.

I am very grateful to Professor Markku Heikinheimo and Professor Debbie Trinder for their valuable comments on this thesis.

I want to express my gratitude to all my co-authors for their valuable contributions: Professor Bruce Bacon, Professor Robert Britton, Professor Robert Fleming, Dr. Mika Hilvo, Leena Kytömäki, Tiina Luukkaala, Professor Onni Niemelä, and Dr. Peiwen Pan.

I would like to thank the people in the Finnish DNA microarray Centre at Turku Centre for Biotechnology, especially Päivi Junni, for skilful technical assistance. I wish to say thank you to people working in CSC as well, particularly to Eija Korpelainen and Jarno Tuimala, for their technical support with microarray data analysis.

I am grateful to all the people with whom I have worked in the laboratory during these years: Alise, Anna-Maria, Eeva, Heini, Henna, Jonna, Jukka, Maria, Mikaela, Milla, Piia and specially my officemate Peiwen, for everything she has taught me and above all for her friendship. I wish to give a special thanks to Aulikki for her excellent technical assistance, her ability to find the solution for practically anything and for all the Finnish culture she has taught me on the way. I also want to thank all the people at IMT who have helped me in any way during these years.

I want to express my deepest gratitude to my friends in the distance and my friends “las latinas”, for sharing ups and downs and cheering me up when I most needed it.

Quiero agradecer de todo corazón a mis padres, Adela y Pelegrín, y a mi hermana, Beatriz, por creer en mí y por su apoyo y amor incondicionales, que no conocen distancias.

Finally, my dearest thanks go to Ville for sharing the good and the bad and for his love and patience over the years. I also want to express my gratitude to my “Finnish family” for taking me in and making me feel at home.

This work has been financially supported by the Tampere Graduate School in Biomedicine and Biotechnology (TGSBB).

Tampere, September 2009

Alejandra Rodríguez Martínez

REFERENCES

Abboud S and Haile DJ (2000): A novel mammalian iron-regulated protein involved in intracellular iron metabolism. J Biol Chem 275:19906-19912.

Abgueguen E, Toutain B, Bedrine H, Chicault C, Orhant M, Aubry M, Monnier A, Mottier S, Jouan H, Bahram S, Mosser J and Fergelot P (2006): Differential expression of genes related to HFE and iron status in mouse duodenal epithelium. Mamm Genome 17:430-450.

Adams P, Brissot P and Powell LW (2000): EASL International Consensus Conference on Haemochromatosis. J Hepatol 33:485-504.

Adams PC, Reboussin DM, Barton JC, McLaren CE, Eckfeldt JH, McLaren GD, Dawkins FW, Acton RT, Harris EL, Gordeuk VR, Leiendecker-Foster C, Speechley M, Snively BM, Holup JL, Thomson E and Sholinsky P (2005): Hemochromatosis and iron-overload screening in a racially diverse population. N Engl J Med 352:1769-1778.

Adamsky K, Weizer O, Amariglio N, Breda L, Harmelin A, Rivella S, Rachmilewitz E and Rechavi G (2004): Decreased hepcidin mRNA expression in thalassemic mice. Br J Haematol 124:123-124.

Ahmad KA, Ahmann JR, Migas MC, Waheed A, Britton RS, Bacon BR, Sly WS and Fleming RE (2002): Decreased liver hepcidin expression in the Hfe knockout mouse. Blood Cells Mol Dis 29:361-366.

Aisen P, Enns C and Wessling-Resnick M (2001): Chemistry and biology of eukaryotic iron metabolism. Int J Biochem Cell Biol 33:940-959.

Allen KJ, Gurrin LC, Constantine CC, Osborne NJ, Delatycki MB, Nicoll AJ, McLaren CE, Bahlo M, Nisselle AE, Vulpe CD, Anderson GJ, Southey MC, Giles GG, English DR, Hopper JL, Olynyk JK, Powell LW and Gertig DM (2008): Iron-overload-related disease in HFE hereditary hemochromatosis. N Engl J Med 358:221-230.

Alvarez-Hernandez X, Smith M and Glass J (1998): The effect of apotransferrin on iron release from Caco-2 cells, an intestinal epithelial cell line. Blood 91:3974-3979.

Andrews NC (1999): Disorders of iron metabolism. N Engl J Med 341:1986-1995.

Andrews NC (2000): Iron homeostasis: insights from genetics and animal models. Nat Rev Genet 1:208-217.

Asare GA, Paterson AC, Kew MC, Khan S and Mossanda KS (2006): Iron-free neoplastic nodules and hepatocellular carcinoma without cirrhosis in Wistar rats fed a diet high in iron. J Pathol 208:82-90.

Babitt JL, Huang FW, Wrighting DM, Xia Y, Sidis Y, Samad TA, Campagna JA, Chung RT, Schneyer AL, Woolf CJ, Andrews NC and Lin HY (2006): Bone morphogenetic protein signaling by hemojuvelin regulates hepcidin expression. Nat Genet 38:531-539.

Babitt JL, Huang FW, Xia Y, Sidis Y, Andrews NC and Lin HY (2007): Modulation of bone morphogenetic protein signaling in vivo regulates systemic iron balance. J Clin Invest 117:1933-1939.

Bacon BR, Healey JF, Brittenham GM, Park CH, Nunnari J, Tavill AS and Bonkovsky HL (1986): Hepatic microsomal function in rats with chronic dietary iron overload. Gastroenterology 90:1844-1853.

Bacon BR, Park CH, Brittenham GM, O'Neill R and Tavill AS (1985): Hepatic mitochondrial oxidative metabolism in rats with chronic dietary iron overload. Hepatology 5:789-797.

Bahram S, Gilfillan S, Kuhn LC, Moret R, Schulze JB, Lebeau A and Schumann K (1999): Experimental hemochromatosis due to MHC class I HFE deficiency: immune status and iron metabolism. Proc Natl Acad Sci U S A 96:13312-13317.

Barisani D, Berg CL, Wessling-Resnick M and Gollan JL (1995): Evidence for a low Km transporter for non-transferrin-bound iron in isolated rat hepatocytes. Am J Physiol 269:G570-576.

Bastin JM, Jones M, O'Callaghan CA, Schimanski L, Mason DY and Townsend AR (1998): Kupffer cell staining by an HFE-specific monoclonal antibody: implications for hereditary haemochromatosis. Br J Haematol 103:931-941.

Bayele HK, McArdle H and Srai SK (2006): Cis and trans regulation of hepcidin expression by upstream stimulatory factor. Blood 108:4237-4245.

Bennett MJ, Lebron JA and Bjorkman PJ (2000): Crystal structure of the hereditary haemochromatosis protein HFE complexed with transferrin receptor. Nature 403:46-53.

Beutler E, Felitti VJ, Koziol JA, Ho NJ and Gelbart T (2002): Penetrance of 845G--> A (C282Y) HFE hereditary haemochromatosis mutation in the USA. Lancet 359:211-218.

Beutler E, Gelbart T, Lee P, Trevino R, Fernandez MA and Fairbanks VF (2000): Molecular characterization of a case of atransferrinemia. Blood 96:4071-4074.

Beutler E, Gelbart T, West C, Lee P, Adams M, Blackstone R, Pockros P, Kosty M, Venditti CP, Phatak PD, Seese NK, Chorney KA, Ten Elshof AE, Gerhard GS and

Chorney M (1996): Mutation analysis in hereditary hemochromatosis. Blood Cells Mol Dis 22:187-194; discussion 194a-194b.

Bondi A, Valentino P, Daraio F, Porporato P, Gramaglia E, Carturan S, Gottardi E, Camaschella C and Roetto A (2005): Hepatic expression of hemochromatosis genes in two mouse strains after phlebotomy and iron overload. Haematologica 90:1161-1167.

Breuer W, Hershko C and Cabantchik ZI (2000): The importance of non-transferrin bound iron in disorders of iron metabolism. Transfus Sci 23:185-192.

Bridle KR, Frazer DM, Wilkins SJ, Dixon JL, Purdie DM, Crawford DH, Subramaniam VN, Powell LW, Anderson GJ and Ramm GA (2003): Disrupted hepcidin regulation in HFE-associated haemochromatosis and the liver as a regulator of body iron homoeostasis. Lancet 361:669-673.

Brittenham G (1994): The red cell cycle. In: Iron Metabolism in Health and Disease, pp. 31-62. JH FH Brock, MJ Pippard, LW Powell, Saunders, London.

Britton RS (1996): Metal-induced hepatotoxicity. Semin Liver Dis 16:3-12.

Brown KE, Broadhurst KA, Mathahs MM and Weydert J (2007): Differential expression of stress-inducible proteins in chronic hepatic iron overload. Toxicol Appl Pharmacol 223:180-186.

Brown KE, Mathahs MM, Broadhurst KA and Weydert J (2006): Chronic iron overload stimulates hepatocyte proliferation and cyclin D1 expression in rodent liver. Transl Res 148:55-62.

Brunet S, Thibault L, Delvin E, Yotov W, Bendayan M and Levy E (1999): Dietary iron overload and induced lipid peroxidation are associated with impaired plasma lipid transport and hepatic sterol metabolism in rats. Hepatology 29:1809-1817.

Calzolari A, Raggi C, Deaglio S, Sposi NM, Stafsnes M, Fecchi K, Parolini I, Malavasi F, Peschle C, Sargiacomo M and Testa U (2006): TfR2 localizes in lipid raft domains and is released in exosomes to activate signal transduction along the MAPK pathway. J Cell Sci 119:4486-4498.

Camaschella C (1998): Juvenile haemochromatosis. Baillieres Clin Gastroenterol 12:227-235.

Camaschella C (2005): Understanding iron homeostasis through genetic analysis of hemochromatosis and related disorders. Blood 106:3710-3717.

Camaschella C, Roetto A, Cali A, De Gobbi M, Garozzo G, Carella M, Majorano N, Totaro A and Gasparini P (2000): The gene TFR2 is mutated in a new type of haemochromatosis mapping to 7q22. Nat Genet 25:14-15.

Camaschella C, Roetto A and De Gobbi M (2002): Juvenile hemochromatosis. Semin Hematol 39:242-248.

Canonne-Hergaux F, Gruenheid S, Ponka P and Gros P (1999): Cellular and subcellular localization of the Nramp2 iron transporter in the intestinal brush border and regulation by dietary iron. Blood 93:4406-4417.

Canonne-Hergaux F, Zhang AS, Ponka P and Gros P (2001): Characterization of the iron transporter DMT1 (NRAMP2/DCT1) in red blood cells of normal and anemic mk/mk mice. Blood 98:3823-3830.

Cauza E, Peck-Radosavljevic M, Ulrich-Pur H, Datz C, Gschwantler M, Schoniger-Hekele M, Hackl F, Polli C, Rasoul-Rockenschaub S, Muller C, Wrba F, Gangl A and Ferenci P (2003): Mutations of the HFE gene in patients with hepatocellular carcinoma. Am J Gastroenterol 98:442-447.

Chatterjee IB, Majumder AK, Nandi BK and Subramanian N (1975): Synthesis and some major functions of vitamin C in animals. Ann N Y Acad Sci 258:24-47.

Chen J, Chloupkova M, Gao J, Chapman-Arvedson TL and Enns CA (2007): HFE modulates transferrin receptor 2 levels in hepatoma cells via interactions that differ from transferrin receptor 1-HFE interactions. J Biol Chem 282:36862-36870.

Chen TT, Li L, Chung DH, Allen CD, Torti SV, Torti FM, Cyster JG, Chen CY, Brodsky FM, Niemi EC, Nakamura MC, Seaman WE and Daws MR (2005): TIM-2 is expressed on B cells and in liver and kidney and is a receptor for H-ferritin endocytosis. J Exp Med 202:955-965.

Cherukuri S, Potla R, Sarkar J, Nurko S, Harris ZL and Fox PL (2005): Unexpected role of ceruloplasmin in intestinal iron absorption. Cell Metab 2:309-319.

Cole SJ, Bradford D and Cooper HM (2007): Neogenin: A multi-functional receptor regulating diverse developmental processes. Int J Biochem Cell Biol 39:1569-1575.

Conner SD and Schmid SL (2003): Differential requirements for AP-2 in clathrin-mediated endocytosis. J Cell Biol 162:773-779.

Conrad ME, Benjamin BI, Williams HL and Foy AL (1967): Human absorption of hemoglobin-iron. Gastroenterology 53:5-10.

Conrad ME and Umbreit JN (2002): Pathways of iron absorption. Blood Cells Mol Dis 29:336-355.

Conrad ME, Umbreit JN and Moore EG (1991): A role for mucin in the absorption of inorganic iron and other metal cations. A study in rats. Gastroenterology 100:129-136.

Conrad ME, Umbreit JN, Moore EG, Hainsworth LN, Porubcin M, Simovich MJ, Nakada MT, Dolan K and Garrick MD (2000): Separate pathways for cellular uptake of ferric and ferrous iron. Am J Physiol Gastrointest Liver Physiol 279:G767-774.

Coppin H, Darnaud V, Kautz L, Meynard D, Aubry M, Mosser J, Martinez M and Roth MP (2007): Gene expression profiling of Hfe-/- liver and duodenum in mouse strains with differing susceptibilities to iron loading: identification of transcriptional regulatory targets of Hfe and potential hemochromatosis modifiers. Genome Biol 8:R221.

Cornejo P, Varela P, Videla LA and Fernandez V (2005): Chronic iron overload enhances inducible nitric oxide synthase expression in rat liver. Nitric Oxide 13:54-61.

Courselaud B, Pigeon C, Inoue Y, Inoue J, Gonzalez FJ, Leroyer P, Gilot D, Boudjema K, Guguen-Guillouzo C, Brissot P, Loreal O and Ilyin G (2002): C/EBPalpha regulates hepatic transcription of hepcidin, an antimicrobial peptide and regulator of iron metabolism. Cross-talk between C/EBP pathway and iron metabolism. J Biol Chem 277:41163-41170.

Courselaud B, Troadec MB, Fruchon S, Ilyin G, Borot N, Leroyer P, Coppin H, Brissot P, Roth MP and Loreal O (2004): Strain and gender modulate hepatic hepcidin 1 and 2 mRNA expression in mice. Blood Cells Mol Dis 32:283-289.

Crosby WH (1966): Mucosal block. An evaluation of concepts relating to control of iron absorption. Semin Hematol 3:299-313.

Damdinsuren B, Nagano H, Kondo M, Yamamoto H, Hiraoka N, Yamamoto T, Marubashi S, Miyamoto A, Umeshita K, Dono K, Nakamori S, Wakasa K, Sakon M and Monden M (2005): Expression of Id proteins in human hepatocellular carcinoma: relevance to tumor dedifferentiation. Int J Oncol 26:319-327.

Darshan D and Anderson GJ (2009): Interacting signals in the control of hepcidin expression. Biometals 22:77-87.

Davila-Hicks P, Theil EC and Lonnerdal B (2004): Iron in ferritin or in salts (ferrous sulfate) is equally bioavailable in nonanemic women. Am J Clin Nutr 80:936-940.

De Domenico I, McVey Ward D and Kaplan J (2008): Regulation of iron acquisition and storage: consequences for iron-linked disorders. Nat Rev Mol Cell Biol 9:72-81.

De Domenico I, Ward DM, di Patti MC, Jeong SY, David S, Musci G and Kaplan J (2007a): Ferroxidase activity is required for the stability of cell surface ferroportin in cells expressing GPI-ceruloplasmin. Embo J 26:2823-2831.

De Domenico I, Ward DM, Langelier C, Vaughn MB, Nemeth E, Sundquist WI, Ganz T, Musci G and Kaplan J (2007b): The molecular mechanism of hepcidin-mediated ferroportin down-regulation. Mol Biol Cell 18:2569-2578.

De Domenico I, Ward DM, Musci G and Kaplan J (2006a): Iron overload due to mutations in ferroportin. Haematologica 91:92-95.

De Domenico I, Ward DM, Musci G and Kaplan J (2007c): Evidence for the multimeric structure of ferroportin. Blood 109:2205-2209.

De Domenico I, Ward DM, Nemeth E, Vaughn MB, Musci G, Ganz T and Kaplan J (2005): The molecular basis of ferroportin-linked hemochromatosis. Proc Natl Acad Sci U S A 102:8955-8960.

De Domenico I, Vaughn MB, Li L, Bagley D, Musci G, Ward DM and Kaplan J (2006b): Ferroportin-mediated mobilization of ferritin iron precedes ferritin degradation by the proteasome. Embo J 25:5396-5404.

de Sousa M, Reimao R, Lacerda R, Hugo P, Kaufmann SH and Porto G (1994): Iron overload in beta 2-microglobulin-deficient mice. Immunol Lett 39:105-111.

De Vries M and Cooper HM (2008): Emerging roles for neogenin and its ligands in CNS development. J Neurochem 106:1483-1492.

DeNardo DG, Kim HT, Hilsenbeck S, Cuba V, Tsimelzon A and Brown PH (2005): Global gene expression analysis of estrogen receptor transcription factor cross talk in breast cancer: identification of estrogen-induced/activator protein-1-dependent genes. Mol Endocrinol 19:362-378.

Dennis G, Jr., Sherman BT, Hosack DA, Yang J, Gao W, Lane HC and Lempicki RA (2003): DAVID: Database for Annotation, Visualization, and Integrated Discovery. Genome Biol 4:P3.

Deugnier Y and Turlin B (2001): Iron and hepatocellular carcinoma. J Gastroenterol Hepatol 16:491-494.

Devireddy LR, Gazin C, Zhu X and Green MR (2005): A cell-surface receptor for lipocalin 24p3 selectively mediates apoptosis and iron uptake. Cell 123:1293-1305.

Donovan A, Brownlie A, Zhou Y, Shepard J, Pratt SJ, Moynihan J, Paw BH, Drejer A, Barut B, Zapata A, Law TC, Brugnara C, Lux SE, Pinkus GS, Pinkus JL, Kingsley PD, Palis J, Fleming MD, Andrews NC and Zon LI (2000): Positional cloning of zebrafish ferroportin1 identifies a conserved vertebrate iron exporter. Nature 403:776-781.

Donovan A, Lima CA, Pinkus JL, Pinkus GS, Zon LI, Robine S and Andrews NC (2005): The iron exporter ferroportin/Slc40a1 is essential for iron homeostasis. Cell Metab 1:191-200.

Drake SF, Morgan EH, Herbison CE, Delima R, Graham RM, Chua AC, Leedman PJ, Fleming RE, Bacon BR, Olynyk JK and Trinder D (2007): Iron absorption and hepatic iron uptake are increased in a transferrin receptor 2 (Y245X) mutant mouse model of hemochromatosis type 3. Am J Physiol Gastrointest Liver Physiol 292:G323-328.

Drakesmith H, Schimanski LM, Ormerod E, Merryweather-Clarke AT, Viprakasit V, Edwards JP, Sweetland E, Bastin JM, Cowley D, Chinthammitr Y, Robson KJ

and Townsend AR (2005): Resistance to hepcidin is conferred by hemochromatosis-associated mutations of ferroportin. Blood 106:1092-1097.

Du X, She E, Gelbart T, Truksa J, Lee P, Xia Y, Khovananth K, Mudd S, Mann N, Moresco EM, Beutler E and Beutler B (2008): The serine protease TMPRSS6 is required to sense iron deficiency. Science 320:1088-1092.

Feder JN, Gnirke A, Thomas W, Tsuchihashi Z, Ruddy DA, Basava A, Dormishian F, Domingo R, Jr., Ellis MC, Fullan A, Hinton LM, Jones NL, Kimmel BE, Kronmal GS, Lauer P, Lee VK, Loeb DB, Mapa FA, McClelland E, Meyer NC, Mintier GA, Moeller N, Moore T, Morikang E, Prass CE, Quintana L, Starnes SM, Schatzman RC, Brunke KJ, Drayna DT, Risch NJ, Bacon BR and Wolff RK (1996): A novel MHC class I-like gene is mutated in patients with hereditary haemochromatosis. Nat Genet 13:399-408.

Feder JN, Penny DM, Irrinki A, Lee VK, Lebron JA, Watson N, Tsuchihashi Z, Sigal E, Bjorkman PJ and Schatzman RC (1998): The hemochromatosis gene product complexes with the transferrin receptor and lowers its affinity for ligand binding. Proc Natl Acad Sci U S A 95:1472-1477.

Feder JN, Tsuchihashi Z, Irrinki A, Lee VK, Mapa FA, Morikang E, Prass CE, Starnes SM, Wolff RK, Parkkila S, Sly WS and Schatzman RC (1997): The hemochromatosis founder mutation in HLA-H disrupts beta2-microglobulin interaction and cell surface expression. J Biol Chem 272:14025-14028.

Feldhoff PW, Arnold J, Oesterling B and Vary TC (1993): Insulin-induced activation of pyruvate dehydrogenase complex in skeletal muscle of diabetic rats. Metabolism 42:615-623.

Fergelot P, Ropert-Bouchet M, Abgueguen E, Orhant M, Radosavljevic M, Grimber G, Jouan H, Le Gall JY, Mosser J, Gilfillan S and Bahram S (2002): Iron overload in mice expressing HFE exclusively in the intestinal villi provides evidence that HFE regulates a functional cross-talk between crypt and villi enterocytes. Blood Cells Mol Dis 28:348-360.

Fillet G, Beguin Y and Baldelli L (1989): Model of reticuloendothelial iron metabolism in humans: abnormal behavior in idiopathic hemochromatosis and in inflammation. Blood 74:844-851.

Fleming MD, Romano MA, Su MA, Garrick LM, Garrick MD and Andrews NC (1998): Nramp2 is mutated in the anemic Belgrade (b) rat: evidence of a role for Nramp2 in endosomal iron transport. Proc Natl Acad Sci U S A 95:1148-1153.

Fleming MD, Trenor CC, 3rd, Su MA, Foernzler D, Beier DR, Dietrich WF and Andrews NC (1997): Microcytic anaemia mice have a mutation in Nramp2, a candidate iron transporter gene. Nat Genet 16:383-386.

Fleming RE, Britton RS, Waheed A, Sly WS and Bacon BR (2005): Pathophysiology of hereditary hemochromatosis. Semin Liver Dis 25:411-419.

Fleming RE, Migas MC, Holden CC, Waheed A, Britton RS, Tomatsu S, Bacon BR and Sly WS (2000): Transferrin receptor 2: continued expression in mouse liver in the face of iron overload and in hereditary hemochromatosis. Proc Natl Acad Sci U S A 97:2214-2219.

Fleming RE, Migas MC, Zhou X, Jiang J, Britton RS, Brunt EM, Tomatsu S, Waheed A, Bacon BR and Sly WS (1999): Mechanism of increased iron absorption in murine model of hereditary hemochromatosis: increased duodenal expression of the iron transporter DMT1. Proc Natl Acad Sci U S A 96:3143-3148.

Fleming RE and Sly WS (2002): Mechanisms of iron accumulation in hereditary hemochromatosis. Annu Rev Physiol 64:663-680.

Folgueras AR, de Lara FM, Pendas AM, Garabaya C, Rodriguez F, Astudillo A, Bernal T, Cabanillas R, Lopez-Otin C and Velasco G (2008): Membrane-bound serine protease matriptase-2 (Tmprss6) is an essential regulator of iron homeostasis. Blood 112:2539-2545.

Frazer DM, Wilkins SJ, Becker EM, Murphy TL, Vulpe CD, McKie AT and Anderson GJ (2003): A rapid decrease in the expression of DMT1 and Dcytb but not Ireg1 or hephaestin explains the mucosal block phenomenon of iron absorption. Gut 52:340-346.

Frazer DM, Wilkins SJ, Becker EM, Vulpe CD, McKie AT, Trinder D and Anderson GJ (2002): Hepcidin expression inversely correlates with the expression of duodenal iron transporters and iron absorption in rats. Gastroenterology 123:835-844.

Fuller SJ and Randle PJ (1984): Reversible phosphorylation of pyruvate dehydrogenase in rat skeletal-muscle mitochondria. Effects of starvation and diabetes. Biochem J 219:635-646.

Galy B, Ferring-Appel D, Kaden S, Grone HJ and Hentze MW (2008): Iron regulatory proteins are essential for intestinal function and control key iron absorption molecules in the duodenum. Cell Metab 7:79-85.

Giannetti AM and Bjorkman PJ (2004): HFE and transferrin directly compete for transferrin receptor in solution and at the cell surface. J Biol Chem 279:25866-25875.

Glahn RP and Van Campen DR (1997): Iron uptake is enhanced in Caco-2 cell monolayers by cysteine and reduced cysteinyl glycine. J Nutr 127:642-647.

Goetz DH, Holmes MA, Borregaard N, Bluhm ME, Raymond KN and Strong RK (2002): The neutrophil lipocalin NGAL is a bacteriostatic agent that interferes with siderophore-mediated iron acquisition. Mol Cell 10:1033-1043.

Gomme PT, McCann KB and Bertolini J (2005): Transferrin: structure, function and potential therapeutic actions. Drug Discov Today 10:267-273.

Goncalves AS, Muzeau F, Blaybel R, Hetet G, Driss F, Delaby C, Canonne-Hergaux F and Beaumont C (2006): Wild-type and mutant ferroportins do not form oligomers in transfected cells. Biochem J 396:265-275.

Goswami T and Andrews NC (2006): Hereditary hemochromatosis protein, HFE, interaction with transferrin receptor 2 suggests a molecular mechanism for mammalian iron sensing. J Biol Chem 281:28494-28498.

Graham RM, Reutens GM, Herbison CE, Delima RD, Chua AC, Olynyk JK and Trinder D (2008): Transferrin receptor 2 mediates uptake of transferrin-bound and non-transferrin-bound iron. J Hepatol 48:327-334.

Grootveld M, Bell JD, Halliwell B, Aruoma OI, Bomford A and Sadler PJ (1989): Non-transferrin-bound iron in plasma or serum from patients with idiopathic hemochromatosis. Characterization by high performance liquid chromatography and nuclear magnetic resonance spectroscopy. J Biol Chem 264:4417-4422.

Gunshin H, Fujiwara Y, Custodio AO, Direnzo C, Robine S and Andrews NC (2005): Slc11a2 is required for intestinal iron absorption and erythropoiesis but dispensable in placenta and liver. J Clin Invest 115:1258-1266.

Gunshin H, Mackenzie B, Berger UV, Gunshin Y, Romero MF, Boron WF, Nussberger S, Gollan JL and Hediger MA (1997): Cloning and characterization of a mammalian proton-coupled metal-ion transporter. Nature 388:482-488.

Han O, Failla ML, Hill AD, Morris ER and Smith JC, Jr. (1995): Reduction of Fe(III) is required for uptake of nonheme iron by Caco-2 cells. J Nutr 125:1291-1299.

Harris ZL, Takahashi Y, Miyajima H, Serizawa M, MacGillivray RT and Gitlin JD (1995): Aceruloplasminemia: molecular characterization of this disorder of iron metabolism. Proc Natl Acad Sci U S A 92:2539-2543.

Harrison PM, Fischbach FA, Hoy TG and Haggis GH (1967): Ferric oxyhydroxide core of ferritin. Nature 216:1188-1190.

Hedrich HB, GR (2004): The laboratory mouse. Academic Press, New York.

Hentze MW and Kuhn LC (1996): Molecular control of vertebrate iron metabolism: mRNA-based regulatory circuits operated by iron, nitric oxide, and oxidative stress. Proc Natl Acad Sci U S A 93:8175-8182.

Hentze MW, Muckenthaler MU and Andrews NC (2004): Balancing acts: molecular control of mammalian iron metabolism. Cell 117:285-297.

Houglum K, Filip M, Witztum JL and Chojkier M (1990): Malondialdehyde and 4-hydroxynonenal protein adducts in plasma and liver of rats with iron overload. J Clin Invest 86:1991-1998.

Huang FW, Pinkus JL, Pinkus GS, Fleming MD and Andrews NC (2005): A mouse model of juvenile hemochromatosis. J Clin Invest 115:2187-2191.

Hvidberg V, Maniecki MB, Jacobsen C, Hojrup P, Moller HJ and Moestrup SK (2005): Identification of the receptor scavenging hemopexin-heme complexes. Blood 106:2572-2579.

Ilyin G, Courselaud B, Troadec MB, Pigeon C, Alizadeh M, Leroyer P, Brissot P and Loreal O (2003): Comparative analysis of mouse hepcidin 1 and 2 genes: evidence for different patterns of expression and co-inducibility during iron overload. FEBS Lett 542:22-26.

Inman RS, Coughlan MM and Wessling-Resnick M (1994): Extracellular ferrireductase activity of K562 cells is coupled to transferrin-independent iron transport. Biochemistry 33:11850-11857.

Jeong SY and David S (2003): Glycosylphosphatidylinositol-anchored ceruloplasmin is required for iron efflux from cells in the central nervous system. J Biol Chem 278:27144-27148.

Johnson MB, Chen J, Murchison N, Green FA and Enns CA (2007): Transferrin receptor 2: evidence for ligand-induced stabilization and redirection to a recycling pathway. Mol Biol Cell 18:743-754.

Johnson MB and Enns CA (2004): Diferric transferrin regulates transferrin receptor 2 protein stability. Blood 104:4287-4293.

Kang JO, Jones C and Brothwell B (1998): Toxicity associated with iron overload found in hemochromatosis: possible mechanism in a rat model. Clin Lab Sci 11:350-354.

Kang JS, Yi MJ, Zhang W, Feinleib JL, Cole F and Krauss RS (2004): Netrins and neogenin promote myotube formation. J Cell Biol 167:493-504.

Kautz L, Meynard D, Monnier A, Darnaud V, Bouvet R, Wang RH, Deng C, Vaulont S, Mosser J, Coppin H and Roth MP (2008): Iron regulates phosphorylation of Smad1/5/8 and gene expression of Bmp6, Smad7, Id1, and Atoh8 in the mouse liver. Blood 112:1503-1509.

Kawabata H, Fleming RE, Gui D, Moon SY, Saitoh T, O'Kelly J, Umehara Y, Wano Y, Said JW and Koeffler HP (2005): Expression of hepcidin is down-regulated in TfR2 mutant mice manifesting a phenotype of hereditary hemochromatosis. Blood 105:376-381.

Kawabata H, Yang R, Hirama T, Vuong PT, Kawano S, Gombart AF and Koeffler HP (1999): Molecular cloning of transferrin receptor 2. A new member of the transferrin receptor-like family. J Biol Chem 274:20826-20832.

Kawakami H and Lonnerdal B (1991): Isolation and function of a receptor for human lactoferrin in human fetal intestinal brush-border membranes. Am J Physiol 261:G841-846.

Keel SB, Doty RT, Yang Z, Quigley JG, Chen J, Knoblaugh S, Kingsley PD, De Domenico I, Vaughn MB, Kaplan J, Palis J and Abkowitz JL (2008): A heme export protein is required for red blood cell differentiation and iron homeostasis. Science 319:825-828.

Keeling SL, Gad JM and Cooper HM (1997): Mouse Neogenin, a DCC-like molecule, has four splice variants and is expressed widely in the adult mouse and during embryogenesis. Oncogene 15:691-700.

Khachigian LM (2006): Early growth response-1 in cardiovascular pathobiology. Circ Res 98:186-191.

Khan MF, Wu X, Tipnis UR, Ansari GA and Boor PJ (2002): Protein adducts of malondialdehyde and 4-hydroxynonenal in livers of iron loaded rats: quantitation and localization. Toxicology 173:193-201.

Kozyraki R, Fyfe J, Verroust PJ, Jacobsen C, Dautry-Varsat A, Gburek J, Willnow TE, Christensen EI and Moestrup SK (2001): Megalin-dependent cubilin-mediated endocytosis is a major pathway for the apical uptake of transferrin in polarized epithelia. Proc Natl Acad Sci U S A 98:12491-12496.

Krause A, Neitz S, Magert HJ, Schulz A, Forssmann WG, Schulz-Knappe P and Adermann K (2000): LEAP-1, a novel highly disulfide-bonded human peptide, exhibits antimicrobial activity. FEBS Lett 480:147-150.

Krijt J, Cmejla R, Sykora V, Vokurka M, Vyoral D and Necas E (2004): Different expression pattern of hepcidin genes in the liver and pancreas of C57BL/6N and DBA/2N mice. J Hepatol 40:891-896.

Kristiansen M, Graversen JH, Jacobsen C, Sonne O, Hoffman HJ, Law SK and Moestrup SK (2001): Identification of the haemoglobin scavenger receptor. Nature 409:198-201.

Kumari MV, Hiramatsu M and Ebadi M (1998): Free radical scavenging actions of metallothionein isoforms I and II. Free Radic Res 29:93-101.

Kuninger D, Kuns-Hashimoto R, Kuzmickas R and Rotwein P (2006): Complex biosynthesis of the muscle-enriched iron regulator RGMc. J Cell Sci 119:3273-3283.

Kuninger D, Kuns-Hashimoto R, Nili M and Rotwein P (2008): Pro-protein convertases control the maturation and processing of the iron-regulatory protein, RGMc/hemojuvelin. BMC Biochem 9:9.

Kuo YM, Su T, Chen H, Attieh Z, Syed BA, McKie AT, Anderson GJ, Gitschier J and Vulpe CD (2004): Mislocalisation of hephaestin, a multicopper ferroxidase

involved in basolateral intestinal iron transport, in the sex linked anaemia mouse. Gut 53:201-206.

Laftah AH, Latunde-Dada GO, Fakih S, Hider RC, Simpson RJ and McKie AT (2008): Haem and folate transport by proton-coupled folate transporter/haem carrier protein 1 (SLC46A1). Br J Nutr1-7.

Latunde-Dada GO, Takeuchi K, Simpson RJ and McKie AT (2006): Haem carrier protein 1 (HCP1): Expression and functional studies in cultured cells. FEBS Lett 580:6865-6870.

Lebron JA, Bennett MJ, Vaughn DE, Chirino AJ, Snow PM, Mintier GA, Feder JN and Bjorkman PJ (1998): Crystal structure of the hemochromatosis protein HFE and characterization of its interaction with transferrin receptor. Cell 93:111-123.

Lebron JA, West AP, Jr. and Bjorkman PJ (1999): The hemochromatosis protein HFE competes with transferrin for binding to the transferrin receptor. J Mol Biol 294:239-245.

Lesbordes-Brion JC, Viatte L, Bennoun M, Lou DQ, Ramey G, Houbron C, Hamard G, Kahn A and Vaulont S (2006): Targeted disruption of the hepcidin 1 gene results in severe hemochromatosis. Blood 108:1402-1405.

Levy JE, Jin O, Fujiwara Y, Kuo F and Andrews NC (1999a): Transferrin receptor is necessary for development of erythrocytes and the nervous system. Nat Genet 21:396-399.

Levy JE, Montross LK, Cohen DE, Fleming MD and Andrews NC (1999b): The C282Y mutation causing hereditary hemochromatosis does not produce a null allele. Blood 94:9-11.

Li C (2006): Genetics and regulation of angiopoietin-like proteins 3 and 4. Curr Opin Lipidol 17:152-156.

Lin L, Goldberg YP and Ganz T (2005): Competitive regulation of hepcidin mRNA by soluble and cell-associated hemojuvelin. Blood 106:2884-2889.

Lin L, Nemeth E, Goodnough JB, Thapa DR, Gabayan V and Ganz T (2008): Soluble hemojuvelin is released by proprotein convertase-mediated cleavage at a conserved polybasic RNRR site. Blood Cells Mol Dis 40:122-131.

Liu XB, Yang F and Haile DJ (2005): Functional consequences of ferroportin 1 mutations. Blood Cells Mol Dis 35:33-46.

Liuzzi JP, Aydemir F, Nam H, Knutson MD and Cousins RJ (2006): Zip14 (Slc39a14) mediates non-transferrin-bound iron uptake into cells. Proc Natl Acad Sci U S A 103:13612-13617.

Lonnerdal B (2007): The importance and bioavailability of phytoferritin-bound iron in cereals and legume foods. Int J Vitam Nutr Res 77:152-157.

Lonnerdal B and Bryant A (2006): Absorption of iron from recombinant human lactoferrin in young US women. Am J Clin Nutr 83:305-309.

Lou DQ, Nicolas G, Lesbordes JC, Viatte L, Grimber G, Szajnert MF, Kahn A and Vaulont S (2004): Functional differences between hepcidin 1 and 2 in transgenic mice. Blood 103:2816-2821.

Ludwiczek S, Theurl I, Artner-Dworzak E, Chorney M and Weiss G (2004): Duodenal HFE expression and hepcidin levels determine body iron homeostasis: modulation by genetic diversity and dietary iron availability. J Mol Med 82:373-382.

Ma Y, Specian RD, Yeh KY, Yeh M, Rodriguez-Paris J and Glass J (2002): The transcytosis of divalent metal transporter 1 and apo-transferrin during iron uptake in intestinal epithelium. Am J Physiol Gastrointest Liver Physiol 283:G965-974.

Masini A, Ceccarelli D, Trenti T, Corongiu FP and Muscatello U (1989): Perturbation in liver mitochondrial Ca2+ homeostasis in experimental iron overload: a possible factor in cell injury. Biochim Biophys Acta 1014:133-140.

Matsunaga E, Tauszig-Delamasure S, Monnier PP, Mueller BK, Strittmatter SM, Mehlen P and Chedotal A (2004): RGM and its receptor neogenin regulate neuronal survival. Nat Cell Biol 6:749-755.

McGregor JA, Shayeghi M, Vulpe CD, Anderson GJ, Pietrangelo A, Simpson RJ and McKie AT (2005): Impaired iron transport activity of ferroportin 1 in hereditary iron overload. J Membr Biol 206:3-7.

McKie AT, Barrow D, Latunde-Dada GO, Rolfs A, Sager G, Mudaly E, Mudaly M, Richardson C, Barlow D, Bomford A, Peters TJ, Raja KB, Shirali S, Hediger MA, Farzaneh F and Simpson RJ (2001): An iron-regulated ferric reductase associated with the absorption of dietary iron. Science 291:1755-1759.

McKie AT, Marciani P, Rolfs A, Brennan K, Wehr K, Barrow D, Miret S, Bomford A, Peters TJ, Farzaneh F, Hediger MA, Hentze MW and Simpson RJ (2000): A novel duodenal iron-regulated transporter, IREG1, implicated in the basolateral transfer of iron to the circulation. Mol Cell 5:299-309.

McLaren GD, Nathanson MH, Jacobs A, Trevett D and Thomson W (1991): Regulation of intestinal iron absorption and mucosal iron kinetics in hereditary hemochromatosis. J Lab Clin Med 117:390-401.

Merle U, Fein E, Gehrke SG, Stremmel W and Kulaksiz H (2007): The iron regulatory peptide hepcidin is expressed in the heart and regulated by hypoxia and inflammation. Endocrinology 148:2663-2668.

Meyerhardt JA, Look AT, Bigner SH and Fearon ER (1997): Identification and characterization of neogenin, a DCC-related gene. Oncogene 14:1129-1136.

Monnier PP, Sierra A, Macchi P, Deitinghoff L, Andersen JS, Mann M, Flad M, Hornberger MR, Stahl B, Bonhoeffer F and Mueller BK (2002): RGM is a repulsive guidance molecule for retinal axons. Nature 419:392-395.

Montosi G, Donovan A, Totaro A, Garuti C, Pignatti E, Cassanelli S, Trenor CC, Gasparini P, Andrews NC and Pietrangelo A (2001): Autosomal-dominant hemochromatosis is associated with a mutation in the ferroportin (SLC11A3) gene. J Clin Invest 108:619-623.

Morey JS, Ryan JC and Van Dolah FM (2006): Microarray validation: factors influencing correlation between oligonucleotide microarrays and real-time PCR. Biol Proced Online 8:175-193.

Morgan EH (1981): Inhibition of reticulocyte iron uptake by NH4Cl and CH3NH2. Biochim Biophys Acta 642:119-134.

Muckenthaler M, Gray NK and Hentze MW (1998): IRP-1 binding to ferritin mRNA prevents the recruitment of the small ribosomal subunit by the cap-binding complex eIF4F. Mol Cell 2:383-388.

Muckenthaler M, Roy CN, Custodio AO, Minana B, deGraaf J, Montross LK, Andrews NC and Hentze MW (2003): Regulatory defects in liver and intestine implicate abnormal hepcidin and Cybrd1 expression in mouse hemochromatosis. Nat Genet 34:102-107.

Muckenthaler MU, Galy B and Hentze MW (2008): Systemic iron homeostasis and the iron-responsive element/iron-regulatory protein (IRE/IRP) regulatory network. Annu Rev Nutr 28:197-213.

Munro HN (1986): Back to basics: an evolutionary odyssey with reflections on the nutrition research of tomorrow. Annu Rev Nutr 6:1-12.

Mwanjewe J and Grover AK (2004): Role of transient receptor potential canonical 6 (TRPC6) in non-transferrin-bound iron uptake in neuronal phenotype PC12 cells. Biochem J 378:975-982.

Myers BM, Prendergast FG, Holman R, Kuntz SM and LaRusso NF (1991): Alterations in the structure, physicochemical properties, and pH of hepatocyte lysosomes in experimental iron overload. J Clin Invest 88:1207-1215.

Nemeth E, Rivera S, Gabayan V, Keller C, Taudorf S, Pedersen BK and Ganz T (2004a): IL-6 mediates hypoferremia of inflammation by inducing the synthesis of the iron regulatory hormone hepcidin. J Clin Invest 113:1271-1276.

Nemeth E, Roetto A, Garozzo G, Ganz T and Camaschella C (2005): Hepcidin is decreased in TFR2 hemochromatosis. Blood 105:1803-1806.

Nemeth E, Tuttle MS, Powelson J, Vaughn MB, Donovan A, Ward DM, Ganz T and Kaplan J (2004b): Hepcidin regulates cellular iron efflux by binding to ferroportin and inducing its internalization. Science 306:2090-2093.

Nicolas G, Bennoun M, Devaux I, Beaumont C, Grandchamp B, Kahn A and Vaulont S (2001): Lack of hepcidin gene expression and severe tissue iron overload in upstream stimulatory factor 2 (USF2) knockout mice. Proc Natl Acad Sci U S A 98:8780-8785.

Nicolas G, Bennoun M, Porteu A, Mativet S, Beaumont C, Grandchamp B, Sirito M, Sawadogo M, Kahn A and Vaulont S (2002a): Severe iron deficiency anemia in transgenic mice expressing liver hepcidin. Proc Natl Acad Sci U S A 99:4596-4601.

Nicolas G, Chauvet C, Viatte L, Danan JL, Bigard X, Devaux I, Beaumont C, Kahn A and Vaulont S (2002b): The gene encoding the iron regulatory peptide hepcidin is regulated by anemia, hypoxia, and inflammation. J Clin Invest 110:1037-1044.

Nicolas G, Viatte L, Lou DQ, Bennoun M, Beaumont C, Kahn A, Andrews NC and Vaulont S (2003): Constitutive hepcidin expression prevents iron overload in a mouse model of hemochromatosis. Nat Genet 34:97-101.

Niederau C, Fischer R, Purschel A, Stremmel W, Haussinger D and Strohmeyer G (1996): Long-term survival in patients with hereditary hemochromatosis. Gastroenterology 110:1107-1119.

Niederkofler V, Salie R and Arber S (2005): Hemojuvelin is essential for dietary iron sensing, and its mutation leads to severe iron overload. J Clin Invest 115:2180-2186.

Niederkofler V, Salie R, Sigrist M and Arber S (2004): Repulsive guidance molecule (RGM) gene function is required for neural tube closure but not retinal topography in the mouse visual system. J Neurosci 24:808-818.

Nunez MT and Tapia V (1999): Transferrin stimulates iron absorption, exocytosis, and secretion in cultured intestinal cells. Am J Physiol 276:C1085-1090.

Oates PS (2007): The relevance of the intestinal crypt and enterocyte in regulating iron absorption. Pflugers Arch 455:201-213.

Ohgami RS, Campagna DR, Greer EL, Antiochos B, McDonald A, Chen J, Sharp JJ, Fujiwara Y, Barker JE and Fleming MD (2005): Identification of a ferrireductase required for efficient transferrin-dependent iron uptake in erythroid cells. Nat Genet 37:1264-1269.

Ohgami RS, Campagna DR, McDonald A and Fleming MD (2006): The Steap proteins are metalloreductases. Blood 108:1388-1394.

Olynyk JK, Cullen DJ, Aquilia S, Rossi E, Summerville L and Powell LW (1999): A population-based study of the clinical expression of the hemochromatosis gene. N Engl J Med 341:718-724.

Oudit GY, Sun H, Trivieri MG, Koch SE, Dawood F, Ackerley C, Yazdanpanah M, Wilson GJ, Schwartz A, Liu PP and Backx PH (2003): L-type Ca2+ channels

provide a major pathway for iron entry into cardiomyocytes in iron-overload cardiomyopathy. Nat Med 9:1187-1194.

Oudit GY, Trivieri MG, Khaper N, Liu PP and Backx PH (2006): Role of L-type Ca2+ channels in iron transport and iron-overload cardiomyopathy. J Mol Med 84:349-364.

Pan PW, Rodriguez A and Parkkila S (2007): A systematic quantification of carbonic anhydrase transcripts in the mouse digestive system. BMC Mol Biol 8:22.

Papanikolaou G, Samuels ME, Ludwig EH, MacDonald ML, Franchini PL, Dube MP, Andres L, MacFarlane J, Sakellaropoulos N, Politou M, Nemeth E, Thompson J, Risler JK, Zaborowska C, Babakaiff R, Radomski CC, Pape TD, Davidas O, Christakis J, Brissot P, Lockitch G, Ganz T, Hayden MR and Goldberg YP (2004): Mutations in HFE2 cause iron overload in chromosome 1q-linked juvenile hemochromatosis. Nat Genet 36:77-82.

Park CH, Bacon BR, Brittenham GM and Tavill AS (1987): Pathology of dietary carbonyl iron overload in rats. Lab Invest 57:555-563.

Park CH, Valore EV, Waring AJ and Ganz T (2001): Hepcidin, a urinary antimicrobial peptide synthesized in the liver. J Biol Chem 276:7806-7810.

Parkes JG, Randell EW, Olivieri NF and Templeton DM (1995): Modulation by iron loading and chelation of the uptake of non-transferrin-bound iron by human liver cells. Biochim Biophys Acta 1243:373-380.

Parkkila S, Niemela O, Britton RS, Fleming RE, Waheed A, Bacon BR and Sly WS (2001): Molecular aspects of iron absorption and HFE expression. Gastroenterology 121:1489-1496.

Parkkila S, Waheed A, Britton RS, Bacon BR, Zhou XY, Tomatsu S, Fleming RE and Sly WS (1997a): Association of the transferrin receptor in human placenta with HFE, the protein defective in hereditary hemochromatosis. Proc Natl Acad Sci U S A 94:13198-13202.

Parkkila S, Waheed A, Britton RS, Feder JN, Tsuchihashi Z, Schatzman RC, Bacon BR and Sly WS (1997b): Immunohistochemistry of HLA-H, the protein defective in patients with hereditary hemochromatosis, reveals unique pattern of expression in gastrointestinal tract. Proc Natl Acad Sci U S A 94:2534-2539.

Petrak J, Myslivcova D, Halada P, Cmejla R, Cmejlova J, Vyoral D and Vulpe CD (2007a): Iron-independent specific protein expression pattern in the liver of HFE-deficient mice. Int J Biochem Cell Biol 39:1006-1015.

Petrak J, Myslivcova D, Man P, Cmejla R, Cmejlova J, Vyoral D, Elleder M and Vulpe CD (2007b): Proteomic analysis of hepatic iron overload in mice suggests dysregulation of urea cycle, impairment of fatty acid oxidation, and changes in the methylation cycle. Am J Physiol Gastrointest Liver Physiol 292:G1490-1498.

Peyssonnaux C, Zinkernagel AS, Schuepbach RA, Rankin E, Vaulont S, Haase VH, Nizet V and Johnson RS (2007): Regulation of iron homeostasis by the hypoxia-inducible transcription factors (HIFs). J Clin Invest 117:1926-1932.

Pigeon C, Ilyin G, Courselaud B, Leroyer P, Turlin B, Brissot P and Loreal O (2001): A new mouse liver-specific gene, encoding a protein homologous to human antimicrobial peptide hepcidin, is overexpressed during iron overload. J Biol Chem 276:7811-7819.

Ponka P (1997): Tissue-specific regulation of iron metabolism and heme synthesis: distinct control mechanisms in erythroid cells. Blood 89:1-25.

Ponka P and Lok CN (1999): The transferrin receptor: role in health and disease. Int J Biochem Cell Biol 31:1111-1137.

Poss KD and Tonegawa S (1997): Heme oxygenase 1 is required for mammalian iron reutilization. Proc Natl Acad Sci U S A 94:10919-10924.

Qiu A, Jansen M, Sakaris A, Min SH, Chattopadhyay S, Tsai E, Sandoval C, Zhao R, Akabas MH and Goldman ID (2006): Identification of an intestinal folate transporter and the molecular basis for hereditary folate malabsorption. Cell 127:917-928.

Raje CI, Kumar S, Harle A, Nanda JS and Raje M (2007): The macrophage cell surface glyceraldehyde-3-phosphate dehydrogenase is a novel transferrin receptor. J Biol Chem 282:3252-3261.

Ramm GA (2000): Animal models of iron overload based on excess exogenous iron. In: Hemochromatosis: Genetics, Pathophysiology, Diagnosis and treatment, pp. 494-507. JC Bartonand CQ Edwards, Cambridge University Press, New York.

Ramm GA and Ruddell RG (2005): Hepatotoxicity of iron overload: mechanisms of iron-induced hepatic fibrogenesis. Semin Liver Dis 25:433-449.

Robb A and Wessling-Resnick M (2004): Regulation of transferrin receptor 2 protein levels by transferrin. Blood 104:4294-4299.

Roberts FD, Charalambous P, Fletcher L, Powell LW and Halliday JW (1993): Effect of chronic iron overload on procollagen gene expression. Hepatology 18:590-595.

Roeser HP, Lee GR, Nacht S and Cartwright GE (1970): The role of ceruloplasmin in iron metabolism. J Clin Invest 49:2408-2417.

Roetto A, Daraio F, Alberti F, Porporato P, Cali A, De Gobbi M and Camaschella C (2002): Hemochromatosis due to mutations in transferrin receptor 2. Blood Cells Mol Dis 29:465-470.

Roetto A, Papanikolaou G, Politou M, Alberti F, Girelli D, Christakis J, Loukopoulos D and Camaschella C (2003): Mutant antimicrobial peptide hepcidin is associated with severe juvenile hemochromatosis. Nat Genet 33:21-22.

Roy CN, Mak HH, Akpan I, Losyev G, Zurakowski D and Andrews NC (2007): Hepcidin antimicrobial peptide transgenic mice exhibit features of the anemia of inflammation. Blood 109:4038-4044.

Sacher A, Cohen A and Nelson N (2001): Properties of the mammalian and yeast metal-ion transporters DCT1 and Smf1p expressed in Xenopus laevis oocytes. J Exp Biol 204:1053-1061.

Santoni V, Molloy M and Rabilloud T (2000): Membrane proteins and proteomics: un amour impossible? Electrophoresis 21:1054-1070.

Santos M, Schilham MW, Rademakers LH, Marx JJ, de Sousa M and Clevers H (1996): Defective iron homeostasis in beta 2-microglobulin knockout mice recapitulates hereditary hemochromatosis in man. J Exp Med 184:1975-1985.

Sarkar J, Seshadri V, Tripoulas NA, Ketterer ME and Fox PL (2003): Role of ceruloplasmin in macrophage iron efflux during hypoxia. J Biol Chem 278:44018-44024.

Schaer DJ, Alayash AI and Buehler PW (2007): Gating the radical hemoglobin to macrophages: the anti-inflammatory role of CD163, a scavenger receptor. Antioxid Redox Signal 9:991-999.

Schmidt PJ, Toran PT, Giannetti AM, Bjorkman PJ and Andrews NC (2008): The transferrin receptor modulates Hfe-dependent regulation of hepcidin expression. Cell Metab 7:205-214.

Sharp P and Srai SK (2007): Molecular mechanisms involved in intestinal iron absorption. World J Gastroenterol 13:4716-4724.

Shayeghi M, Latunde-Dada GO, Oakhill JS, Laftah AH, Takeuchi K, Halliday N, Khan Y, Warley A, McCann FE, Hider RC, Frazer DM, Anderson GJ, Vulpe CD, Simpson RJ and McKie AT (2005): Identification of an intestinal heme transporter. Cell 122:789-801.

Silvestri L, Pagani A and Camaschella C (2008a): Furin-mediated release of soluble hemojuvelin: a new link between hypoxia and iron homeostasis. Blood 111:924-931.

Silvestri L, Pagani A, Fazi C, Gerardi G, Levi S, Arosio P and Camaschella C (2007): Defective targeting of hemojuvelin to plasma membrane is a common pathogenetic mechanism in juvenile hemochromatosis. Blood 109:4503-4510.

Silvestri L, Pagani A, Nai A, De Domenico I, Kaplan J and Camaschella C (2008b): The serine protease matriptase-2 (TMPRSS6) inhibits hepcidin activation by cleaving membrane hemojuvelin. Cell Metab 8:502-511.

Smith A and Hunt RC (1990): Hemopexin joins transferrin as representative members of a distinct class of receptor-mediated endocytic transport systems. Eur J Cell Biol 53:234-245.

Smith A and Morgan WT (1978): Transport of heme by hemopexin to the liver: evidence for receptor-mediated uptake. Biochem Biophys Res Commun 84:151-157.

Smith A and Morgan WT (1979): Haem transport to the liver by haemopexin. Receptor-mediated uptake with recycling of the protein. Biochem J 182:47-54.

Smith SR, Ghosh MC, Ollivierre-Wilson H, Hang Tong W and Rouault TA (2006): Complete loss of iron regulatory proteins 1 and 2 prevents viability of murine zygotes beyond the blastocyst stage of embryonic development. Blood Cells Mol Dis 36:283-287.

Stal P, Hultcrantz R, Moller L and Eriksson LC (1995): The effects of dietary iron on initiation and promotion in chemical hepatocarcinogenesis. Hepatology 21:521-528.

Stal P, Wang GS, Olsson JM and Eriksson LC (1999): Effects of dietary iron overload on progression in chemical hepatocarcinogenesis. Liver 19:326-334.

Sturrock A, Alexander J, Lamb J, Craven CM and Kaplan J (1990): Characterization of a transferrin-independent uptake system for iron in HeLa cells. J Biol Chem 265:3139-3145.

Surgenor DM, Koechlin BA and Strong LE (1949): Chemical, Clinical, and Immunological Studies on the Products of Human Plasma Fractionation. Xxxvii. the Metal-Combining Globulin of Human Plasma. J Clin Invest 28:73-78.

Swain JH, Tabatabai LB and Reddy MB (2002): Histidine content of low-molecular-weight beef proteins influences nonheme iron bioavailability in Caco-2 cells. J Nutr 132:245-251.

Tanno T, Bhanu NV, Oneal PA, Goh SH, Staker P, Lee YT, Moroney JW, Reed CH, Luban NL, Wang RH, Eling TE, Childs R, Ganz T, Leitman SF, Fucharoen S and Miller JL (2007): High levels of GDF15 in thalassemia suppress expression of the iron regulatory protein hepcidin. Nat Med 13:1096-1101.

Torrance JD and Bothwell TH (1968): A simple technique for measuring storage iron concentrations in formalinised liver samples. S Afr J Med Sci 33:9-11.

Trinder D, Olynyk JK, Sly WS and Morgan EH (2002): Iron uptake from plasma transferrin by the duodenum is impaired in the Hfe knockout mouse. Proc Natl Acad Sci U S A 99:5622-5626.

Truksa J, Peng H, Lee P and Beutler E (2006): Bone morphogenetic proteins 2, 4, and 9 stimulate murine hepcidin 1 expression independently of Hfe, transferrin receptor 2 (Tfr2), and IL-6. Proc Natl Acad Sci U S A 103:10289-10293.

Umbreit JN, Conrad ME, Hainsworth LN and Simovich M (2002): The ferrireductase paraferritin contains divalent metal transporter as well as mobilferrin. Am J Physiol Gastrointest Liver Physiol 282:G534-539.

Umbreit JN, Conrad ME, Moore EG, Desai MP and Turrens J (1996): Paraferritin: a protein complex with ferrireductase activity is associated with iron absorption in rats. Biochemistry 35:6460-6469.

Waheed A, Parkkila S, Saarnio J, Fleming RE, Zhou XY, Tomatsu S, Britton RS, Bacon BR and Sly WS (1999): Association of HFE protein with transferrin receptor in crypt enterocytes of human duodenum. Proc Natl Acad Sci U S A 96:1579-1584.

Waheed A, Parkkila S, Zhou XY, Tomatsu S, Tsuchihashi Z, Feder JN, Schatzman RC, Britton RS, Bacon BR and Sly WS (1997): Hereditary hemochromatosis: effects of C282Y and H63D mutations on association with beta2-microglobulin, intracellular processing, and cell surface expression of the HFE protein in COS-7 cells. Proc Natl Acad Sci U S A 94:12384-12389.

Wallace DF, Summerville L and Subramaniam VN (2007): Targeted disruption of the hepatic transferrin receptor 2 gene in mice leads to iron overload. Gastroenterology 132:301-310.

van Renswoude J, Bridges KR, Harford JB and Klausner RD (1982): Receptor-mediated endocytosis of transferrin and the uptake of fe in K562 cells: identification of a nonlysosomal acidic compartment. Proc Natl Acad Sci U S A 79:6186-6190.

Vandesompele J, De Preter K, Pattyn F, Poppe B, Van Roy N, De Paepe A and Speleman F (2002): Accurate normalization of real-time quantitative RT-PCR data by geometric averaging of multiple internal control genes. Genome Biol 3:RESEARCH0034.

Wang RH, Li C, Xu X, Zheng Y, Xiao C, Zerfas P, Cooperman S, Eckhaus M, Rouault T, Mishra L and Deng CX (2005): A role of SMAD4 in iron metabolism through the positive regulation of hepcidin expression. Cell Metab 2:399-409.

Weinstein DA, Roy CN, Fleming MD, Loda MF, Wolfsdorf JI and Andrews NC (2002): Inappropriate expression of hepcidin is associated with iron refractory anemia: implications for the anemia of chronic disease. Blood 100:3776-3781.

Weizer-Stern O, Adamsky K, Margalit O, Ashur-Fabian O, Givol D, Amariglio N and Rechavi G (2007): Hepcidin, a key regulator of iron metabolism, is transcriptionally activated by p53. Br J Haematol 138:253-262.

Verga Falzacappa MV, Casanovas G, Hentze MW and Muckenthaler MU (2008): A bone morphogenetic protein (BMP)-responsive element in the hepcidin promoter

controls HFE2-mediated hepatic hepcidin expression and its response to IL-6 in cultured cells. J Mol Med 86:531-540.

Verga Falzacappa MV, Vujic Spasic M, Kessler R, Stolte J, Hentze MW and Muckenthaler MU (2007): STAT3 mediates hepatic hepcidin expression and its inflammatory stimulation. Blood 109:353-358.

West AP, Jr., Bennett MJ, Sellers VM, Andrews NC, Enns CA and Bjorkman PJ (2000): Comparison of the interactions of transferrin receptor and transferrin receptor 2 with transferrin and the hereditary hemochromatosis protein HFE. J Biol Chem 275:38135-38138.

West AR and Oates PS (2008): Mechanisms of heme iron absorption: current questions and controversies. World J Gastroenterol 14:4101-4110.

Vielmetter J, Chen XN, Miskevich F, Lane RP, Yamakawa K, Korenberg JR and Dreyer WJ (1997): Molecular characterization of human neogenin, a DCC-related protein, and the mapping of its gene (NEO1) to chromosomal position 15q22.3-q23. Genomics 41:414-421.

Wixom RL, Prutkin L and Munro HN (1980): Hemosiderin: nature, formation, and significance. Int Rev Exp Pathol 22:193-225.

World CJ, Yamawaki H and Berk BC (2006): Thioredoxin in the cardiovascular system. J Mol Med 84:997-1003.

Wrighting DM and Andrews NC (2006): Interleukin-6 induces hepcidin expression through STAT3. Blood 108:3204-3209.

Wu P, Sato J, Zhao Y, Jaskiewicz J, Popov KM and Harris RA (1998): Starvation and diabetes increase the amount of pyruvate dehydrogenase kinase isoenzyme 4 in rat heart. Biochem J 329 (Pt 1):197-201.

Wu WH, Meydani M, Meydani SN, Burklund PM, Blumberg JB and Munro HN (1990): Effect of dietary iron overload on lipid peroxidation, prostaglandin synthesis and lymphocyte proliferation in young and old rats. J Nutr 120:280-289.

Vujic Spasic M, Kiss J, Herrmann T, Kessler R, Stolte J, Galy B, Rathkolb B, Wolf E, Stremmel W, Hentze MW and Muckenthaler MU (2007): Physiologic systemic iron metabolism in mice deficient for duodenal Hfe. Blood 109:4511-4517.

Vulpe CD, Kuo YM, Murphy TL, Cowley L, Askwith C, Libina N, Gitschier J and Anderson GJ (1999): Hephaestin, a ceruloplasmin homologue implicated in intestinal iron transport, is defective in the sla mouse. Nat Genet 21:195-199.

Xia Y, Babitt JL, Sidis Y, Chung RT and Lin HY (2008): Hemojuvelin regulates hepcidin expression via a selective subset of BMP ligands and receptors independently of neogenin. Blood 111:5195-5204.

Yan QW, Yang Q, Mody N, Graham TE, Hsu CH, Xu Z, Houstis NE, Kahn BB and Rosen ED (2007): The adipokine lipocalin 2 is regulated by obesity and promotes insulin resistance. Diabetes 56:2533-2540.

Yang F, West AP, Jr., Allendorph GP, Choe S and Bjorkman PJ (2008): Neogenin interacts with hemojuvelin through its two membrane-proximal fibronectin type III domains. Biochemistry 47:4237-4245.

Yu PB, Hong CC, Sachidanandan C, Babitt JL, Deng DY, Hoyng SA, Lin HY, Bloch KD and Peterson RT (2008): Dorsomorphin inhibits BMP signals required for embryogenesis and iron metabolism. Nat Chem Biol 4:33-41.

Yu X, Burgess SC, Ge H, Wong KK, Nassem RH, Garry DJ, Sherry AD, Malloy CR, Berger JP and Li C (2005): Inhibition of cardiac lipoprotein utilization by transgenic overexpression of Angptl4 in the heart. Proc Natl Acad Sci U S A 102:1767-1772.

Zhang AS, Anderson SA, Meyers KR, Hernandez C, Eisenstein RS and Enns CA (2007): Evidence that inhibition of hemojuvelin shedding in response to iron is mediated through neogenin. J Biol Chem 282:12547-12556.

Zhang AS, West AP, Jr., Wyman AE, Bjorkman PJ and Enns CA (2005): Interaction of hemojuvelin with neogenin results in iron accumulation in human embryonic kidney 293 cells. J Biol Chem 280:33885-33894.

Zhang AS, Xiong S, Tsukamoto H and Enns CA (2004): Localization of iron metabolism-related mRNAs in rat liver indicate that HFE is expressed predominantly in hepatocytes. Blood 103:1509-1514.

Zhou XY, Tomatsu S, Fleming RE, Parkkila S, Waheed A, Jiang J, Fei Y, Brunt EM, Ruddy DA, Prass CE, Schatzman RC, O'Neill R, Britton RS, Bacon BR and Sly WS (1998): HFE gene knockout produces mouse model of hereditary hemochromatosis. Proc Natl Acad Sci U S A 95:2492-2497.

Zoller H, Pietrangelo A, Vogel W and Weiss G (1999): Duodenal metal-transporter (DMT-1, NRAMP-2) expression in patients with hereditary haemochromatosis. Lancet 353:2120-2123.

SUPPLEMENTARY DATA

Appendix 1. *Functional annotation of genes regulated in the heart of iron-fed mice.*

Functional Category	Gene Symbol	Description	GenBank Number	FC	Q-PCR
Protein folding and response to stress	*Hspb1*	heat shock protein 1	NM_013560	-1.48	
	Hspcb	heat shock protein 1, beta	NM_008302	-1.49	
	Hspca	heat shock protein 1, alpha	NM_010480	-1.53	
	Dnajb1	DnaJ (Hsp40) homolog, subfamily B, member 1	NM_018808	-1.90	-2.70
	Hspa1b	heat shock protein 1B	NM_010478	-2.25	-8.78
	Hsp105	heat shock protein 105	NM_013559	-2.25	
Carbohydrate metabolic process	*Pdk4*	pyruvate dehydrogenase kinase, isoenzyme 4	NM_013743	2.06	3.76
	Fbp2	fructose bisphosphatase 2	NM_007994	1.40	
	Ppp1r3c	protein phosphatase 1, regulatory (inhibitor) subunit 3C	NM_016854	-1.44	
	Acdc	adipocyte, C1Q and collagen domain containing	NM_009605	-1.50	
Regulation of angiogenesis	*Angptl4*	angiopoietin-like 4	NM_020581	2.79	5.06
	Cited2	Cbp/p300-interacting transactivator, with Glu/Asp-rich carboxy-terminal domain, 2	NM_010828	1.41	
	Adamts1	a disintegrin-like and metalloprotease (reprolysin type) with thrombospondin type 1 motif, 1	NM_009621	1.40	
Motor activity	*Myl7*	myosin, light polypeptide 7, regulatory	NM_008182	7.68	9.85
	Myl4	myosin, light polypeptide 4, alkali	NM_008184	6.32	10.03
	Myh7	myosin, heavy polypeptide 7, cardiac muscle, beta	NM_025569	1.42	
	Acta1	actin, alpha 1, skeletal muscle	NM_010359	-2.79	-3.26
Calcium ion binding	*Myl7*	myosin, light polypeptide 7, regulatory	NM_022879	7.68	
	Myl4	myosin, light polypeptide 4, alkali	NM_010858	6.32	
	S100a8	S100 calcium binding protein A8 (calgranulin A)	NM_013650	1.96	2.88
	S100a9	S100 calcium binding protein A9 (calgranulin B)	NM_009114	1.95	3.09
	Chordc1	cysteine and histidine-rich domain (CHORD)-containing, zinc-binding protein 1	NM_025844	-1.40	
Regulation of progression through cell cycle	*Fos*	FBJ osteosarcoma oncogene	NM_010234	1.49	2.33
	Cited2	Cbp/p300-interacting transactivator, with Glu/Asp-rich carboxy-terminal domain, 2	NM_010828	1.41	
	Cdkn1a	cyclin-dependent kinase inhibitor 1A	NM_007669	-1.49	
Negative regulation of apoptosis	*Angptl4*	angiopoietin-like 4	NM_020581	2.79	5.06
	Cdkn1a	cyclin-dependent kinase inhibitor 1A	NM_007669	-1.49	
	Hspa1b	heat shock protein 1B	NM_010478	-2.25	-8.78
Transcriptional regulation	*Txnip*	thioredoxin interacting protein	NM_023719	1.78	
	Dbp	D site albumin promoter binding protein	NM_016974	1.65	
	Fos	FBJ osteosarcoma oncogene	NM_010234	1.49	2.33
	Egr1	early growth response 1	NM_007913	1.46	
	Irx3	Iroquois related homeobox 3 (Drosophila)	NM_008393	1.43	
	Cited2	Cbp/p300-interacting transactivator, with Glu/Asp-rich carboxy-terminal domain, 2	NM_010828	1.41	
	Idb1	inhibitor of DNA binding 1	NM_010495	-1.40	
	Sox18	SRY-box containing gene 18	NM_009236	-1.42	

Appendix 2. *Functional annotation of genes regulated in the skeletal muscle of iron-fed mice.*

Functional Category	Gene Symbol	Description	GenBank Number	FC	Q-PCR
Protein folding and response to stress	*Hspb1*	heat shock protein 1	NM_013560	-1.48	
	Hspa1a	heat shock protein 1A	NM_010479	-1.48	
	Hsp105	heat shock protein 105	NM_013559	-1.72	
	Hspca	heat shock protein 1, alpha	NM_010480	-1.91	
	Hspa1b	Heat shock protein 1B	NM_010478	-2.4	-3.77
	Dnajb1	DnaJ (Hsp40) homolog, subfamily B, member 1	NM_018808	-2.52	-4.61
Regulation of angiogenesis	*Cited2*	Cbp/p300-interacting transactivator, with Glu/Asp-rich carboxy-terminal domain, 2	NM_010828	1.46	
	Angptl4	angiopoietin-like 4	NM_020581	1.45	2.26
	Ctgf	connective tissue growth factor	NM_010217	-1.59	
	Idb1	inhibitor of DNA binding 1	NM_010495	-1.66	
Carbohydrate metabolic process	*Pdk4*	pyruvate dehydrogenase kinase, isoenzyme 4	NM_013743	1.4	1.59
	Pfkfb3	6-phosphofructo-2-kinase/fructose-2,6-biphosphatase 3	NM_133232	1.4	
	Atf3	activating transcription factor 3	NM_007498	-1.49	
Calcium ion binding	*S100a8*	Calgranulin A, S100 calcium binding protein A8	NM_013650	2.8	4.44
	S100a9	Calgranulin B, S100 calcium binding protein A9	NM_009114	2.26	6.42
	Myl2	Myosin light polypeptide 2	NM_010861	1.6	
	Slc25a25	solute carrier family 25 (mitochondrial carrier, phosphate carrier), member 25	NM_146118	-2.22	
Actin cytosqueleton organization and biogenesis	*S100a9*	Calgranulin B, S100 calcium binding protein A9	NM_009114	2.26	
	Myl2	Myosin light polypeptide 2	NM_010861	1.6	
	Actc1	actin, alpha, cardiac	NM_009608	-1.46	
Negative regulation of apoptosis	*Angptl4*	angiopoietin-like 4	NM_020581	1.45	2.26
	Cdkn1a	cyclin-dependent kinase inhibitor 1A	NM_007669	-1.62	
	Hspa1b	Heat shock protein 1B	NM_010478	-2.4	-3.77
Transcriptional regulation	*Cited2*	Cbp/p300-interacting transactivator, with Glu/Asp-rich carboxy-terminal domain, 2	NM_010828	1.46	
	Fosl2	fos-like antigen 2	NM_008037	-1.42	
	Atf3	activating transcription factor 3	NM_007498	-1.49	
	Pdlim1	PDZ and LIM domain 1	NM_016861	-1.51	
	Nfil3	nuclear factor, interleukin 3, regulated	NM_017373	-1.64	
	Klf4	Kruppel-like factor 4	NM_010637	-1.65	
	Idb1	inhibitor of DNA binding 1	NM_010495	-1.66	
	Egr3	early growth response 3	NM_018781	-1.79	
	Fos	FBJ osteosarcoma oncogene	NM_010234	-2.1	-2.40
Cell adhesion	*Mllt4*	myeloid/lymphoid or mixed lineage-leukemia	XM_890447	1.4	
	Col1a1	procollagen, type I, alpha 1	NM_007742	-1.41	
	Nedd9	neural precursor cell expressed, developmentally down-regulated gene 9	NM_017464	-1.58	
	Ctgf	connective tissue growth factor	NM_010217	-1.59	

Appendix 3. *Genes that display altered mRNA expression in the liver of Hfe$^{-/-}$ mice.*

FC	P value	Symbol	Description	GenBank no	Illumina probe	Q-RT-PCR
9.83	0.039	Saa2	serum amyloid A 2	NM_011314	1090139	39.36
9.54	0.013	Lcn2	lipocalin 2	NM_008491	2510112	19.95
6.30	0.039	Saa1	serum amyloid A 1	NM_009117	5390520	16.36
4.61	0.025	Rgs16	regulator of G-protein signaling 16	NM_011267	780091	
4.17	0.039	Mt1	metallothionein 1	NM_013602	4850164	5.35
4.12	0.027	Moxd1	monooxygenase, DBH-like 1	NM_021509	2450301	
3.29	0.068	Orm2	orosomucoid 2	NM_011016	2100048	
2.89	0.222	Saa3	serum amyloid A 3	NM_011315	6510390	
2.38	0.132	G6pc	glucose-6-phosphatase, catalytic	NM_008061	430093	
2.36	0.105	Apoa4	apolipoprotein A-IV	NM_007468	102450537	
2.30	0.132	Angptl4	angiopoietin-like 4	NM_020581	6760593	1.67
2.23	0.132	Hp	haptoglobin	NM_017370	2940551	
2.09	0.168	Apoa4	apolipoprotein A-IV	NM_007468	4120451	
2.01	0.301	Serpina12	serine (or cysteine) peptidase inhibitor, clade A (alpha-1 antiproteinase, antitrypsin), member 12	NM_026535	1230128	
1.92	0.263	Slc2a2	solute carrier family 2 (facilitated glucose transporter), member 2	NM_031197	6770079	
1.92	0.274	Lpin1	lipin 1	NM_015763	102940241	
1.89	0.301	Slco1b2	solute carrier organic anion transporter family, member 1b2	NM_020495	610605	
1.71	0.301	Gna14	guanine nucleotide binding protein, alpha 14	NM_008137	3390017	
1.70	0.301	G0s2	G0/G1 switch gene 2	NM_008059	6550020	
1.70	0.301	Il6ra	interleukin 6 receptor, alpha	AK020663	102640121	
1.68	0.301	Mfsd2	major facilitator superfamily domain containing 2	NM_029662	1400594	
1.68	0.301	Orm1	orosomucoid 1	NM_008768	1500563	
1.67	0.301	Ugt1a6a	UDP glucuronosyltransferase 1 family, polypeptide A6A	NM_145079	6900086	
1.67	0.301	Cyp2a5	cytochrome P450, family 2, subfamily a, polypeptide 5	NM_007812	4070632	
1.66	0.301	AI132487	expressed sequence AI132487	NM_001012310	5720048	
1.65	0.301	Slc46a3	solute carrier family 46, member 3	NM_027872	6840484	2.25
1.65	0.301	Wfdc2	WAP four-disulfide core domain 2	NM_026323	2900465	
1.64	0.304	Wdfy1	WD repeat and FYVE domain containing 1	NM_027057	101170044	
1.64	0.301	Cyp27a1	cytochrome P450, family 27, subfamily a, polypeptide 1	NM_024264	4050195	
1.63	0.301	D11Ertd636e	DNA segment, Chr 11, ERATO Doi 636, expressed	NM_029794	5260427	
1.63	0.301	Serpina3n	serine (or cysteine) peptidase inhibitor, clade A, member 3N	NM_009252	5340400	
1.62	0.301	Plg	plasminogen	NM_008877	3360270	
1.62	0.301	Sfrs5	splicing factor, arginine/serine-rich 5 (SRp40, HRS)	NM_009159	6350008	
1.62	0.324	Sbk1	SH3-binding kinase 1	NM_145587	940452	
1.61	0.301	Vasn	vasorin	NM_139307	1770722	
1.61	0.301	Rnase4	ribonuclease, RNase A family 4	NM_201239	6900519	
1.60	0.301	Ugt1a6b	UDP glucuronosyltransferase 1 family, polypeptide A6B	NM_201410	4810601	
1.59	0.301	Lcn13	lipocalin 13	NM_153558	6110435	
1.59	0.301	Slc6a9	solute carrier family 6 (neurotransmitter transporter, glycine), member 9	NM_008135	2470520	
1.59	0.306	Mela	melanoma antigen	NM_008581	104560161	
1.59	0.301	Cyp2d26	cytochrome P450, family 2, subfamily d, polypeptide 26	NM_029562	780021	
1.59	0.304	Cyp2a5	cytochrome P450, family 2, subfamily a, polypeptide 5	NM_007812	6380047	
1.58	0.301	Slc2a2	solute carrier family 2 (facilitated glucose transporter), member 2	NM_031197	5720722	
1.58	0.301	Gstt2	glutathione S-transferase, theta 2	NM_010361	1580519	
1.57	0.323	Slc39a4	solute carrier family 39 (zinc transporter), member 4	NM_028064	450717	
1.57	0.330	Dio1	deiodinase, iodothyronine, type I	NM_007860	5420148	
1.57	0.306	AI428936	expressed sequence AI428936	NM_153577	2650433	
1.57	0.324	Ppp1r3c	protein phosphatase 1, regulatory (inhibitor) subunit 3C	NM_016854	2640170	
1.56	0.306	1810011O10Rik	RIKEN cDNA 1810011O10 gene	NM_026931	840670	
1.55	0.330	Mt2	metallothionein 2	NM_008630	6860286	
1.55	0.318	Ppp1r3b	protein phosphatase 1, regulatory (inhibitor) subunit 3B	NM_177741	101450309	
1.54	0.323	Hspd1	heat shock protein 1 (chaperonin)	NM_010477	60097	

1.54	0.323	Hadhb	hydroxyacyl-Coenzyme A dehydrogenase/3-ketoacyl-Coenzyme A thiolase/enoyl-Coenzyme A hydratase (trifunctional protein), beta subunit	NM_145558	60064
1.52	0.323	Tmem50a	transmembrane protein 50A	NM_027935	2690440
1.52	0.346	Bhlhb2	basic helix-loop-helix domain containing, class B2	NM_011498	7040603
1.52	0.330	Acaa2	acetyl-Coenzyme A acyltransferase 2 (mitochondrial 3-oxoacyl-Coenzyme A thiolase)	NM_177470	2360324
1.51	0.330	Dcn	decorin	NM_007833	5900711
1.51	0.330	Lrg1	leucine-rich alpha-2-glycoprotein 1	NM_029796	5690605
1.51	0.330	Prei4	hypothetical Glycerophosphoryl diester phosphodiesterase/Glycosyl hydrolase, starch-binding domain containing protein	AK030645	101990368
1.51	0.330	1500003O03Rik	RIKEN cDNA 1500003O03 gene	NM_019769	1050239
1.50	0.361	Dct	dopachrome tautomerase	NM_010024	3840494
1.50	0.396	Dusp1	dual specificity phosphatase 1	NM_013642	6860121
1.50	0.333	Ppp1r3b	protein phosphatase 1, regulatory (inhibitor) subunit 3B	NM_177741	6130253
1.50	0.333	Psmb8	proteasome (prosome, macropain) subunit, beta type 8 (large multifunctional peptidase 7)	NM_010724	100780427
1.50	0.333	Fn1	fibronectin 1	NM_010233	2970647
1.49	0.333	Ppap2b	phosphatidic acid phosphatase type 2B	NM_080555	4730280
1.49	0.346	Lbp	lipopolysaccharide binding protein	NM_008489	6860019
1.48	0.348	Txnip	thioredoxin interacting protein	NM_023719	102640017
1.48	0.341	Pcsk4	proprotein convertase subtilisin/kexin type 4	NM_008793	130687
1.48	0.341	Kmo	kynurenine 3-monooxygenase (kynurenine 3-hydroxylase)	NM_133809	101660358
1.48	0.361	Dio1	deiodinase, iodothyronine, type I	NM_007860	5290112
1.48	0.361	Pklr	pyruvate kinase liver and red blood cell	NM_013631	2470114
1.48	0.361	Dct	dopachrome tautomerase	NM_010024	1090347
1.48	0.348	Itih4	inter alpha-trypsin inhibitor, heavy chain 4	NM_018746	4210411
1.47	0.342	C1s	complement component 1, s subcomponent	NM_144938	6840114
1.47	0.361	Hnrpa2b1	heterogeneous nuclear ribonucleoprotein A2/B1	NM_182650	6200494
1.45	0.361	Thrsp	thyroid hormone responsive SPOT14 homolog (Rattus)	AK050300	102690609
1.45	0.361	Fgl1	fibrinogen-like protein 1	NM_145594	2350358
1.44	0.388	Eif4ebp3	eukaryotic translation initiation factor 4E binding protein 3	NM_201256	1230725
1.44	0.361	Nsdhl	NAD(P) dependent steroid dehydrogenase-like	NM_010941	3360402
1.44	0.396	Mup4	major urinary protein 4	NM_008648	670253
1.44	0.371	Tsc22d3	TSC22 domain family 3	NM_010286	6510072
1.43	0.361	Es31	PREDICTED: esterase 31	XM_356125	3290458
1.43	0.377	Col4a2	procollagen, type IV, alpha 2	NM_009932	2350619
1.42	0.406	Apcs	serum amyloid P-component	NM_011318	2060500
1.41	0.230	Nsdhl	NAD(P) dependent steroid dehydrogenase-like	NM_010941	6380563
-1.41	0.232	Rnf186	ring finger protein 186	NM_025786	520286
-1.41	0.233	Hamp1	hepcidin antimicrobial peptide 1	NM_032541	4920112
-1.42	0.396	Ddc	dopa decarboxylase	NM_016672	670408
-1.42	0.385	Hbb-b1	hemoglobin, beta adult major chain	AK010993	101660133
-1.42	0.396	Hmgcs1	3-hydroxy-3-methylglutaryl-Coenzyme A synthase 1	NM_145942	6620452
-1.43	0.369	Ddah1	dimethylarginine dimethylaminohydrolase 1	NM_026993	6400750
-1.44	0.371	Cyp4a14	cytochrome P450, family 4, subfamily a, polypeptide 14	NM_007822	2370110
-1.45	0.361	Ddah1	dimethylarginine dimethylaminohydrolase 1	NM_026993	107000184
-1.45	0.361	H47	histocompatibility 47	NM_024439	1190161
-1.45	0.361	Lss	lanosterol synthase	NM_146006	3170129
-1.46	0.361	Iigp2	interferon inducible GTPase 2	NM_019440	6110440
-1.47	0.361	Slc25a25	solute carrier family 25 (mitochondrial carrier, phosphate carrier), member 25	NM_146118	1230605
-1.48	0.341	Hsp90ab1	heat shock protein 90kDa alpha (cytosolic), class B member 1	NM_008302	3170358
-1.48	0.361	Ddc	dopa decarboxylase	NM_016672	102850113
-1.50	0.361	Hmgcr	3-hydroxy-3-methylglutaryl-Coenzyme A reductase	NM_008255	2630242
-1.51	0.330	5033411D12Rik	RIKEN cDNA 5033411D12 gene	NM_138654	2320471
-1.52	0.330	Gsta2	glutathione S-transferase, alpha 2 (Yc2)	NM_008182	106770161
-1.54	0.318	Nme6	expressed in non-metastatic cells 6, protein	NM_018757	510136
-1.55	0.323	Mcm10	minichromosome maintenance deficient 10 (S. cerevisiae)	AK041749	100510239
-1.55	0.369	Hhex	hematopoietically expressed homeobox	NM_008245	2340575
-1.56	0.306	Mbd1	methyl-CpG binding domain protein 1	AK007371	101580722

-1.56	0.317	Cbs	cystathionine beta-synthase	NM_144855	6660039	
-1.57	0.304	Cxcl9	chemokine (C-X-C motif) ligand 9	NM_008599	1570673	
-1.57	0.318	Elovl5	ELOVL family member 5, elongation of long chain fatty acids (yeast)	NM_134255	3800170	
-1.58	0.301	Cyp3a11	cytochrome P450, family 3, subfamily a, polypeptide 11	NM_007818	6770332	
-1.59	0.301	Mrps27	mitochondrial ribosomal protein S27	NM_173757	4850546	
-1.59	0.301	Cdk2ap2	CDK2-associated protein 2	NM_026373	4070577	
-1.59	0.301	Cd74	CD74 antigen (invariant polypeptide of major histocompatibility complex, class II antigen-associated)	NM_010545	6400162	
-1.60	0.301	H2-Ab1	histocompatibility 2, class II antigen A, beta 1	NM_207105	4230427	
-1.62	0.301	Erdr1	erythroid differentiation regulator 1	NM_133362	5890184	
-1.62	0.301	Serpinh1	serine (or cysteine) peptidase inhibitor, clade H, member 1	NM_009825	6130014	
-1.62	0.301	Morf4l2	mortality factor 4 like 2	NM_019768	6450133	
-1.63	0.301	H2-Eb1	histocompatibility 2, class II antigen E beta	NM_010382	2350079	
-1.63	0.301	BC048546	cDNA sequence BC048546	NM_001001179	106650576	
-1.65	0.341	Esm1	endothelial cell-specific molecule 1	NM_023612	1410594	
-1.66	0.301	Hspb1	heat shock protein 1	NM_013560	6760435	
-1.67	0.301	Mvd	mevalonate (diphospho) decarboxylase	NM_138656	2060717	
-1.70	0.301	Hspa8	heat shock protein 8	NM_031165	1050132	
-1.71	0.301	Hsp90b1	heat shock protein 90kDa beta (Grp94), member 1	NM_011631	5670576	
-1.71	0.301	Gsta2	glutathione S-transferase, alpha 2 (Yc2)	NM_008182	6550139	
-1.72	0.301	Hsp90aa1	heat shock protein 90kDa alpha (cytosolic), class A member 1	NM_010480	2120722	
-1.72	0.301	Cbr1	carbonyl reductase 1	NM_007620	2120253	
-1.73	0.301		hypothetical Proline-rich region containing protein	AK085505	101090504	
-1.74	0.301	Es22	esterase 22	NM_133660	1090184	
-1.76	0.306	ACP	ACYL CARRIER PROTEIN homolog	AK018717	105670398	
-1.76	0.301	Csad	cysteine sulfinic acid decarboxylase	NM_144942	770215	
-1.77	0.301	H2-Ab1	histocompatibility 2, class II antigen A, beta 1	NM_207105	2370433	
-1.77	0.301	Egr1	early growth response 1	NM_007913	4610347	
-1.79	0.301	Entpd4	ectonucleoside triphosphate diphosphohydrolase 4	NM_026174	7040288	
-1.81	0.301	H2-Aa	histocompatibility 2, class II antigen A, alpha	NM_010378	5290673	
-1.82	0.301	Stip1	stress-induced phosphoprotein 1	NM_016737	6450390	
-1.85	0.301	Insc	inscuteable homolog (Drosophila)	NM_173767	380605	
-1.92	0.250	Tfrc	transferrin receptor	NM_011638	4050551	-2.19
-1.93	0.301	Cish	cytokine inducible SH2-containing protein	NM_009895	840315	
-1.96	0.274	Socs3	suppressor of cytokine signaling 3	NM_007707	5550563	
-1.97	0.274	Gadd45g	growth arrest and DNA-damage-inducible 45 gamma	NM_011817	2510142	
-1.99	0.222	Hist1h1c	histone cluster 1, H1c	NM_015786	3870603	
-2.14	0.150	Hspa5	heat shock protein 5	NM_022310	5130671	
-2.16	0.189	Hsph1	heat shock 105kDa/110kDa protein 1	NM_013559	1690017	-2.43
-2.20	0.236	Phlda1	pleckstrin homology-like domain, family A, member 1	NM_009344	2450020	
-2.23	0.301	Plk3	polo-like kinase 3 (Drosophila)	NM_013807	2640592	
-2.39	0.135	Cyp26b1	cytochrome P450, family 26, subfamily b, polypeptide 1	NM_175475	2630142	-2.18
-2.45	0.105	Syvn1	synovial apoptosis inhibitor 1, synoviolin	NM_028769	6940594	
-2.53	0.255	Foxq1	forkhead box Q1	NM_008239	4850088	1.91
-3.47	0.039	Creld2	cysteine-rich with EGF-like domains 2	NM_029720	5670184	-4.25

Appendix 4. *Genes showing changes in mRNA expression in the liver of mice with dietary iron overload.*

FC	P value	Symbol	Description	GenBank	Illumina probe	Q-RT-PCR
13.58	0.001	Cyp2b10	cytochrome P450, family 2, subfamily b, polypeptide 10	NM_009999	6200139	
10.03	0.001	Hamp2	hepcidin antimicrobial peptide 2	NM_183257	2940050	24.77
7.64	0.001	Id1	inhibitor of DNA binding 1	NM_010495	360398	
7.41	0.023	Cyp2b9	cytochrome P450, family 2, subfamily b, polypeptide 9	NM_010000	360152	
7.29	0.031	Dbp	D site albumin promoter binding protein	NM_016974	4200270	16.29
6.97	0.002	Cyp4a14	cytochrome P450, family 4, subfamily a, polypeptide 14	NM_007822	2370110	16.06

6.56	0.001	Apoa4	apolipoprotein A-IV	NM_007468	102450537	
5.35	0.001	Apoa4	apolipoprotein A-IV	NM_007468	4120451	
5.06	0.007	Rgs16	regulator of G-protein signaling 16	NM_011267	780091	
4.45	0.007	Ccnd1	cyclin D1	NM_007631	460524	
3.95	0.053	Mt1	metallothionein 1	NM_013602	4850164	
3.69	0.007	Foxq1	forkhead box Q1	NM_008239	4850088	
3.61	0.007	Ccnd1	cyclin D1	NM_007631	6980398	
3.59	0.007	Mfsd2	major facilitator superfamily domain containing 2	NM_029662	1400594	
3.48	0.240	Dmbt1	deleted in malignant brain tumors 1	NM_007769	7050270	
3.34	0.011	Cxcl1	chemokine (C-X-C motif) ligand 1	NM_008176	2690537	
3.31	0.005	Axud1	AXIN1 up-regulated 1	NM_153287	1230053	
3.12	0.007	Id3	inhibitor of DNA binding 3	NM_008321	6450403	8.38
3.03	0.007	Apoa5	apolipoprotein A-V	NM_080434	6130471	
3.01	0.010	Rad51l1	RAD51-like 1 (S. cerevisiae)	NM_009014	4010112	
2.92	0.023	Id2	inhibitor of DNA binding 2	NM_010496	870324	5.2
2.72	0.015	Ccnd1	cyclin D1	NM_007631	770309	
2.65	0.011	Cib3	PREDICTED:calcium and integrin binding family member 3	XM_356089	2350400	
2.62	0.015	S100a8	S100 calcium binding protein A8 (calgranulin A)	NM_013650	70112	
2.56	0.016	Cyp4a10	cytochrome P450, family 4, subfamily a, polypeptide 10	NM_010011	6130131	
2.55	0.064	Egr1	early growth response 1	NM_007913	4610347	
2.52	0.015	Cyp4a10	cytochrome P450, family 4, subfamily a, polypeptide 10	NM_010011	3170288	
2.47	0.062	Aacs	acetoacetyl-CoA synthetase	NM_030210	6100438	
2.44	0.012	Cyp4a31	cytochrome P450, family 4, subfamily a, polypeptide 31	NM_201640	107000113	
2.40	0.015	EG226654	predicted gene, EG226654	XM_129558	105570368	
2.37	0.131	Cish	cytokine inducible SH2-containing protein	NM_009895	840315	
2.37	0.015	Ccnd1	cyclin D1	NM_007631	3120576	
2.36	0.027	Acot3	acyl-CoA thioesterase 3	NM_134246	130494	16.6
2.35	0.013	Bhlhb2	basic helix-loop-helix domain containing, class B2	NM_011498	7040603	
2.30	0.149	Acta2	actin, alpha 2, smooth muscle, aorta	NM_007392	3390619	
2.24	0.041	Cyp26b1	cytochrome P450, family 26, subfamily b, polypeptide 1	NM_175475	2630142	
2.22	0.032	Fasn	fatty acid synthase	NM_007988	430717	
2.17	0.029	Slc2a2	solute carrier family 2 (facilitated glucose transporter), member 2	NM_031197	6770079	
2.15	0.026	Chrna4	cholinergic receptor, nicotinic, alpha polypeptide 4	NM_015730	2680091	
2.15	0.027	Dusp1	dual specificity phosphatase 1	NM_013642	6860121	
2.14	0.029	Zfp36l1	zinc finger protein 36, C3H type-like 1	NM_007564	4120048	
2.12	0.021	Serpina7	serine (or cysteine) peptidase inhibitor, clade A (alpha-1 antiproteinase, antitrypsin), member 7	NM_177920	2510537	
2.11	0.017	Akr1b3	aldo-keto reductase family 1, member B3 (aldose reductase)	NM_009658	6650494	
2.10	0.026	Lcn2	lipocalin 2	NM_008491	2510112	4.4
2.09	0.016	Adam23	a disintegrin and metallopeptidase domain 23	NM_011780	7000484	
2.08	0.027	Abcd2	ATP-binding cassette, sub-family D (ALD), member 2	NM_011994	4070315	
2.04	0.021	Serpina3m	serine (or cysteine) peptidase inhibitor, clade A, member 3M	NM_009253	130253	
2.04	0.021	Il1b	interleukin 1 beta	NM_008361	2640364	
2.02	0.022	Rsad2	radical S-adenosyl methionine domain containing 2	NM_021384	2120619	4.74
2.02	0.025	Abcd2	ATP-binding cassette, sub-family D (ALD), member 2	NM_011994	6220162	
1.96	0.028	Ehhadh	enoyl-Coenzyme A, hydratase/3-hydroxyacyl Coenzyme A dehydrogenase	NM_023737	6200315	
1.95	0.021	Ly6a	lymphocyte antigen 6 complex, locus A	NM_010738	6110605	
1.94	0.028	Gsta1	glutathione S-transferase, alpha 1 (Ya)	NM_008181	106840133	
1.93	0.023	Akr1b8	aldo-keto reductase family 1, member B8	NM_008012	3120288	
1.93	0.032	S100a9	S100 calcium binding protein A9 (calgranulin B)	NM_009114	7050528	
1.91	0.165	Ly6d	lymphocyte antigen 6 complex, locus D	NM_010742	4050010	
1.89	0.029	Socs3	suppressor of cytokine signaling 3	NM_007707	5550563	
1.89	0.027	Serpina7	serine (or cysteine) peptidase inhibitor, clade A (alpha-1 antiproteinase, antitrypsin), member 7	NM_177920	104670131	
1.87	0.037	Elovl6	ELOVL family member 6, elongation of long chain fatty acids (yeast)	NM_130450	5340746	
1.87	0.027	Id4	inhibitor of DNA binding 4	NM_031166	3830152	
1.86	0.029	Gstt2	glutathione S-transferase, theta 2	AK079739	106650102	

1.85	0.034	Arrdc4	arrestin domain containing 4	NM_025549	2810019	
1.84	0.075	Gsta1	glutathione S-transferase, alpha 1 (Ya)	NM_008181	3780112	
1.84	0.026	Nudt18	nudix (nucleoside diphosphate linked moiety X)-type motif 18	NM_153136	3520041	
1.83	0.047	Gsta2	glutathione S-transferase, alpha 2 (Yc2)	NM_008182	2600047	
1.82	0.133	Tef	thyrotroph embryonic factor	NM_017376	3120397	
1.82	0.027	BC089597	cDNA sequence BC089597	NM_145424	110484	
1.82	0.027	Zc3h12d	zinc finger CCCH type containing 12D	NM_172785	1410056	
1.82	0.029	Pltp	phospholipid transfer protein	NM_011125	630110	
1.82	0.037	Slc2a2	solute carrier family 2 (facilitated glucose transporter), member 2	NM_031197	5720722	
1.81	0.037	Mod1	malic enzyme, supernatant	NM_008615	1980239	
1.81	0.060	H2-Aa	histocompatibility 2, class II antigen A, alpha	NM_010378	5290673	
1.81	0.035	Rnf186	ring finger protein 186	NM_025786	520286	
1.81	0.040	Acaca	acetyl-Coenzyme A carboxylase alpha	NM_133360	2680369	
1.80	0.027	Mycl1	v-myc myelocytomatosis viral oncogene homolog 1, lung carcinoma derived (avian)	NM_008506	1980309	
1.79	0.067	Gsta2	glutathione S-transferase, alpha 2 (Yc2)	NM_008182	106770161	
1.78	0.065	Asns	asparagine synthetase	NM_012055	7100687	
1.78	0.031	Gstm6	glutathione S-transferase, mu 6	NM_008184	3940358	
1.77	0.119	Cyp2c29	cytochrome P450, family 2, subfamily c, polypeptide 29	NM_007815	6420601	
1.76	0.029	Cyp2c54	cytochrome P450, family 2, subfamily c, polypeptide 54	NM_206537	6130193	2.37
1.76	0.038	Oasl1	2'-5' oligoadenylate synthetase-like 1	NM_145209	5270687	
1.74	0.032	Tm4sf4	transmembrane 4 superfamily member 4	NM_145539	540600	
1.73	0.030	A230106M15Rik	RIKEN cDNA A230106M15 gene	NM_175474	5270435	
1.73	0.040	Hamp1	hepcidin antimicrobial peptide 1	NM_032541	4920112	5.27
1.72	0.041	Mgst3	microsomal glutathione S-transferase 3	NM_025569	5290736	
1.72	0.036	Ctsc	cathepsin C	NM_009982	2230739	
1.71	0.038	Ctsc	cathepsin C	NM_009982	4670408	
1.70	0.043	Aqp8	aquaporin 8	NM_007474	6770402	
1.69	0.051	Mgst3	microsomal glutathione S-transferase 3	NM_025569	3450338	
1.68	0.133	H2-Ab1	histocompatibility 2, class II antigen A, beta 1	NM_207105	4810050	
1.67	0.041	A530050D06Rik	RIKEN cDNA A530050D06 gene	NM_001081169	104070037	
1.67	0.046	Sqrdl	sulfide quinone reductase-like (yeast)	NM_021507	6290132	
1.66	0.110	Gadd45g	growth arrest and DNA-damage-inducible 45 gamma	NM_011817	2510142	
1.66	0.121	Gnat1	guanine nucleotide binding protein, alpha transducing 1	NM_008140	6100170	
1.65	0.060	Cyp2a5	cytochrome P450, family 2, subfamily a, polypeptide 5	NM_007812	4070632	
1.65	0.063	Esr1	estrogen receptor 1 (alpha)	NM_007956	5860193	
1.65	0.133	Cd74	CD74 antigen (invariant polypeptide of major histocompatibility complex, class II antigen-associated)	NM_010545	6400162	
1.64	0.062	2010003K11Rik	RIKEN cDNA 2010003K11 gene	NM_027237	6940368	
1.62	0.162	H2-Ab1	histocompatibility 2, class II antigen A, beta 1	NM_207105	2370433	
1.62	0.086	Nr1d1	nuclear receptor subfamily 1, group D, member 1	NM_145434	770746	
1.61	0.208	S100a6	S100 calcium binding protein A6 (calcyclin)	NM_011313	1690204	
1.60	0.118	Fgg	fibrinogen, gamma polypeptide	NM_133862	4610717	
1.59	0.077	Gstm3	glutathione S-transferase, mu 3	NM_010359	101170047	
1.57	0.144	Cp	ceruloplasmin	NM_007752	2570484	1.8
1.57	0.272	Actg2	actin, gamma 2, smooth muscle, enteric	NM_009610	4780180	
1.55	0.110	Gclc	glutamate-cysteine ligase, catalytic subunit	NM_010295	2810731	
1.54	0.110	Cyp2a5	cytochrome P450, family 2, subfamily a, polypeptide 5	NM_007812	6380047	
1.54	0.196	Osgin1	oxidative stress induced growth inhibitor 1	NM_027950	1450053	
1.53	0.161	Ppp1r3c	protein phosphatase 1, regulatory (inhibitor) subunit 3C	NM_016854	2640170	
1.52	0.371	Spink4	serine peptidase inhibitor, Kazal type 4	NM_011463	4610619	
1.51	0.136	Phlda1	pleckstrin homology-like domain, family A, member 1	NM_009344	2450020	
1.51	0.332	Psmc1	protease (prosome, macropain) 26S subunit, ATPase 1	NM_008947	6350538	
1.50	0.165	1100001G20Rik	RIKEN cDNA 1100001G20 gene	NM_183249	3610368	
1.50	0.207	Cyp2b13	cytochrome P450, family 2, subfamily b, polypeptide 13	NM_007813	5420672	
1.49	0.181	H2-Ab1	histocompatibility 2, class II antigen A, beta 1	NM_207105	4230427	
1.45	0.190	Hbb-b1	hemoglobin, beta adult major chain	NM_008220	4050717	
1.43	0.335	Klf5	Kruppel-like factor 5	NM_009769	3840348	
1.43	0.207	H2-Eb1	histocompatibility 2, class II antigen E beta	NM_010382	2350079	
1.42	0.252	Fos	FBJ osteosarcoma oncogene	NM_010234	1850315	

1.41	0.350	Ltf	lactotransferrin	NM_008522	6770364	71.08
1.41	0.224	Rps6	ribosomal protein S6	NM_009096	2060168	
1.41	0.311	Sftpd	surfactant associated protein D	NM_009160	6510181	
1.41	0.211	Hbb-b1	hemoglobin, beta adult major chain	AK005442	105690048	
-1.41	0.275	Arntl	aryl hydrocarbon receptor nuclear translocator-like	NM_007489	3170463	
-1.45	0.350	Alas1	aminolevulinic acid synthase 1	NM_020559	6400440	
-1.46	0.173	C730048C13Rik	RIKEN cDNA C730048C13 gene	NM_177002	6590021	
-1.55	0.110	Scp2	sterol carrier protein 2, liver	NM_011327	6200537	
-1.55	0.110	2810007J24Rik	RIKEN cDNA 2810007J24 gene	NM_175250	1740400	
-1.55	0.115	Mcm10	minichromosome maintenance deficient 10 (S. cerevisiae)	NM_027290	4920632	
-1.55	0.152	Pnkd	paroxysmal nonkinesiogenic dyskinesia	NM_019999	3520592	
-1.56	0.133	Egfr	epidermal growth factor receptor	NM_207655	6480521	
-1.59	0.167	Lpin1	lipin 1	NM_015763	102940241	
-1.59	0.097	Spon2	spondin 2, extracellular matrix protein	NM_133903	2680136	
-1.62	0.119	Rdh9	retinol dehydrogenase 9	NM_153133	2810195	
-1.62	0.146	Plek	pleckstrin	NM_019549	1090039	
-1.62	0.065	Whsc1l1	Wolf-Hirschhorn syndrome candidate 1-like 1 (human)	NM_001001735	107000603	
-1.62	0.085	Gck	glucokinase	NM_010292	2370273	
-1.64	0.094	Creld2	cysteine-rich with EGF-like domains 2	NM_029720	5670184	-2.09
-1.68	0.066	BC057022	cDNA sequence BC057022	NM_001004180	6350441	
-1.68	0.113	Clpx	caseinolytic peptidase X (E.coli)	NM_011802	6220156	
-1.69	0.041	Hp	haptoglobin	NM_017370	2940551	
-1.70	0.041	Pik3r1	phosphatidylinositol 3-kinase, regulatory subunit, polypeptide 1 (p85 alpha), transcript variant 1	NM_001024955	105420551	
-1.70	0.034	Bok	Bcl-2-related ovarian killer protein	NM_016778	1170373	
-1.71	0.041	Herpud1	homocysteine-inducible, endoplasmic reticulum stress-inducible, ubiquitin-like domain member 1	NM_022331	7100440	
-1.71	0.133	Cdkn1a	cyclin-dependent kinase inhibitor 1A (P21)	NM_007669	4050088	
-1.73	0.030	Egfr	epidermal growth factor receptor	NM_007912	105130452	
-1.74	0.029	Arl4d	ADP-ribosylation factor-like 4D	NM_025404	6200040	
-1.74	0.033	Tfrc	transferrin receptor	NM_011638	4050551	
-1.75	0.039	Socs2	suppressor of cytokine signaling 2	NM_007706	4760692	
-1.76	0.108	Ddc	dopa decarboxylase	NM_016672	102850113	
-1.76	0.054	Car3	carbonic anhydrase 3	NM_007606	5890390	
-1.77	0.038	Hes6	hairy and enhancer of split 6 (Drosophila)	NM_019479	6550504	
-1.77	0.028	Ethe1	ethylmalonic encephalopathy 1	NM_023154	3440133	
-1.78	0.032	Slc41a2	solute carrier family 41, member 2	NM_177388	2260333	
-1.78	0.037	Car3	carbonic anhydrase 3	NM_007606	870687	
-1.80	0.027	Dio1	deiodinase, iodothyronine, type I	NM_007860	5420148	
-1.81	0.032	Gstp1	glutathione S-transferase, pi 1	NM_013541	3170102	
-1.81	0.041	Scarb1	scavenger receptor class B, member 1	AK080894	101500463	
-1.81	0.052	Hspb1	heat shock protein 1	NM_013560	6760435	
-1.82	0.026	Slco2a1	solute carrier organic anion transporter family, member 2a1	NM_033314	102570500	
-1.82	0.031	Cyp4v3	cytochrome P450, family 4, subfamily v, polypeptide 3	NM_133969	5550390	
-1.82	0.041	Saa3	serum amyloid A 3	NM_011315	6510390	
-1.85	0.029	Ormdl3	ORM1-like 3 (S. cerevisiae)	NM_025661	1340711	
-1.86	0.029	Serpina1e	serine (or cysteine) peptidase inhibitor, clade A, member 1e	NM_009247	2630180	
-1.87	0.026	Dio1	deiodinase, iodothyronine, type I	NM_007860	4570279	
-1.87	0.027	Pfkfb3	6-phosphofructo-2-kinase/fructose-2,6-biphosphatase 3	NM_133232	630706	
-1.87	0.049	Nudt7	nudix (nucleoside diphosphate linked moiety X)-type motif 7	NM_024437	5910097	
-1.89	0.026	Ppp1r3b	protein phosphatase 1, regulatory (inhibitor) subunit 3B	NM_177741	6130253	
-1.90	0.031	Srd5a1	steroid 5 alpha-reductase 1	NM_175283	5910347	
-1.91	0.037	Tff3	trefoil factor 3, intestinal	NM_011575	1580129	
-1.91	0.025	Saa4	serum amyloid A 4	NM_011316	430706	
-1.91	0.038	Lpin2	lipin 2	AK048657	102570497	
-1.94	0.021	Slc11a2	solute carrier family 11 (proton-coupled divalent metal ion transporters), member 2	AK049856	100430138	-1.13
-1.95	0.023	Ppp1r3b	protein phosphatase 1, regulatory (inhibitor) subunit 3B	NM_177741	101450309	
-1.95	0.062	Ccrn4l	CCR4 carbon catabolite repression 4-like (S. cerevisiae)	NM_009834	50438	

-1.96	0.029	Tsc22d1	TSC22 domain family, member 1	NM_009366	6040181	
-1.97	0.041	Ddc	dopa decarboxylase	NM_016672	670408	
-1.97	0.084	8430408G22Rik	RIKEN cDNA 8430408G22 gene	NM_145980	6100736	
-1.99	0.025	C9	complement component 9	NM_013485	5550452	
-2.03	0.019	Angptl4	angiopoietin-like 4	NM_020581	6760593	
-2.05	0.037	Hhex	hematopoietically expressed homeobox	NM_008245	2340575	
-2.06	0.024	Car14	carbonic anhydrase 14	NM_011797	1450528	
-2.08	0.025	Il6ra	interleukin 6 receptor, alpha	AK020663	102640121	
-2.08	0.029	EG241041	predicted gene, EG241041	NR_002858	105550524	
-2.11	0.016	Mmd2	monocyte to macrophage differentiation-associated 2	NM_175217	4920100	
-2.13	0.016	Hsph1	heat shock 105kDa/110kDa protein 1	NM_013559	1690017	-3.62
-2.14	0.068	Nfil3	nuclear factor, interleukin 3, regulated	NM_017373	4070377	
-2.16	0.015	Selenbp2	selenium binding protein 2	NM_019414	2650372	
-2.16	0.027	Aox3	aldehyde oxidase 3	NM_023617	4180592	
-2.17	0.023	2810439F02Rik	RIKEN cDNA 2810439F02 gene	NM_028341	3870300	
-2.19	0.032	Serpina12	serine (or cysteine) peptidase inhibitor, clade A (alpha-1 antiproteinase, antitrypsin), member 12	NM_026535	1230128	
-2.20	0.015	Alas2	aminolevulinic acid synthase 2, erythroid	NM_009653	6550176	
-2.21	0.015	Slco1a1	solute carrier organic anion transporter family, member 1a1	NM_013797	104230484	
-2.22	0.026	Hes6	hairy and enhancer of split 6 (Drosophila)	NM_019479	540411	
-2.23	0.016	2810439F02Rik	RIKEN cDNA 2810439F02 gene	NM_028341	1410725	
-2.26	0.012	Dct	dopachrome tautomerase	NM_010024	1090347	
-2.26	0.016	Aatk	apoptosis-associated tyrosine kinase	NM_007377	5890280	
-2.32	0.084	Cdkn1a	cyclin-dependent kinase inhibitor 1A (P21)	NM_007669	6400706	
-2.49	0.012	4732465J04Rik	RIKEN cDNA 4732465J04 gene	AK076359	103060563	
-2.50	0.026	Cyp7b1	cytochrome P450, family 7, subfamily b, polypeptide 1	NM_007825	1190309	
-2.51	0.016	Cabyr	calcium-binding tyrosine-(Y)-phosphorylation regulated (fibrousheathin 2)	NM_181731	7040040	
-2.61	0.176	Bcl6	B-cell leukemia/lymphoma 6	NM_009744	940100	
-2.63	0.007	Susd4	sushi domain containing 4	NM_144796	1850017	
-2.72	0.007	Dct	dopachrome tautomerase	NM_010024	3840494	
-2.73	0.035	Cyp4a12b	cytochrome P450, family 4, subfamily a, polypeptide 12B	NM_172306	6660170	
-2.79	0.110	Saa2	serum amyloid A 2	NM_011314	1090139	-3.36
-2.80	0.007	Nnmt	nicotinamide N-methyltransferase	NM_010924	450471	
-2.80	0.012	Cyp7a1	cytochrome P450, family 7, subfamily a, polypeptide 1	NM_007824	6980603	
-2.88	0.017	Serpine2	serine (or cysteine) peptidase inhibitor, clade E, member 2	AK045954	101940008	
-2.91	0.009	C6	complement component 6	NM_016704	2900129	
-3.15	0.026	Mup2	major urinary protein 2	NM_008647	770088	
-3.32	0.009	Hsd3b5	hydroxy-delta-5-steroid dehydrogenase, 3 beta- and steroid delta-isomerase 5	NM_008295	3290112	-3.01
-3.39	0.005	Susd4	sushi domain containing 4	NM_144796	101230504	
-3.62	0.022	Cyp4a12a	cytochrome P450, family 4, subfamily a, polypeptide 12a	NM_177406	4210288	
-3.96	0.062	Saa1	serum amyloid A 1	NM_009117	5390520	-4.31
-4.28	0.007	Mup4	major urinary protein 4	NM_008648	670253	
-5.00	0.007	Elovl3	elongation of very long chain fatty acids (FEN1/Elo2, SUR4/Elo3, yeast)-like 3	NM_007703	6860050	
-7.46	0.001	2200001I15Rik	RIKEN cDNA 2200001I15 gene	NM_183278	2450324	

Appendix 5. *Genes that exhibit transcriptional regulation in the duodenum of Hfe$^{-/-}$ mice.*

FC	P value	Symbol	Description	GenBank no	Illumina Probe	Q-RT-PCR
15.67	0.042	Ela3	elastase 3, pancreatic	NM_026419	4060731	14.77
14.12	0.057	Ela3	elastase 3, pancreatic	NM_026419	3990711	
13.09	0.062	Try4	trypsin 4	NM_011646	5860044	
12.51	0.044	Cpb1	carboxypeptidase B1 (tissue)	NM_029706	290600	14.55
12.42	0.062	Cpa1	carboxypeptidase A1	NM_025350	4730022	
12.17	0.051	Pnlip	pancreatic lipase	NM_026925	6450341	
11.51	0.085	Gkn2	gastrokine 2	NM_025467	2120575	
11.35	0.065	Prss1	protease, serine, 1 (trypsin 1)	NM_053243	6370400	
10.56	0.093	Gkn1	gastrokine 1	NM_025466	5420091	

10.34	0.019	Reg2	regenerating islet-derived 2	NM_009043	2470072	
10.20	0.081	Ela2a	elastase 2A	NM_007919	5270129	
9.99	0.075	Ctrl	chymotrypsin-like	NM_023182	2120301	
9.82	0.063	Cel	carboxyl ester lipase	NM_009885	2640278	
9.71	0.067	Sycn	syncollin	NM_026716	2570040	
9.68	0.085	Ctrb1	chymotrypsinogen B1	NM_025583	1050347	
8.57	0.085	Pdia2	protein disulfide isomerase associated 2	NM_001081070	5360706	
8.17	0.089	Pnliprp1	pancreatic lipase related protein 1	NM_018874	360433	
8.14	0.049	Rnase1	ribonuclease, RNase A family, 1 (pancreatic)	NM_011271	6550364	
8.14	0.071	Cpa2	carboxypeptidase A2, pancreatic	NM_001024698	100380021	
7.49	0.070	Cuzd1	CUB and zona pellucida-like domains 1	NM_008411	7100673	
7.41	0.046	Prss2	protease, serine, 2	NM_009430	1090286	
7.14	0.064	2210010C04Rik	RIKEN cDNA 2210010C04 gene	NM_023333	5690332	
6.87	0.017	Reg3b	regenerating islet-derived 3 beta	NM_011036	2690524	
6.19	0.107	Amy2	amylase 2, pancreatic	NM_009669	580138	
5.84	0.100	Ela1	elastase 1, pancreatic	NM_033612	3390167	
5.35	0.099	Clps	colipase, pancreatic	NM_025469	6220524	
4.86	0.117	Pla2g1b	phospholipase A2, group IB, pancreas	NM_011107	460500	
4.50	0.117	Pnliprp2	pancreatic lipase-related protein 2	NM_011128	130131	
4.38	0.123	Prss1	protease, serine, 1 (trypsin 1)	NM_053243	3290162	
4.24	0.129	Cabp2	calcium binding protein 2	NM_013878	840142	
4.21	0.196	Tff1	trefoil factor 1	NM_009362	3850452	
4.06	0.150	Erp27	endoplasmic reticulum protein 27	NM_026983	6380142	
3.90	0.103	Reg3d	regenerating islet-derived 3 delta	NM_013893	4010075	
3.81	0.148	Rbpjl	recombination signal binding protein for immunoglobulin kappa J region-like	NM_009036	5390019	
3.61	0.117	Serpini2	serine (or cysteine) peptidase inhibitor, clade I, member 2	NM_026460	1570427	
3.59	0.237	Psca	prostate stem cell antigen	NM_028216	2450161	
3.27	0.139	Gp2	glycoprotein 2 (zymogen granule membrane)	NM_025989	5860563	
3.27	0.149	Cldn10	claudin 10	NM_021386	4920097	
3.01	0.191	Tmed6	transmembrane emp24 protein transport domain containing 6	NM_025458	6510048	
3.01	0.232	Clps	colipase, pancreatic	NM_025469	1340056	
2.93	0.181	Mat1a	methionine adenosyltransferase I, alpha	NM_133653	2690239	
2.90	0.183	Klk1b5	kallikrein 1-related peptidase b5	NM_008456	105420707	
2.78	0.176	Bhlhb8	basic helix-loop-helix domain containing, class B, 8	NM_010800	6620020	
2.78	0.249	Gal	galanin	NM_010253	3930279	
2.74	0.275	Hamp2	hepcidin antimicrobial peptide 2	NM_183257	2940050	6.66
2.67	0.214	Klk1b5	kallikrein 1-related peptidase b5	NM_008456	6590139	
2.65	0.177	Sepp1	selenoprotein P, plasma, 1	NM_009155	450273	
2.62	0.234	Aqp12	aquaporin 12	NM_177587	360519	
2.62	0.244	Chac1	ChaC, cation transport regulator-like 1 (E. coli)	NM_026929	7100725	
2.51	0.244	Sox21	SRY-box containing gene 21	NM_177753	4670041	
2.51	0.270	Ctrc	chymotrypsin C (caldecrin)	NM_001033875	3060152	
2.45	0.255	Fgf21	fibroblast growth factor 21	NM_020013	3780377	
2.39	0.283	Gamt	guanidinoacetate methyltransferase	NM_010255	6980301	
2.34	0.257	Klk1b11	kallikrein 1-related peptidase b11	NM_010640	101190114	
2.33	0.250	Bhlhb8	basic helix-loop-helix domain containing, class B, 8	NM_010800	5550725	
2.31	0.264	Mal	myelin and lymphocyte protein, T-cell differentiation protein	NM_010762	4590239	
2.30	0.319	Cldn18	claudin 18	NM_019815	2030193	
2.29	0.266	Klk1	kallikrein 1	NM_010639	104730373	
2.29	0.281	Dusp26	dual specificity phosphatase 26 (putative)	NM_025869	1170593	
2.28	0.328	2900093B09Rik	RIKEN cDNA 2900093B09 gene	NM_021387	3780497	
2.25	0.265	Slc6a9	solute carrier family 6 (neurotransmitter transporter, glycine), member 9	NM_008135	2470520	
2.22	0.277	Klk1b27	kallikrein 1-related peptidase b27	NM_020268	5900632	
2.18	0.275	Scara3	scavenger receptor class A, member 3	NM_172604	5890487	
2.16	0.305	Cldn10	claudin 10	NM_023878	6620270	
2.15	0.302	Itih4	inter alpha-trypsin inhibitor, heavy chain 4	NM_018746	2690471	
2.14	0.282	Mt1	metallothionein 1	NM_013602	4850164	9.63

2.14	0.289	Klk1b5	kallikrein 1-related peptidase b5	NM_008456	2350528	
2.14	0.308	Klk1b27	kallikrein 1-related peptidase b27	NM_020268	2810008	
2.14	0.323	Slc38a5	solute carrier family 38, member 5	NM_172479	540093	
2.13	0.283	Sec11c	SEC11 homolog C (S. cerevisiae)	NM_025468	1500056	
2.11	0.317	Klk1b4	kallikrein 1-related pepidase b4	NM_010915	5900605	
2.10	0.306	Klk1b24	kallikrein 1-related peptidase b24	NM_010643	106130471	
2.09	0.292	Alpi	alkaline phosphatase, intestinal	NM_001081082	70050	
2.09	0.358	Arhgdig	Rho GDP dissociation inhibitor (GDI) gamma	NM_008113	5130338	
2.06	0.304	Pabpc1	poly A binding protein, cytoplasmic 1	NM_008774	6020632	
2.05	0.310	Mela	melanoma antigen	NM_008581	104560161	
2.03	0.312	H3f3a	H3 histone, family 3A	NM_008210	2900086	
2.03	0.352	C130090K23Rik	RIKEN cDNA C130090K23 gene	NM_145560	3800722	
1.98	0.347	Klk1b4	kallikrein 1-related pepidase b4	NM_010915	630348	
1.97	0.360	Rab26	PREDICTED: RAB26, member RAS oncogene family	XM_283428	104590114	
1.97	0.365	Ptf1a	pancreas specific transcription factor, 1a	NM_018809	6450377	
1.91	0.408	Ctse	cathepsin E	NM_007799	2030292	2.32
1.91	0.366	Nupr1	nuclear protein 1	NM_019738	1990524	
1.90	0.368	Klf4	Kruppel-like factor 4 (gut)	NM_010637	5570750	
1.90	0.415	Mal	myelin and lymphocyte protein, T-cell differentiation protein	NM_010762	4280487	
1.87	0.391	Amy1	amylase 1, salivary	NM_007446	2360148	
1.85	0.388	Acsm3	acyl-CoA synthetase medium-chain family member 3	NM_016870	2650706	
1.82	0.406	Gls2	glutaminase 2 (liver, mitochondrial)	NM_001033264	102900647	
1.81	0.413	Inmt	indolethylamine N-methyltransferase	NM_009349	2320020	
1.80	0.421	Muc1	mucin 1, transmembrane	NM_013605	6220131	
1.80	0.487	Ins2	insulin II	NM_008387	610040	
1.80	0.418	Gcat	glycine C-acetyltransferase (2-amino-3-ketobutyrate-coenzyme A ligase)	NM_013847	5270672	
1.80	0.423	Vill	villin-like	NM_011700	130672	
1.78	0.450	Suox	sulfite oxidase	NM_173733	5220286	
1.78	0.430	Lcmt1	leucine carboxyl methyltransferase 1	NM_025304	2230551	
1.78	0.433	2310042E22Rik	RIKEN cDNA 2310042E22 gene	NM_025634	5420707	
1.77	0.441	Clu	clusterin	NM_013492	5420075	
1.77	0.448	Krt23	keratin 23	NM_033373	1190369	
1.75	0.451	Bcas1	breast carcinoma amplified sequence 1	NM_029815	2030711	
1.75	0.440	Tcfcp2l1	transcription factor CP2-like 1	NM_023755	5340497	
1.75	0.460	Areg	amphiregulin	NM_009704	4920025	
1.74	0.436	Muc1	mucin 1, transmembrane	NM_013605	3140082	
1.74	0.437	Klk1b26	kallikrein 1-related petidase b26	NM_010644	101850092	
1.73	0.449	Syt16	synaptotagmin XVI	NM_172804	2690504	
1.73	0.459	Tle6	transducin-like enhancer of split 6, homolog of Drosophila E(spl)	NM_053254	3170242	
1.71	0.462	4732474O15Rik	RIKEN cDNA 4732474O15 gene	XM_138397	6770014	
1.71	0.477	Anxa3	annexin A3	NM_013470	5570494	
1.69	0.458	Klk1b4	kallikrein 1-related pepidase b4	NM_010915	100130301	
1.69	0.567	Psapl1	prosaposin-like 1	NM_175249	3520735	
1.68	0.498	S100a6	S100 calcium binding protein A6 (calcyclin)	NM_011313	1690204	
1.66	0.484	Cpb1	carboxypeptidase B1 (tissue)	AK007944	103170132	
1.66	0.491	Sult1c2	sulfotransferase family, cytosolic, 1C, member 2	NM_026935	5910538	
1.65	0.491	C130090K23Rik	RIKEN cDNA C130090K23 gene	NM_181323	4280435	
1.64	0.489	Fkbp11	FK506 binding protein 11	NM_024169	3170575	
1.60	0.507	Capn5	calpain 5	NM_007602	4050706	
1.60	0.515	Tead2	TEA domain family member 2	NM_011565	6450079	
1.60	0.519	Col7a1	procollagen, type VII, alpha 1	NM_007738	2190072	
1.60	0.529	Akr1b8	aldo-keto reductase family 1, member B8	NM_008012	3120288	
1.60	0.519	AI428936	expressed sequence AI428936	NM_153577	2650433	
1.58	0.617	Dpcr1	diffuse panbronchiolitis critical region 1 (human)	NM_001033366	101240301	
1.57	0.528	Nqo1	NAD(P)H dehydrogenase, quinone 1	NM_008706	6840121	
1.56	0.562	Il33	interleukin 33	NM_133775	6590687	
1.55	0.537	Mknk1	MAP kinase-interacting serine/threonine kinase 1	NM_021461	6510161	
1.54	0.546	BC034090	cDNA sequence BC034090	XM_148974	4070609	
1.54	0.560	Ero1lb	ERO1-like beta (S. cerevisiae)	NM_026184	5550358	

1.54	0.561	Mup1	major urinary protein 1	NM_031188	430685	
1.53	0.562	Aldh3a1	aldehyde dehydrogenase family 3, subfamily A1	NM_007436	580095	
1.53	0.560	Rgs17	regulator of G-protein signaling 17	NM_019958	1400603	
1.52	0.561	Gif	gastric intrinsic factor	NM_008118	2260056	
1.52	0.563	Rbp1	retinol binding protein 1, cellular	NM_011254	1690072	
1.49	0.584	Slc5a5	solute carrier family 5 (sodium iodide symporter), member 5	NM_053248	106590070	
1.49	0.588	P2ry14	purinergic receptor P2Y, G-protein coupled, 14	NM_133200	6100497	
1.48	0.594	Gsdm2	gasdermin 2	NM_029727	3130102	
1.47	0.600	Anxa10	annexin A10	AK018597	106400500	
1.46	0.593	Clca3	chloride channel calcium activated 3	NM_017474	6510167	
1.46	0.606	Mboat1	membrane bound O-acyltransferase domain containing 1	NM_153546	4010309	
1.45	0.60	Car2	carbonic anhydrase 2	NM_009801	1660600	
1.44	0.613	Tmem97	transmembrane protein 97	NM_133706	4540300	
1.44	0.610	Dhx34	DEAH (Asp-Glu-Ala-His) box polypeptide 34	NM_027883	2900133	
1.43	0.633	Vtn	vitronectin	NM_011707	3360044	
1.42	0.626	Slc39a5	solute carrier family 39 (metal ion transporter), member 5	NM_028051	4610440	
1.40	0.635	Vsig2	V-set and immunoglobulin domain containing 2	NM_020518	6420075	
1.40	0.639	P2rx1	purinergic receptor P2X, ligand-gated ion channel, 1	NM_008771	2940021	
-1.44	0.607	LOC620017	PREDICTED: similar to Ig kappa chain V-V region L7 precursor	XM_357633	510347	
-1.47	0.586	Apoa4	apolipoprotein A-IV	NM_007468	102450537	
-1.51	0.617	Lct	lactase	NM_001081078	102350138	
-1.55	0.566	Igk-V21-2	IgK chain mRNA V-region, from hybridoma M195.	M83099	1050121	
-1.56	0.534	Eme1	essential meiotic endonuclease 1 homolog 1 (S. pombe)	NM_177752	2680670	
-1.60	0.520	Defcr-rs1	defensin related sequence cryptdin peptide (paneth cells)	NM_007844	107100142	
-1.62	0.503	Muc3	PREDICTED: mucin 3, intestinal	XM_355711	101690750	
-1.63	0.532	Guca2b	guanylate cyclase activator 2b (retina)	NM_008191	4200014	
-1.68	0.471	Lyz1	lysozyme 1	NM_013590	5700609	
-1.68	0.473	Slc9a1	solute carrier family 9 (sodium/hydrogen exchanger), member 1	NM_016981	2650093	
-1.70	0.455	Fcgr4	Fc receptor, IgG, low affinity IV	NM_144559	2810059	
-1.78	0.416	Hist1h2ao	histone cluster 1, H2ao	NM_178185	2480093	
-1.79	0.426	Apoc3	apolipoprotein C-III	NM_023114	2030168	
-1.85	0.383	Hist1h2ai	histone cluster 1, H2ai	NM_178182	4540039	
-1.95	0.355	Pkp4	similar to PLAKOPHILIN 4	AK021168	106940451	
-1.97	0.342	Guca2a	guanylate cyclase activator 2a (guanylin)	NM_008190	7050253	
-2.00	0.329	Defcr6	defensin related cryptdin 6	NM_007852	6900706	
-2.07	0.301	Hspb1	heat shock protein 1	NM_013560	6760435	
-2.11	0.287	Defcr6	defensin related cryptdin 6	NM_007852	100430075	
-2.11	0.324	AY761184	cDNA sequence AY761184	NM_001007582	6650465	
-2.11	0.287	Hsp90ab1	heat shock protein 90kDa alpha (cytosolic), class B member 1	NM_008302	6040093	
-2.14	0.317	Muc3	PREDICTED: mucin 3, intestinal	XM_355711	105670541	
-2.19	0.286	Atp5b	ATP synthase, H+ transporting mitochondrial F1 complex, beta subunit	NM_016774	3870138	
-2.23	0.256	Serpinh1	serine (or cysteine) peptidase inhibitor, clade H, member 1	NM_009825	6130014	
-2.29	0.240	Hsp90ab1	heat shock protein 90kDa alpha (cytosolic), class B	NM_008302	3170358	
-2.32	0.246	Ddb1	damage specific DNA binding protein 1	NM_015735	6110687	1.25
-2.50	0.199	Khk	ketohexokinase	NM_008439	3870204	
-2.69	0.180	Defcr20	defensin related cryptdin 20	NM_183268	5080575	
-2.93	0.143	Erdr1	erythroid differentiation regulator 1	NM_133362	5890184	-3.45
-3.14	0.120	Cyp26b1	cytochrome P450, family 26, subfamily b, polypeptide 1	NM_175475	2630142	-2.04

Appendix 6. *Genes that display altered mRNA expression in the duodenum of mice with dietary iron overload.*

FC	P value	Symbol	Description	GenBank no	Illumina Probe	Q-RT-PCR
6.07	0.001	Slc5a4b	solute carrier family 5 (neutral amino acid transporters, system A), member 4b	NM_023219	430563	
4.97	0.002	Cbr3	carbonyl reductase 3	NM_173047	6590148	

4.62	0.002	Cyp4a10	cytochrome P450, family 4, subfamily a, polypeptide 10	NM_010011	6130131	
4.42	0.002	Gstm1	glutathione S-transferase, mu 1	NM_010358	6590463	4.29
4.27	0.002	Gsta3	glutathione S-transferase, alpha 3	NM_010356	2470193	
4.17	0.004	Akr1b8	aldo-keto reductase family 1, member B8	NM_008012	3120288	
3.68	0.008	Tm4sf4	transmembrane 4 superfamily member 4	NM_145539	540600	
3.61	0.004	Ephx1	epoxide hydrolase 1, microsomal	NM_010145	1740136	
3.61	0.005	Acaa1b	acetyl-Coenzyme A acyltransferase 1B	NM_146230	6100750	6.13
3.51	0.007	Gsta1	glutathione S-transferase, alpha 1 (Ya)	NM_008181	3780112	
3.04	0.012	Mod1	malic enzyme, supernatant	NM_008615	1980239	
2.93	0.038	Gsta2	glutathione S-transferase, alpha 2 (Yc2)	NM_008182	106770161	
2.80	0.011	Gstm6	glutathione S-transferase, mu 6	NM_008184	3940358	
2.78	0.014	Gsta2	glutathione S-transferase, alpha 2 (Yc2)	NM_008182	2600047	
2.65	0.020	Gsta2	glutathione S-transferase, alpha 2 (Yc2)	NM_008182	6550139	
2.57	0.021	Gprc5a	G protein-coupled receptor, family C, group 5, member A	NM_181444	3870095	7.75
2.49	0.027	Il1rl1	interleukin 1 receptor-like 1	NM_010743	6020347	
2.41	0.023	Gstm4	glutathione S-transferase, mu 4	NM_026764	2340181	
2.36	0.037	Cldn4	claudin 4	NM_009903	4920739	
2.36	0.023	Slc37a1	solute carrier family 37 (glycerol-3-phosphate transporter), member 1	AK028984	100060707	
2.29	0.056	Aldh1a1	aldehyde dehydrogenase family 1, subfamily A1	NM_013467	6520706	
2.26	0.070	Hmox1	heme oxygenase (decycling) 1	NM_010442	1740687	16.67
2.26	0.037	Gsta4	glutathione S-transferase, alpha 4	NM_010357	1660369	
2.23	0.077	Cyp2c66	cytochrome P450, family 2, subfamily c, polypeptide 66	NM_001011707	100630446	
2.14	0.178	Reg2	regenerating islet-derived 2	NM_009043	2470072	
2.13	0.038	Cyp4a10	cytochrome P450, family 4, subfamily a, polypeptide 10	NM_010011	3170288	
2.02	0.070	Htatip2	HIV-1 tat interactive protein 2, homolog (human)	NM_016865	3120465	
1.99	0.058	Ldlr	low density lipoprotein receptor	NM_010700	106400053	
1.99	0.154	Dbp	D site albumin promoter binding protein	NM_016974	4200270	2.7
1.97	0.069	Pmm1	phosphomannomutase 1	NM_013872	6840112	
1.96	0.057	Cyp51	cytochrome P450, family 51	NM_020010	106760403	
1.96	0.079	Gsta1	glutathione S-transferase, alpha 1 (Ya)	NM_008181	106840133	
1.95	0.081	Gch1	GTP cyclohydrolase 1	NM_008102	670364	
1.95	0.069	Sfrs5	splicing factor, arginine/serine-rich 5 (SRp40, HRS)	NM_009159	6350008	
1.90	0.077	Gstm6	glutathione S-transferase, mu 6	NM_008184	102370750	
1.90	0.079	Aldh1a7	aldehyde dehydrogenase family 1, subfamily A7	NM_011921	3800086	
1.88	0.079	Slc30a10	solute carrier family 30, member 10	NM_001033286	102760133	
1.88	0.082	Hmgcs2	3-hydroxy-3-methylglutaryl-Coenzyme A synthase 2	NM_008256	770725	
1.88	0.100	Gstm3	glutathione S-transferase, mu 3	NM_010359	101170047	
1.86	0.190	Ugt2b36	UDP glucuronosyltransferase 2 family, polypeptide B36	NM_001029867	103060504	
1.85	0.094	Aldh3a2	aldehyde dehydrogenase family 3, subfamily A2	NM_007437	101170242	
1.82	0.104	Ppme1	protein phosphatase methylesterase 1	NM_028292	2650592	
1.82	0.109	Cyp2b10	cytochrome P450, family 2, subfamily b, polypeptide 10	NM_009999	6200139	
1.81	0.113	Mboat1	membrane bound O-acyltransferase domain containing 1	NM_153546	4010309	
1.72	0.157	Defcr20	defensin related cryptdin 20	NM_183268	102900750	
1.71	0.158	Alpi	alkaline phosphatase, intestinal	NM_001081082	70050	
1.65	0.186	Tef	thyrotroph embryonic factor	NM_017376	3120397	
1.58	0.267	Capg	capping protein (actin filament), gelsolin-like	NM_007599	770373	
1.55	0.268	5730469M10Rik	RIKEN cDNA 5730469M10 gene	NM_027464	5080593	
-1.40	0.597	Gng12	guanine nucleotide binding protein (G protein), gamma 12	NM_025278	100520079	
-1.40	0.650	Hod	homeobox only domain	AK003784	103850021	
-1.41	0.569	Klf3	Kruppel-like factor 3 (basic)	NM_008453	103170438	
-1.41	0.611	Defcr5	defensin related cryptdin 5	NM_007851	101940653	
-1.42	0.621	Dsg2	desmoglein 2	NM_007883	105340750	
-1.43	0.519	Glg1	golgi apparatus protein 1	NM_009149	101340162	
-1.45	0.415	Ppp4r2	protein phosphatase 4, regulatory subunit 2	NM_182939	102680609	
-1.47	0.357	9130404H23Rik	RIKEN cDNA 9130404H23 gene	XM_484657	106040022	
-1.47	0.348	Irf2bp2	interferon regulatory factor 2 binding protein 2, transcript variant 1	XM_284454	102850446	
-1.47	0.560	Sec23a	SEC23A (S. cerevisiae)	NM_009147	101500095	
-1.56	0.261	Reg3g	regenerating islet-derived 3 gamma	NM_011260	1340520	

-1.58	0.552	D17Wsu92e	DNA segment, Chr 17, Wayne State University 92, expressed	NM_001033279	103450372	
-1.71	0.169	Cxcl13	chemokine (C-X-C motif) ligand 13	NM_018866	6290402	
-1.74	0.150	Cd52	CD52 antigen	NM_013706	5910242	
-1.77	0.140	Ly6d	lymphocyte antigen 6 complex, locus D	NM_010742	4050010	
-1.78	0.120	Reg3b	regenerating islet-derived 3 beta	NM_011036	1780593	
-1.78	0.170	C3	complement component 3	NM_009778	1740372	
-1.80	0.127	Klk1b26	kallikrein 1-related petidase b26	NM_010644	101850092	
-1.83	0.114	Anpep	alanyl (membrane) aminopeptidase	NM_008486	6510138	
-1.87	0.112	Klk1b27	kallikrein 1-related peptidase b27	NM_020268	5900632	
-1.88	0.117	Lyzs	lysozyme	NM_017372	6770717	
-1.90	0.082	Herpud1	homocysteine-inducible, endoplasmic reticulum stress-inducible, ubiquitin-like domain member 1	NM_022331	7100440	
-1.91	0.073	Hspa1a	heat shock protein 1A	NM_010479	105130121	
-1.91	0.076	Tfrc	transferrin receptor	NM_011638	4050551	-2.43
-1.93	0.170	Faim3	Fas apoptotic inhibitory molecule 3	NM_026976	4060537	
-1.95	0.090	Cd74	CD74 antigen (invariant polypeptide of major histocompatibility complex, class II antigen-associated)	BC003476	101940500	
-2.00	0.049	Igtp	interferon gamma induced GTPase	NM_018738	2570056	
-2.00	0.054	Ccl5	chemokine (C-C motif) ligand 5	NM_013653	3710397	
-2.03	0.056	Apol7a	apolipoprotein L 7a	NM_029419	5130102	
-2.03	0.045	BC020489	PREDICTED: cDNA sequence BC020489, transcript variant 1	XM_128064	3060497	
-2.06	0.043	H2-Ab1	histocompatibility 2, class II antigen A, beta 1	NM_207105	4230427	
-2.06	0.046	H2-Eb1	histocompatibility 2, class II antigen E beta	NM_010382	2350079	
-2.07	0.040	H2-DMa	histocompatibility 2, class II, locus DMa	NM_010386	6290463	
-2.07	0.044	Psmb8	proteasome (prosome, macropain) subunit, beta type 8 (large multifunctional peptidase 7)	NM_010724	100780427	
-2.10	0.108	Dnase1	deoxyribonuclease I	NM_010061	1190167	
-2.11	0.042	Bag3	Bcl2-associated athanogene 3	NM_013863	4200487	
-2.11	0.042	Hsp90aa1	heat shock protein 90kDa alpha (cytosolic), class A member 1	NM_010480	2120722	
-2.11	0.046	Indo	indoleamine-pyrrole 2,3 dioxygenase	NM_008324	2680390	
-2.13	0.091	Reg3b	regenerating islet-derived 3 beta	NM_011036	2690524	
-2.13	0.036	H2-Ab1	histocompatibility 2, class II antigen A, beta 1	NM_207105	2370433	
-2.16	0.038	H2-DMb2	histocompatibility 2, class II, locus Mb2	NM_010388	6450593	
-2.16	0.040	2010001M09Rik	RIKEN cDNA 2010001M09 gene	NM_027222	6520136	
-2.17	0.041	Hspb1	heat shock protein 1	NM_013560	6760435	
-2.23	0.160	Dnase1	deoxyribonuclease I	NM_010061	6840546	
-2.25	0.028	Chordc1	cysteine and histidine-rich domain (CHORD)-containing, zinc-binding protein 1	NM_025844	6650577	
-2.29	0.026	Ubd	ubiquitin D	NM_023137	5570632	
-2.31	0.253	LOC620017	PREDICTED: similar to Ig kappa chain V-V region L7 precursor	XM_357633	510347	
-2.31	0.026	Slc38a5	solute carrier family 38, member 5	NM_172479	540093	
-2.37	0.030	Car4	carbonic anhydrase 4	NM_007607	130100	-4.08
-2.41	0.353	Rpl5	ribosomal protein L5	NM_016980	105270520	
-2.53	0.019	H2-Aa	histocompatibility 2, class II antigen A, alpha	NM_010378	5290673	
-2.62	0.019	Dnajb1	DnaJ (Hsp40) homolog, subfamily B, member 1	NM_018808	1090041	-2.17
-2.65	0.017	Cd74	CD74 antigen (invariant polypeptide of major histocompatibility complex, class II antigen-associated)	NM_010545	6400162	
-2.73	0.277	Tpt1	tumor protein, translationally-controlled 1	NM_009429	102570132	
-2.76	0.015	H2-Ab1	histocompatibility 2, class II antigen A, beta 1	NM_207105	4810050	
-3.23	0.249	Defcr-rs1	defensin related sequence cryptdin peptide (paneth cells)	NM_007844	107100142	
-3.28	0.286	Defa1	defensin, alpha 1	NM_010031	101050609	
-3.33	0.019	Egr1	early growth response 1	NM_007913	4610347	-2.32
-5.64	0.003	Hsph1	heat shock 105kDa/110kDa protein 1	NM_013559	1690017	-6.55

ORIGINAL COMMUNICATIONS

Iron Metabolism • Research Paper

Hepatic and extrahepatic expression of the new iron regulatory protein hemojuvelin

[haematologica]
2004;89:1441-1445

ALEJANDRA RODRIGUEZ MARTINEZ
ONNI NIEMELÄ
SEPPO PARKKILA

A B S T R A C T

Background and Objectives. Hereditary hemochromatosis (HH) is a common disorder of iron overload. A rare variant of the disease, juvenile hemochromatosis, is an early-onset form which is caused by mutations in a recently identified gene, called *HJV* or *HFE2*. A previous report based on Northern blotting showed human HJV mRNA expression only in the skeletal muscle, liver and heart.

Design and Methods. In this study we analyzed the expression of HJV mRNA in a number of human and mouse tissues by a sensitive reverse transcription-polymerase chain reaction method. We also studied the expression of HJV protein in mouse tissues using Western blotting. A polyclonal rabbit antibody was raised against a synthetic peptide which was designed based on the predicted sequence of human and mouse HJV protein.

Results. Human HJV mRNA expression was detected in the liver, heart, esophagus, pancreas, descending colon, ileocecum and skeletal muscle. Mouse tissues that were positive for expression included brain, liver, heart, lung, stomach, spleen, kidney, duodenum, jejunum, ileum, colon, skeletal muscle, testis and blood. By Western blotting, HJV protein expression was detected in the mouse liver, heart, kidney, brain and muscle.

Interpretation and Conclusions. The facts that HJV protein is expressed in the liver and mutations in the *HJV* gene induce hepatic iron accumulation point to a possibility that HJV protein may modulate iron transport in hepatocytes. The wide expression of HJV as shown in the present study suggests that its role in regulating iron allocation could be extended to other tissues beyond the liver.

Key words: expression, hemochromatosis, hemojuvelin, *HFE2*, mRNA.

From the Institute of Medical Technology (ARM, SP) and Department of Clinical Chemistry, University of Tampere and Tampere University Hospital, Tampere, Finland (ARM, ON, SP); Laboratory of EP Central Hospital, Seinäjoki, Finland (ON); Department of Clinical Chemistry, University of Oulu, Oulu, Finland (SP).

Correspondence:
Prof. Seppo Parkkila, MD, PhD, Institute of Medical Technology, University of Tampere, Biokatu 6, FI-33520 Tampere, Finland.
E-mail: seppo.parkkila@uta.fi

Hereditary hemochromatosis (HH) consists of a group of genetic disorders which lead to iron deposition in several tissues and consequent damage of organs, such as the liver, heart, and pancreas. Several variant forms of HH have been described with heterogeneous etiology and slight clinical differences (Table 1). In the classical form of HH (type 1), late complications in the absence of treatment usually appear between the 4th and the 5th decades of life. The medical problems manifested in HH include cirrhosis, hepatocellular carcinoma, cardiomyopathy, diabetes mellitus and hypogonadism. Type 1 HH is associated with mutations within the *HFE* gene.[1-3] Nevertheless, HH is genetically a heterogeneous disease, and the penetrance of different genotypes has remained unknown.[4] The HFE protein appears to have direct functional links to iron transport, since it was found to associate and interact with transferrin receptor (TfR) in cryptal enterocytes and in placental syncytiotrophoblasts.[5-7] In these locations, HFE protein is believed to have an important role in TfR-mediated iron transport. The ultimate proof that deficiency or functional derangement of the *HFE* gene product is the molecular basis of HH was provided when *HFE* gene knockout mice were found to exhibit hepatic iron accumulation in a manner similar to that in the classical form of HH.[8]

In juvenile hemochromatosis (JH), also called type 2 hemochromatosis, iron overload occurs at a young age, leading to clinical symptoms usually before 30 years of age. Severe and early development of cardiomyopathy and hypogonadism are characteristic features of this disorder, which affects both sexes equally.[9] Mutations in the hepcidin gene have been reported in some JH

Table 1. Background information on hereditary hemochromatosis (HH).

Genes of iron metabolism		*Types of HH*	
Gene/protein	*OMIM*	*Name of disorder*	*locus*
HFE/HFE	235200	Type 1, HFE-related HH	6p21.3
HFE2, HJV/Hemojuvelin	608374	Type 2A, juvenile hemochromatosis	1q21
HAMP/Hepcidin	606464	Type 2B, juvenile hemochromatosis	19q13
TFR2/Transferin receptor-2	604720	Type 3	7q22

patients.[10] Hepcidin is a small disulfide-bonded peptide with antimicrobial activity which is expressed primarily in the liver.[11,12] However, several reports demonstrated linkage to a locus on chromosome 1q21 in the majority of JH cases.[13-16] This locus was recently shown to contain a gene, called *HJV* or *HFE2*, which is probably the main causative gene of JH.[17] In the original report, Papanikolaou *et al.*[17] identified four missense mutations, one nonsense mutation and one frameshift mutation from 12 patients. In a subsequent report, Lee *et al.*[18] described two other mutations in the same gene. The *HJV* gene is 4,265 bp long and contains four exons.[17] It is transcribed into a full-length messenger-RNA with five spliced isoforms. Hemojuvelin (HJV), the protein product of the *HJV* gene, exists in three isoforms of 426, 313 and 200 amino acids. The possible function of HJV protein as a membrane-bound receptor or secreted polypeptide hormone was hypothesized based on several protein motifs identified in its amino acid sequence. Even though the exact function of HJV protein has not been established it is believed to have a role in iron metabolism.

A previous report based on Northern blotting analysis showed human HJV mRNA expression in skeletal muscle, liver and heart.[17] The present study was designed to investigate further the expression of HJV mRNA in human and mouse tissues as well as to provide the first evidence on HJV protein expression in mouse tissues.

Design and Methods

Polymerase chain reaction (PCR) analysis

The expression of human and mouse HJV mRNA was first examined using cDNA kits purchased from BD Biosciences (Palo Alto, CA, USA). The cDNA included in MTC™ panels were used as templates for PCR using *HJV* gene-specific primers. The human MTC™ digestive panel, panel I and panel II and mouse MTC™ panel I (BD Biosciences) contained first-strand cDNA preparations produced from total poly(A) RNA isolated from a number of different tissues. All human cDNA were derived from adult tissues. Another set of mouse cDNA was prepared in our laboratory. Total RNA from mouse tissue samples (pooled from 5 adult Balb/c mice) was prepared using TRIZOL reagent (Invitrogen, Carlsbad, CA, USA). cDNA was synthesized from total RNA using M-MuLV reverse transcriptase (Finnzymes, Espoo, Finland) using random primers (500 μg/mL) according to the manufacturer's instructions.

Two primers for amplifying human HJV cDNA were chosen based on the human mRNA sequence (GenBank database accession No. AY372521) which is the translated portion of the gene's longest transcript; forward 5′-TCACTTTCACACATGCCG-3' (nucleotides 540-557 in exon 3) and reverse 5'-GATCGAGAGAGTCGCTGAC-3' (nucleotides 971-989 in exon 4), which generated a 450-bp product corresponding to amino acids 180-330 of the protein sequence. The primers were produced by Sigma Genosys (Cambridgeshire, UK). Primers for β2-microglobulin were used to monitor the quantity of mRNA in the study samples.

To amplify mouse HJV cDNA, two primers (Sigma Genosys) were chosen based on the mouse HJV mRNA sequence published in GenBank (NM_027126); forward 5'-AGGCTGAGGTGGACAATC-3' (nucleotides 945-962) and reverse 5'-CAAGAAGACTCGGGCATC-3' (nucleotides 1382-1399), which generated a 455-bp product corresponding to amino acids 230-381 of the murine HJV protein sequence.[17] Primers for β-actin were used to assess the quantity of mRNA.

Amplification was performed using 2-3 ng of total cDNA as a template. The PCR reactions were amplified in a thermal cycler (Biometra, Göttingen, Germany). After initial denaturation at 94°C for 1 min, amplification was performed for 30-31 cycles of denaturation at 94°C for 30 s, annealing at 55-56°C for 30 s and extension at 72°C for 1 min 30 s, followed by a final extension at 72°C for 3 min. The PCR products were analyzed by electrophoresis on 1.5% agarose gel containing 0.1 μg/mL ethidium bromide with DNA standard (100 bp DNA Ladder, New England Biolabs, Beverly, MA, USA). Primers for glyceraldehyde 3-phosphate dehydrogenase (G3PDH, BD Biosciences) were used in all the performed experiments to monitor the amplification reaction.

The amplification products obtained from the human liver and muscle and mouse blood and 17-day old

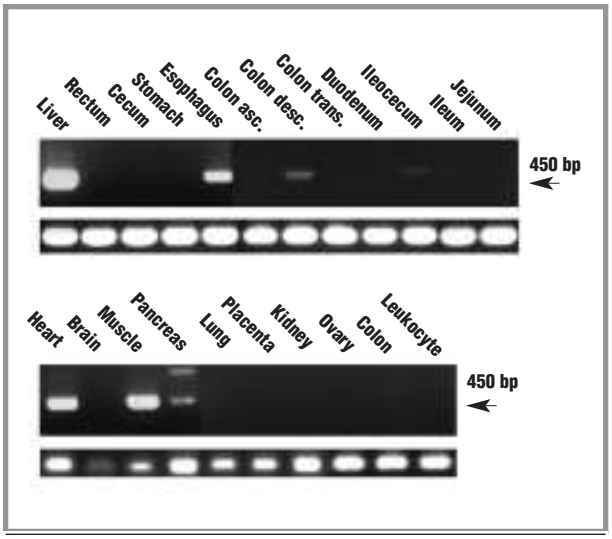

Figure 1. PCR analysis of human HJV mRNA expression. The amplified sequence partially includes exons 3 and 4. The strongest 450 bp signals are seen in the liver, esophagus, heart and muscle. Weaker bands are present in the descending colon and pancreas. A faint signal is present in the ileocecum. β-2-microglobulin primers were used to monitor the quantity of mRNA in the samples.

embryos were purified from agarose gel using GFX™ PCR DNA and Gel Band Purification kit (Amersham Biosciences, Buckinghamshire, UK). DNA sequencing reactions were performed using ABI PRISM™ Big Dye Terminator Cycle Sequencing Ready Reaction Kit, version 3.1 (Applied Biosystems, Foster City, CA, USA) according to manufacturer's protocol. The sequencing was finally performed on the ABI PRISM™ 3100 Genetic Analyzer (Applied Biosystems).

Antibodies

The rabbit anti-human/mouse HJV serum was raised by Innovagen AB (Lund, Sweden) against a synthetic peptide (NH_2-) SRSERNRRGAITIDTARRLC (-COOH) which was designed based on the predicted amino acid sequences of human and mouse HJV (amino acids 328-347 and 321-340 from human and murine HJV molecules, respectively).[17] Both mouse and human HJV mRNA sequences are available in GenBank (accession numbers AY372521 and NM_027126).

Western blotting

Samples of heart, lung, stomach, duodenum, jejunum, liver, ileum, colon, spleen, kidney, muscle, testis and brain were obtained from adult Balb/c mice. The procedures were approved by the institutional animal care committee (University of Tampere). The tissue samples were homogenized in phosphate-buffered saline (PBS) in the presence of protease inhibitors, and approximately 1 mg of protein from each sample was analyzed by SDS-PAGE (NuPAGE 10% Bis-Tris, Invitrogen) under reducing conditions according to Laemmli.[19] The separated proteins were transferred electrophoretically from the gel to a Parablot polyvinylidene fluoride membrane (Macherey-Nagel, Düren, Germany) in a Novex Xcell II blot module (Invitrogen). After the transblotting, HJV protein was detected by the electroluminescence method (Amersham Biosciences) according to the manufacturer's instructions. The primary antibody was diluted 1:2000. Control experiments were performed using preimmune serum (1:1000) instead of the anti-HJV serum.

Results

HJV gene expression in human tissues

The expression of the human *HJV* gene was studied by PCR amplification of a commercially available set of cDNA produced from selected human tissues, including liver, rectum, cecum, stomach, esophagus, ascending colon, descending colon, transverse colon, duodenum, ileocecum, ileum, jejunum, heart, brain, muscle, pancreas, lung, placenta, kidney, ovary, colon and leukocytes. Figure 1 shows a strong 450-bp band in the liver, esophagus, heart and muscle and weaker reactions in the descending colon and pancreas. A faint signal was also observed in the ileocecum. Rectum, cecum, stomach, ascending colon, transverse colon, duodenum, ileum, jejunum, brain, lung, placenta, kidney, ovary, colon and leukocytes were negative.

HJV gene expression in mouse tissues

The expression of the murine *HJV* gene was investigated by PCR amplification of cDNA samples produced in our laboratory out of 5 Balb/c mice (including blood, heart, lung, stomach, duodenum, jejunum, liver, ileum, colon, spleen, kidney, muscle, testis and brain) (Figure 2, upper panel). In addition, we used a commercially available set of cDNA produced from selected mouse specimens (including heart, brain, spleen, lung, testis, 7-day old embryo, 11-day old embryo, 15-day old embryo and 17-day old embryo) (Figure 2, lower panel). Positive 455-bp bands were observed in all tissue samples except for the brain and spleen of the commercial panel. It is of interest that a strong positive signal was amplified from the brain and spleen cDNA prepared in our laboratory. The three oldest embryos showed positive bands. Even though the PCR method was not quantitative, the signal became stronger with increasing age of the embryo, which could indicate a developmental regulation.

Expression of hemojuvelin in mouse tissues

Expression of mouse HJV protein was analyzed using Western blotting. Compared to the results in RT-PCR, the

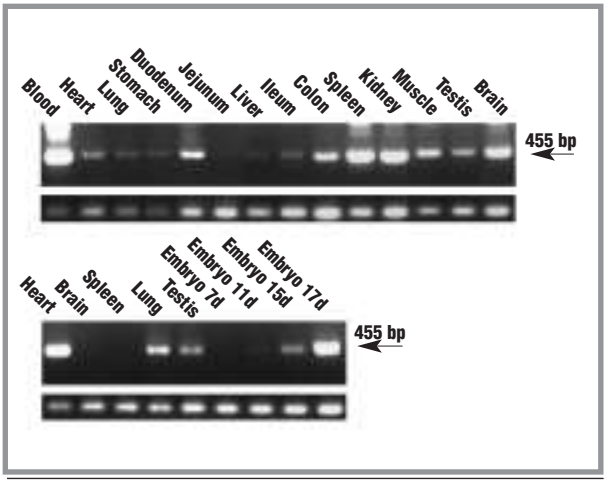

Figure 2. Expression of HJV mRNA in mouse tissues. The upper panel shows the results derived from the cDNA samples produced in our laboratory. The lower panel represents the commercial cDNA samples. Positive bands are observed in most tissue specimens except the brain and spleen in the lower panel. Note that the bands in the embryo samples become stronger with age. β-actin primers were used as an internal control to assess the quantity of mRNA.

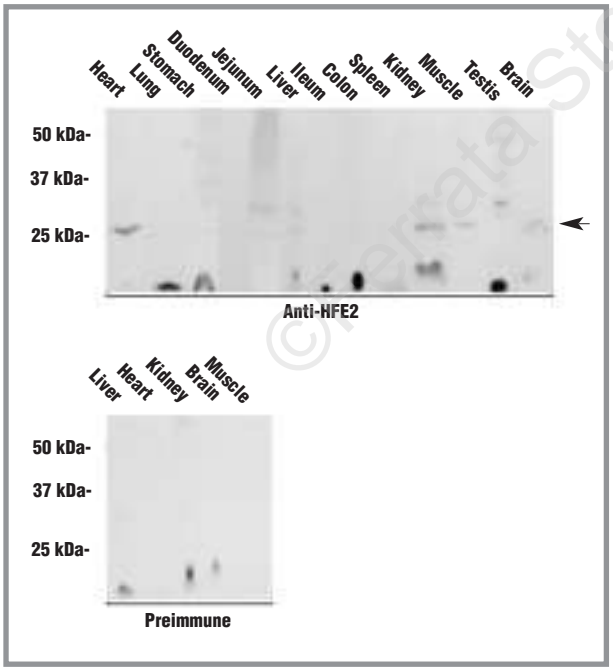

Figure 3. Western blotting of HJV protein in mouse tissues. The antibody was raised against a synthetic peptide which was designed based on the predicted amino acid sequences of human and mouse HJV. A positive polypeptide band of 26 kDa is present in the samples from heart, liver, kidney, muscle and brain. A band of 30 kDa is also observed in the samples from jejunum, liver, kidney and testis.

protein expression showed a more limited pattern of distribution. The results are shown in Figure 3. A 26 kDa positive band was observed in the liver, heart, kidney, brain and muscle. A 30 kDa band was also observed in the jejunum, liver, kidney and testis. These two bands most likely correspond to different HJV isoforms.[17] Both the antiserum and pre-immune serum showed low molecular weight bands in several lanes. These non-specific bands are probably present because of the high protein content in each lane.

Discussion

The present study was designed to elucidate HJV protein and mRNA expression in different human and mouse tissues. The RT-PCR results for human HJV agreed quite well with the distribution pattern recently reported by Papanikolaou *et al.*[17] In addition to the previously documented sites of expression (skeletal muscle, liver and heart), we found positive signals in four other tissues: descending colon, esophagus, ileocecum and pancreas. Of these, the last three were not previously tested for HJV expression.[17] The RT-PCR results indicated positive expression only in the descending colon, whereas the other segments of the large intestine were negative. Therefore, it is not surprising that the Northern blot result for colon has previously remained negative.[17] The observed variation may simply reflect different sampling. It is also notable that the signal intensities of RT-PCR and Northern blot did not correlate with each other.[17] This discrepancy can be attributed to the nature of the different methods. The RT-PCR method employed in the present study is not quantitative, although it is considered more sensitive than the Northern blotting.

In this paper, we also report the first results on HJV expression in mouse tissues. The data indicate that the transcript is more widely expressed than its human ortholog. In fact, the mRNA seems to be present in nearly every mouse tissue tested. This difference in the distribution of HJV mRNA may point to a physiological interspecies variation of iron metabolism. On the other hand, it is possible that the heterogeneity of primers could affect the results in the sensitive RT-PCR method. To confirm the specificity of the PCR reactions, the amplification products obtained from the human liver and muscle and mouse blood and 17-day old embryo were purified from agarose gel and subjected to DNA sequencing. The correct product was amplified from each tissue (*data not shown*). Even though we must be careful with attributing a quantification relevance to RT-PCR results, it is noteworthy that the *HJV* transcript seems to emerge during embryogenesis. No signal was visible at embryonic day 7, a positive band became

apparent in 11-day old embryos, and was found to further increase during the later stages. Absence of the specific mRNA during the early stages of development could indicate that HJV protein is not required during early processes such as blastocyst formation and implantation. However, the transcript was present at 11 days, which represents the peak time for organogenesis in mice. Based on those preliminary results, it would be interesting to correlate HJV expression to the developmental stages in more detailed investigations using *in situ* hybridization or immunohistochemistry.

Figure 2 showed some heterogeneity in HJV mRNA expression between different mice. Positive HJV signals were amplified from all cDNA samples, which were produced in our laboratory. In contrast, no amplification product was obtained from the commercial brain and spleen cDNA. The former cDNA were pooled from 5 mice and the latter cDNA from 200 mice. Thus, it is unlikely that any coincidences could explain this variation. Previous studies have demonstrated the influence of mouse strain on the severity of iron accumulation.[20, 21] Therefore, one can hypothesize that the expression of iron regulatory proteins including HJV could be affected by genetic factors linked to different strains or mouse colonies. Therefore, further studies should be conducted to evaluate HJV expression in several mouse strains as well as in mice with defective regulation of iron metabolism. According to our observations mouse HJV mRNA is more widely expressed than the corresponding protein. The differences in the distribution could be due to a higher sensitivity of the PCR amplification method as compared to the immunodetection. Another possibility is that the more limited protein expression pattern derives from post-transcriptional regulation. Nevertheless, the data suggests that HJV mRNA is expressed in a number of different human and mouse tissues. Thus, the role of the HJV protein may not be restricted to those organs, which are classically considered most important for orchestrating iron allocation. Mouse HJV protein was also detected in tissues where iron is primarily accumulated during the development of juvenile hemochromatosis, which supports a role for the HJV protein in the regulation of iron transport in these tissues. Although as yet only little is known about this interesting protein, the present results should open avenues for cell level-oriented studies on the role and mechanisms of HJV protein in the regulation of iron homeostasis.

All authors (ARM, ON, SP) gave substantial contributions to the conception and design of the study, analysis and interpretation of data, drafting and revising the article critically, and gave the final approval of the present version of the manuscript. ARM performed most of the laboratory analyses. SP and ON supervised the study.

This work was supported by grants from the Sigrid Juselius Foundation and Academy of Finland to SP, and from the Finnish Foundation for Alcohol Studies to ON.

The authors reported no potential conflicts of interest.

Manucript received June 22, 2004. Accepted September 6, 2004.

References

1. Feder JN, Gnirke A, Thomas W, Tsuchihashi Z, Ruddy DA, Basava A, et al. A novel MHC class I-like gene is mutated in patients with hereditary haemochromatosis. Nat Genet 1996; 13:399-408.
2. Trinder D, Fox C, Vautier G, Olynyk JK. Molecular pathogenesis of iron overload. Gut 2002;51:290-5.
3. Parkkila S, Niemela O, Britton RS, Fleming RE, Waheed A, Bacon BR, et al. Molecular aspects of iron absorption and HFE expression. Gastroenterology 2001;121:1489-96.
4. Merryweather-Clarke AT, Cadet E, Bomford A, Capron D, Viprakasit V, Miller A, et al. Digenic inheritance of mutations in HAMP and HFE results in different types of haemochromatosis. Hum Mol Genet 2003;12:2241-7.
5. Lebron JA, Bennett MJ, Vaughn DE, Chirino AJ, Snow PM, Mintier GA, et al. Crystal structure of the hemochromatosis protein HFE and characterization of its interaction with transferrin receptor. Cell 1998;93:111-23.
6. Parkkila S, Waheed A, Britton RS, Bacon BR, Zhou XY, Tomatsu S, et al. Association of the transferrin receptor in human placenta with HFE, the protein defective in hereditary hemochromatosis. Proc Natl Acad Sci USA 1997;94:13198-202.
7. Waheed A, Parkkila S, Saarnio J, Fleming RE, Zhou XY, Tomatsu S, et al. Association of HFE protein with transferrin receptor in crypt enterocytes of human duodenum. Proc Natl Acad Sci USA 1999;96:1579-84.
8. Zhou XY, Tomatsu S, Fleming RE, Parkkila S, Waheed A, Jiang J, et al. HFE gene knockout produces mouse model of hereditary hemochromatosis. Proc Natl Acad Sci USA 1998; 95:2492-7.
9. De Gobbi M, Roetto A, Piperno A, Mariani R, Alberti F, Papanikolaou G, et al. Natural history of juvenile haemochromatosis. Br J Haematol 2002;117:973-9.
10. Roetto A, Papanikolaou G, Politou M, Alberti F, Girelli D, Christakis J, et al. Mutant antimicrobial peptide hepcidin is associated with severe juvenile hemochromatosis. Nat Genet 2003;33:21-2.
11. Krause A, Neitz S, Magert HJ, Schulz A, Forssmann WG, Schulz-Knappe P, et al. LEAP-1, a novel highly disulfide-bonded human peptide, exhibits antimicrobial activity. FEBS Lett 2000;480:147-50.
12. Park CH, Valore EV, Waring AJ, Ganz T. Hepcidin, a urinary antimicrobial peptide synthesized in the liver. J Biol Chem 2001; 276: 7806-10.
13. Roetto A, Totaro A, Cazzola M, Cicilano M, Bosio S, D'Ascola G, et al. Juvenile hemochromatosis locus maps to chromosome 1q. Am J Hum Genet 1999;64:1388-93.
14. Papanikolaou G, Politou M, Roetto A, Bosio S, Sakelaropoulos N, Camaschella C, et al. Linkage to chromosome 1q in Greek families with juvenile hemochromatosis. Blood Cells Mol Dis 2001;27:744-9.
15. Barton JC, Rao SV, Pereira NM, Gelbart T, Beutler E, Rivers CA, et al. Juvenile hemochromatosis in the southeastern United States: a report of seven cases in two kinships. Blood Cells Mol Dis 2002; 29:104-15.
16. Rivard SR, Lanzara C, Grimard D, Carella M, Simard H, Ficarella R, et al. Juvenile hemochromatosis locus maps to chromosome 1q in a French Canadian population. Eur J Hum Genet 2003;11:585-9.
17. Papanikolaou G, Samuels ME, Ludwig EH, MacDonald ML, Franchini PL, Dube MP, et al. Mutations in HFE2 cause iron overload in chromosome 1q-linked juvenile hemochromatosis. Nat Genet 2004;36:77-82.
18. Lee PL, Beutler E, Rao SV, Barton JC. Genetic abnormalities and juvenile hemochromatosis: mutations of the HJV gene encoding hemojuvelin. Blood 2004;103:4669-71.
19. Laemmli UK. Cleavage of structural proteins during the assembly of the head of bacteriophage T4. Nature 1970;227:680-5.
20. Fleming RE, Holden CC, Tomatsu S, Waheed A, Brunt EM, Britton RS, et al. Mouse strain differences determine severity of iron accumulation in Hfe knockout model of hereditary hemochromatosis. Proc Natl Acad Sci USA 2001;98:2707-11.
21. Leboeuf RC, Tolson D, Heinecke JW. Dissociation between tissue iron concentrations and transferrin saturation among inbred mouse strains. J Lab Clin Med 1995;126:128-36.

BMC Genomics

BioMed Central

Research article

Effects of iron loading on muscle: genome-wide mRNA expression profiling in the mouse

Alejandra Rodriguez*[1], Mika Hilvo[1], Leena Kytömäki[2], Robert E Fleming[3,4], Robert S Britton[5], Bruce R Bacon[5] and Seppo Parkkila[1,6]

Address: [1]Institute of Medical Technology, University of Tampere and Tampere University Hospital, Tampere, Finland, [2]Turku Centre for Biotechnology, University of Turku, Turku, Finland, [3]Department of Pediatrics, Saint Louis University School of Medicine, St. Louis, USA, [4]Edward A. Doisy Department of Biochemistry and Molecular Biology, Saint Louis University School of Medicine, St. Louis, USA, [5]Department of Internal Medicine, Saint Louis University School of Medicine, St. Louis, USA and [6]Department of Clinical Chemistry, University of Oulu, Oulu, Finland

Email: Alejandra Rodriguez* - alejandra.rodriguez.martinez@uta.fi; Mika Hilvo - mika.hilvo@uta.fi; Leena Kytömäki - leena.kytomaki@btk.fi; Robert E Fleming - flemingr@slu.edu; Robert S Britton - brittonr@slu.edu; Bruce R Bacon - baconbr@slu.edu; Seppo Parkkila - seppo.parkkila@uta.fi

* Corresponding author

Published: 19 October 2007

BMC Genomics 2007, **8**:379 doi:10.1186/1471-2164-8-379

Received: 21 May 2007
Accepted: 19 October 2007

This article is available from: http://www.biomedcentral.com/1471-2164/8/379

Abstract

Background: Hereditary hemochromatosis (HH) encompasses genetic disorders of iron overload characterized by deficient expression or function of the iron-regulatory hormone hepcidin. Mutations in 5 genes have been linked to this disease: *HFE*, *TFR2* (encoding transferrin receptor 2), *HAMP* (encoding hepcidin), *SLC40A1* (encoding ferroportin) and *HJV* (encoding hemojuvelin). Hepcidin inhibits iron export from cells into plasma. Hemojuvelin, an upstream regulator of hepcidin expression, is expressed in mice mainly in the heart and skeletal muscle. It has been suggested that soluble hemojuvelin shed by the muscle might reach the liver to influence hepcidin expression. Heart muscle is one of the target tissues affected by iron overload, with resultant cardiomyopathy in some HH patients. Therefore, we investigated the effect of iron overload on gene expression in skeletal muscle and heart using Illumina™ arrays containing over 47,000 probes. The most apparent changes in gene expression were confirmed using real-time RT-PCR.

Results: Genes with up-regulated expression after iron overload in both skeletal and heart muscle included angiopoietin-like 4, pyruvate dehydrogenase kinase 4 and calgranulin A and B. The expression of transferrin receptor, heat shock protein 1B and DnaJ homolog B1 were down-regulated by iron in both muscle types. Two potential hepcidin regulatory genes, hemojuvelin and neogenin, showed no clear change in expression after iron overload.

Conclusion: Microarray analysis revealed iron-induced changes in the expression of several genes involved in the regulation of glucose and lipid metabolism, transcription and cellular stress responses. These may represent novel connections between iron overload and pathological manifestations of HH such as cardiomyopathy and diabetes.

Background

It is crucial for the human body to maintain iron homeostasis. Since there is no adjustable mechanism to influence iron loss from the body, tight regulation of iron absorption at the intestinal level is vital [1]. In order to maintain iron balance, iron export from enterocytes, reticuloendothelial macrophages and hepatocytes into the blood stream has to be controlled as well. Functional derangement of proteins involved in these regulatory mechanisms can cause hereditary hemochromatosis (HH, OMIM-235200). This genetic disorder of iron overload is characterized by high transferrin saturation, low iron content in macrophages, and deposition of iron in several organs including the liver, heart, and pancreas. Causative mutations for HH have been described in several genes, namely *HFE*, *TFR2* (encoding transferrin receptor 2), *HJV* (encoding hemojuvelin), and *HAMP* (encoding hepcidin) [2-7]. It has been proposed that these mutations cause deficient hepcidin synthesis [4,5,8,9].

The antimicrobial peptide hepcidin is the central regulator of iron metabolism. It is produced mainly in the liver and exerts its function by binding to the iron export protein, ferroportin, inducing its internalization and degradation [10]. Ferroportin is located in the cellular membranes of enterocytes, reticuloendothelial cells, hepatocytes and placental cells [11]. Therefore, hepcidin acts to decrease the export of iron from these cells into the circulation.

Hemojuvelin is a glycosyl phosphatidylinositol-anchored protein which belongs to the repulsive guidance molecule (RGM) protein family [4,12]. Recent studies suggest that hemojuvelin exists in two forms. One is a rarer full-length protein shed to the extracellular fluid, where it has a long half-life. The other is a smaller, membrane-associated disulfide-linked heterodimer, which is a more abundant but shorter-lived form composed of N- and C-terminal fragments [13,14]. According to latest studies the most common mutation in hemojuvelin (G320V) affects the targeting of the membrane-associated form and reduces the amount of the soluble form [15]. Interestingly, studies in cultured cells suggest that the two forms regulate hepcidin expression reciprocally by competing for a receptor binding site [14]. Evidence shows that hemojuvelin is a bone morphogenetic protein co-receptor, and its interaction with BMP initiates a signaling cascade that leads to regulation of hepcidin expression [16,17]. On the other hand, it has been observed that overexpressed hemojuvelin binds to the membrane receptor neogenin and that this interaction is required for the accumulation of iron in cultured cells [12]. Zhang *et al*. also showed that the G320V mutated hemojuvelin overexpressed *in vitro* was not able to bind neogenin, and that iron did not accumulate in the cells under these conditions. Furthermore, a recent study in cultured cells suggested that neogenin may mediate inhibition of hemojuvelin shedding in response to iron [18]. We have previously determined the sites of simultaneous expression of hemojuvelin and neogenin [19]. The highest expression of hemojuvelin transcript is found in the skeletal muscle and heart. Although *in vivo* evidence of a combined role of hemojuvelin and neogenin in iron homeostasis has not been provided yet, it has been suggested that hemojuvelin shed from skeletal muscle and heart by neogenin-dependent mechanism could reach the liver to influence hepcidin expression [12].

Cardiomyopathy develops in some HH patients [20]. In order to better understand the mechanisms behind pathological effects of iron overload in muscle cells, we have performed a genome-wide expression analysis of genes in skeletal muscle and heart of mice with or without dietary iron loading. Microarray data analysis identified several genes whose expression was either down- or up-regulated due to iron overload. These results may reveal novel links between iron overload and pathological manifestations of HH.

Results

Documentation of iron overload in the liver and heart of iron-fed mice

The mice were fed either standard (0.02% carbonyl iron) or high-iron (2% carbonyl iron) diet for 6 weeks. Iron concentrations of liver and heart specimens were determined to confirm the validity of the animal model. Figure 1A demonstrates that the livers of mice of all three strains were highly iron-loaded when fed an iron-rich diet. A much smaller increment in cardiac iron content after a high-iron diet was observed also in all three strains and in both genders (Figure 1B), although statistical significance was not reached in all the cases. Basal cardiac iron levels were lower than basal hepatic contents. In general, female mice showed slightly higher hepatic and cardiac iron levels than male mice.

Identification and validation of changes in gene expression induced by dietary iron overload in skeletal muscle and heart

We obtained a list of 14 genes with iron-induced up-regulated expression in skeletal muscle (Table 1) and forty with down-regulated expression (Table 2). In the heart, iron loading resulted in the up-regulation of 35 genes (Table 3), while forty genes had down-regulated expression after iron overload (Table 4). There were seven genes which were up-regulated in both the heart and skeletal muscle, while nine genes were down-regulated in both tissues.

From the lists of microarray results we selected 15 genes which presented the highest fold change values. The

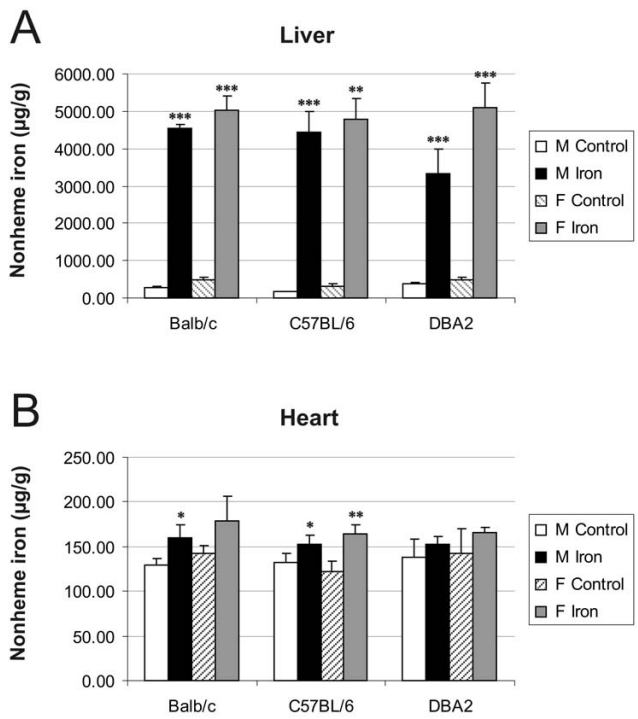

Figure 1

Hepatic and cardiac non-heme iron concentrations. Iron contents were studied in three strains of male and female mice fed either the control or high-iron diet. The result values are expressed as mean +/- standard deviation. Statistical significant differences relative to control diet fed mice were determined. *$p < 0,05$; **$p < 0,01$; ***$p < 0,001$. F = female; M = male.

expression levels of these genes were then analyzed in the same mouse strain (C57BL/6) by Q-RT-PCR (quantitative reverse-transcription PCR). Certainly, the results from these analyses showed a good correlation between the two methods; the expression of all the genes was regulated and displayed the same direction of change. The fold change values obtained from PCR experiments were all over 1.4 except for the Tfrc gene whose downregulation in the skeletal muscle reached the value of -1.36.

Representations of these Q-RT-PCR results are depicted in figures 2 and 3. In general, the fold-change values obtained by microarray analysis were smaller than those determined by Q-RT-PCR. This phenomenon has been described previously and is probably due to the fact that array analyses are less quantitative than Q-PCR [21].

The hepatic mRNA levels of these 15 genes were also analyzed by Q-RT-PCR. The results for genes whose expression varied in the same direction in both skeletal muscle and heart after iron loading are shown together with their expression in the liver in Figure 4. The expression of four of the 15 genes (*Myl4*, *Myl7*, *Acta1 and Adn*) was considered negligible in the liver because of very low signal intensity. Among the 11 remaining genes only the hepatic expression of *Pdk4* (shown in figure 4B) and Cxcl7 (fold change of +1.38, data not shown) was not significantly regulated by dietary iron.

Expression of genes involved in hepcidin regulatory pathway during dietary iron overload

One of the aims of this study was to explore the effect of dietary iron overload on the expression of the iron-related genes hemojuvelin (*Hjv*) and neogenin (*Neo*) in skeletal muscle and heart. We did not observe differential expression of these genes or any of the traditional iron-regulatory genes (such as *Cybrd1*, *Slc11a2*, *Slc40a1*, *Heph*, *Trfr2*, *Hfe* or *Hamp*) by the microarray approach, except for the transferrin receptor gene (*Tfrc*), which was down-regulated by iron in heart, skeletal muscle and liver (Figure 4E). Even though the microarray method we used proved to be very accurate, we wanted to verify these results and to explore the response of hepcidin expression in the studied tissues by Q-RT-PCR.

The expression of hepcidin1 and hepcidin2 in the liver was greatly up-regulated by iron overload and varied according to mouse strain and gender [22,23]. In Balb/c and C57BL/6 mice, hepcidin 1 was the predominant form expressed in the liver, while in DBA2 mice, the hepatic expression of hepcidin 2 was dominant (Figures 5C and Figure 6C). The expression of hepcidin1 in the skeletal muscle was negligible in all strains (Figure 5A). In the heart muscle, it showed a slight tendency towards decreased expression in most iron fed mice, although the baseline signal in control mice was already quite low (Figure 5B). Only DBA2 mice expressed hepcidin2 in the skeletal muscle and heart, and this expression was not clearly regulated by iron overload (Figure 6A and 6B).

The results for hemojuvelin expression did not indicate any clear regulation by iron overload, strain or gender in any of the tissues studied (Figure 7). This is in agreement with previous studies of hepatic expression [24,25]. Hemojuvelin expression only showed a minor trend downwards in skeletal muscle and heart of mice fed with high-iron diet. No significant changes were observed for neogenin expression (Figure 8).

Discussion

Excess free iron participates in the formation of free radicals causing oxidative stress and cell damage, which is evidenced as a series of pathological manifestations [26]. While some studies have analyzed the effects of iron on the transcriptional profiles in liver and duodenum, this is the first study reporting changes in mRNA expression that may contribute to iron-induced effects on skeletal muscle

Table 1: Genes with up-regulated expression in skeletal muscle during iron overload

Gene name	Symbol	Accession.	Fold change
Calgranulin A, S100 calcium binding protein A8	S100a8	NM_013650	2.80
Calgranulin B, S100 calcium binding protein A9	S100a9	NM_009114	2.26
Stearoyl-Coenzyme A desaturase 1	Scd1	NM_009127	1.75
Adipsin, complement factor D	Adn	NM_013459	1.62
Myosin light polypeptide 2	Myl2	NM_010861	1.60
UDP-N-acetyl-alpha-D-galactosamine:polypeptide N-acetylgalactosaminyl transferase-like 2	Galntl2	XM_127638	1.56
cytochrome P450, family 26, subfamily b, polypeptide 1	Cyp26b1	NM_175475	1.49
cold inducible RNA binding protein	Cirbp	NM_007705	1.48
Cbp/p300-interacting transactivator, with Glu/Asp-rich carboxy-terminal domain, 2	Cited2	NM_010828	1.46
angiopoietin-like 4	Angptl4	NM_020581	1.45
epididymal protein Av381126		NM_183143	1.45
pyruvate dehydrogenase kinase, isoenzyme 4	Pdk4	NM_013743	1.40
myeloid/lymphoid or mixed lineage-leukemia translocation to 4 homolog (Drosophila)	Mllt4	XM_890447	1.40
6-phosphofructo-2-kinase/fructose-2,6-biphosphatase 3	Pfkfb3	NM_133232	1.40

Data obtained with 3 high-iron and 3 control samples.

and heart. We used a genome-wide mRNA expression profiling approach and validated the most substantive changes by Q-RT-PCR.

Expression of antioxidant enzymes is considered a protective mechanism against oxidative stress-induced damage. However, the regulation of antioxidant enzymes in response to oxidative stress is a rather controversial issue, as the results vary greatly depending on the type and length of the stimulus and the type of cells or tissue tested. We did not find increased expression of oxidative stress-related genes or antioxidant enzymes after iron overload, except for glutathione peroxidase 3, whose expression was induced by 1.35-fold change in heart (data not shown).

The data analysis identified two genes encoding calcium- and zinc-binding proteins, *S100a8* (calgranulin A) and *S100a9* (calgranulin B) among the up-regulated genes presenting the highest fold changes. These proteins form a rather ubiquitous heterodimer called calprotectin. The highest amounts of this protein complex are located in neutrophil granulocytes, monocytes and keratinocytes [27]. Calprotectin is a pro-inflammatory cytokine that is upregulated in many inflammatory conditions, and is involved in innate immunity, leukocyte adhesion, endothelial transmigration and processes of chronic inflammation [28]. *In vitro* studies have shown that reactive oxygen species (ROS) induce protein levels of S100a9 [29]. Additionally, S100a8 expression is induced in keratinocytes upon exposure to ultraviolet A (UVA) radiation, a stimulus causing oxidative stress. Interestingly, the antioxidant enzymes superoxide dismutase and catalase, whose mRNA expression was unaffected in our microarray, abrogate S100a8 induction [30]. We found that both S100a8 and S100a9 transcripts were substantially up-regulated in skeletal muscle, heart and liver of iron-loaded mice, although the levels of S100a8 transcript in skeletal muscle were negligible and, in general, both genes were weakly expressed. This demonstrates the high sensitivity and accuracy of both the microarray analysis and the Q-RT-PCR method. It is noteworthy that S100a8 and S100a9 transcripts showed a very similar up-regulation pattern in the tissues studied, which agrees with the concept of the two proteins forming a heterodimer. The transcriptional regulation of the *S100a8* and *S100a9* genes seems to be rather complex, with promoter binding sites for transcription factors such as activator protein 1 (AP-1), nuclear factor kappa B (NF-κB) and C/EBP. Consistently, at least AP-1 and NF-κB have been previously identified to be regulated by the intracellular redox state [31].

Pyruvate dehydrogenase kinase 4 (Pdk4) phosphorylates and inactivates the pyruvate dehydrogenase complex, decreasing the rate of glucose oxidation and thus increasing blood glucose levels. Increased Pdk4 expression and activity has been observed in both skeletal muscle [32,33] and heart [34] of insulin-resistant mouse models. The question arises of whether Pdk4 overexpression causes insulin resistance or *vice versa*. Insulin suppresses Pdk4 expression in skeletal muscle [35] and, according to a recent study by Kim and coworkers [36], this effect is impaired in insulin resistance, suggesting that insulin resistance may indeed induce Pdk4 expression. However, several studies using high-fat dietary models of insulin resistance indicate that Pdk4 overexpression occurs before the development of insulin resistance [37-39]. Although it has not been documented directly that increased Pdk4 mRNA levels can indeed cause insulin resistance, it seems possible that a vicious cycle may exist between these two phenomena. In the present study, we show an up-regulation of Pdk4 mRNA levels in skeletal muscle and heart but not in the liver of iron-loaded mice. Diabetes mellitus is

Table 2: Genes with down-regulated expression in skeletal muscle during iron overload

Gene name	Symbol	Accession.	Fold change
major urinary protein 1	Mup1	NM_031188	-2.61
DnaJ (Hsp40) homolog, subfamily B, member 1	Dnajb1	NM_018808	-2.52
Heat shock protein 1B	Hspa1b	NM_010478	-2.40
solute carrier family 25 (mitochondrial carrier, phosphate carrier), member 25	Slc25a25	NM_146118	-2.22
major urinary protein 3	Mup3	NM_010845	-2.21
FBJ osteosarcoma oncogene	Fos	NM_010234	-2.10
heat shock protein 1, alpha	Hspca	NM_010480	-1.91
early growth response 3	Egr3	NM_018781	-1.79
metallothionein 1	Mt1	NM_013602	-1.78
heat shock protein 105	Hsp105	NM_013559	-1.72
RIKEN full-length enriched library, clone:A530098C11 product: hypothetical SAM (and some other nucleotide) binding motif containing protein		AK041301	-1.70
ERBB receptor feedback inhibitor 1	Errfi1	NM_133753	-1.69
inhibitor of DNA binding 1	Idb1	NM_010495	-1.66
Transthyretin	Ttr	NM_013697	-1.65
Kruppel-like factor 4	Klf4	NM_010637	-1.65
nuclear factor, interleukin 3, regulated	Nfil3	NM_017373	-1.64
cyclin-dependent kinase inhibitor 1A	Cdkn1a	NM_007669	-1.62
RIKEN full-length enriched library, clone:D830037I21 product:weakly similar to RING ZINC FINGER PROTEIN SMRZ [Homo sapiens]		AK052911	-1.61
protein phosphatase 1, regulatory subunit 10	Ppp1r10	NM_175934	-1.61
connective tissue growth factor	Ctgf	NM_010217	-1.59
serine (or cysteine) proteinase inhibitor, clade H, member 1	Serpinh1	NM_009825	-1.58
cerebellar degeneration-related 2	Cdr2	NM_007672	-1.58
neural precursor cell expressed, developmentally down-regulated gene 9	Nedd9	NM_017464	-1.58
apolipoprotein A-II	Apoa2	NM_013474	-1.54
DNA-damage-inducible transcript 4	Ddit4	NM_029083	-1.54
PDZ and LIM domain 1	Pdlim1	NM_016861	-1.51
activating transcription factor 3	Atf3	NM_007498	-1.49
heat shock protein 1A	Hspa1a	NM_010479	-1.48
heat shock protein 1	Hspb1	NM_013560	-1.48
neural precursor cell expressed, developmentally down-regulated gene 9	Nedd9	NM_017464	-1.47
actin, alpha, cardiac	Actc1	NM_009608	-1.46
inositol hexaphosphate kinase 3	Ihpk3	NM_173027	-1.45
kidney androgen regulated protein	Kap	NM_010594	-1.44
metallothionein 2	Mt2	NM_008630	-1.44
8430408G22Rik		NM_145980	-1.43
cyclin-dependent kinase inhibitor 1A	Cdkn1a	NM_007669	-1.42
G0/G1 switch gene 2	G0s2	NM_008059	-1.42
fos-like antigen 2	Fosl2	NM_008037	-1.42
procollagen, type I, alpha 1	Col1a1	NM_007742	-1.41
dysferlin interacting protein 1	Dysfip1	NM_026814	-1.40

Data obtained with 3 high-iron and 3 control samples.

the major endocrine disorder associated with HH. The mechanisms responsible for this clinical manifestation are still obscure, but two processes have been proposed: the pancreatic β-cell iron accumulation results in cell damage and diminished insulin secretion, and liver iron overload leads to insulin resistance [40]. The herein reported induction of Pdk4 expression in the skeletal and heart muscle might represent a novel mechanism involved in the development of diabetes mellitus in HH.

Angiopoietin-like 4 (Angptl4) is a secreted protein produced mainly in fat tissue, and to a lesser extent in liver, placenta, skeletal muscle and heart. It is directly involved in regulating glucose homeostasis, lipid metabolism, and insulin sensitivity. Angptl4 decreases the activity of lipoprotein lipase (LPL), thus inhibiting lipoprotein metabolism and increasing plasma triglyceride levels. Transgenic mice with Angptl4 overexpression directed to heart muscle (lipoprotein-derived fatty acids are the major energy source in this tissue) show reduced cardiac LPL activity, decreased triglyceride utilization and impaired cardiac function resulting in cardiomyopathy [41]. Transgenic overexpression of Angptl4 from a liver-specific promoter causes hypertriglyceridemia similar to that induced by

adenoviral over-expression [42]. These results support the hypothesis that Angptl4 has LPL-dependent actions [43]. Accordingly, in LPL-expressing tissues (muscle, heart and adipose tissue) Angptl4 may bind directly and inactivate LPL, restricting acquisition of free fatty acids to these sites: it is not shed into plasma from these tissues but rather acts in an autocrine/paracrine fashion. On the other hand, in the liver, which has low LPL expression, Angptl4 is shed to plasma and inhibits LPL in other locations, causing a general reduction of triglyceride utilization and acting as an endocrine factor. Interestingly, we showed a 5-fold increase in the level of Angptl4 transcript in the heart of iron-loaded mice, raising the possibility that early induction of Angptl4 expression could contribute to the pathogenesis of cardiomyopathy in HH. The increased expression of Pdk4 and Angptl4 observed in skeletal muscle and heart of iron-loaded mice might have its origin in a common mechanism. The forkhead transcription factor Foxo1 is a major regulator of insulin action in insulin-sensitive tissues (liver, skeletal muscle and adipose tissues) and it is involved in insulin's action to suppress Pdk4 and Angptl4 [36,44].

Table 3: Genes with up-regulated expression in the heart during iron overload

Gene name	Symbol	Accession.	Fold change
myosin, light polypeptide 7, regulatory	Myl7	NM_022879	7.68 **
myosin, light polypeptide 4, alkali	Myl4	NM_010858	6.32 **
seminal vesicle secretion 5	Svs5	NM_009301	5.21 **
seminal vesicle protein 2	Svp2	NM_009300	4.25 **
myosin binding protein H-like	Mybphl	NM_026831	4.14 **
angiopoietin-like 4	Angptl4	NM_020581	2.79 *
seminal vesicle protein, secretion 2	Svs2	NM_017390	2.61 **
pyruvate dehydrogenase kinase, isoenzyme 4	Pdk4	NM_013743	2.06 *
S100 calcium binding protein A8 (calgranulin A)	S100a8	NM_013650	1.96 *
S100 calcium binding protein A9 (calgranulin B)	S100a9	NM_009114	1.95 *
3-hydroxy-3-methylglutaryl-Coenzyme A synthase 2	Hmgcs2	NM_008256	1.82 **
Ras-related associated with diabetes	Rrad	NM_019662	1.81 **
thioredoxin interacting protein	Txnip	NM_023719	1.78 *
secretory leukocyte protease inhibitor	Slpi	NM_011414	1.69 **
dickkopf homolog 3 (Xenopus laevis)	Dkk3	NM_015814	1.68 **
START domain containing 10	Stard10	NM_019990	1.68 **
D site albumin promoter binding protein	Dbp	NM_016974	1.65 *
lectin, galactose binding, soluble 4	Lgals4	NM_010706	1.65 **
cytochrome P450, family 26, subfamily b, polypeptide 1	Cyp26b1	NM_175475	1.62 **
2310043N10Rik		XM_979471	1.55 *
cold inducible RNA binding protein	Cirbp	NM_007705	1.49 *
FBJ osteosarcoma oncogene	Fos	NM_010234	1.49 **
2900060B14Rik			1.49 *
early growth response 1	Egr1	NM_007913	1.46 *
1810015C04Rik		NM_025459	1.45 *
seminal vesicle secretion 1	Svs1	NM_172888	1.44 **
Iroquois related homeobox 3 (Drosophila)	Irx3	NM_008393	1.43 **
	BC031353	NM_153584	1.43 *
folliculin interacting protein 1	Fnip1	NM_173753	1.42 **
myosin, heavy polypeptide 7, cardiac muscle, beta	Myh7	NM_080728	1.42 **
Cbp/p300-interacting transactivator, with Glu/Asp-rich carboxy-terminal domain, 2	Cited2	NM_010828	1.41*
2610035D17Rik		XM_990633	1.41 **
a disintegrin-like and metalloprotease (reprolysin type) with thrombospondin type 1 motif, 1	Adamts1	NM_009621	1.40 *
fructose bisphosphatase 2	Fbp2	NM_007994	1.40 *
2300009N04Rik			1.40 *

*Data obtained with 2 high-iron and 2 control samples.
** Data obtained with 3 high-iron and 3 control samples.

Myosin light polypeptide 4 (Myl4) (encoding the alkali atrial essential light chain (ELCa)) and myosin light polypeptide 7 (Myl7) (encoding the regulatory light chain (RLC-A)) show a 10-fold up-regulation in the cardiac muscle of iron-loaded mice. Both genes belong to the EF-hand family of Ca^{2+} binding proteins and are part of the myosin molecular complex. They appear to be involved in force development during muscle contraction. ELC is important in the interaction between myosin and actin

Table 4: Genes with down-regulated expression in the heart during iron overload

Gene name	Symbol	Accession.	Fold change
uncoupling protein 1, mitochondrial	Ucp1	NM_009463	-4.47 **
actin, alpha 1, skeletal muscle	Acta1	NM_009606	-2.79 *
chemokine (C-X-C motif) ligand 7	Cxcl7	NM_023785	-2.41 *
stearoyl-Coenzyme A desaturase 1	Scd1	NM_009127	-2.40 **
heat shock protein 1B	Hspa1b	NM_010478	-2.25 **
heat shock protein 105	Hsp105	NM_013559	-2.25 **
tubulin, beta 1, 2810484G07Rik	Tubb1		-2.15 *
Adipsin	Adn	NM_013459	-1.92 **
carbonic anhydrase 3	Car3	NM_007606	-1.91 **
DnaJ (Hsp40) homolog, subfamily B, member 1	Dnajb1	NM_018808	-1.90 **
ERBB receptor feedback inhibitor 1	Errfi1	NM_133753	-1.81 **
RIKEN full-length enriched library, clone:F830002E14 product: hypothetical Phenylalanine-rich region profile containing protein		AK089567	-1.69 **
fatty acid synthase	Fasn	NM_007988	-1.65 **
dickkopf homolog 3 (Xenopus laevis)	Dkk3	NM_015814	-1.61 *
Wnt inhibitory factor 1	Wif1	NM_011915	-1.60 **
glycoprotein 5 (platelet)	Gp5	NM_008148	-1.57 *
heat shock protein 1, alpha	Hspca	NM_010480	-1.53 **
	mt-Nd5		-1.52 *
adipocyte, C1Q and collagen domain containing	Acdc	NM_009605	-1.50 **
3-hydroxybutyrate dehydrogenase (heart, mitochondrial)	Bdh	NM_175177	-1.50 *
heat shock protein 1, beta	Hspcb	NM_008302	-1.49 **
4-aminobutyrate aminotransferase	Abat	NM_172961	-1.49 **
DNA-damage-inducible transcript 4	Ddit4	NM_029083	-1.49 **
cyclin-dependent kinase inhibitor 1A	Cdkn1a	NM_007669	-1.49 **
heat shock protein 1	Hspb1	NM_013560	-1.48 **
potassium voltage-gated channel, shaker-related subfamily, member 5	Kcna5	NM_145983	-1.46 **
CD9 antigen	Cd9	NM_007657	-1.45 *
protein phosphatase 1, regulatory (inhibitor) subunit 3C	Ppp1r3c	NM_016854	-1.44 **
RIKEN full-length enriched library, clone:2510042H12 product: weakly similar to RAT HEMOGLOBIN ALPHA CHAIN (FRAGMENT) [Rattus norvegicus]		AK011092	-1.44 *
immunoglobulin superfamily, member 1	Igsf1	NM_183336	-1.43 **
SRY-box containing gene 18	Sox18	NM_009236	-1.42 *
phosphatidylinositol (4,5) bisphosphate 5-phosphatase, A	Pib5pa	NM_172439	-1.41 *
transferrin receptor	Tfrc	NM_011638	-1.41 **
cysteine and histidine-rich domain (CHORD)-containing, zinc-binding protein 1	Chordc1	NM_025844	-1.40 **
eukaryotic translation elongation factor 2	Eef2	NM_007907	-1.40 **
FERM domain containing 5	Frmd5	NM_172673	-1.40 **
inhibitor of DNA binding 1	Idb1	NM_010495	-1.40 **
procollagen-proline, 2-oxoglutarate 4-dioxygenase (proline 4-hydroxylase), alpha 1 polypeptide	P4ha1	NM_011030	-1.40 **
protein O-fucosyltransferase 2	Pofut2	NM_030262	-1.40 *
1500015O10Rik		NM_024283	-1.40 **

*Data obtained with 2 high-iron and 2 control samples.
** Data obtained with 3 high-iron and 3 control samples.

[45]. There are two forms of ELC in the cardiac muscle, ELCa and ELCv (encoded by Myl3). ELCa has a higher performance than ELCv and its elevated accumulation in diseased heart is considered a compensatory response in heart failure [46]. Furthermore, transgenic rats overexpressing ELCa in the heart show an improvement in contractile parameters [47]. These observations open the possibility that the induction of cardiac Myl4 and Myl7 expression observed in our experiments is a compensatory response to early damage produced by iron accumulation. Additionally, according to our microarray results, other myosin genes were induced by iron in mouse heart (*Myh7*) and skeletal muscle (*Myl2*). Actin filaments play an essential role, along with myosin, in muscle contraction. Curiously, in the present work, iron suppressed the expression of skeletal muscle and smooth muscle isoforms of actin (acta1 and acta2) in the heart, as well as the cardiac isoform (actc1) in skeletal muscle.

The present microarray data analysis identified one gene (Stearoyl-coenzyme A desaturase 1, *Scd1*), which showed marked upregulation (1.75 fold) in the skeletal muscle and downregulation (-2.40 fold) in the heart after iron overload. This finding was also confirmed by Q-RT-PCR.

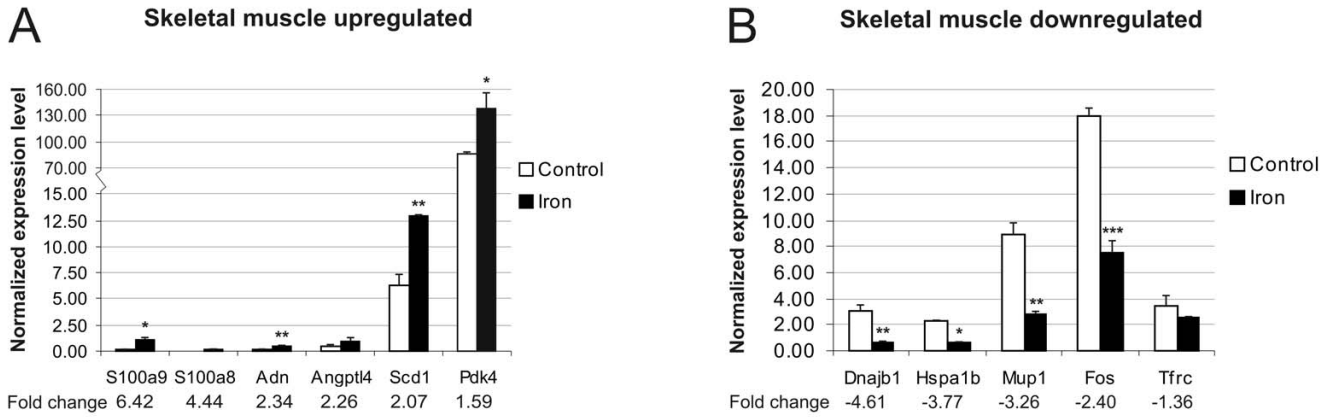

Figure 2

Confirmation of microarray results for skeletal muscle by Q-RT-PCR. The experiments were performed on samples derived from C57BL/6 male mice. The result values are expressed as mean of triplicate runs +/- standard deviation. Statistical significant differences relative to control diet fed mice were determined. **p* < 0,05; ***p* < 0,01; ****p* < 0,001. A, Q-RT-PCR analysis of 6 genes with up-regulated expression after iron overload. B, Q-RT-PCR evaluation of 5 genes with iron-induced down-regulation of expression by microarray analysis.

Scd1 is an iron-containing enzyme with a central lipogenic role. It catalyzes the insertion of a double bond into fatty acyl-CoA substrates, the preferred one being stearoyl-CoA, and yielding oleoyl-CoA. Oleic acid is the major monounsaturated fatty acid of membrane phospholipids, triglycerides, cholesterol esters, wax esters and alkyl-1,2-diacylglicerol. The (stearic acid/oleic acid) ratio has important effects on cell membrane fluidity and signal transduction. The overexpression of Scd1 has been shown to be associated with genetic predisposition to hepatocarcinogenesis [48]. Scd1 mRNA levels were induced 2.49 times in mouse liver during iron overload (data not shown), an effect that was previously shown in both enteral and parenteral models of iron overload [49]. As Pigeon and coworkers have discussed, most likely the effect of iron on Scd1 expression in the liver is not direct, but a compensatory mechanism in response to the need to renew unsaturated fatty acids.

The FBJ osteosarcoma oncogene (Fos) is a major component of activator-protein-1 (AP-1), a redox-sensitive transcription factor complex, which also includes members of

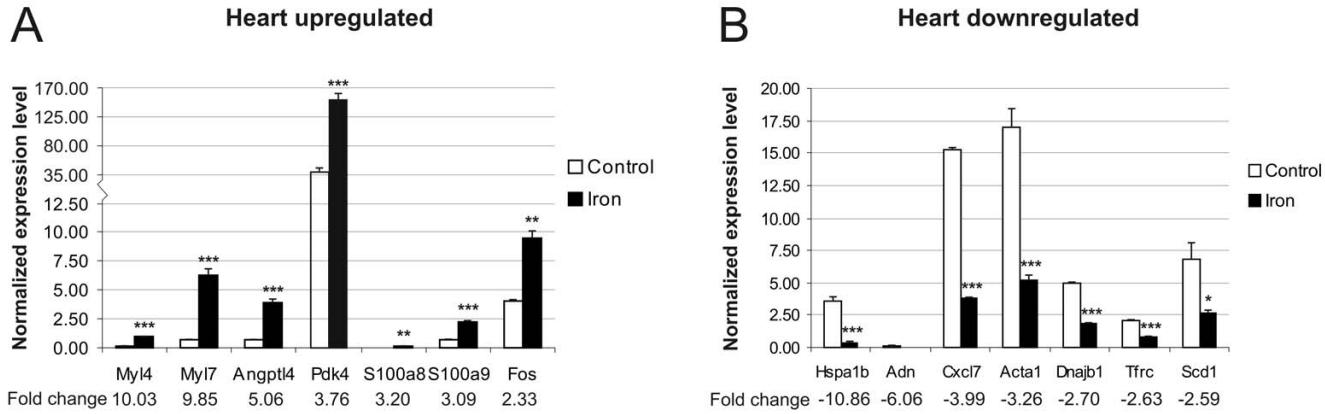

Figure 3

Verification of data obtained for heart samples by microarray analysis using Q-RT-PCR. Samples from C57BL/6 male mice were used in these experiments. The result values are expressed as mean of triplicate runs +/- standard deviation. Statistical significant differences relative to control diet fed mice were determined. **p* < 0,05; ***p* < 0,01; ****p* < 0,001. A, Q-RT-PCR evaluation of seven genes with up-regulated expression after iron overload. B, Q-RT-PCR analysis of seven genes with iron-induced down-regulation of expression by microarray.

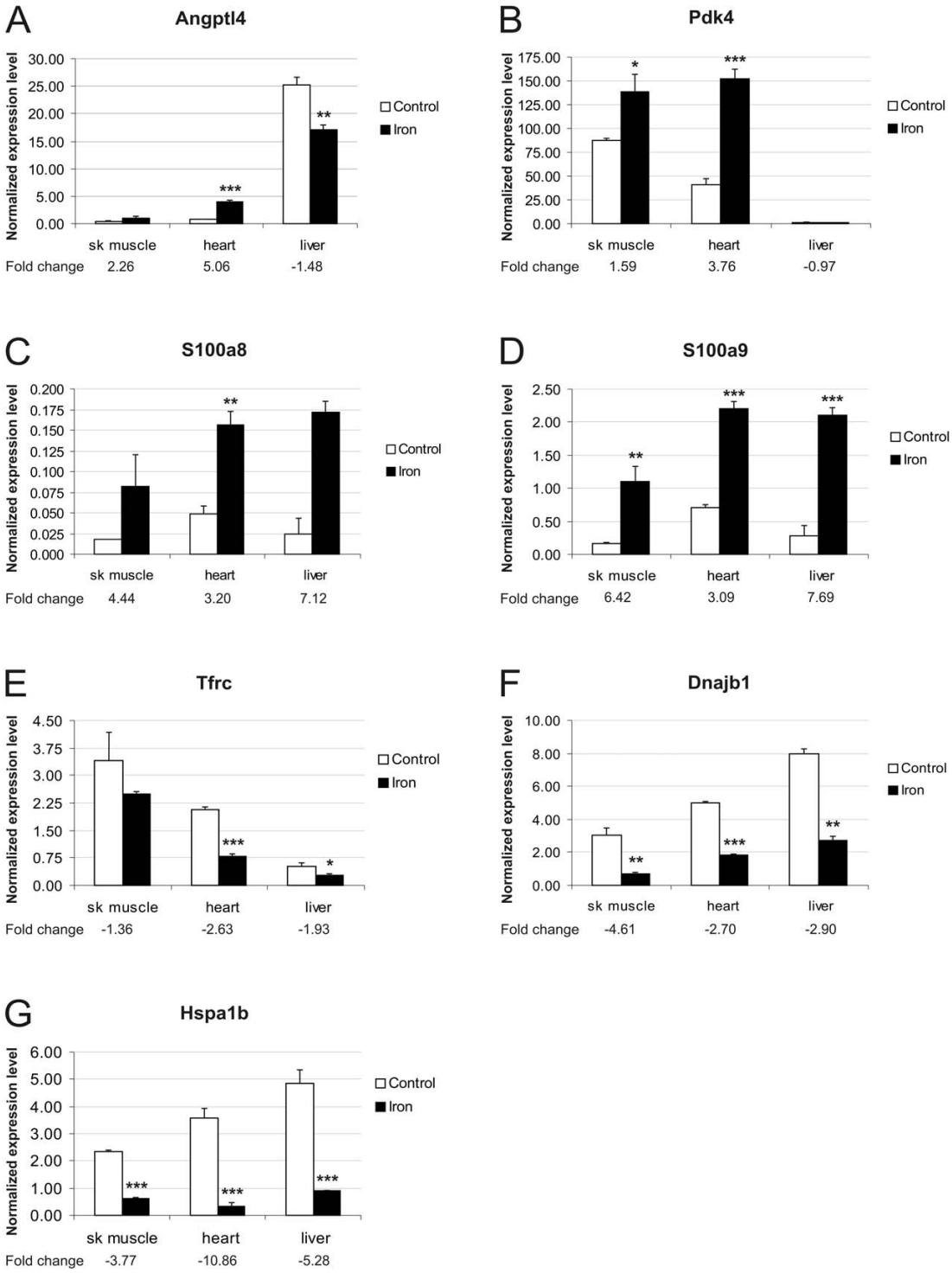

Figure 4

Expression analysis of genes presenting same trend in muscular tissues and comparison with hepatic expression. C57BL/6 male mice were used in this analysis. The result values are expressed as mean of triplicate runs +/- standard deviation. Statistical significant differences relative to control diet fed mice were determined. *$p < 0,05$; **$p < 0,01$; ***$p <$ 0,001. A-D, Genes with up-regulated expression in both skeletal muscle and heart after iron overload. E-G, Genes with down-regulated expression in skeletal muscle and heart after iron overload.

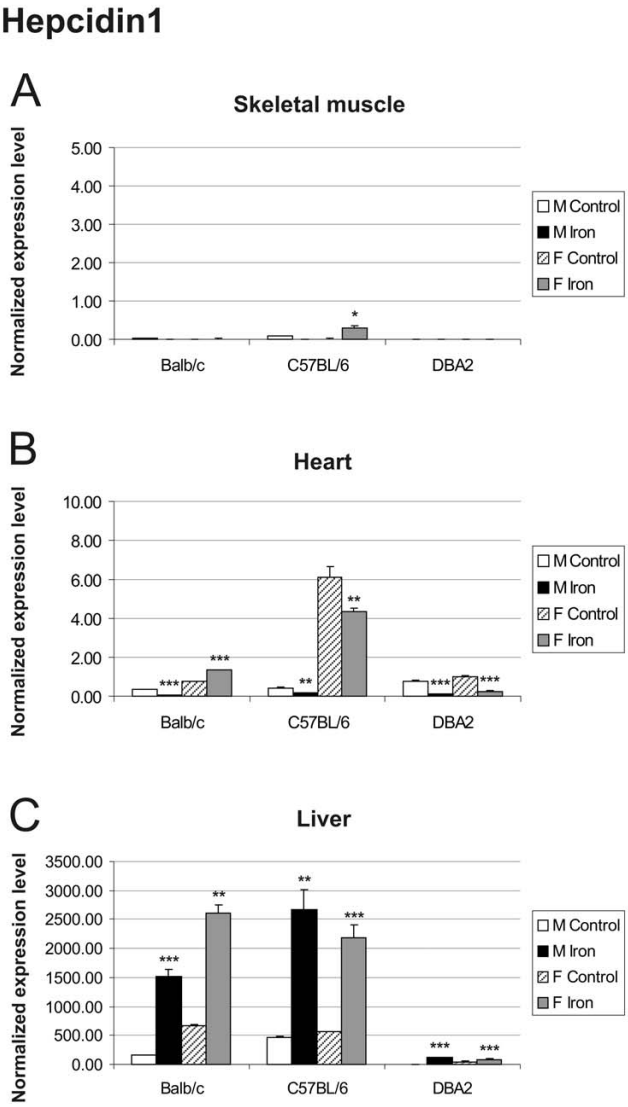

Figure 5
Expression of hepcidin1 in skeletal muscle (A), heart (B) and liver (C) assessed by Q-RT-PCR. The expression of hepcidin1 transcripts was assessed in control *versus* iron fed mice of 3 strains (Balb/c, C57BL/6, DBA2). The result values are expressed as mean of triplicate runs +/- standard deviation. Statistical significant differences relative to control diet fed mice were determined. *$p < 0,05$; **$p < 0,01$; ***$p < 0,001$. F = female; M = male.

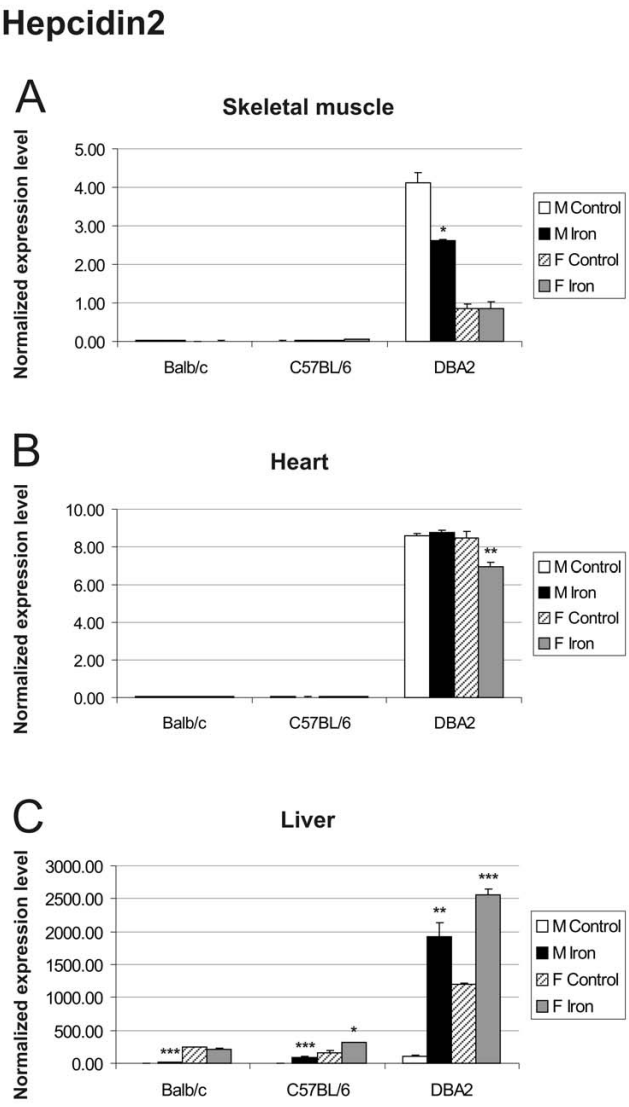

Figure 6
Q-RT-PCR analysis of hepcidin2 mRNA expression in skeletal muscle (A), heart (B) and liver (C). The expression of hepcidin2 in control *versus* iron overloaded mice was analyzed in 3 strains (Balb/c, C57BL/6, DBA2). The result values are expressed as mean of triplicate runs +/- standard deviation. Statistical significant differences relative to control diet fed mice were determined. *$p < 0,05$; **$p < 0,01$; ***$p < 0,001$. F = female; M = male.

the Jun (c-Jun, JunB, JunD), Maf and ATF subfamilies. Fos is thought to have an important role in signal transduction, cell proliferation and differentiation. Expression of c-fos and c-jun can be induced by many stimuli and compounds, including some metals such as iron [50]. Accordingly, the present work shows increased expression of c-Fos in the heart and liver of iron-loaded mice. However, in skeletal muscle, c-Fos was down-regulated and, according to the microarray results, the same is true for c-Jun. Probably other mechanisms are influencing the transcription of c-Fos and c-Jun in skeletal muscle. Interestingly, a recent study suggested that c-Jun and JunB negatively regulate the transcription of *S100a8* and *S100a9* [51]. Furthermore, AP-1 activity had been previously connected to iron metabolism in several ways. For example, AP-1 regulates transcription of ceruloplasmin (the plasma iron oxi-

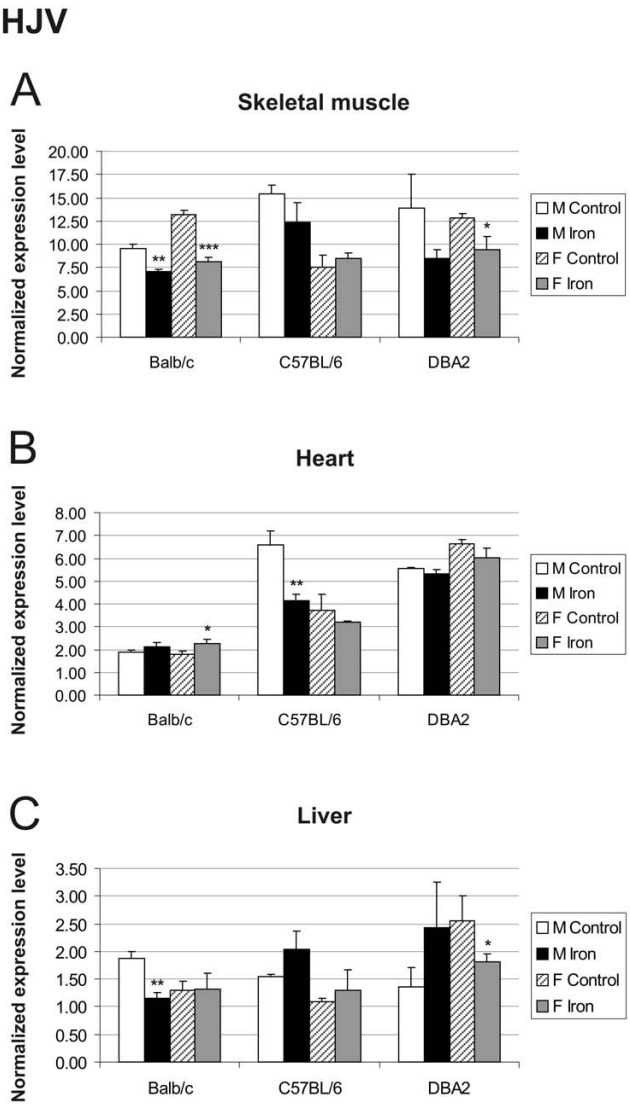

Figure 7
Expression of hemojuvelin (HJV) in skeletal muscle (A), heart (B) and liver (C). Q-RT-PCR analysis of HJV mRNA levels in control *versus* iron overloaded mice of 3 strains (Balb/c, C57BL/6, DBA2). The result values are expressed as mean of triplicate runs +/- standard deviation. Statistical significant differences relative to control diet fed mice were determined. *$p < 0,05$; **$p < 0,01$; ***$p < 0,001$. F = female; M = male.

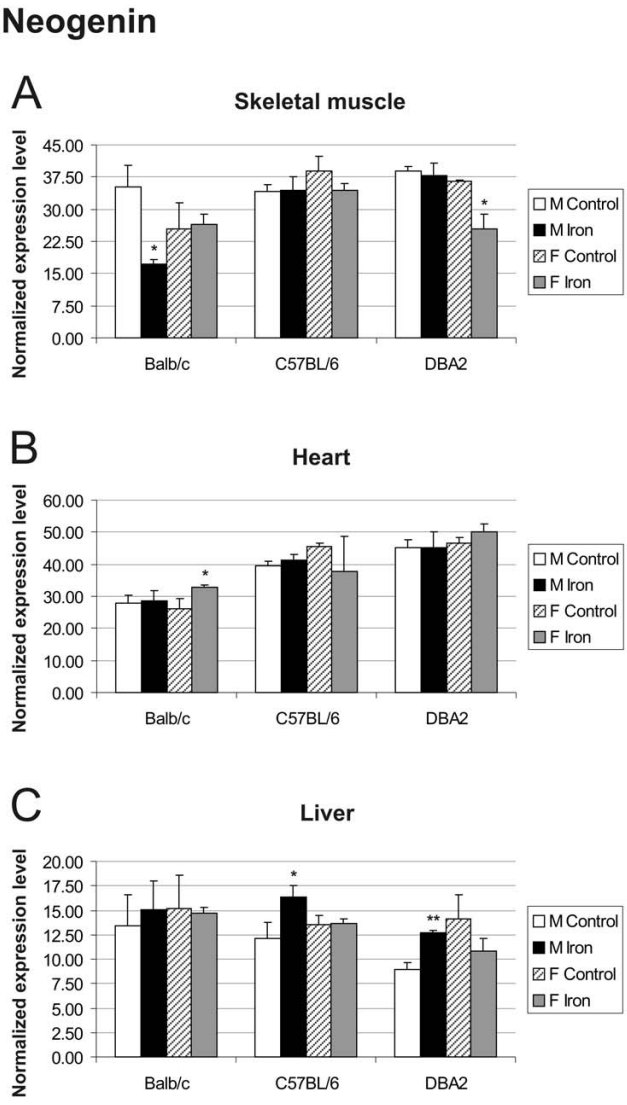

Figure 8
Neogenin transcript levels in skeletal muscle (A), heart (B) and liver (C). 3 mouse strains (Balb/c, C57BL/6, DBA2) were used for this Q-RT-PCR analysis. The result values are expressed as mean of triplicate runs +/- standard deviation. Statistical significant differences relative to control diet fed mice were determined. *$p < 0,05$; **$p < 0,01$; ***$p < 0,001$. F = female; M = male.

dase) [52], and the promoter region of *HFE* contains an AP-1 transcription element [53].

Heat shock proteins, or stress proteins, are expressed in response to heat shock and a variety of other stress stimuli including oxidative free radicals and toxic metal ions. The members of the 70-kDa heat shock protein family (Hsp70) assist cells in maintaining functional proteins under stressful conditions [54]. Hsp40 proteins stimulate the ATPase activity of Hsp70 proteins and stabilize the interaction of these chaperons with their substrate proteins [55]. In the present study, dietary iron overload decreased the expression of *Hspa1b* (a member of Hsp70 family) and *Dnajb1* (a member of Hsp40 family) in skeletal muscle, heart and liver of mice as validated by Q-RT-PCR. In accordance with these findings, our microarray results also showed decreased expression of several other

heat shock protein genes in skeletal muscle (*Hsp105*, *Hspca*, *Hspb1* and *Hspa1a*) and heart (*Hsp105*, *Hspcb*, *Hspca* and *Hspb1*) of iron-loaded mice. This unexpected result might represent novel regulatory mechanisms specific to these concrete experimental conditions.

The post-transcriptional regulation of transferrin receptor 1 and divalent metal transporter 1 by iron is mediated through iron-responsive elements located in the 3'-untranslated region of their mRNAs [56,57]. As expected, we found decreased Tfrc mRNA expression in skeletal muscle, heart and liver of iron-loaded mice but, surprisingly, the expression of divalent metal transporter 1 was not changed substantially.

The expression levels of hepcidin1 and hepcidin2 transcripts in the liver are markedly influenced by strain and gender, in accordance with previous reports [22,23]. DBA2 mice differ markedly in the expression levels of their hepcidin genes when compared with Balb/c and C57BL/6 mice. For DBA2, the difference in hepcidin2 expression was evident not only in liver, but also in the heart and skeletal muscle. These results further demonstrate that iron responses can vary between different mouse strains.

Conclusion

To conclude, we have identified genes whose expression is altered in skeletal muscle and heart during iron overload. The number of the affected genes and the magnitude of the changes were relatively low, which is probably due to the fact that skeletal muscle and heart are not the primary targets of iron loading. Interestingly, some of the regulated genes identified in this study are involved in modulation of glucose and lipid metabolism, transcription and cellular stress responses. These might represent novel links between iron overload and the pathogenesis of cardiomyopathy and diabetes in HH. Further investigation of these genes may help to understand how iron excess leads to these common HH manifestations.

Methods

Animal care and experimental iron overload

The experiments with mice were performed in the laboratory animal centre of the University of Oulu. The mice were kept under specific pathogen-free conditions and the experiments were approved by the Animal Care and Use Committee of the University of Oulu (permission No 102/05). Five male and five female mice from each of three strains (Balb/c, C57BL/6, and DBA/2) were placed on a diet (Lactamin, Stockholm, Sweden) supplemented with 2% carbonyl iron (Sigma-Aldrich Sweden AB, Stockholm, Sweden, #C3518) at the age of 10–12 weeks. Equivalent groups of littermates were fed control chow diet without iron supplementation (0.02% iron). After 6 weeks of treatment, blood was collected from the mice under anaesthesia. Animals were then sacrificed and liver, skeletal muscle (extensor digitorum longus, EDL) and heart samples were immediately collected and immersed in RNAlater (Ambion, Huntingdon, UK). EDL is relatively easy to identify and isolate and it has been used as a reference muscle in many physiological studies. Liver samples were also collected and stored frozen before measurement of iron content.

Determination of hepatic and cardiac iron content

Liver and heart tissue samples were analyzed for non-heme iron content using the bathophenanthroline method as described by Torrance and Bothwell [58]. The values are expressed as μg of iron per g dry weight.

RNA isolation

Total RNA was obtained using RNeasy RNA isolation kit (Qiagen, Valencia, CA) as recommended by the manufacturer. Residual DNA was removed from the samples using RNase-free DNase (Qiagen). RNA concentration and purity were determined using optical density (OD) measurements at 260 and 280 nm. All the samples had an OD260/OD280 ratio of 1.95 or higher.

Microarray analysis

Microarray studies were performed in the Finnish DNA Microarray Centre at Turku Centre for Biotechnology. Heart and skeletal muscle specimens derived from 3 male C57BL/6 mice of each group (iron diet and control diet) were subjected to total RNA extraction. The resulting samples were analyzed individually. 200 ng of total RNA from each sample was amplified using the Illumina™ RNA TotalPrep Amplification kit (Ambion) following the manufacturer's instructions. The *in vitro* transcription reaction, which was conducted for 14 h, included labelling of the cRNA by biotinylation.

Hybridization and scanning

Labelled and amplified material (1.5 μg/array) was hybridized to Illumina's Sentrix Mouse-6 Expression BeadChips™ (Illumina, Inc., San Diego, CA) (12 samples, 2 chips) at 55°C for 18 h according to Illumina BeadStation 500X™ protocol. Arrays were washed and then stained with 1 μg/ml cyanine3-streptavidin (Amersham Biosciences, Buckinghamshire, UK). The Illumina BeadArray™ reader was used to scan the arrays according to the manufacturer's instructions. Samples were analyzed using the BeadStudio™ software from Illumina. The hybridization control report showed problems in 2 of the arrays, corresponding to 2 heart samples, one from a control mouse and the other from an iron-loaded mouse. In both cases, 228 probes failed to hybridize, and therefore, these probes were excluded from the analyses of these 2 samples.

Data analysis

Array data were normalized with Inforsense KDE version 2.0.4 (Inforsense, London, UK) using quantile normalization method. The fold-change values were calculated for each gene using the same software. The resulting data were filtered according to a fold-change of 1.4 and -1.4 for up- and down-regulated expression, respectively. This value has been proposed as an adequate compromise above which there is a high correlation between microarray and quantitative PCR data, regardless of other factors such as spot intensity and cycle threshold [59].

Quantitative real-time PCR

The RNA extracts from 5 mice within each study group were equally pooled and RNA samples (3 μg from liver and 1.5 μg from heart and skeletal muscle) were converted into first strand cDNA with a First Strand cDNA Synthesis kit (Fermentas, Burlington, Canada) using random hexamer primers according to the protocol recommended by the manufacturer. The relative expression levels of target genes in mouse liver, skeletal muscle and heart were assessed by quantitative real-time RT-PCR using the Lightcycler detection system (Roche, Rotkreuz, Switzerland). The validations of microarray data were performed on samples obtained from C57BL/6 mice, while mRNA expression of hepcidin1, hepcidin2, hemojuvelin and neogenin was studied in three strains (Balb/c, C57BL/6, and DBA/2). Four housekeeping genes (*Actb* (β-actin), *Gapdh* (glyceraldehyde-3-phosphate dehydrogenase), *Hprt1* (hypoxanthine phosphoribosyl-transferase I), and *Sdha* (succinate dehydrogenase complex subunit A)) were used as internal controls to normalize the cDNA samples for potential quality and quantity differences. The primers for the housekeeping genes and for mouse *Hjv* and *Neo* target genes have been described earlier [19]. Mouse Hamp1 and Hamp2 primers have been also previously characterized [60]. The primer sets for the remaining target genes in this study are shown in Table 5. Most of them were designed using Primer3 [61], based on the complete cDNA sequences deposited in GenBank. The specificity of the primers was verified using NCBI Basic Local Alignment and Search Tool (Blast) [62]. When possible, and in order to avoid amplification of contaminating genomic DNA, both primers from each set were specific to different exons.

Each PCR reaction was performed in a total volume of 20 μl containing 0.5 μl of first strand cDNA, 1× of QuantiTect SYBR Green PCR Master Mix (Qiagen, Hilden, Germany), and 0.5 μM of each primer. Amplification and detection were carried out as follows: After an initial 15-min activation step at 95°C, amplification was performed in a 3-step cycling procedure: denaturation at 95°C, 15 s, ramp rate 20°C/s; annealing temperature determined according to the melting temperature for each primer pair, 20 s, ramp rate 20°C/s; and elongation at 72°C, 15s, ramp rate 20°C/s for 45 cycles and final cooling step. Melting curve analysis was always performed after the amplification to check PCR specificity. To quantify the levels of transcripts in the studied tissues, a standard curve was established for each gene using 5-fold serial dilutions of known concentrations of purified PCR products generated from the same primer sets. Every cDNA sample was tested in triplicate and the obtained crossing point (Cp) value facilitated the determination of the levels of starting message using a specific standard curve. The geometric mean of the 4 internal control genes was used as an accurate normalization factor for gene expression levels [63]. The normalization factor is always considered as a value of 100 and the final result is expressed as relative mRNA expression level.

Statistical analyses

The mean values and standard deviations were calculated from the individuals in each group for the iron measurements and from technical triplicates for the Q-RT-PCR experiments. The Student's *t*-test (unpaired, 2-tailed) was used to analyze statistically the differences in iron content and in gene expression between control and iron loaded mice. Theoretically, the Q-PCR technology used herein can detect a minimum of 100 copies of starting material. In order to avoid wrong use of the statistical methods, these were not applied to data with raw values below 300 copies.

List of Abbreviations

BMP- bone morphogenetic protein;

ELC- essential light chain;

HH- hereditary hemochromatosis;

LPL- lipoprotein lipase;

OD- optical density;

Q-RT-PCR - quantitative reverse-transcription PCR;

RGM- repulsive guidance molecule;

RLC- regulatory light chain.

Authors' contributions

AR participated in sample collection and preparation, designed primers, carried out the Q-RT-PCR and drafted the manuscript. MH performed microarray data analysis. LK carried out microarray data analysis. REF, RSB and BRB provided materials, participated in experimental design and made critical reviewing of the manuscript. SP conceived the study, participated in its design and coordination, participated in sample collection and made critical reviewing of the manuscript. All authors read and approved the final manuscript.

Table 5: Sequences of the primers used in this study

Symbol	Name	GenBank Accession No.	Forward primer (5'-3')	Reverse primer (5'-3')	Source
Angptl4	Angiopoietin – like 4	NM_020581	CACGCACCTAGACAATGGA	AGAGGCTGGATCTGGAAA	*
Pdk4	Pyruvate dehydrogenase kinase, isoenzyme 4	NM_013743	GATTGACATCCTGCCTGACC	TCTGGTCTTCTGGGCTCTTC	*
S100a8	Calgranulin A, S100 calcium binding protein A8	NM_013650	GGAAATCACCATGCCCTCTAC	GCCACACCCACTTTTATCACC	*
S100a9	Calgranulin B, S100 calcium binding protein A9	NM_009114	CGACACCTTCCATCAATACTC	GAGGGCTTCATTTCTCTTCTC	*
Fos	FBJ osteosarcoma oncogene	NM_010234	CGGGTTTCAACGCCGACTA	TTGGCACTAGAGACGGACAGA	RTprimerDB, 3328
Myl4	Myosin light polypeptide 4	NM_010858	GGGTAAAGCACGTTTCTCCA	AGGGAAGGTTGTGGGTCAG	*
Myl7	Myosin light polypeptide 7	NM_022879	TCACCGTCTTCCTCACACTC	GCTGCTTGAACTCTTCCTTG	*
Acta1	Actin alpha 1	NM_009606	CCAAAGCTAACCGGGAGAA	CCCCAGAATCCAACACGA	*
Cxcl7	Chemokine (C-X-C motif) ligand 7	NM_023785	GCCCACTTCATAACCTCCA	ATCACTTCCACATCAGCACA	*
Tfrc	Transferrin receptor 1	NM_011638	TCATGAGGGAAATCAATGATCGTA	GCCCCAGAAGATATGTCGGAA	QPPD, 1607
Scd1	Stearoyl-Coenzyme A desaturase 1	NM_009127	TGGGTTGGCTGCTTGTG	GCGTGGGCAGGATGAAG	QPPD, 1847
Adn	Adipsin, complement factor D	NM_013459	AACCGGACAACCTGCAATC	CCCACGTAACCACACCTTC	*
Mup1	Major urinary protein 1	NM_031188	CTCTATGGCCGAGAACCAGA	AGCGATTGGCATTGGATAGG	*
Dnajb1	DnaJ (Hsp40) homolog, subfamily B, member 1	NM_018808	CGACCGCTATGGAGAGGAA	GCCACCGAAGAACTCAGCA	*
Hspa1b	Heat shock protein 1B	NM_010478	GAGGAGTTCAAGAGGAAGCA	GCGTGATGGATGTGTAGAAG	*

* designed using Primer3 http://puma.fmvz.usp.br/primer3/primer3_www.cgi

Acknowledgements

We thank Dr. Jokke Hannuksela and Dr. Mari Leppilampi for their help with tissue sample collection, and Rosemary O'Neill for iron measurements. We are grateful to the staff of the Finnish microarray core facility at Turku Centre of Biotechnology, especially Päivi Junni, for skilful technical assistance. This work was supported by grants from the Academy of Finland, Finnish Cultural Foundation, Emil Aaltonen Foundation, U.S. Public Health Services (NIH grants DK41816 and HL66225), and Sigrid Juselius Foundation.

References

1. Fleming RE, Bacon BR: **Orchestration of iron homeostasis.** *N Engl J Med* 2005, **352(17):**1741-1744.
2. Camaschella C, Roetto A, Cali A, De Gobbi M, Garozzo G, Carella M, Majorano N, Totaro A, Gasparini P: **The gene TFR2 is mutated in a new type of haemochromatosis mapping to 7q22.** *Nat Genet* 2000, **25(1):**14-15.
3. Feder JN, Gnirke A, Thomas W, Tsuchihashi Z, Ruddy DA, Basava A, Dormishian F, Domingo R Jr., Ellis MC, Fullan A, Hinton LM, Jones NL, Kimmel BE, Kronmal GS, Lauer P, Lee VK, Loeb DB, Mapa FA, McClelland E, Meyer NC, Mintier GA, Moeller N, Moore T, Morikang E, Prass CE, Quintana L, Starnes SM, Schatzman RC, Brunke KJ, Drayna DT, Risch NJ, Bacon BR, Wolff RK: **A novel MHC class I-like gene is mutated in patients with hereditary haemochromatosis.** *Nat Genet* 1996, **13(4):**399-408.
4. Papanikolaou G, Samuels ME, Ludwig EH, MacDonald ML, Franchini PL, Dube MP, Andres L, MacFarlane J, Sakellaropoulos N, Politou M, Nemeth E, Thompson J, Risler JK, Zaborowska C, Babakaiff R, Radomski CC, Pape TD, Davidas O, Christakis J, Brissot P, Lockitch G, Ganz T, Hayden MR, Goldberg YP: **Mutations in HFE2 cause iron overload in chromosome 1q-linked juvenile hemochromatosis.** *Nat Genet* 2004, **36(1):**77-82.
5. Roetto A, Papanikolaou G, Politou M, Alberti F, Girelli D, Christakis J, Loukopoulos D, Camaschella C: **Mutant antimicrobial peptide hepcidin is associated with severe juvenile hemochromatosis.** *Nat Genet* 2003, **33(1):**21-22.
6. Montosi G, Donovan A, Totaro A, Garuti C, Pignatti E, Cassanelli S, Trenor CC, Gasparini P, Andrews NC, Pietrangelo A: **Autosomal-dominant hemochromatosis is associated with a mutation in the ferroportin (SLC11A3) gene.** *J Clin Invest* 2001, **108(4):**619-623.
7. Njajou OT, Vaessen N, Joosse M, Berghuis B, van Dongen JW, Breuning MH, Snijders PJ, Rutten WP, Sandkuijl LA, Oostra BA, van Duijn CM, Heutink P: **A mutation in SLC11A3 is associated with autosomal dominant hemochromatosis.** *Nat Genet* 2001, **28(3):**213-214.
8. Bridle KR, Frazer DM, Wilkins SJ, Dixon JL, Purdie DM, Crawford DH, Subramaniam VN, Powell LW, Anderson GJ, Ramm GA: **Disrupted hepcidin regulation in HFE-associated haemochromatosis and the liver as a regulator of body iron homoeostasis.** *Lancet* 2003, **361(9358):**669-673.
9. Nemeth E, Roetto A, Garozzo G, Ganz T, Camaschella C: **Hepcidin is decreased in TFR2 hemochromatosis.** *Blood* 2005, **105(4):**1803-1806.
10. Nemeth E, Tuttle MS, Powelson J, Vaughn MB, Donovan A, Ward DM, Ganz T, Kaplan J: **Hepcidin regulates cellular iron efflux by binding to ferroportin and inducing its internalization.** *Science* 2004, **306(5704):**2090-2093.
11. Abboud S, Haile DJ: **A novel mammalian iron-regulated protein involved in intracellular iron metabolism.** *J Biol Chem* 2000, **275(26):**19906-19912.
12. Zhang AS, West AP Jr., Wyman AE, Bjorkman PJ, Enns CA: **Interaction of hemojuvelin with neogenin results in iron accumulation in human embryonic kidney 293 cells.** *J Biol Chem* 2005, **280(40):**33885-33894.
13. Kuninger D, Kuns-Hashimoto R, Kuzmickas R, Rotwein P: **Complex biosynthesis of the muscle-enriched iron regulator RGMc.** *J Cell Sci* 2006, **119(Pt 16):**3273-3283.
14. Lin L, Goldberg YP, Ganz T: **Competitive regulation of hepcidin mRNA by soluble and cell-associated hemojuvelin.** *Blood* 2005, **106(8):**2884-2889.
15. Silvestri L, Pagani A, Fazi C, Gerardi G, Levi S, Arosio P, Camaschella C: **Defective targeting of hemojuvelin to plasma membrane is a common pathogenetic mechanism in juvenile hemochromatosis.** *Blood* 2007, **109(10):**4503-4510.
16. Babitt JL, Huang FW, Wrighting DM, Xia Y, Sidis Y, Samad TA, Campagna JA, Chung RT, Schneyer AL, Woolf CJ, Andrews NC, Lin HY: **Bone morphogenetic protein signaling by hemojuvelin regulates hepcidin expression.** *Nat Genet* 2006, **38(5):**531-539.
17. Babitt JL, Huang FW, Xia Y, Sidis Y, Andrews NC, Lin HY: **Modulation of bone morphogenetic protein signaling in vivo regulates systemic iron balance.** *J Clin Invest* 2007, **117(7):**1933-1939.
18. Zhang AS, Anderson SA, Meyers KR, Hernandez C, Eisenstein RS, Enns CA: **Evidence that inhibition of hemojuvelin shedding in response to iron is mediated through neogenin.** *J Biol Chem* 2007, **282(17):**12547-12556.
19. Rodriguez A, Pan P, Parkkila S: **Expression studies of neogenin and its ligand hemojuvelin in mouse tissues.** *J Histochem Cytochem* 2007, **55(1):**85-96.
20. Niederau C, Fischer R, Purschel A, Stremmel W, Haussinger D, Strohmeyer G: **Long-term survival in patients with hereditary hemochromatosis.** *Gastroenterology* 1996, **110(4):**1107-1119.
21. DeNardo DG, Kim HT, Hilsenbeck S, Cuba V, Tsimelzon A, Brown PH: **Global gene expression analysis of estrogen receptor transcription factor cross talk in breast cancer: identification of estrogen-induced/activator protein-1-dependent genes.** *Mol Endocrinol* 2005, **19(2):**362-378.
22. Courselaud B, Troadec MB, Fruchon S, Ilyin G, Borot N, Leroyer P, Coppin H, Brissot P, Roth MP, Loreal O: **Strain and gender modulate hepatic hepcidin 1 and 2 mRNA expression in mice.** *Blood Cells Mol Dis* 2004, **32(2):**283-289.
23. Krijt J, Cmejla R, Sykora V, Vokurka M, Vyoral D, Necas E: **Different expression pattern of hepcidin genes in the liver and pancreas of C57BL/6N and DBA/2N mice.** *J Hepatol* 2004, **40(6):**891-896.
24. Krijt J, Vokurka M, Chang KT, Necas E: **Expression of Rgmc, the murine ortholog of hemojuvelin gene, is modulated by development and inflammation, but not by iron status or erythropoietin.** *Blood* 2004, **104(13):**4308-4310.
25. Bondi A, Valentino P, Daraio F, Porporato P, Gramaglia E, Carturan S, Gottardi E, Camaschella C, Roetto A: **Hepatic expression of hemochromatosis genes in two mouse strains after phlebotomy and iron overload.** *Haematologica* 2005, **90(9):**1161-1167.
26. Britton RS: **Metal-induced hepatotoxicity.** *Semin Liver Dis* 1996, **16(1):**3-12.
27. Johne B, Fagerhol MK, Lyberg T, Prydz H, Brandtzaeg P, Naess-Andresen CF, Dale I: **Functional and clinical aspects of the myelomonocyte protein calprotectin.** *Mol Pathol* 1997, **50(3):**113-123.
28. Gebhardt C, Nemeth J, Angel P, Hess J: **S100A8 and S100A9 in inflammation and cancer.** *Biochem Pharmacol* 2006, **72(11):**1622-1631.
29. Carlsson H, Yhr M, Petersson S, Collins N, Polyak K, Enerback C: **Psoriasin (S100A7) and calgranulin-B (S100A9) induction is dependent on reactive oxygen species and is downregulated by Bcl-2 and antioxidants.** *Cancer Biol Ther* 2005, **4(9):**998-1005.
30. Grimbaldeston MA, Geczy CL, Tedla N, Finlay-Jones JJ, Hart PH: **S100A8 induction in keratinocytes by ultraviolet A irradiation is dependent on reactive oxygen intermediates.** *J Invest Dermatol* 2003, **121(5):**1168-1174.
31. Sen CK, Packer L: **Antioxidant and redox regulation of gene transcription.** *Faseb J* 1996, **10(7):**709-720.
32. Fuller SJ, Randle PJ: **Reversible phosphorylation of pyruvate dehydrogenase in rat skeletal-muscle mitochondria. Effects of starvation and diabetes.** *Biochem J* 1984, **219(2):**635-646.
33. Feldhoff PW, Arnold J, Oesterling B, Vary TC: **Insulin-induced activation of pyruvate dehydrogenase complex in skeletal muscle of diabetic rats.** *Metabolism* 1993, **42(5):**615-623.
34. Wu P, Sato J, Zhao Y, Jaskiewicz J, Popov KM, Harris RA: **Starvation and diabetes increase the amount of pyruvate dehydrogenase kinase isoenzyme 4 in rat heart.** *Biochem J* 1998, **329 (Pt 1):**197-201.
35. Lee FN, Zhang L, Zheng D, Choi WS, Youn JH: **Insulin suppresses PDK-4 expression in skeletal muscle independently of plasma FFA.** *Am J Physiol Endocrinol Metab* 2004, **287(1):**E69-74.
36. Kim YI, Lee FN, Choi WS, Lee S, Youn JH: **Insulin regulation of skeletal muscle PDK4 mRNA expression is impaired in acute insulin-resistant states.** *Diabetes* 2006, **55(8):**2311-2317.
37. Peters SJ, Harris RA, Wu P, Pehleman TL, Heigenhauser GJ, Spriet LL: **Human skeletal muscle PDH kinase activity and isoform**

expression during a 3-day high-fat/low-carbohydrate diet. *Am J Physiol Endocrinol Metab* 2001, **281(6):**E1151-8.
38. Kraegen EW, Clark PW, Jenkins AB, Daley EA, Chisholm DJ, Storlien LH: **Development of muscle insulin resistance after liver insulin resistance in high-fat-fed rats.** *Diabetes* 1991, **40(11):**1397-1403.
39. Kim JK, Wi JK, Youn JH: **Metabolic impairment precedes insulin resistance in skeletal muscle during high-fat feeding in rats.** *Diabetes* 1996, **45(5):**651-658.
40. Bacon BR: **Hemochromatosis: diagnosis and management.** *Gastroenterology* 2001, **120(3):**718-725.
41. Yu X, Burgess SC, Ge H, Wong KK, Nassem RH, Garry DJ, Sherry AD, Malloy CR, Berger JP, Li C: **Inhibition of cardiac lipoprotein utilization by transgenic overexpression of Angptl4 in the heart.** *Proc Natl Acad Sci U S A* 2005, **102(5):**1767-1772.
42. Koster A, Chao YB, Mosior M, Ford A, Gonzalez-DeWhitt PA, Hale JE, Li D, Qiu Y, Fraser CC, Yang DD, Heuer JG, Jaskunas SR, Eacho P: **Transgenic angiopoietin-like (angptl)4 overexpression and targeted disruption of angptl4 and angptl3: regulation of triglyceride metabolism.** *Endocrinology* 2005, **146(11):**4943-4950.
43. Li C: **Genetics and regulation of angiopoietin-like proteins 3 and 4.** *Curr Opin Lipidol* 2006, **17(2):**152-156.
44. Yamada T, Ozaki N, Kato Y, Miura Y, Oiso Y: **Insulin downregulates angiopoietin-like protein 4 mRNA in 3T3-L1 adipocytes.** *Biochem Biophys Res Commun* 2006, **347(4):**1138-1144.
45. VanBuren P, Waller GS, Harris DE, Trybus KM, Warshaw DM, Lowey S: **The essential light chain is required for full force production by skeletal muscle myosin.** *Proc Natl Acad Sci U S A* 1994, **91(26):**12403-12407.
46. Abdelaziz AI, Pagel I, Schlegel WP, Kott M, Monti J, Haase H, Morano I: **Human atrial myosin light chain 1 expression attenuates heart failure.** *Adv Exp Med Biol* 2005, **565:**283-92; discussion 92, 405-15.
47. Abdelaziz AI, Segaric J, Bartsch H, Petzhold D, Schlegel WP, Kott M, Seefeldt I, Klose J, Bader M, Haase H, Morano I: **Functional characterization of the human atrial essential myosin light chain (hALC-1) in a transgenic rat model.** *J Mol Med* 2004, **82(4):**265-274.
48. Falvella FS, Pascale RM, Gariboldi M, Manenti G, De Miglio MR, Simile MM, Dragani TA, Feo F: **Stearoyl-CoA desaturase 1 (Scd1) gene overexpression is associated with genetic predisposition to hepatocarcinogenesis in mice and rats.** *Carcinogenesis* 2002, **23(11):**1933-1936.
49. Pigeon C, Legrand P, Leroyer P, Bouriel M, Turlin B, Brissot P, Loreal O: **Stearoyl coenzyme A desaturase 1 expression and activity are increased in the liver during iron overload.** *Biochim Biophys Acta* 2001, **1535(3):**275-284.
50. Maki A, Berezesky IK, Fargnoli J, Holbrook NJ, Trump BF: **Role of [Ca2+]i in induction of c-fos, c-jun, and c-myc mRNA in rat PTE after oxidative stress.** *Faseb J* 1992, **6(3):**919-924.
51. Zenz R, Eferl R, Kenner L, Florin L, Hummerich L, Mehic D, Scheuch H, Angel P, Tschachler E, Wagner EF: **Psoriasis-like skin disease and arthritis caused by inducible epidermal deletion of Jun proteins.** *Nature* 2005, **437(7057):**369-375.
52. Das D, Tapryal N, Goswami SK, Fox PL, Mukhopadhyay CK: **Regulation of ceruloplasmin in human hepatic cells by redox active copper: identification of a novel AP-1 site in the ceruloplasmin gene.** *Biochem J* 2007, **402(1):**135-141.
53. Sanchez M, Queralt R, Bruguera M, Rodes J, Oliva R: **Cloning, sequencing and characterization of the rat hereditary hemochromatosis promoter: comparison of the human, mouse and rat HFE promoter regions.** *Gene* 1998, **225(1-2):**77-87.
54. Mayer MP, Bukau B: **Hsp70 chaperones: cellular functions and molecular mechanism.** *Cell Mol Life Sci* 2005, **62(6):**670-684.
55. Fan CY, Lee S, Cyr DM: **Mechanisms for regulation of Hsp70 function by Hsp40.** *Cell Stress Chaperones* 2003, **8(4):**309-316.
56. Casey JL, Hentze MW, Koeller DM, Caughman SW, Rouault TA, Klausner RD, Harford JB: **Iron-responsive elements: regulatory RNA sequences that control mRNA levels and translation.** *Science* 1988, **240(4854):**924-928.
57. Cairo G, Pietrangelo A: **Iron regulatory proteins in pathobiology.** *Biochem J* 2000, **352 Pt 2:**241-250.
58. Torrance JD, Bothwell TH: **A simple technique for measuring storage iron concentrations in formalinised liver samples.** *S Afr J Med Sci* 1968, **33:**9-11.
59. Morey JS, Ryan JC, Van Dolah FM: **Microarray validation: factors influencing correlation between oligonucleotide microarrays and real-time PCR.** *Biol Proced Online* 2006, **8:**175-193.
60. Ilyin G, Courselaud B, Troadec MB, Pigeon C, Alizadeh M, Leroyer P, Brissot P, Loreal O: **Comparative analysis of mouse hepcidin 1 and 2 genes: evidence for different patterns of expression and co-inducibility during iron overload.** *FEBS Lett* 2003, **542(1-3):**22-26.
61. **Primer3** [http://puma.fmvz.usp.br/primer3/primer3_www.cgi]
62. **BLAST: Basic Local Alignment and Search Tool** [http://www.ncbi.nlm.nih.gov/BLAST/]
63. Vandesompele J, De Preter K, Pattyn F, Poppe B, Van Roy N, De Paepe A, Speleman F: **Accurate normalization of real-time quantitative RT-PCR data by geometric averaging of multiple internal control genes.** *Genome Biol* 2002, **3(7):**RESEARCH0034.

OPEN ACCESS Freely available online

PLoS one

Global Transcriptional Response to *Hfe* Deficiency and Dietary Iron Overload in Mouse Liver and Duodenum

Alejandra Rodriguez[1]*, Tiina Luukkaala[2], Robert E. Fleming[3,4,5], Robert S. Britton[5,6], Bruce R. Bacon[5,6], Seppo Parkkila[1,7]

1 Institute of Medical Technology, University of Tampere and Tampere University Hospital, Tampere, Finland, **2** Science Center, Pirkanmaa Hospital District and Tampere School of Public Health, University of Tampere, Tampere, Finland, **3** Department of Pediatrics, Saint Louis University School of Medicine, St. Louis, Missouri, United States of America, **4** Edward A. Doisy Department of Biochemistry and Molecular Biology, Saint Louis University School of Medicine, St. Louis, Missouri, United States of America, **5** Saint Louis University Liver Center, St. Louis, Missouri, United States of America, **6** Division of Gastroenterology and Hepatology, Department of Internal Medicine, Saint Louis University School of Medicine, St. Louis, Missouri, United States of America, **7** School of Medicine, University of Tampere and Tampere University Hospital, Tampere, Finland

Abstract

Iron is an essential trace element whose absorption is usually tightly regulated in the duodenum. *HFE*-related hereditary hemochromatosis (HH) is characterized by abnormally low expression of the iron-regulatory hormone, hepcidin, which results in increased iron absorption. The liver is crucial for iron homeostasis as it is the main production site of hepcidin. The aim of this study was to explore and compare the genome-wide transcriptome response to *Hfe* deficiency and dietary iron overload in murine liver and duodenum. Illumina™ arrays containing over 47,000 probes were used to study global transcriptional changes. Quantitative RT-PCR (Q-RT-PCR) was used to validate the microarray results. In the liver, the expression of 151 genes was altered in $Hfe^{-/-}$ mice while dietary iron overload changed the expression of 218 genes. There were 173 and 108 differentially expressed genes in the duodenum of $Hfe^{-/-}$ mice and mice with dietary iron overload, respectively. There was 93.5% concordance between the results obtained by microarray analysis and Q-RT-PCR. Overexpression of genes for acute phase reactants in the liver and a strong induction of digestive enzyme genes in the duodenum were characteristic of the *Hfe*-deficient genotype. In contrast, dietary iron overload caused a more pronounced change of gene expression responsive to oxidative stress. In conclusion, *Hfe* deficiency caused a previously unrecognized increase in gene expression of hepatic acute phase proteins and duodenal digestive enzymes.

Citation: Rodriguez A, Luukkaala T, Fleming RE, Britton RS, Bacon BR, et al. (2009) Global Transcriptional Response to *Hfe* Deficiency and Dietary Iron Overload in Mouse Liver and Duodenum. PLoS ONE 4(9): e7212. doi:10.1371/journal.pone.0007212

Editor: Juan Valcarcel, Centre de Regulació Genòmica, Spain

Received June 4, 2009; **Accepted** August 28, 2009; **Published** September 29, 2009

Funding: This work was supported by grants from the U.S. Public Health Services (NIH grants DK41816 and HL66225, http://www.nih.gov/), and Sigrid Juselius Foundation (http://www.sigridjuselius.fi/). The funders had no role in study design, data collection and analysis, decision to publish, or preparation of the manuscript.

Competing Interests: The authors have declared that no competing interests exist.

* E-mail: alejandra.rodriguez.martinez@uta.fi

Introduction

Iron plays crucial roles in cellular metabolism but, in excess, it can catalyze the formation of free radicals leading to oxidative stress and cell damage [1]. Iron is absorbed in the duodenum, where it crosses the apical and basolateral membranes of absorptive enterocytes to enter the blood stream [2]. There is no regulated mechanism of iron excretion, and thus the absorption of iron must be tightly regulated to maintain iron balance. *HFE*-related hereditary hemochromatosis (HH, OMIM-235200) is an autosomal recessive disorder in which absorption of iron is inappropriately high [3,4]. HH is characterized by high transferrin saturation and low iron content in macrophages. Iron is deposited primarily in the parenchymal cells of various organs, particularly the liver, but also the pancreas, heart, skin, and testes, resulting in tissue damage and organ failure. Clinical complications in untreated HH patients include hepatic fibrosis, cirrhosis, hepatocellular carcinoma, diabetes, cardiomyopathy, hypogonadism, and arthritis [4].

HH is characterized by inappropriately low expression of the iron-regulatory hormone hepcidin [5]. Hepcidin, a small peptide hormone expressed mainly in the liver, is a central player in the maintenance of iron balance [6]. The only known molecule capable of transporting iron out of cells is ferroportin [7–9]. This iron exporter is located in the plasma membrane of enterocytes, reticuloendothelial cells, hepatocytes, and placental cells [7]. Hepcidin binds to ferroportin and induces its internalization and degradation, therefore suppressing the transport of iron into the circulation [10]. The expression of hepcidin is induced by increased iron stores and inflammation, and suppressed by hypoxia and anemia [11,12].

Mice homozygous for a null allele of *Hfe* ($Hfe^{-/-}$) provide a genetic animal model of HH [13]. There are several animal models of iron overload based on administration of exogenous iron [14]. According to the route of iron delivery, these can be divided into two main types: enteral (i.e. dietary) and parenteral models. For example, dietary supplementation with carbonyl iron in mice reproduces the HH pattern of hepatic iron loading, with predominantly parenchymal iron deposition [14]. Although both $Hfe^{-/-}$ mice and carbonyl iron-fed mice develop iron overload, there are important differences between these two models. $Hfe^{-/-}$ mice lack Hfe protein and therefore have decreased expression of hepcidin [15,16], while mice

with dietary iron overload express functional Hfe protein and their hepcidin expression is elevated [12].

Current RNA microarray technology allows expression profiling of the whole transcriptome. This methodology has been used to explore the effects of *Hfe* gene disruption on mRNA expression in the liver and duodenum, two organs with crucial roles in iron metabolism [17]. In the present study, we used this approach to study gene expression in the liver and duodenum of $Hfe^{-/-}$ mice and wild-type mice, with or without dietary iron overload. This allowed the identification of genes whose expression is changed during iron overload and those genes whose expression is differentially influenced by lack of Hfe protein.

Results

We used global microarray analysis to study gene expression in the liver and duodenum of $Hfe^{-/-}$ mice and carbonyl iron loaded mice, and comparing it with that of wild-type mice fed a standard diet. This approach allowed the identification of genes whose expression is changed during iron overload and those genes whose expression is differentially influenced by lack of Hfe protein. All the mice used were males and all had the same genetic background (C57BL/6).

Hepatic transcriptional response to *Hfe* deficiency and dietary iron overload

Hepatic RNA from 3 $Hfe^{-/-}$ mice and 2 wild-type mice was subjected to microarray analysis. The Pearson correlation coefficient between the knock out mice and between the controls was in both cases 0.989. The results revealed 86 induced genes and 65 repressed genes, using a cutoff value of $\pm$1.4-fold (Table 1 and Dataset S1). This cutoff value has been proposed as an adequate compromise above which there is a high correlation between microarray and Q-RT-PCR data, regardless of other factors such as spot intensity and cycle threshold [18]. The fold-changes ranged from 9.83 to $-$3.47. Functional annotation of the gene lists highlighted the biological processes that may be modified by *Hfe* deficiency. This analysis revealed enrichment of heat shock proteins and proteins related to inflammatory responses or antigen processing and presentation, among others (Table 2).

Another microarray experiment was performed using hepatic RNA from 3 mice with dietary iron overload and 2 mice fed a standard diet. The similarity between samples from individual mice was measured as the Pearson correlation coefficient, which was 0.989 between iron overloaded mice and 0.991 between control mice. The expression of 123 genes was upregulated and that of 95 genes was downregulated, applying a cutoff value of $\pm$1.4-fold (Table 1 and Dataset S2). The fold-changes ranged between 13.58 and $-$7.46. The list of regulated genes was functionally annotated (Table 3), showing enrichment of cytochrome P450 proteins as well as others involved in glutathione metabolism, acute-phase response, organic acid biosynthetic process and cellular iron homeostasis, among others.

There were 11 upregulated and 7 downregulated genes that were affected by both *Hfe* deficiency and dietary iron overload in similar fashion, while 27 genes were regulated in opposite directions by these two conditions in the liver (Table 4). In some cases, several genes belonging to the same gene family showed divergent regulation (e.g., *Saa1*, *Saa2*, *Saa3*) with upregulation in $Hfe^{-/-}$ mice and downregulation by dietary iron overload.

Altered expression of iron-related genes in the liver. The expression of 3 iron-related genes was altered in the liver of $Hfe^{-/-}$ mice. The expression of *Hamp1* and *Tfrc* was decreased and that of *Lcn2* was induced. We confirmed these results using Q-RT-PCR, and also tested the expression of *Hamp2*, which was downregulated (Figure 1). Dietary iron overload changed the expression of 5 iron-related genes in the liver. The expression of *Hamp1*, *Hamp2*, *Lcn2* and *Cp* were upregulated using both microarray analysis and Q-RT-PCR, while *Tfrc* expression was down-regulated by 1.7-fold (Figure 2).

Confirmation of hepatic microarray results by Q-RT-PCR. Microarray analysis for the expression of several genes was confirmed by performing Q-RT-PCR on hepatic samples from 5 $Hfe^{-/-}$ mice, 4 wild-type control mice, 5 iron-fed mice and 4 mice fed a standard diet. For this purpose, we selected iron-related genes and others whose expression was substantially altered in the experimental groups. A total of 29 results from the hepatic microarray data, corresponding to 24 different genes, were tested by Q-RT-PCR, and 27 (93.1%) of them showed concordant results by these two methods (Figures 1 and 2). Changes in *Foxq1* and *Dmt1* expression were false-positives in the microarray analysis for $Hfe^{-/-}$ mice and dietary iron overload, respectively. The upregulation of *Ltf* expression by dietary iron overload observed by microarray analysis could not be confirmed by Q-RT-PCR because the expression levels in samples from all but one of the treated mice and all control mice were below the detection threshold.

Duodenal gene expression response to *Hfe* deficiency and dietary iron supplementation

Microarray analysis of duodenal RNA from 2 $Hfe^{-/-}$ mice and 2 wild-type mice revealed that the expression of 143 genes was upregulated and that of 30 genes was downregulated when a cutoff value of $\pm$1.4-fold was used (Table 1 and Dataset S3). The fold-changes ranged from 15.67 to $-$3.14. The Pearson correlation coefficient between knockout mice and between controls was 0.976 and 0.971, respectively. Functional categories overrepresented among the genes regulated by *Hfe* deficiency included proteins with endopeptidase activity, and others involved in lipid catabolism and antimicrobial activity (Table 5).

Table 1. Number of genes regulated by *Hfe* deficiency or dietary iron overload in murine liver and duodenum.

Tissue	Model	Total regulated genes	Upregulated genes	Downregulated genes	Proportion of results confirmed by Q-RT-PCR
Liver	$Hfe^{-/-}$	151	86	65	11/12
	Dietary Iron	218	123	95	16/17
Duodenum	$Hfe^{-/-}$	173	143	30	6/7
	Dietary Iron	108	49	59	10/10

Genes with changes in mRNA expression greater than $\pm$1.4-fold were considered as regulated.
doi:10.1371/journal.pone.0007212.t001

Table 2. Functional annotation of genes regulated in the liver of *Hfe*$^{-/-}$ mice.

Functional Category	Gene Symbol	Description	GenBank Number	FC	Q-PCR
Response to unfolded protein	Hspd1	heat shock protein 1 (chaperonin)	NM_010477	1.54	
	H47	histocompatibility 47	NM_024439	−1.45	
	Hsp90ab1	heat shock protein 90 kDa alpha (cytosolic), class B member 1	NM_008302	−1.48	
	Hspb1	heat shock protein 1	NM_013560	−1.66	
	Hspa8	heat shock protein 8	NM_031165	−1.70	
	Hsp90b1	heat shock protein 90 kDa beta (Grp94), member 1	NM_011631	−1.71	
	Hsp90aa1	heat shock protein 90 kDa alpha (cytosolic), class A member 1	NM_010480	−1.72	
	Hspa5	heat shock protein 5	NM_022310	−2.14	
	Hsph1	heat shock 105 kDa/110 kDa protein 1	NM_013559	−2.16	−2.43
	Syvn1	synovial apoptosis inhibitor 1, synoviolin	NM_028769	−2.45	
Inflammatory response	Saa2	serum amyloid A 2	NM_011314	9.83	39.36
	Saa1	serum amyloid A 1	NM_009117	6.30	16.36
	Orm2	orosomucoid 2	NM_011016	3.29	
	Saa3	serum amyloid A 3	NM_011315	2.89	
	Orm1	orosomucoid 1	NM_008768	1.68	
	Serpina3n	serine (or cysteine) peptidase inhibitor, clade A, member 3N	NM_009252	1.63	
	C1s	complement component 1, s subcomponent	NM_144938	1.47	
	Cxcl9	chemokine (C-X-C motif) ligand 9	NM_008599	−1.57	
Apolipoprotein associated with HDL	Saa2	serum amyloid A 2	NM_011314	9.83	39.36
	Saa1	serum amyloid A 1	NM_009117	6.30	16.36
	Saa3	serum amyloid A 3	NM_011315	2.89	
	Apoa4	apolipoprotein A-IV	NM_007468	2.36	
Monooxygenase activity	Moxd1	monooxygenase, DBH-like 1	NM_021509	4.12	
	Cyp2a5	cytochrome P450, family 2, subfamily a, polypeptide 5	NM_007812	1.67	
	Cyp27a1	cytochrome P450, family 27, subfamily a, polypeptide 1	NM_024264	1.64	
	Cyp2d26	cytochrome P450, family 2, subfamily d, polypeptide 26	NM_029562	1.59	
	Kmo	kynurenine 3-monooxygenase (kynurenine 3-hydroxylase)	NM_133809	1.48	
	Cyp4a14	cytochrome P450, family 4, subfamily a, polypeptide 14	NM_007822	−1.44	
	Cyp3a11	cytochrome P450, family 3, subfamily a, polypeptide 11	NM_007818	−1.58	
	Cyp26b1	cytochrome P450, family 26, subfamily b, polypeptide 1	NM_175475	−2.39	−2.18
Steroid biosynthetic process	Nsdhl	NAD(P) dependent steroid dehydrogenase-like	NM_010941	1.44	
	Hmgcs1	3-hydroxy-3-methylglutaryl-Coenzyme A synthase 1	NM_145942	−1.42	
	Lss	lanosterol synthase	NM_146006	−1.45	
	Hmgcr	3-hydroxy-3-methylglutaryl-Coenzyme A reductase	NM_008255	−1.50	
	Mvd	mevalonate (diphospho) decarboxylase	NM_138656	−1.67	
Antigen processing and presentation	Psmb8	proteasome (prosome, macropain) subunit, beta type 8 (large multifunctional peptidase 7)	NM_010724	1.50	
	Cd74	CD74 antigen (invariant polypeptide of major histocompatibility complex, class II antigen-associated)	NM_010545	−1.59	
	H2-Eb1	histocompatibility 2, class II antigen E beta	NM_010382	−1.63	
	H2-Ab1	histocompatibility 2, class II antigen A, beta 1	NM_207105	−1.77	
	H2-Aa	histocompatibility 2, class II antigen A, alpha	NM_010378	−1.81	
Endopeptidase inhibitor activity	Serpina12	serine (or cysteine) peptidase inhibitor, clade A (alpha-1 antiproteinase, antitrypsin), member 12	NM_026535	2.01	
	Wfdc2	WAP four-disulfide core domain 2	NM_026323	1.65	
	Serpina3n	serine (or cysteine) peptidase inhibitor, clade A, member 3N	NM_009252	1.63	
	Itih4	inter alpha-trypsin inhibitor, heavy chain 4	NM_018746	1.48	
carboxy-lyase activity	Ddc	dopa decarboxylase	NM_016672	−1.48	
	Mvd	mevalonate (diphospho) decarboxylase	NM_138656	−1.67	
	Csad	cysteine sulfinic acid decarboxylase	NM_144942	−1.76	

Table 2. Cont.

Functional Category	Gene Symbol	Description	GenBank Number	FC	Q-PCR
T cell differentiation	Cd74	CD74 antigen (invariant polypeptide of major histocompatibility complex, class II antigen-associated)	NM_010545	−1.59	
	Hsp90aa1	heat shock protein 90 kDa alpha (cytosolic), class A member 1	NM_010480	−1.72	
	Egr1	early growth response 1	NM_007913	−1.77	
	H2-Aa	histocompatibility 2, class II antigen A, alpha	NM_010378	−1.81	
	Gadd45g	growth arrest and DNA-damage-inducible 45 gamma	NM_011817	−1.97	
Glycogen metabolic process	G6pc	glucose-6-phosphatase, catalytic	NM_008061	2.38	
	Ppp1r3c	protein phosphatase 1, regulatory (inhibitor) subunit 3C	NM_016854	1.57	
	Ppp1r3b	protein phosphatase 1, regulatory (inhibitor) subunit 3B	NM_177741	1.55	

doi:10.1371/journal.pone.0007212.t002

Global transcriptional regulation was also studied in the duodenum of mice fed an iron-supplemented diet, using 3 treated mice and 2 controls. The Pearson correlation coefficient was 0.985 between treated mice and 0.983 between controls. The expression of 49 genes was induced and 59 genes were repressed, applying a cutoff value of ±1.4-fold (Table 1 and Dataset S4). The fold-changes ranged between 6.07 and −5.64. Functional annotation of the gene list evidenced enrichment of genes involved in glutathione metabolism, antigen processing and presentation and inflammatory response, among others (Table 6).

We identified genes whose expression was affected by both *Hfe* deficiency and dietary iron supplementation in the duodenum. There were 4 genes whose expression was induced in both conditions, 3 genes whose expression was decreased, and 4 genes with opposite regulation (Table 7).

Altered expression of iron-related genes in the duodenum. In the duodenum of $Hfe^{-/-}$ mice, *Hamp2* expression was increased by 2.7-fold using microarray analysis. However, this could not be confirmed by Q-RT-PCR, because *Hamp2* mRNA levels in the samples from wild-type mice and in one $Hfe^{-/-}$ sample were below the detection threshold. In mice fed the iron-supplemented diet, the duodenal expression of *Tfrc* was downregulated and that for *Hmox1* was upregulated: both of these results were validated by Q-RT-PCR (Figure 3).

Confirmation of duodenal microarray results by Q-RT-PCR. Q-RT-PCR analyses were done on duodenal RNA samples from 5 $Hfe^{-/-}$ mice, 4 wild-type control mice, 5 iron-fed mice and 4 mice fed a standard diet in order to confirm the microarray results. The mRNA expression of a total of 17 different genes was tested and 16 (94.1%) showed concordant results between microarray analysis and Q-RT-PCR (Figures 3 and 4). The sole discrepant result concerned the expression of *Ddb1* that was downregulated according to microarray analysis, while Q-RT-PCR revealed a slight induction (1.25-fold) of expression.

Discussion

The goal of this study was to explore and compare the genome-wide transcriptome response to *Hfe* deficiency and dietary iron overload in murine liver and duodenum. This approach allowed the identification of genes whose expression is changed during iron overload and those genes whose expression is differentially influenced by lack of Hfe protein. The global transcriptional response to *Hfe* deficiency has been explored previously in the liver and duodenum of two mouse strains [17]. However, it is notable that only a few analogous changes in gene expression are seen when comparing our data with those of the previous study, even for mice of the same genetic background. Two other reports have explored expression of selected genes by using dedicated arrays in $Hfe^{-/-}$ mice and in mice with secondary iron overload produced by intraperitoneal injection of iron-dextran [19,20]. In one study, duodenum and liver samples were analyzed using an array of iron-related genes [19]. The results for duodenal gene expression in $Hfe^{-/-}$ mice have no concordance with ours. Regulation of hepatic gene expression, on the other hand, is similar for several genes, such as *Hamp1*, *Tfrc* and *Mt1*. The second report focused on gene expression in the duodenum [20], and again, there is little concordance between their observations and ours. The lack of agreement between these studies is probably due to differences in the animal models (parenteral vs. enteral iron loading; mouse strains) and in the microarray methodology.

The hepatic expression of acute phase proteins (APPs) can be induced by inflammatory mediators such as interleukin-6. Interestingly, the liver of $Hfe^{-/-}$ mice has upregulated expression of APPs such as serum amyloids, lipocalins and orosomucoids. Notably, the expression of serum amyloid genes (*Saa1*, *Saa2*, *Saa3*) was upregulated in the $Hfe^{-/-}$ mice compared to being downregulated in dietary iron overload, suggesting that *Hfe* deficiency induces this gene expression by an iron-independent mechanism. However, hepatic interleukin-6 mRNA expression was not significantly changed by *Hfe* deficiency, so the potential involvement of this cytokine in the observed upregulation of APPs remains uncertain.

Lipocalin2 (human Ngal from neutrophil gelatinase-associated lipocalin) is an APP with antimicrobial properties through a mechanism of iron deprivation by siderophore binding [21]. It can donate iron to various types of cells [22,23] and seems to be capable of intracellular iron chelation and iron excretion [24]. Furthermore, a recent study has shown that lipocalin2 is an adipokine with potential importance in insulin resistance associated with obesity [25]. We observed that *Lcn2* expression is increased in the liver of both $Hfe^{-/-}$ mice and those with dietary iron overload, suggesting that this induction is iron-related.

Dietary iron overload of the liver led to increased expression of both hepcidin genes (*Hamp1*, *Hamp2*) as previously reported [26,27], and these results were verified by Q-RT-PCR. In the liver of $Hfe^{-/-}$ mice, *Hamp1* expression was downregulated as expected [15,16,19]. We also examined the levels of *Hamp2* mRNA by Q-RT-PCR and found a -1.92-fold change. The low expression of hepatic *Hamp1* in $Hfe^{-/-}$ mice is likely responsible for the increased iron absorption and low microphage iron content in these mice [15,16,19].

Inhibitor of DNA-binding/differentiation proteins, also known as Id proteins, comprise a family of proteins that heterodimerize

Table 3. Functional annotation of genes regulated in the liver of iron-fed mice.

Functional Category	Gene Symbol	Description	GenBank Number	FC	Q-PCR
Electron transport, containing heme and monooxygenase activity	Cyp2b10	cytochrome P450, family 2, subfamily b, polypeptide 10	NM_009999	13.58	
	Cyp2b9	cytochrome P450, family 2, subfamily b, polypeptide 9	NM_010000	7.41	
	Cyp4a14	cytochrome P450, family 4, subfamily a, polypeptide 14	NM_007822	6.97	16.06
	Cyp26b1	cytochrome P450, family 26, subfamily b, polypeptide 1	NM_175475	2.24	
	Cyp2c29	cytochrome P450, family 2, subfamily c, polypeptide 29	NM_007815	1.77	
	Cyp2c54	cytochrome P450, family 2, subfamily c, polypeptide 54	NM_206537	1.76	2.37
	Cyp2a5	cytochrome P450, family 2, subfamily a, polypeptide 5	NM_007812	1.65	
	Cyp2b13	cytochrome P450, family 2, subfamily b, polypeptide 13	NM_007813	1.50	
	Cyp4v3	cytochrome P450, family 4, subfamily v, polypeptide 3	NM_133969	−1.82	
	Cyp7b1	cytochrome P450, family 7, subfamily b, polypeptide 1	NM_007825	−2.50	
	Cyp4a12b	cytochrome P450, family 4, subfamily a, polypeptide 12B	NM_172306	−2.73	
	Cyp7a1	cytochrome P450, family 7, subfamily a, polypeptide 1	NM_007824	−2.80	
	Cyp4a12a	cytochrome P450, family 4, subfamily a, polypeptide 12a	NM_177406	−3.62	
Glutathione metabolism	Gsta1	glutathione S-transferase, alpha 1 (Ya)	NM_008181	1.94	
	Gstt2	glutathione S-transferase, theta 2	AK079739	1.86	
	Gsta2	glutathione S-transferase, alpha 2 (Yc2)	NM_008182	1.83	
	Gstm6	glutathione S-transferase, mu 6	NM_008184	1.78	
	Mgst3	microsomal glutathione S-transferase 3	NM_025569	1.72	
	Gstm3	glutathione S-transferase, mu 3	NM_010359	1.59	
	Gclc	glutamate-cysteine ligase, catalytic subunit	NM_010295	1.55	
	Gstp1	glutathione S-transferase, pi 1	NM_013541	−1.81	
Acute-phase response	Il1b	interleukin 1 beta	NM_008361	2.04	
	Saa3	serum amyloid A 3	NM_011315	−1.82	
	Saa4	serum amyloid A 4	NM_011316	−1.91	
	Saa2	serum amyloid A 2	NM_011314	−2.79	−3.36
	Saa1	serum amyloid A 1	NM_009117	−3.96	−4.31
Organic acid biosynthetic process	Fasn	fatty acid synthase	NM_007988	2.22	
	Elovl6	ELOVL family member 6, elongation of long chain fatty acids	NM_130450	1.87	
	Acaca	acetyl-Coenzyme A carboxylase alpha	NM_133360	1.81	
	Cd74	CD74 antigen (invariant polypeptide of major histocompatibility complex, class II antigen-associated)	NM_010545	1.65	
	Cyp7b1	cytochrome P450, family 7, subfamily b, polypeptide 1	NM_007825	−2.50	
	Elovl3	elongation of very long chain fatty acids-like 3	NM_007703	−5.00	
Cellular iron ion homeostasis	Hamp2	hepcidin antimicrobial peptide 2	NM_183257	10.03	24.77
	Hamp1	hepcidin antimicrobial peptide 1	NM_032541	1.73	5.27
	Tfrc	transferrin receptor	NM_011638	−1.74	
	Alas2	aminolevulinic acid synthase 2, erythroid	NM_009653	−2.20	
Hemopoiesis and immune system development	Id2	inhibitor of DNA binding 2	NM_010496	2.92	5.2
	Egr1	early growth response 1	NM_007913	2.55	
	H2-Aa	histocompatibility 2, class II antigen A, alpha	NM_010378	1.81	
	Gadd45g	growth arrest and DNA-damage-inducible 45 gamma	NM_011817	1.66	
	Cd74	CD74 antigen (invariant polypeptide of major histocompatibility complex, class II antigen-associated)	NM_010545	1.65	
	Hbb-b1	hemoglobin, beta adult major chain	NM_008220	1.45	
	Pik3r1	phosphatidylinositol 3-kinase, regulatory subunit, polypeptide 1 (p85 alpha), transcript variant 1	NM_001024955	−1.70	
	Alas2	aminolevulinic acid synthase 2, erythroid	NM_009653	−2.20	
	Bcl6	B-cell leukemia/lymphoma 6	NM_009744	−2.61	
Serine-type endopeptidase inhibitor activity	Serpina7	serine (or cysteine) peptidase inhibitor, clade A (alpha-1 antiproteinase, antitrypsin), member 7	NM_177920	2.12	

Table 3. Cont.

Functional Category	Gene Symbol	Description	GenBank Number	FC	Q-PCR
	Serpina3m	serine (or cysteine) peptidase inhibitor, clade A, member 3 M	NM_009253	2.04	
	Spink4	serine peptidase inhibitor, Kazal type 4	NM_011463	1.52	
	Serpina1e	serine (or cysteine) peptidase inhibitor, clade A, member 1e	NM_009247	−1.86	
	Serpina12	serine (or cysteine) peptidase inhibitor, clade A (alpha-1 antiproteinase, antitrypsin), member 12	NM_026535	−2.19	
	Serpine2	serine (or cysteine) peptidase inhibitor, clade E, member 2	AK045954	−2.88	
Antigen processing and presentation via MHC class II	H2-Aa	histocompatibility 2, class II antigen A, alpha	NM_010378	1.81	
	H2-Ab1	histocompatibility 2, class II antigen A, beta 1	NM_207105	1.68	
	Cd74	CD74 antigen (invariant polypeptide of major histocompatibility complex, class II antigen-associated)	NM_010545	1.65	
	H2-Eb1	histocompatibility 2, class II antigen E beta	NM_010382	1.43	

doi:10.1371/journal.pone.0007212.t003

with basic-helix-loop-helix (bHLH) transcription factors to inhibit their binding to DNA. Several studies have reported that Id proteins have important roles in differentiation, cell cycle and angiogenesis in various cell types [28]. Expression of *Id1*, *2*, and *3* is increased during liver disease, with levels that escalate as liver disease progresses from hepatitis to cirrhosis. In hepatocellular carcinoma, high expression is observed in well-differentiated tumors, and it decreases as the tumor cells become undifferentiated [29]. In light of these findings, it has been suggested that *Id1*, *2*, and *3* may play a role in the early stages of hepatocarcinogenesis. Given that, it is notable that we found that the expression of *Id1*, *2*, *3*, and *4* was increased in the liver of mice with dietary iron overload, but was unaffected in $Hfe^{-/-}$ mice. Increased hepatic expression of *Id1* mRNA has previously been reported in mice fed an iron-supplemented diet [30]. The same study showed upregulation of the gene for bone morphogenetic protein 6 (*Bmp6*) in the same experimental mice. Recent work demonstrates that Bmp6 is a key player in the signalling pathway that controls hepcidin expression [31]. Unexpectedly, upregulation of hepatic *Bmp6* mRNA expression by dietary iron overload was not evident in the current study.

The gene expression of several heat shock proteins was downregulated in the liver and duodenum by both Hfe deficiency and dietary iron overload, with a considerably greater number of these genes downregulated in the liver of *Hfe*−/− mice. Although these genes are induced under certain stress conditions, such as heat shock and ischemia–reperfusion, their expression is decreased by iron overload [19,27,32]. Currently, the physiological implications of this downregulation are unknown.

Our results indicate that disruption of the *Hfe* gene induces the expression of many genes in the duodenum coding for digestive enzymes, such as elastases, carboxypeptidases, trypsins, chymotrypsins, amylases, and lipases. In contrast, feeding mice with an iron-supplemented diet did not affect the expression of any of these genes. The upregulation of gene expression for digestive enzymes in $Hfe^{-/-}$ mice is surprising because overexpression of these enzymes has not been associated with HH.

A common feature of the duodenal response to both *Hfe* deficiency and dietary iron overload was the transcriptional repression of genes involved in antimicrobial activities, such as cryptdins. In mice fed an iron-supplemented diet, there was also a decrease in mRNA expression for genes involved in antigen processing and presentation, such as some genes of the MHC class II family.

The solute carrier molecules constitute a large family of proteins involved in membrane transport of diverse molecules. The gene expression of many family members was affected by *Hfe* deficiency or dietary iron overload. In the duodenum, the expression of the sodium-coupled neutral amino acid transporter *Slc38a5* was induced in $Hfe^{-/-}$ mice and repressed in mice fed an iron-supplemented diet. In the liver, the expression of *Slc46a3* was upregulated in $Hfe^{-/-}$ mice. This gene belongs to the Slc46 subfamily of heme transporters. It is thus a close relative of *Slc46a1* (also known as *HCP1*), a recently identified, although controversial, heme transporter [33,34]. The iron transporter Dmt1, encoded by *Slc11a2*, contains an iron-responsive element (IRE) in the 3′UTR of its mRNA. This permits the regulation of *Dmt1* mRNA levels according to the cellular labile iron pool by mediation of the iron regulatory proteins, IRP1 and IRP2. Under iron-replete conditions, IRP activity is reduced rendering the *Dmt1* mRNA vulnerable to degradation. The opposite is true under iron-deficient conditions, which is believed to be the situation inside the enterocytes of HH patients and $Hfe^{-/-}$ mice [35,36]. Accordingly, in some studies, increased expression of *Dmt1* has been observed in the duodenum of HH patients [37] as well as in $Hfe^{-/-}$ mice [38]. However, we did not find a significant change in the expression of *Dmt1* in the $Hfe^{-/-}$ duodenum. This may be explained by the inability of our microarray probes and PCR primers to discriminate between IRE-positive and IRE–negative transcripts.

The post-transcriptional regulation of *Tfrc* (transferrin receptor 1) by iron is also mediated through the IRE/IRP system [39]. Tfrc is involved in the uptake of transferrin-bound iron by cells. Analogous to our observations, suppression of *Tfrc* expression in the duodenum [40] and liver [27] of mice fed an iron-supplemented diet, and in the liver of $Hfe^{-/-}$ mice [19] has been reported previously. Our microarray analysis indicates that the expression of *Tfrc* was not significantly changed in the duodenum of $Hfe^{-/-}$ mice, a result that agrees with a previous report [19].

Excess free iron increases oxidant production [1]. Subsequently, some antioxidant defense mechanisms are upregulated in order to provide resistance to iron-related toxicity. It is notable from our data that this response is elicited in both liver and duodenum, as seen in the upregulation of glutathione S-transferase genes. Interestingly, dietary iron overload seems to induce a stronger response than *Hfe* deficiency, especially in the regulation of enzymes involved in glutathione-related detoxification of reactive intermediates.

Table 4. Comparison of hepatic gene regulation by *Hfe* deficiency or dietary iron overload.

	Gene Symbol	Description	GenBank Number	FC $Hfe^{-/-}$	FC diet
Increased in $Hfe^{-/-}$ and by diet	*Lcn2*	lipocalin 2	NM_008491	9.54	2.10
	Rgs16	regulator of G-protein signaling 16	NM_011267	4.61	5.06
	Mt1	metallothionein 1	NM_013602	4.17	3.95
	Apoa4	apolipoprotein A-IV	NM_007468	2.36	6.56
	Slc2a2	solute carrier family 2 (facilitated glucose transporter), member 2	NM_031197	1.92	2.17
	Mfsd2	major facilitator superfamily domain containing 2	NM_029662	1.68	3.59
	Cyp2a5	cytochrome P450, family 2, subfamily a, polypeptide 5	NM_007812	1.67	1.65
	Gstt2	glutathione S-transferase, theta 2	NM_010361	1.58	1.86
	Ppp1r3c	protein phosphatase 1, regulatory (inhibitor) subunit 3C	NM_016854	1.57	1.53
	Bhlhb2	basic helix-loop-helix domain containing, class B2	NM_011498	1.52	2.35
	Dusp1	dual specificity phosphatase 1	NM_013642	1.50	2.15
Increased in $Hfe^{-/-}$ and decreased by diet	*Saa2*	serum amyloid A 2	NM_011314	9.83	−2.79
	Saa1	serum amyloid A 1	NM_009117	6.30	−3.96
	Saa3	serum amyloid A 3	NM_011315	2.89	−1.82
	Angptl4	angiopoietin-like 4	NM_020581	2.30	−2.03
	Hp	haptoglobin	NM_017370	2.23	−1.69
	Serpina12	serine (or cysteine) peptidase inhibitor, clade A (alpha-1 antiproteinase, antitrypsin), member 12	NM_026535	2.01	−2.19
	Lpin1	lipin 1	NM_015763	1.92	−1.59
	Il6ra	interleukin 6 receptor, alpha	AK020663	1.70	−2.08
	Dio1	deiodinase, iodothyronine, type I	NM_007860	1.57	−1.87
	Ppp1r3b	protein phosphatase 1, regulatory (inhibitor) subunit 3B	NM_177741	1.55	−1.95
	Dct	dopachrome tautomerase	NM_010024	1.50	−2.72
	Mup4	major urinary protein 4	NM_008648	1.44	−4.28
Decreased in $Hfe^{-/-}$ and increased by diet	*Cyp26b1*	cytochrome P450, family 26, subfamily b, polypeptide 1	NM_175475	−2.39	2.24
	Phlda1	pleckstrin homology-like domain, family A, member 1	NM_009344	−2.20	1.51
	Gadd45g	growth arrest and DNA-damage-inducible 45 gamma	NM_011817	−1.97	1.66
	Socs3	suppressor of cytokine signaling 3	NM_007707	−1.96	1.89
	Cish	cytokine inducible SH2-containing protein	NM_009895	−1.93	2.37
	H2-Aa	histocompatibility 2, class II antigen A, alpha	NM_010378	−1.81	1.81
	Egr1	early growth response 1	NM_007913	−1.77	2.55
	H2-Ab1	histocompatibility 2, class II antigen A, beta 1	NM_207105	−1.77	1.68
	Gsta2	glutathione S-transferase, alpha 2 (Yc2)	NM_008182	−1.71	1.83
	H2-Eb1	histocompatibility 2, class II antigen E beta	NM_010382	−1.63	1.43
	Cd74	CD74 antigen (invariant polypeptide of major histocompatibility complex, class II antigen-associated)	NM_010545	−1.59	1.65
	Cyp4a14	cytochrome P450, family 4, subfamily a, polypeptide 14	NM_007822	−1.44	6.97
	Hbb-b1	hemoglobin, beta adult major chain	AK010993	−1.42	1.45
	Rnf186	ring finger protein 186	NM_025786	−1.41	1.81
	Hamp1	hepcidin antimicrobial peptide 1	NM_032541	−1.41	1.73
Decreased in $Hfe^{-/-}$ and by diet	*Creld2*	cysteine-rich with EGF-like domains 2	NM_029720	−3.47	−1.64
	Hsph1	heat shock 105 kDa/110 kDa protein 1	NM_013559	−2.16	−2.13
	Tfrc	transferrin receptor	NM_011638	−1.92	−1.74
	Hspb1	heat shock protein 1	NM_013560	−1.66	−1.81
	Hhex	hematopoietically expressed homeobox	NM_008245	−1.55	−2.05
	Mcm10	minichromosome maintenance deficient 10 (S. cerevisiae)	NM_027290	−1.55	−1.55
	Ddc	dopa decarboxylase	NM_016672	−1.48	−1.97

FC, fold-change; diet, iron-supplemented diet.

doi:10.1371/journal.pone.0007212.t004

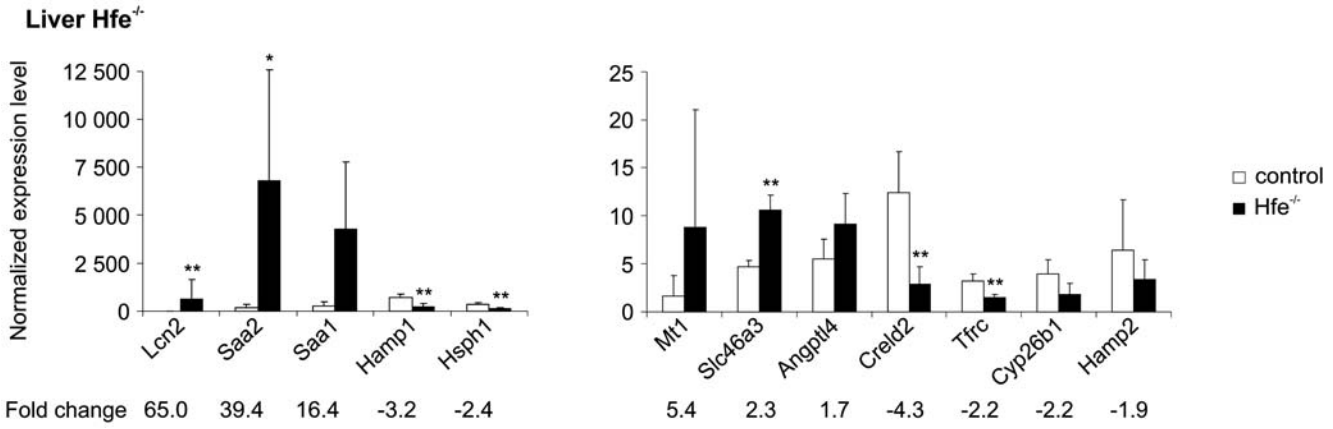

Figure 1. Validation of liver microarray data from *Hfe*$^{-/-}$ mice by Q-RT-PCR. The expression of various mRNA species in 5 *Hfe*$^{-/-}$ mice is compared to those in 4 wild-type controls. Each sample was run in triplicate. (mean±SD). *$p<0.05$; **$p<0.025$; ***$p<0.01$.
doi:10.1371/journal.pone.0007212.g001

In conclusion, *Hfe* deficiency results in increased gene expression of hepatic APPs and duodenal digestive enzymes. In contrast, dietary iron overload causes a more pronounced change of gene expression responsive to oxidative stress.

Materials and Methods

Ethics Statement

The animal protocols were approved by the Animal Care and Use Committees of Saint Louis University and the University of Oulu (permission No 102/05).

Animal care and animal models

Five male C57BL/6 mice homozygous for a disruption of the *Hfe* gene and 4 male wild-type control mice were fed a standard rodent diet (250 ppm of iron) and sacrificed at approximately 10 weeks of age. The generation of the *Hfe*$^{-/-}$ mice has been described elsewhere [13]. In addition, 5 male C57BL/6 mice fed an iron-supplemented diet (2% carbonyl iron) and 4 male control mice fed a standard diet (200 ppm of iron) for 6 weeks were used [27]. The mice with dietary iron overload had a hepatic iron concentration that was approximately 2.5 times higher than the *Hfe*$^{-/-}$ mice. The duodenum and liver samples were immediately collected from anesthetized mice and immersed in RNAlater solution (Ambion, Huntingdon, UK).

RNA isolation

Total RNA extraction and quality control have been described previously [27].

Microarray analysis

All microarray data reported in the present article are described in accordance with MIAME guidelines, have been deposited in NCBI's Gene Expression Omnibus public repository [41], and are accessible through GEO Series accession number GSE17969 [42]. Microarray experiments were performed in the Finnish DNA Microarray Centre at Turku Centre for Biotechnology using Illumina's Sentrix Mouse-6 Expression Beadchips. Duodenal and liver RNA samples from 3 *Hfe*$^{-/-}$ mice and 3 mice with dietary iron overload were used. As controls, RNA samples from the duodenum and liver of 4 wild-type mice (2 controls of the *Hfe*$^{-/-}$ mice and 2 controls of the mice with dietary iron overload) were used. All 10 samples were analyzed individually. The amplification of total RNA (300 ng), *in vitro* transcription, hybridization and scanning have been described before [27].

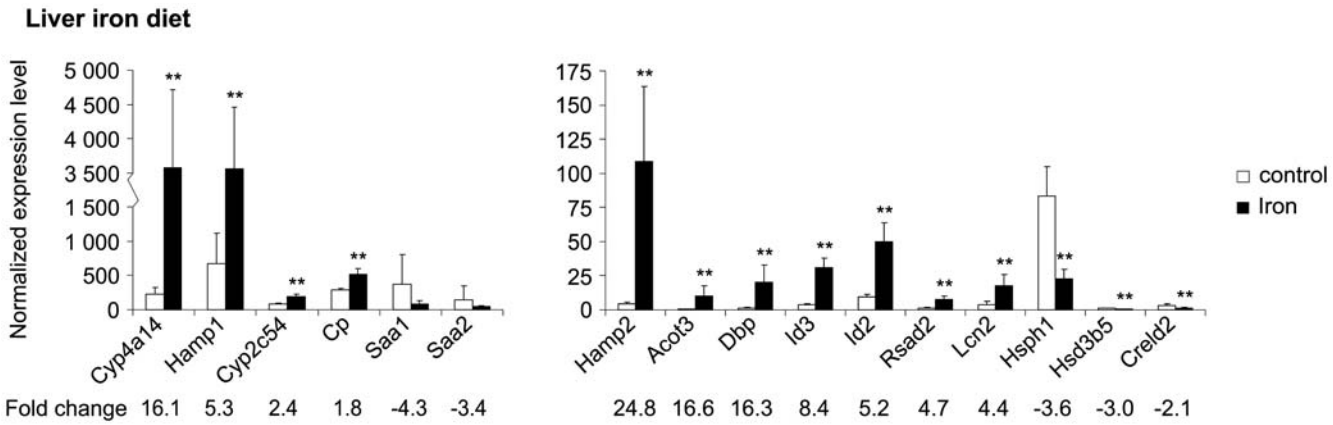

Figure 2. Expression of genes affected by dietary iron overload in the liver, as confirmed by Q-RT-PCR. Samples from 5 mice fed an iron-supplemented diet and 4 mice fed a control diet were used, and each sample was run in triplicate. (mean±SD). *$p<0.05$; **$p<0.025$; ***$p<0.01$.
doi:10.1371/journal.pone.0007212.g002

Table 5. Functional annotation of genes regulated in the duodenum of *Hfe*$^{-/-}$ mice.

Functional Category	Gene Symbol	Description	GenBank Number	FC	Q-PCR
Endopeptidase activity	Ela3	elastase 3, pancreatic	NM_026419	15.67	14.77
	Try4	trypsin 4	NM_011646	13.09	
	RP23-395H4.4	elastase 2A	NM_007919	10.20	
	Ctrl	chymotrypsin-like	NM_023182	9.99	
	Ctrb1	chymotrypsinogen B1	NM_025583	9.68	
	Prss2	protease, serine, 2	NM_009430	7.41	
	2210010C04Rik	RIKEN cDNA 2210010C04 gene	NM_023333	7.14	
	Ela1	elastase 1, pancreatic	NM_033612	5.84	
	Klk1b5	kallikrein 1-related peptidase b5	NM_008456	2.90	
	Ctrc	chymotrypsin C (caldecrin)	NM_001033875	2.51	
	Klk1b11	kallikrein 1-related peptidase b11	NM_010640	2.34	
	Klk1	kallikrein 1	NM_010639	2.29	
	Klk1b27	kallikrein 1-related peptidase b27	NM_020268	2.22	
	Klk1b4	kallikrein 1-related pepidase b4	NM_010915	2.11	
	Klk1b24	kallikrein 1-related peptidase b24	NM_010643	2.10	
	Mela	melanoma antigen	NM_008581	2.05	
	Ctse	cathepsin E	NM_007799	1.91	2.32
	Klk1b26	kallikrein 1-related petidase b26	NM_010644	1.74	
	Capn5	calpain 5	NM_007602	1.60	
Lipid catabolic function	Cel	carboxyl ester lipase	NM_009885	9.82	
	Pnliprp1	pancreatic lipase related protein 1	NM_018874	8.17	
	Clps	colipase, pancreatic	NM_025469	5.35	
	Pla2g1b	phospholipase A2, group IB, pancreas	NM_011107	4.86	
	Pnliprp2	pancreatic lipase-related protein 2	NM_011128	4.50	
	Apoc3	apolipoprotein C-III	NM_023114	−1.79	
Triacylglycerol lipase activity	Cel	carboxyl ester lipase	NM_009885	9.82	
	Pnliprp1	pancreatic lipase related protein 1	NM_018874	8.17	
	Pnliprp2	pancreatic lipase-related protein 2	NM_011128	4.50	
Antimicrobial	Hamp2	hepcidin antimicrobial peptide 2	NM_183257	2.74	6.66
	Defcr-rs1	defensin related sequence cryptdin peptide (paneth cells)	NM_007844	−1.60	
	Lyz1	lysozyme 1	NM_013590	−1.68	
	Defcr6	defensin related cryptdin 6	NM_007852	−2.11	
	Defcr20	defensin related cryptdin 20	NM_183268	−2.69	
Metallocarboxypeptidase activity	Cpa1	carboxypeptidase A1	NM_025350	12.42	
	Cpa2	carboxypeptidase A2, pancreatic	NM_001024698	8.14	
	Cpb1	carboxypeptidase B1 (tissue)	NM_029706	12.51	14.55

doi:10.1371/journal.pone.0007212.t005

Data analysis

Array data were normalized with Chipster (v1.1.1) using the quantile normalization method. Quality control of the data included non-metric multidimensional scaling, dendrograms, hierarchical clustering, and 2-way clustering (heat maps). These analyses showed that data from one of the three duodenal samples from *Hfe*$^{-/-}$ mice were highly divergent from the other two. Thus, this sample was excluded from further analyses. The data were then filtered according to the SD of the probes. The percentage of data that did not pass through the filter was adjusted to 99.4%, implicating a SD value of almost 3. At this point, statistical analysis was performed using the empirical Bayes t-test for the comparison of 2 groups. Due to the small number of samples, the statistical results were considered as orientative and thus no filtering was applied to the data according to p-values. The remaining 280 probes were further filtered according to fold-change with ± 1.4 as cut-off values for up- and down-regulated expression, respectively. The functional annotation tool DAVID (Database for Annotation, Visualization and Integrated Discovery) [43,44] was used to identify enriched biological categories among the regulated genes as compared to all the genes present in Illumina's Sentrix Mouse-6 Expression Beadchip. The annotation groupings analyzed were: Gene Ontology biological process and molecular functions, SwissProt Protein Information Resources keywords, SwissProt comments, Kyoto Encyclopedia of Genes and Genomes and Biocarta pathways. Results were filtered to remove categories with EASE (expression analysis systematic explorer) scores greater than 0.05. Redundant categories with the same gene members were removed to yield a single representative category.

Table 6. Functional annotation of genes regulated in the duodenum of mice fed an iron-supplemented diet.

Functional Category	Gene Symbol	Description	GenBank Number	FC	Q-PCR
Glutatione metabolism	Gstm1	glutathione S-transferase, mu 1	NM_010358	4.42	4.29
	Gsta3	glutathione S-transferase, alpha 3	NM_010356	4.27	
	Gsta1	glutathione S-transferase, alpha 1 (Ya)	NM_008181	3.51	
	Gsta2	glutathione S-transferase, alpha 2 (Yc2)	NM_008182	2.93	
	Gstm6	glutathione S-transferase, mu 6	NM_008184	2.80	
	Gstm4	glutathione S-transferase, mu 4	NM_026764	2.41	
	Gsta4	glutathione S-transferase, alpha 4	NM_010357	2.26	
	Gstm3	glutathione S-transferase, mu 3	NM_010359	1.88	
	Anpep	alanyl (membrane) aminopeptidase	NM_008486	−1.83	
Antigen processing and presentation	Cd74	CD74 antigen (invariant polypeptide of major histocompatibility complex, class II antigen-associated)	BC003476	−1.95	
	H2-Eb1	histocompatibility 2, class II antigen E beta	NM_010382	−2.06	
	H2-DMa	histocompatibility 2, class II, locus DMa	NM_010386	−2.07	
	Psmb8	proteasome (prosome, macropain) subunit, beta type 8 (large multifunctional peptidase 7)	NM_010724	−2.07	
	H2-DMb2	histocompatibility 2, class II, locus Mb2	NM_010388	−2.16	
	H2-Aa	histocompatibility 2, class II antigen A, alpha	NM_010378	−2.53	
	H2-Ab1	histocompatibility 2, class II antigen A, beta 1	NM_207105	−2.76	
Chaperone cofactor-dependent protein folding	Cd74	CD74 antigen (invariant polypeptide of major histocompatibility complex, class II antigen-associated)	BC003476	−1.95	
	H2-DMa	histocompatibility 2, class II, locus DMa	NM_010386	−2.07	
	H2-DMb2	histocompatibility 2, class II, locus Mb2	NM_010388	−2.16	
	Dnajb1	DnaJ (Hsp40) homolog, subfamily B, member 1	NM_018808	−2.62	−2.17
	Hsph1	heat shock 105 kDa/110 kDa protein 1	NM_013559	−5.64	−6.55
MHCII	H2-Eb1	histocompatibility 2, class II antigen E beta	NM_010382	−2.06	
	H2-DMa	histocompatibility 2, class II, locus DMa	NM_010386	−2.07	
	H2-DMb2	histocompatibility 2, class II, locus Mb2	NM_010388	−2.16	
	H2-Aa	histocompatibility 2, class II antigen A, alpha	NM_010378	−2.53	
	H2-Ab1	histocompatibility 2, class II antigen A, beta 1	NM_207105	−2.76	
T cell differentiation and activation	Cd74	CD74 antigen (invariant polypeptide of major histocompatibility complex, class II antigen-associated)	BC003476	−1.95	
	H2-DMa	histocompatibility 2, class II, locus DMa	NM_010386	−2.07	
	H2-Aa	histocompatibility 2, class II antigen A, alpha	NM_010378	−2.53	
	Egr1	early growth response 1	NM_007913	−3.33	−2.32
	Hsp90aa1	heat shock protein 90 kDa alpha (cytosolic), class A member 1	NM_010480	−2.11	
Inflammatory response	Reg3g	regenerating islet-derived 3 gamma	NM_011260	−1.56	
	Cxcl13	chemokine (C-X-C motif) ligand 13	NM_018866	−1.71	
	C3	complement component 3	NM_009778	−1.78	
	Ccl5	chemokine (C-C motif) ligand 5	NM_013653	−2.00	
	Pap	pancreatitis-associated protein	NM_011036	−2.13	
Antimicrobial	Defcr20	defensin related cryptdin 20	NM_183268	1.72	
	Defcr5	defensin related cryptdin 5	NM_007851	−1.41	
	Lyzs	lysozyme	NM_017372	−1.88	
	Defcr-rs1	defensin related sequence cryptdin peptide (paneth cells)	NM_007844	−3.23	
Lectin	Reg2	regenerating islet-derived 2	NM_009043	2.14	
	Glg1	golgi apparatus protein 1	NM_009149	−1.43	
	Reg3g	regenerating islet-derived 3 gamma	NM_011260	−1.56	
	Pap	pancreatitis-associated protein	NM_011036	−2.13	
B cell mediated immunity	C3	complement component 3	NM_009778	−1.78	
	Cd74	CD74 antigen (invariant polypeptide of major histocompatibility complex, class II antigen-associated)	BC003476	−1.95	

Table 6. Cont.

Functional Category	Gene Symbol	Description	GenBank Number	FC	Q-PCR
	H2-DMa	histocompatibility 2, class II, locus DMa	NM_010386	−2.07	
Cholesterol metabolic process	Ldlr	low density lipoprotein receptor	NM_010700	1.99	
	Cyp51	cytochrome P450, family 51	NM_020010	1.96	
	Hmgcs2	3-hydroxy-3-methylglutaryl-Coenzyme A synthase 2	NM_008256	1.88	
Response to heat	Hspa1a	heat shock protein 1A	NM_010479	−1.91	
	Hsp90aa1	heat shock protein 90 kDa alpha (cytosolic), class A member 1	NM_010480	−2.11	
	Hsph1	heat shock 105 kDa/110 kDa protein 1	NM_013559	−5.64	−6.55

doi:10.1371/journal.pone.0007212.t006

Quantitative Reverse-Transcriptase PCR

For this analysis, duodenal and liver RNA samples from 5 mice of each experimental group ($Hfe^{-/-}$ and dietary iron overload) and 4 mice from each control group (wild-type and normal diet) were used. Exceptionally, for the analysis of mRNA expression in the duodenum of $Hfe^{-/-}$ mice, only 4 samples were used. RNA samples (5 µg) were converted into first strand cDNA with a First Strand cDNA Synthesis kit (Fermentas, Burlington, Canada) using random hexamer primers. The relative expression levels of target genes in the duodenum and liver were assessed by Q-RT-PCR using the LightCycler detection system (Roche, Rotkreuz, Switzerland). The reaction setup, cycling program, standard curve method and primer pairs for *Angptl4*, *Dnajb1* and *Tfrc* have been described before [27]. Mouse *Hamp1* and *Hamp2* primers have also been characterized previously [26]. The primer sets for the other target genes (Dataset S5) were designed using Primer3 [45], based on the complete cDNA sequences deposited in GenBank. The specificity of the primers was verified using NCBI Basic Local Alignment and Search Tool (BLAST) [46]. To avoid amplification of contaminating genomic DNA, both primers from each set were specific to different exons, when possible. Each cDNA sample was tested in triplicate. The mean and SD of the 3 crossing point (Cp) values were calculated for each sample and a SD cutoff level of 0.2 was set. Accordingly, when the SD of the triplicates of a sample was greater than 0.2, the most outlying replicate was excluded and the analysis was continued with the two remaining replicates. Using the standard curve method, the Cp values were then transformed by the LightCycler software into copy numbers. The expression value for each sample was the mean of the copy numbers for the sample's replicates. This value was normalized by dividing it by the geometric mean of the 4 internal control genes, an accurate normalization method [47]. The normalization factor was always considered as a value of 100 and the final result was expressed as relative mRNA expression level.

Statistical analyses

We performed statistical analyses of the microarray data using the empirical Bayes t-test for the comparison of 2 groups, and the p-values are shown in supplementary datasets S1-S4. For the Q-RT-PCR results, we used the Mann-Whitney test to evaluate differences in group values for $Hfe^{-/-}$ mice vs. wild-type mice and mice with dietary iron overload vs. untreated mice. Due to the small sample sizes, the statistical significance is only considered as orientative. Values are expressed as mean±SD.

Supporting Information

Dataset S1 List of genes differentially expressed in the liver of Hfe knockout mice

Found at: doi:10.1371/journal.pone.0007212.s001 (0.04 MB XLS)

Table 7. Genes regulated in the duodenum of mice by *Hfe* deficiency or iron-supplemented diet.

	Gene Symbol	Description	GenBank	FC $Hfe^{-/-}$	FC diet
Increased in $Hfe^{-/-}$ and by diet	*Reg2*	regenerating islet-derived 2	NM_009043	10.34	2.14
	Alpi	alkaline phosphatase, intestinal	NM_001081082	2.09	1.71
	Akr1b8	aldo-keto reductase family 1, member B8	NM_008012	1.60	4.17
	Mboat1	membrane bound O-acyltransferase domain containing 1	NM_153546	1.46	1.81
Increased in $Hfe^{-/-}$ and decreased by diet	*Reg3b*	regenerating islet-derived 3 beta	NM_011036	6.87	−2.13
	Klk1b27	kallikrein 1-related peptidase b27	NM_020268	2.22	−1.87
	Slc38a5	solute carrier family 38, member 5	NM_172479	2.14	−2.31
Decreased in $Hfe^{-/-}$ and increased by diet	*Defcr20*	defensin related cryptdin 20	NM_183268	−2.69	1.72
Decreased in $Hfe^{-/-}$ and by diet	*Hspb1*	heat shock protein 1	NM_013560	−2.07	−2.17
	Defcr-rs1	defensin related sequence cryptdin peptide (Paneth cells)	NM_007844	−1.60	−3.23
	LOC620017	PREDICTED: similar to Ig kappa chain V-V region L7 precursor	XM_357633	−1.44	−2.31

FC, fold-change; diet, iron-supplemented diet.

doi:10.1371/journal.pone.0007212.t007

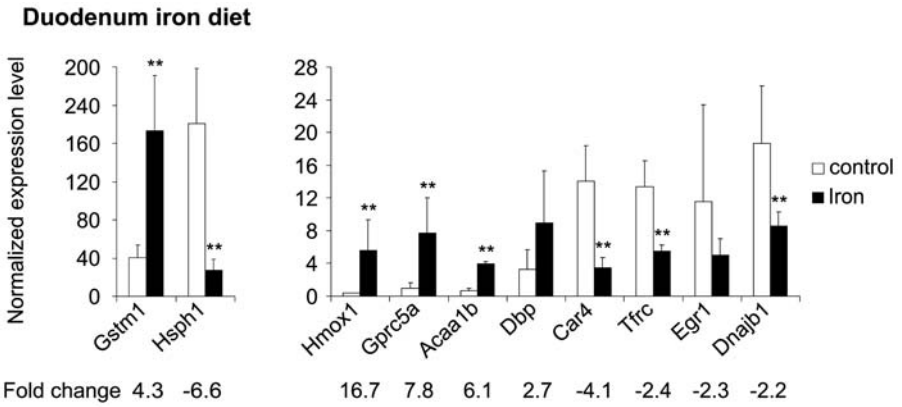

Figure 3. Expression of genes regulated in the duodenum of dietary iron-loaded mice as verified by Q-RT-PCR. Samples from 5 mice fed an iron-supplemented diet and 4 mice fed a control diet were used, and each sample was run in triplicate. (mean±SD). *$p<0.05$; **$p<0.025$; ***$p<0.01$.
doi:10.1371/journal.pone.0007212.g003

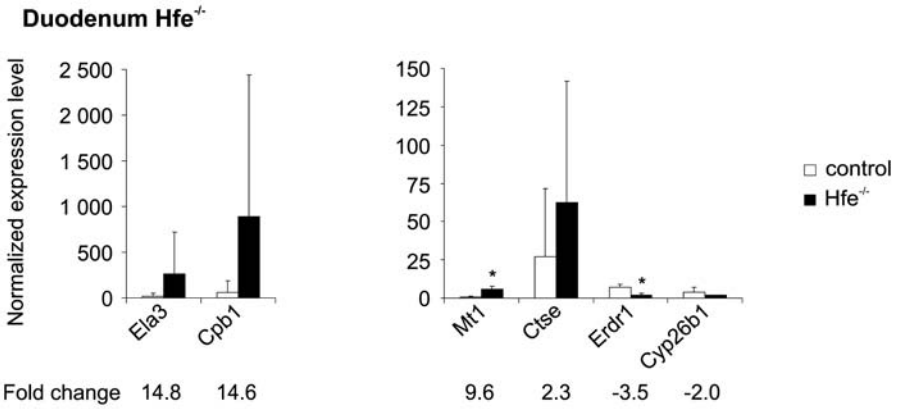

Figure 4. Validation of the duodenal microarray results from *Hfe*$^{-/-}$ mice by Q-RT-PCR. The *Hfe*$^{-/-}$ and control groups contained samples from 4 mice, and each sample was tested in triplicate. (mean±SD). *$p<0.05$; **$p<0.025$; ***$p<0.01$.
doi:10.1371/journal.pone.0007212.g004

Dataset S2 List of genes differentially expressed in the liver of mice fed an iron-supplemented diet
Found at: doi:10.1371/journal.pone.0007212.s002 (0.05 MB XLS)

Dataset S3 Genes whose expression was altered in the duodenum of Hfe knockout mice
Found at: doi:10.1371/journal.pone.0007212.s003 (0.05 MB XLS)

Dataset S4 Genes whose expression was affected in the duodenum of mice fed an iron-supplemented diet
Found at: doi:10.1371/journal.pone.0007212.s004 (0.04 MB XLS)

Dataset S5 Sequences of the primers used in the Q-RT-PCR experiments performed in this study
Found at: doi:10.1371/journal.pone.0007212.s005 (0.06 MB DOC)

Acknowledgments

We thank Mary Migas and Rosemary O'Neill for excellent technical assistance. We are grateful to the staff of the Finnish microarray core facility at Turku Centre of Biotechnology, especially Tiia Heinonen for performing the microarray hybridizations and scanning.

Author Contributions

Conceived and designed the experiments: AR REF RSB BRB SP. Performed the experiments: AR. Analyzed the data: AR TL. Contributed reagents/materials/analysis tools: REF RSB BRB SP. Wrote the paper: AR. Critically reviewed the manuscript and approved its final version: TL REF RSB BRB SP.

References

1. Britton RS (1996) Metal-induced hepatotoxicity. Semin Liver Dis 16: 3–12.
2. Parkkila S, Niemela O, Britton RS, Fleming RE, Waheed A, et al. (2001) Molecular aspects of iron absorption and HFE expression. Gastroenterology 121: 1489–1496.
3. Feder JN, Gnirke A, Thomas W, Tsuchihashi Z, Ruddy DA, et al. (1996) A novel MHC class I-like gene is mutated in patients with hereditary haemochromatosis. Nat Genet 13: 399–408.
4. Fleming RE, Britton RS, Waheed A, Sly WS, Bacon BR (2005) Pathophysiology of hereditary hemochromatosis. Semin Liver Dis 25: 411–419.
5. Papanikolaou G, Samuels ME, Ludwig EH, MacDonald ML, Franchini PL, et al. (2004) Mutations in HFE2 cause iron overload in chromosome 1q-linked juvenile hemochromatosis. Nat Genet 36: 77–82.
6. Nemeth E, Ganz T (2006) Regulation of iron metabolism by hepcidin. Annu Rev Nutr 26: 323–342.
7. Abboud S, Haile DJ (2000) A novel mammalian iron-regulated protein involved in intracellular iron metabolism. J Biol Chem 275: 19906–19912.
8. McKie AT, Marciani P, Rolfs A, Brennan K, Wehr K, et al. (2000) A novel duodenal iron-regulated transporter, IREG1, implicated in the basolateral transfer of iron to the circulation. Mol Cell 5: 299–309.

9. Gunshin H, Mackenzie B, Berger UV, Gunshin Y, Romero MF, et al. (1997) Cloning and characterization of a mammalian proton-coupled metal-ion transporter. Nature 388: 482–488.
10. Nemeth E, Tuttle MS, Powelson J, Vaughn MB, Donovan A, et al. (2004) Hepcidin regulates cellular iron efflux by binding to ferroportin and inducing its internalization. Science 306: 2090–2093.
11. Nicolas G, Chauvet C, Viatte L, Danan JL, Bigard X, et al. (2002) The gene encoding the iron regulatory peptide hepcidin is regulated by anemia, hypoxia, and inflammation. J Clin Invest 110: 1037–1044.
12. Pigeon C, Ilyin G, Courselaud B, Leroyer P, Turlin B, et al. (2001) A new mouse liver-specific gene, encoding a protein homologous to human antimicrobial peptide hepcidin, is overexpressed during iron overload. J Biol Chem 276: 7811–7819.
13. Zhou XY, Tomatsu S, Fleming RE, Parkkila S, Waheed A, et al. (1998) HFE gene knockout produces mouse model of hereditary hemochromatosis. Proc Natl Acad Sci U S A 95: 2492–2497.
14. Ramm GA (2000) Animal models of iron overload based on excess exogenous iron. In: Barton JC, Edwards CQ, eds. Hemochromatosis: Genetics, Pathophysiology, Diagnosis and Treatment. New York: Cambridge University Press. pp 494–507.
15. Bridle KR, Frazer DM, Wilkins SJ, Dixon JL, Purdie DM, et al. (2003) Disrupted hepcidin regulation in HFE-associated haemochromatosis and the liver as a regulator of body iron homoeostasis. Lancet 361: 669–673.
16. Ahmad KA, Ahmann JR, Migas MC, Waheed A, Britton RS, et al. (2002) Decreased liver hepcidin expression in the Hfe knockout mouse. Blood Cells Mol Dis 29: 361–366.
17. Coppin H, Darnaud V, Kautz L, Meynard D, Aubry M, et al. (2007) Gene expression profiling of Hfe−/− liver and duodenum in mouse strains with differing susceptibilities to iron loading: identification of transcriptional regulatory targets of Hfe and potential hemochromatosis modifiers. Genome Biol 8: R221.
18. Morey JS, Ryan JC, Van Dolah FM (2006) Microarray validation: factors influencing correlation between oligonucleotide microarrays and real-time PCR. Biol Proced Online 8: 175–193.
19. Muckenthaler M, Roy CN, Custodio AO, Minana B, deGraaf J, et al. (2003) Regulatory defects in liver and intestine implicate abnormal hepcidin and Cybrd1 expression in mouse hemochromatosis. Nat Genet 34: 102–107.
20. Abgueguen E, Toutain B, Bedrine H, Chicault C, Orhant M, et al. (2006) Differential expression of genes related to HFE and iron status in mouse duodenal epithelium. Mamm Genome 17: 430–450.
21. Goetz DH, Holmes MA, Borregaard N, Bluhm ME, Raymond KN, et al. (2002) The neutrophil lipocalin NGAL is a bacteriostatic agent that interferes with siderophore-mediated iron acquisition. Mol Cell 10: 1033–1043.
22. Yang J, Mori K, Li JY, Barasch J (2003) Iron, lipocalin, and kidney epithelia. Am J Physiol Renal Physiol 285: F9–18.
23. Devireddy LR, Gazin C, Zhu X, Green MR (2005) A cell-surface receptor for lipocalin 24p3 selectively mediates apoptosis and iron uptake. Cell 123: 1293–1305.
24. Mori K, Lee HT, Rapoport D, Drexler IR, Foster K, et al. (2005) Endocytic delivery of lipocalin-siderophore-iron complex rescues the kidney from ischemia-reperfusion injury. J Clin Invest 115: 610–621.
25. Yan QW, Yang Q, Mody N, Graham TE, Hsu CH, et al. (2007) The adipokine lipocalin 2 is regulated by obesity and promotes insulin resistance. Diabetes 56: 2533–2540.
26. Ilyin G, Courselaud B, Troadec MB, Pigeon C, Alizadeh M, et al. (2003) Comparative analysis of mouse hepcidin 1 and 2 genes: evidence for different patterns of expression and co-inducibility during iron overload. FEBS Lett 542: 22–26.
27. Rodriguez A, Hilvo M, Kytomaki L, Fleming RE, Britton RS, et al. (2007) Effects of iron loading on muscle: genome-wide mRNA expression profiling in the mouse. BMC Genomics 8: 379.
28. Norton JD (2000) ID helix-loop-helix proteins in cell growth, differentiation and tumorigenesis. J Cell Sci 113 (Pt 22): 3897–3905.
29. Damdinsuren B, Nagano H, Kondo M, Yamamoto H, Hiraoka N, et al. (2005) Expression of Id proteins in human hepatocellular carcinoma: relevance to tumor dedifferentiation. Int J Oncol 26: 319–327.
30. Kautz L, Meynard D, Monnier A, Darnaud V, Bouvet R, et al. (2008) Iron regulates phosphorylation of Smad1/5/8 and gene expression of Bmp6, Smad7, Id1, and Atoh8 in the mouse liver. Blood 112: 1503–1509.
31. Andriopoulos B Jr, Corradini E, Xia Y, Faasse SA, Chen S, et al. (2009) BMP6 is a key endogenous regulator of hepcidin expression and iron metabolism. Nat Genet 41: 482–487.
32. Brown KE, Broadhurst KA, Mathahs MM, Weydert J (2007) Differential expression of stress-inducible proteins in chronic hepatic iron overload. Toxicol Appl Pharmacol 223: 180–186.
33. Shayeghi M, Latunde-Dada GO, Oakhill JS, Laftah AH, Takeuchi K, et al. (2005) Identification of an intestinal heme transporter. Cell 122: 789–801.
34. Qiu A, Jansen M, Sakaris A, Min SH, Chattopadhyay S, et al. (2006) Identification of an intestinal folate transporter and the molecular basis for hereditary folate malabsorption. Cell 127: 917–928.
35. Fleming RE, Sly WS (2002) Mechanisms of iron accumulation in hereditary hemochromatosis. Annu Rev Physiol 64: 663–680.
36. Trinder D, Olynyk JK, Sly WS, Morgan EH (2002) Iron uptake from plasma transferrin by the duodenum is impaired in the Hfe knockout mouse. Proc Natl Acad Sci U S A 99: 5622–5626.
37. Zoller H, Pietrangelo A, Vogel W, Weiss G (1999) Duodenal metal-transporter (DMT-1, NRAMP-2) expression in patients with hereditary haemochromatosis. Lancet 353: 2120–2123.
38. Fleming RE, Migas MC, Zhou X, Jiang J, Britton RS, et al. (1999) Mechanism of increased iron absorption in murine model of hereditary hemochromatosis: increased duodenal expression of the iron transporter DMT1. Proc Natl Acad Sci U S A 96: 3143–3148.
39. Owen D, Kuhn LC (1987) Noncoding 3′ sequences of the transferrin receptor gene are required for mRNA regulation by iron. Embo J 6: 1287–1293.
40. Dupic F, Fruchon S, Bensaid M, Loreal O, Brissot P, et al. (2002) Duodenal mRNA expression of iron related genes in response to iron loading and iron deficiency in four strains of mice. Gut 51: 648–653.
41. Edgar R, Domrachev M, Lash AE (2002) Gene Expression Omnibus: NCBI gene expression and hybridization array data repository. Nucleic Acids Res 30: 207–210.
42. GEO. Gene Expression Omnibus. http://www.ncbi.nlm.nih.gov/geo/.
43. The DAVID Bioinformatic Resources. http://david.abcc.ncifcrf.gov.
44. Dennis G Jr, Sherman BT, Hosack DA, Yang J, Gao W, et al. (2003) DAVID: Database for Annotation, Visualization, and Integrated Discovery. Genome Biol 4: P3.
45. Primer3. http://frodo.wi.mit.edu/.
46. BLAST. Basic Local Alignment and Search Tool. http://blast.ncbi.nlm.nih.gov/Blast.cgi.
47. Vandesompele J, De Preter K, Pattyn F, Poppe B, Van Roy N, et al. (2002) Accurate normalization of real-time quantitative RT-PCR data by geometric averaging of multiple internal control genes. Genome Biol 3: RESEARCH0034.